

SOCIEDAD POLIMÉRICA DE MÉXICO



Sociedad Polimérica
de México, A.C.



*Riviera Maya, Quintana Roo del 23 al
27 de octubre de 2016.*

XXIX Congreso Nacional de la S.P.M.

Información Legal:

SOCIEDAD POLIMÉRICA DE MÉXICO, Año 15, No. 15, enero – diciembre 2016, es una publicación anual editada por la Sociedad Polimérica de México, A.C., Carretera Panorámica Prepa Pastita No. 12500, Barrio de la Alameda, C.P. 36000, Tel. 6641738928, <http://www.sociedadpolimerica.mx/portal/?p=memorias>, aliceac@tectijuana.mx.

Editor responsable: Dr. Ángel Licea-Claveríe. Reserva de Derechos al Uso Exclusivo No. 04-2015-052710244200-203, ISSN: 2448-6272, ambos otorgados por el Instituto Nacional del Derecho de Autor. Responsable de la última actualización de este número, Sociedad Polimérica de México, A.C., Carretera Panorámica Prepa Pastita No. 12500, Barrio de la Alameda, C.P. 36000, Tel. 6641738928, a cargo de la Dr. Ángel Licea-Claveríe, fecha última modificación, 16 de diciembre de 2016.

Las opiniones expresadas por los autores, no necesariamente reflejan la postura del editor de la publicación.

Queda prohibida la reproducción total o parcial de los contenidos e imágenes de la publicación sin previa autorización de la Sociedad Polimérica de México, A. C.

COMITÉ EDITORIAL

**Angel Licea Claverie, Iván Zapata
González y Milton Vázquez Lepe**

PATROCINADORES



Anton Paar



**UNIVERSIDAD
AUTÓNOMA
METROPOLITANA**



Preface, Proceedings of SLAP 2016

This volume is a collection of papers presented at the 15th Simposio Latinoamericano de Polímeros and 13th Congreso Iberoamericano de Polímeros: SLAP 2016.

This is the third time that the Sociedad Polimérica de México A.C. (SPM) is pleased to organize the premier meetings among the polymer communities in Latinoamerica, Portugal and Spain.

The first and second SLAP Conferences organized by SPM were held in México in 1990 (Guadalajara) and 2002 (Acapulco). Both Conferences were a success in terms of the quality of the papers presented and the rewarding interaction between scientists, not only from Latinoamerica, Portugal and Spain, but also increasingly from other countries.

SLAP 2016 takes place on October 23rd-27th of 2016 at the Riviera Maya, Quintana Roo, in the Mexican Caribe surrounded by the ancient Maya culture. The conference includes participants from 17 countries, and include 170 oral presentations and 271 posters, surpassing in numbers the two previous versions of this conference held in Mexico. There will be 7 plenary speakers and 22 Keynote speakers from different countries, such as Canada, USA, Mexico, Costa Rica, Colombia, Venezuela, Peru, Chile, Argentina, Brazil, Spain, France, Germany, Italy, Slovenia and Israel.

The rich variety of presentations related to different contemporary issues in polymer science and engineering are organized in the following symposia:

- 1.-Nanotechnology and Polymers
- 2.-Polymers and the environment
- 3.-Polymers for tissue engineering and biomaterials
- 4.-Stimuli-responsive polymers for medicine
- 5.-Polymer composites and nanocomposites.
- 6.-Polymer engineering, processing and rheology.
- 7.-Polymeric membranes and their applications
- 8.-Modern synthetic methods of polymers
- 9.-Modern Methods of Analysis and Characterization of Polymers and Theoretical studies.
- 10.-General Topics on Polymers.

The Organizing SLAP2016 Committee thanks to all contributors and invited speakers for sharing his/her knowledge and expertise during the conference and also for contributing to the success of SLAP2016.

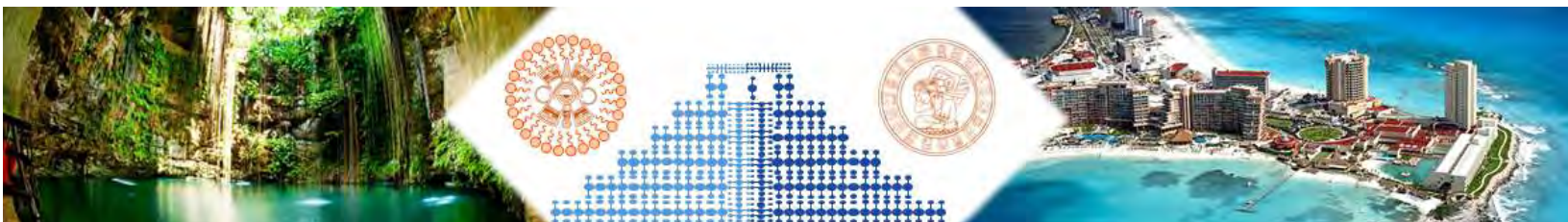
We also would like to thank the sponsors from academia and private companies for their financial support to this conference.

Antonio Martínez Richa, President of SLAP2016 and Angel Licea Claveríe, President of SPM.



LOCAL ORGANIZING COMMITTEE

- Antonio Martínez Richa, Universidad de Guanajuato, Guanajuato, Guanajuato
- Angel Licea Claverie, Instituto Tecnológico de Tijuana, Tijuana, Baja California
- Enrique Saldivar Guerra, CIQA, Saltillo, Coahuila
- José Bonilla Cruz, CIMAV, Monterrey, Nuevo León
- Juan Valerio Cauich Rodríguez, CICY, Mérida, Yucatán
- Milton Oswaldo Vázquez Lepe, Universidad de Guadalajara, Guadalajara, Jalisco
- Eduardo Vivaldo Lima, UNAM, Ciudad de México, D.F.
- Beatriz García Gaitán, Instituto Tecnológico de Toluca, Toluca, México
- Rubén González Núñez, Universidad de Guadalajara, Guadalajara, Jalisco
- Manuel de Jesús Aguilar Vega, CICY, Mérida, Yucatán
- Graciela Elizabeth Morales Balado, CIQA, Saltillo, Coahuila
- Iván de Jesús Zapata González, Instituto Tecnológico de Tijuana, Tijuana, Baja California
- Emilio Bucio Carrillo, UNAM Ciudad de México, D.F.



INTERNATIONAL ADVISORY COMMITTEE

- Julio San Román del Barrio, Centro de Investigaciones Científicas (CSIC) Madrid, España
- José María Kenny, Università degli Studi di Perugia, Perugia, Italia
- Alejandro J. Müller, Universidad del País Vasco, España
- Roberto Olayo González, Universidad Autónoma Metropolitana-Iztapalapa, Ciudad de México, México.
- Juan Carlos Rueda Sánchez, Pontificia Universidad Católica del Perú, Lima, Perú
- Marco Aurelio de Paoli, Universidade Estadual de Campinas, Brasil
- Michael Jaffe, New Jersey Institute of Technology, U.S.A.
- Carlos Peniche Cobas, Universidad de la Habana, La Habana, Cuba
- Bernabé Luis Rivas Quiroz, Universidad de Concepción, Chile



SPONSORS



1. Nanotechnology and Polymers

26	COLLAGEN/PVA/SC ELECTROSPUN SCAFFOLD FOR 3D CELL CULTURE Luis H. Delgado Rangel, Julia Hernández Vargas, J. Betzabe González Campos, Zaira Y. García Carvajal, Judit Aviña Verduzco and José María Ponce-Ortega	1
44	TEMPLATING DOUBLE AND TRIPLE CRYSTALLINE MORPHOLOGIES IN BIODEGRADABLE COPOLYMERS AND TERPOLYMERS Alejandro J. Müller	2
45	PICKERING SILICA-BASED STYRENE EMULSION POLYMERIZATION KINETICS: UNTANGLING MECHANISMS Benoit Fouconnier, Francisco López-Serrano	3
113	ZIRCONOCENE ALUMINOHYDRIDE IMMOBILIZED ON ORGANIC SUPPORTS FOR THE SYNTHESIS OF POLYETHYLENE Alba N. Estrada-Ramirez, Odilia Perez, Rene D. Peralta, Maricela Garcia-Zamora, Victor E. Comparán, Gladys Y. Cortez-Mazatán	4
138	SEMICONDUCTORES POLIMERICOS DEL TIPO PUSH/PULL EN BASE A TIOFENO Y BENZODIOXAZOL Juan Carlos Ahumada, Juan Pablo Soto, Juliet Andrea Aristizabal	5
159	POLÍMEROS CONDUCTORES: SÍNTESIS, CARACTERIZACIÓN Y ELECTROPOLIMERIZACIÓN DE COPOLÍMEROS DE CARBAZOL Y ETILENDIOXITIOFENO Cindy Escalona, Juan Soto, Simon Le Page, Juan Ahumada, Felipe Gallardo, Juliet Aristizabal	6
165	MAGNETOHYPERTERMIA IN A VEGETABLE OIL BASED POLYMER C. Meiorin, D. Muraca, D.G. Actis, P. Mendoza Zélis, M.I. Aranguren, M. Knobel, M.A Mosiewicki	7
168	INFLUENCE OF ELECTROSPINNING PROCESS PARAMETERS ON THE STRUCTURE AND MORPHOLOGY OF SMART POLYMER FIBERS MADE OF POLY(VINYLLIDENE FLUORIDE) Anthony Moulins, Mitasha Swain, Nicole Demarquette, Ricardo Zednik	8
175	LAYER-by-LAYER HYBRID GRAPHENE OXIDE PDADMAC MULTILAYERED FILMS Layza Arizmendi, Raquel Ledezma, Alberto Rodríguez, Sergio Moya and Ronald Ziolo	9
210	PROPIEDADES REOLÓGICAS TRANSITORIAS DE MATERIALES COMPUESTOS A BASE DE POLIPROPILENO REFORZADO CON NANO-ARCILLAS DE PALIGORSKITA Carlos Gamboa Sosa, Genaro Soberanis Monforte, P.I. González-Chi	10
216	NANOPARTÍCULAS DE TALCO EN FILMS ORIENTADOS POR ROLL-CASTING Ma. Gabriela Passaretti, Daniel A. Vega, Marcelo A. Villar	11
240	CARBON NANOTUBES FUNCTIONALIZATION: IN SEARCH OF NANOCOMPOSITES PROPERTIES IMPROVEMENT J. A. Torres-Avalos, F. López-Serrano, S. M. Nuño- Donlucas	12
249	FLUORESCENCE EMISSION COLOR CHANGES OF ACRYLONITRILE DERIVATIVES DUE TO NANOCRYSTALS, MORPHOLOGY. SYNTHESIS, STRUCTURE, AND OPTICAL PROPERTIES M. Judith Percino, Margarita Cerón, Oscar Rodríguez, Guillermo Soriano-Moro, Enrique Pérez-Gutierrez, José Bonilla-Cruz	13



282	SYNTHESIS OF NANOCOMPOSITES WITH STAR SHAPED POLY(ϵ -CAPROLACTONE)-CO-POLY(ETHYLENE GLYCOL) AS POLYMERIC MATRIX	14
	Leonardo Ramses Cajero Zul, Sergio Manuel Nuño Donlucas	
299	EFFECT OF NUCLEATION ON THE CRYSTALLIZATION OF POLY (LACTIC ACID)/POLY (PROPYLENE) BLENDS	15
	Dulce K. Contreras García, Yovana García Morais, Sergio Barrientos Ramírez, Georgina Montes de Oca Ramírez	
300	WELL-DEFINED NANOPARTICLES FROM POLYMER ELECTROLYTES PSSNA VIA RAFT POLYMERIZATION	16
	Claude St Thomas, Enrique J. Jimenez Regalado, Alexis Vélez de la Fuente, Judith Cardoso Martinez, Ramiro Guerrero Santos, Hortensia Maldonado-Textle, Judith Cabello Romero	
318	EFFECT OF THE COMPOSITION IN STATIC AND DYNAMIC MECHANICAL PROPERTIES OF POLYMERS SYNTHESIZED IN TWO STAGES. SYSTEMS: STYRENE – BUTYL ACRYLATE / BUTYL ACRYLATE AND STYRENE – METHYL METHACRYLATE / BUTYL ACRYLATE	17
	Francisco J. Rivera Gálvez, María E. Hernández, Carlos F. Jasso-Gastinel	
339	SYNTHESIS AND CHARACTERIZATION OF TiO ₂ /ZNO NANOFIBERS FROM PVAC ELECTROSPUN MICROFIBER PRECURSORS	18
	Sandra Milena Camargo Silva Efrén Muñoz Prieto, Edwin Gomez Pachon, Ricardo Vera Graziano	
353	SYNTHESIS OF FLUORINATED RANDOM COPOLYMER (P3FM-co-P13FM) BY RAFT AND IT'S CHAIN EXTENTION WITH MMA IN sc(CO ₂). MORPHOLOGY OF DISPERSED MICROSPHERES	19
	Yañez-Macias Roberto; Guerrero-Santos Ramiro, Maldonado-Textle Hortensia, Cabello-Romero Judith Nazareth, Garza-Cepeda Jesús Angel, Torres-Lubián José Román	
370	BIOSYNTHESIS OF SILVER NANOPARTICLES AND ITS USE IN POLYMER SOLAR CELLS	20
	Edgar J. López-Naranjo, I. Paz Hernández-Rosales, Luis J. González-Ortiz, Damaris Velázquez-Páez, Alejandro Manzano-Ramírez	
411	SERS SUBSTRATES FOR ACETONE DETECTION	21
	Iván Alziri Estrada-Moreno, Elsa Anabel Mercado-Gardea, Mónica Elvira Mendoza-Duarte, Sergio Gabriel Flores-Gallardo, Alejandro Vega-Rios, Rocío Domínguez-Cruz, Velia Carolina Osuna-Galindo, Pedro Piza-Ruiz, Alfredo Márquez-Lucero	
413	EXFOLIATION OF LIQUID PHASE GRAPHENE OXIDE VIA INTERCALATION BY FeCl ₃ AND FUNCTIONALIZATION WITH POLY(3,4-ETHYLENEDIOXYTHIOPHENE)	22
	Lorena Carrasco, Alejandro Vega	
417	SAFER ALTERNATIVES TO OBTAIN GRAPHENE OXIDE	23
	Eliana Higueta, Yuliana Franco, Omar Gutiérrez	
424	EXFOLIACIÓN DE GRAFENO EN FASE LÍQUIDA: PRIMERA ETAPA EN LA PRODUCCIÓN DE NANOCOMPUESTOS EPOXI/GRAFENO	24
	Leonel Ignacio Silva, Juan Pablo Tomba, Carmen Cristina Riccardi	
428	ORDENAMIENTO EN FILMS DELGADOS DE COPOLÍMERO BLOQUE BAJO CO ₂ SUPERCRÍTICO	25
	Anabella A. Abate, Cristian M. Piqueras, Marcelo A. Villar2, Daniel A. Vega	



2. Polymers and the environment

12	TRANSFORMING PHYTOCHEMICAL WASTE FROM COLOMBIAN SUGARCANE MILLS INTO POLYMERS WITH ADDED-VALUE Lina M. Delgado, Constan H. Salamanca, Guillermo L. Montoya, Giovanni Rojas	26
17	CASE STUDY: REINFORCED DROP-IN BIOPLASTIC COMPOSED OF GREEN HDPE, CELLULOSE AND LIGNIN Marco Aurelio De Paoli, Renan Gadioli, Walter R Waldman	27
54	THE OPTIMIZATION OF LACCASE IMMOBILIZATION CONDITIONS ONTO TWO DIFFERENT POLYMERIC MICROSPHERES BY RESPONSE SURFACE METHODOLOGY Myleidi Vera, Bernabé L. Rivas	28
56	MONODISPERSE MICROSPHERES OF GLYCIDYL METHACRYLATE AS POLYMERIC SUPPORT FOR LACCASE IMMOBILIZATION Myleidi Vera, Bernabé L. Rivas	29
91	EFFECT OF CHITOSAN-BASED EDIBLE COATINGS WITH NATURAL COMPOUNDS ON THE MICROBIAL PRESERVATION OF MINIMALLY PROCESSED STRAWBERRIES Bárbara Tomadoni, Mirna A. Mosiewicki, Mariana Pereda, Alejandra Ponce	30
110	ESTUDIO DE LA DEGRADACIÓN DE BOLSAS CON ADITIVO PRO-OXIDANTE IRRADIAS CON RADIACIÓN GAMMA MEDIANTE ESPECTROFOTOMETRÍA DE INFRARROJO Jenny Aguilar, Maribel Luna, Vladimir Valle, Miguel Aldás	31
111	ESTUDIO DE LA DEGRADACIÓN DE BOLSAS CON ADITIVO PRO-OXIDANTE IRRADIAS CON RADIACIÓN GAMMA MEDIANTE ESPECTROFOTOMETRÍA DE INFRARROJO Jenny Aguilar, Maribel Luna, Vladimir Valle, Miguel Aldás	32
161	STRESS TRANSFER QUANTIFICATION IN GELATIN-NANOFIBRILLATED CELLULOSE COMPOSITES BY RAMAN SPECTROSCOPY Franck Quero, Stephen J. Eichhorn, Javier Enrione	33
171	EXPLORATORY STUDIES ON POLI(3-HYDROXYBUTYRATE) SOIL DEGRADATION AND ASSESSMENT OF LOSS MASS RATE Matheus Marques Torres, Mariane Igansi Alves, Karine Laste Macagnam, Luciana Bicca Dode, Claire Tondo Vendruscolo, Angelita da Silveira Moreira, Yasser da Silveira Kruger, Patrícia Diaz de Oliveira	34
174	CALCIUM RELEASE EVALUATION DURING SILK FIBROIN DIALYSIS Luisa Storelli dos Reis, Mariana Agostini de Moraes, Pedro de Alcântara Pessôa Filho	35
190	FORMULACIÓN Y EVALUACIÓN DE UN HIDROGEL A BASE DE CARRAGENINA, COMO RECUBRIMIENTO DE FERTILIZANTES NPK DE LIBERACIÓN CONTROLADA Katherine Ávila Viatela, Angie Cifuentes Cetina	36
191	ADSORPTION CAPACITY OF METHYLENE BLUE BY XANTHAN BIOPOLYMER Anderson Correa, Yasser Krüger, Miguel Oliveira, Paula Klaic1, Angelita Moreira, Claire Vendruscolo, Patrícia Oliveira, Ligia Furlan	37
199	EVALUATION OF NATURAL RUBBER WITH FILLERS FROM PYROLYTIC CARBON BLACK POST INDUSTRIAL WASTE William Urrego Yepes, Leyla Yamile Jaramillo Zapata, Juan Carlos Posada Correa, Daniel Santiago Tobón	38



206	REINFORCEMENT OF RECYCLED HIGH DENSITY POLYETHYLENE WITH ALDER SAWDUST (ALNUS ACUMINATA) Katherine Méndez, Guillermo Jiménez	39
222	USE OF INDUSTRIAL WASTE IN ASPHALT MASSES Hélio Wiebeck Jorge Coelho, Antônio Lúcio Duarte Ferreira, Fábio José Esper, Janaina Aline Galvão Barros	40
229	THE INFLUENCE OF ALKALI CONCENTRATION, TEMPERATURE AND TIME ON HEMICELLOSES EXTRACTION FROM CURAUÁ FIBERS Mariana Roldi de Oliveira, Sandra Maria da Luz	41
269	EDIBLE FILM DEVELOPMENT ARRACACHA STARCH BASED Viviane de S. Silva, Renan Primo, Jose I. Velasco, Farayde M. Fakhouri, Rafael A. de Oliveira	42
271	WATERBORNE ACRYLIC/CASEIN LATEXES AND THEIR APPLICATION AS ECOFRIENDLY COATING Matías L. Picchio, Mario C.G. Passeggi (Jr.), María J. Barandiaran, Roque J. Minari, Luis M. Gugliotta	43
272	REMOCIÓN DE ÓXIDOS DE METALES MEDIANTE EL USO DE HIDROGELES BIODEGRADABLES Agustín Martínez-Ruvalcaba, Emilo Cruz-Barba, Juan Carlos Sánchez, Leticia Cázares, Syeni Agredano	44
279	HYDROGELS OF PEG/PVA: METRIBUZIN RESEARCH José Luis Gadea P., Fidel Benjamín Alarcón H., María del Carmen Fuentes A., Angeluz Olvera V.	45
302	ADSORPTION OF HRP ON AGAVE-FIBER/HDPE FOAMED COMPOSITES AND ITS POSSIBLE USE IN THE DEGRADATION OF A TEXTILE DYE Valeria Figueroa Velarde, Mayra García Sánchez, Luis Carlos Rosales Rivera, Pedro Ortega Gudiño, Orfil González Reynoso, Jorge Ramón Robledo Ortiz	46
325	CASTOR OIL POLYURETHANE/CELLULOSE DERIVATIVES AND POLYACRYLIC ACID Mario A. Gómez Jiménez ¹ , Rosa E. Zavala Arce, J.L. Rivera Armenta, Ana Ma. Mendoza Martínez, Nancy P. Díaz Zavala, Norma A. Rangel Vazquez	47
330	ADSORCIÓN DE TARTRACINA EN UN SISTEMA CONTINUO CON UN CRIOGEL Q-C-EDGE: EFECTO DE ALTURA DE LECHO Y FLUJO DE ALIMENTACIÓN A. García-Gonzalez, P. Ávila-Pérez, B. García-Gaitan, J. L. García-Rivas, J. Sánchez-Jaime, R. E. Zavala-Arce	48
336	CARROT PROCESSING WASTE AS RAW MATERIAL FOR EDIBLE FILM PRODUCTION Caio G Otoni, Marcos V Lorevice, Márcia R de Moura, Marcos D Ferreira, Luiz HC Mattoso	49
368	MICROBIOLOGICAL DETERIORATION OF POLYURETHANE/POLY(2-(DIETHYLAMINO)ETHYL METHACRYLATE) HYBRID MATERIALS Paula Faccia, Francisco Pardini, Claudio Gervasi, Javier Amalvy, María Teresa Del Panno	50
401	SYNTHESIS AND CHARACTERIZATION OF CHITOSAN CRYOGELS Anete Jessica Arcos-Arévalo, Rosa Elvira Zavala-Arce, Pedro Ávila-Pérez, Beatriz García-Gaitán, José Luis García-Rivas, María de la Luz Jiménez-Núñez	51



406	EFFECTO DE DOS TAMAÑOS DE PERLAS DE QUITOSANO-CELULOSA-ENTRECRUZADO CON ETILENGLICOL DIGLICIDIL ÉTER (Q-C-EDGE) EN LA ADSORCIÓN DE ROJO No. 2 Adriana Olivares Castro, Rosa Elvira Zavala-Arce, María de la Luz Jiménez Nuñez, Celso Hernández-Tenorio, Beatriz García-Gaitán, Mario Alejandro Gómez-Jiménez	52
409	BIODEGRADABLE POLYMERIC PLA/GO COMPOSITES WITH ENHANCED THERMO MECHANICAL PROPERTIES Mónica Elvira Mendoza Duarte, Iván Alziri Estrada Moreno, Daniel Lardizábal Gutiérrez, Sergio Gabriel Flores Gallardo, Erika Ivonne López Martínez, Alejandro Vega Ríos	53
416	EFFECT OF ACIDITY ON THE CATALYTIC ACTIVITY OF HZSM-5 ZEOLITES FOR ITS APPLICATION IN CHEMICAL RECYCLING OF POLYPROPYLENE PLASTIC WASTES Yuliana Franco, Eliana Higueta, Omar Gutiérrez	54
450	BIODEGRADATION UNDER COMPOSTING CONDITIONS OF PCL-BASED POLYURETHANES PRODUCED BY ENZYMATIC POLYMERIZATION Marina P. Arrieta, Karla A. Barrera-Rivera, Daniel Lopez, Antonio Martinez-Richa, Laura Peponi	55

3. Polymers for tissue engineering and biomaterials

10	DEVELOPMENT OF BIORESORBABLE ELECTROSPUN SMALL-DIAMETER VASCULAR GRAFTS Flores Montini-Ballarín, Pablo C. Caracciolo, Gustavo A. Abraham	56
29	ON THE FRICTION AND WEAR CHARACTERISTICS OF POLY(METHYLMETHACRYLATE)/ BIPHASIC CALCIUM PHOSPHATE COATINGS UNDER LUBRICATED CONDITION L. Daniel Aguilera, Karla J. Moreno, J. Santos García, Julio de Jesús Aguirre, Griselda Castruita de León, Héctor Iván Meléndez Ortiz	57
80	IMPROVED THERMAL PROPERTIES OF NEW CYANOACRYLATE POLYMERS CONTAINING 6-HYDROXYHEXYL ACRYLATE Gabriel Estan-Cerez, Diego A. Alonso, José Miguel Martín-Martínez	58
115	CASTOR OIL BASED POLYURETHANE / TITANIUM COMPOSITE FOAMS Fernando J. Aguilar-Perez, Rossana F. Vargas-Coronado, Juan V. Cauich-Rodríguez, Juan J. Pavon-Palacio, José A. Rodríguez-Ortiz, Yadir Torres-Hernández	59
120	POLYETHYLENE GLYCOL DIGLYCIDYL ETHER CROSSLINKED CHITOSAN AS BIOMATERIAL M. G. Chuc-Gamboa, J. A. Tec-Sánchez, R. Vargas-Coronado, J. V. Cauich-Rodríguez, J.M. Cervantes-Uc, M.P. Gutierrez-Amador	60
123	AN ALTERNATIVE FOR THE TREATMENT OF CHAGAS DISEASE: HYDROGELS FOR BENZNIDAZOLE CONTROLLED RELEASE Valeria S. Garcia, Verónica D. Gonzalez, Luis M. Gugliotta	61
127	POLYURETHANES BASED ON METFORMINE AND ATORVASTATIN FOR THE CONTROL OF METABOLIC SYNDROME Guido Zapata-Catzin, Marcos Bonilla-Hernández, Rossana Vargas-Coronado, Juan V. Cauich-Rodríguez, Stefania Zeppetelli, Assunta Borzacchiello	62



133	ANTIBACTERIAL GLASS IONOMER CEMENT MODIFIED WITH PROPOLIS Maldonado-Gallegos, D. Aguilar-Pérez, J. V. Cauich-Rodríguez, S. E. Hernández-Solis , F. Aguilar-Ayala	63
186	PLASMA POLYMERIZED E-CAPROLACTONE BIOFILMS Roberto Olayo-Valles, José Antonio Lopez-Barrera, Jesús Olayo-Lortia, Omar E. Uribe-Juárez, Ernesto J. Espinosa-Santamaría, Juan-Carlos Ruiz, Juan Morales-Corona	64
231	HYDROGEN PEROXIDE PLASMA TO INCREASING THE POLYANILINE ADHESION ON METALLIC SUBSTRATES FOR MEDICAL APPLICATION Lidia Ma. Gómez, Ma. Guadalupe Olayo, Maribel González-Torres, Francisco González-Salgado, Rafael Basurto, Elena Colín, J. Cuauhtémoc Palacios, Guillermo J. Cruz	65
259	HEPARIN ABSORPTION IN POROUS PPy/I AND ITS RELEASE IN KR SOLUTIONS Maribel González-Torres, Guillermo J. Cruz Cruz, Lidia Ma. Gómez Jiménez, Francisco González Salgado, Rosario Ramírez Segundo, Fernando G. Flores Nava, Rafael Basurto Sánchez, Ma. Guadalupe Olayo González	66
264	CROSSLINKED ELECTROSPINNED FIBERS AND PARTICLES OF PLASMA POLYANILINE Rosario Ramírez, Guillermo J. Cruz, Ma. de los Ángeles Enríquez, Jaime Rosales, Fernando G. Flores, Maribel González-Torres, Lidia Ma. Gómez, Francisco González-Salgado, Juan Morales, Ma. Guadalupe Olayo	67
268	STRUCTURE OF PYRROLE-ALLYLAMINE PLASMA COPOLYMER FILMS Ma. Guadalupe Olayo, E. Jocelyn Alvarado, Maribel González-Torres, Lidia Ma. Gómez, Francisco González-Salgado, Rosario Ramírez-Segundo, Fernando G. Flores-Nava, Guillermo J. Cruz	68
333	KGM/CHI ASYMMETRIC MEMBRANES AS WOUND DRESSING Giovana Genevro, Carla França, Mariana de Moraes, Marisa Beppu	69
373	CHEMICAL STRUCTURES OF BIOCOMPATIBLE PLASMA POLYALLYLAMINE Guillermo J. Cruz, E. Jocelyn Alvarado, Lidia Ma. Gómez, Maribel González- Torres, Francisco González-Salgado, Rosario Ramírez-Segundo, Fernando G. Flores-Nava, Rafael Basurto, Ma. Guadalupe Olayo	70
414	EFFECTO DE LAS TÉCNICAS PARA ELABORACIÓN DE MEMBRANAS EN LAS PROPIEDADES ELÉCTRICAS DE UN POLÍMERO DE CONDUCCIÓN IÓNICA PARA INGENIERÍA DE TEJIDOS Estefanía Correa Muñoz ¹ , María Moncada Acevedo, Víctor Zapata Sanchez	71
427	COMPOSITE OF ZNO NANOPARTICLES AND FISH BONE HYDROXYAPATITE: SYNTHESIS AND CHARACTERIZATION Víctor M. Ovando-Medina, Miguel A. Corona-Rivera, Karla D. Estrada- Martínez, Hugo Martínez-Gutiérrez, Lorena Farías-Cepeda, Nancy E. Dávila- Guzmán	72



4. Stimuli-responsive polymers for medicine

18	EFFICIENT CONDENSATION OF DNA INTO ENVIRONMENT-RESPONSIVE POLYPLEXES PRODUCED FROM A NOVEL BLOCK CATIONIC POLYMER CARRYING TWO AMINE GROUPS	73
	Lindomar Albuquerque, Eliézer Jäger, Petr Stepánek, Vanessa Schmidt, Cristiano Giacomelli, Fernando Carlos Giacomelli	
22	pH AND THERMAL RESPONSIVE HYBRIDS PREPARED FROM ISOPHORONE DIISOCYANATE-BASED POLYURETHANE AND 2-(DIISOPROPYLAMINO) ETHYLMETHACRYLATE	74
	Francisco M. Pardini, Oscar R. Pardini, Paula A. Faccia, Javier I. Amalvy	
84	SCALING-UP OF PDEAEM (CORE) – PEGMA (SHELL) NANOGEL SYNTHESIS	75
	Iván Zapata-González, Angel Licea-Claverie, Edgar Medina-Monroy	
94	THERMORESPONSIVE SYSTEMS FOR DRUG DELIVERY BASED ON XANTHAN AND GELLAN DERIVATIVES	76
	Jacques Desbrieres, Mihaela Hamcerencu, Marcel Popa, Gerard Riess	
361	POLYACRYLAMIDE-BASED RESPONSIVE NANOCOMPOSITE HYDROGELS ADDED BY MAGNETITE NANOPARTICLES AND MONTMORILLONITE CLAY	77
	Adriel Bortolin, Fauze A. Aouada, Luiz H. C. Mattoso, C. Ribeiro	

5. Polymer composites and nanocomposites

16	MAGNETIC FILMS BASED ON BIO-POLYMERS AND NANOMAGNETITE	78
	Gianina A. Kloster, Diego Muraca, Mirna A. Mosiewicki, Norma E. Marcovich	
79	FLAME RETARDANCY AND THERMAL STABILITY BEHAVIOR OF LDPE / EVA / CLAY / METAL HYDROXIDES NANOCOMPOSITES	79
	Eduardo Ramírez, Saúl Sánchez, Mario Valera	
95	CLAY DISTRIBUTION BETWEEN PHASES IN HETEROGENEOUS BLENDS POLYSTYRENE/POLYVINYL CHLORIDE	80
	Helen Inciarte, Angel Ysea1, Haydée Oliva, David Echeverri, Luis Rios	
119	IN-SITU SYNTHESIS AND CHARACTERIZATION OF P3HT-FeO COMPOSITES	81
	Marcos Fuentes Perez, María E. Nicho Diaz, Mérida Sotelo Lerma, Patricia E. Altuzar Coello3, Jesús Castellon Uribe, Giovanni S. Jiménez Bahena	
166	FOTO-DEGRADACIÓN DE NANOCOMPUESTOS DE POLIPROPILENO Y MONTMORILLONITA	82
	Julie Merchan-Sandoval, Roberto Chávez, Lidia Quinzani, Marcelo Failla	
169	SÍNTESIS Y CARACTERIZACIÓN DE NANOCOMPUESTOS DE POLIPROPILENO RAMIFICADO Y MONTMORILLONITA	83
	Aníbal Ferrofino, Facundo Ramos, Lidia Quinzani, Marcelo Failla	
176	ESR AND OTHERS TECHNIQUES IN THE CHARACTERIZATION OF RECYCLED POLYAMIDE WITH MAGNETITE (Fe ₃ O ₄) NANOPARTICLES	84
	Lucas Gabriel dos Santos, Mariana Fontana, Daniel Farinha Valezi, Jonathan Baumí, Carmen Luísa Barbosa Guedes, Alexandre Urbano, Eduardo Di Mauro	
197	STUDY OF COMPOSITES CURED BY MICROWAVES IRRADIATION USING DMA	85
	Daniel Kersting , Hélio Wiebeck , Fábio Esper	



233	A ZOOM INTO THE STRUCTURE OF PYRROLE AND TITANIUM OXIDE HYBRID COMPOUNDS F. González-Salgado, M.G. Olayo, G. García-Rosales, M. González-Torres, L.M. Gómez, R. Basurto, E. Colín, J. C. Palacios, G.J. Cruz	86
274	FLEXURAL BEHAVIOR OF TIMBER STRUCTURES REINFORCED BY POLYMERIC COMPOSITE Andressa Cecília Milanese, Maria Odila Hilário Cioffi	87
275	PRODUCCION DE LATEX ACRILICO / MELAMINICO CON ALTO CONTENIDO DE SOLIDOS PARA SU APLICACIÓN COMO PELICULA CURABLE A ALTA TEMPERATURA Carlos Córdoba, Luis Gugliotta, Roque Minari	88
278	DEGRADATION OF PLA-NATURAL FIBER COMPOSITES UNDER CONTROLLED COMPOSTING CONDITIONS AND ITS EFFECT ON TENSILE PROPERTIES Erick Omar Cisneros-López, Aida Alejandra Pérez-Fonseca, Yolanda González-García, Carlos Federico Jasso-Gastinel, Daniel Edén Ramírez-Areola, Jorge Ramón Robledo-Ortíz	89
281	EFFECT OF AGAVE FIBER SURFACE TREATMENT ON THE TENSILE PROPERTIES OF POLYETHYLENE COMPOSITES PRODUCED BY COMPRESSION MOLDING Erick Omar Cisneros-López, Martíz Estaban Gonzalez-López, Aida Alejandra Pérez-Fonseca, Rubén González-Núñez, Denis Rodrigue, Jorge Ramón Robledo-Ortíz	90
285	INFLUENCE OF NANOCCLAYS ON THE THERMAL AND MECHANICAL PROPERTIES OF POLYLACTIC ACID Alan Salvador Martín del Campo-Flores, Jorge Ramón Robledo-Ortiz, Rubén González-Nuñez, Martín Arellano-Martinez, Aida Alejandra Pérez-Fonseca	91
294	SYNTHESIS AND CHARACTERIZATION OF PVDF/PMMA COMPOSITES J.R. Leppe, M.E. Nicho, F.Z. Sierra, F.F. Hernández, M. Fuentes, G. Alvarado-Tenorio	92
315	ARTIFICIAL WEATHERING OF POLYETHYLENE NANOCOMPOSITES WITHE CARBON NANOPARTICLES FOR OUTDOOR APPLICATION IN SOLAR WATER HEATERS J. Martínez-Colunga, J. Valdéz-Garza, J. Mata-Padilla, V. Cruz-Delgado, C. Ávila-Orta	93
321	INFLUENCE OF CLAYS AND ORGANIC FILLERS ON THE VULCANIZATION CHARACTERISTICS AND MECHANICAL PROPERTIES IN NATURAL RUBBER-ORGANOCLAY NANOCOMPOSITES Marcos G. Fernandes, Christiano G. B. Andrade, Fabio J. Esper, Francisco R. V. Diaz, Hélio Wiebeck	94
367	INCREASED OF ANTIOXIDANT ACTIVITY OF ERIOCITRIN, A CITRIC FLAVONOID, IMMOBILIZED ONTO POLYURETHANE-HEMA/HDTMA-MMT OBTAINED BY PHOTOPOLYMERIZATION Noelia Bertorello, Hugo Destéfanis, Javier Amalvy	95
385	MICROSTRUCTURAL, THERMAL AND MECHANICAL PROPERTIES OF GRAFTED POLYPROPYLENE COMPOSITES WITH ACETYLATED WHEAT STRAW FIBERS Vladimir Fernández, Santiago Duarte, Ramón Sánchez, Jacobo Aguilar, Francisco Moscoso and Gonzalo Canché	96
400	SEMICONTINUOUS EMULSION POLYMERIZATION OF n-BUTYL ACRYLATE IN PRESENCE OF GRAPHENE OXIDE Victoria Padilla, Raquel Ledezma, Esther Treviño	97



410	SYNTHESIS AND DYNAMICAL MECHANICAL CHARACTERIZATION OF POLYURETHANE MATRIX COMPOSITES REINFORCED WITH KERATIN MATERIALS Vicente Amaya Amaya, Ana Laura Martínez Hernández, Miguel de Icaza Herrera, Carlos Velasco Santos	98
412	KERATIN, RENEWABLE MATERIAL IN POLYMER COMPOSITES: NATURAL AND SYNTHETIC MATRICES Martínez-Hernández A.L.1,* , Flores-Hernández C.G.1, Jiménez-Cervantes-A. E.1, Saucedo-Rivalcoba V.1, Rivera-Armenta J.L.2, Velasco-Santos C1	99
415	DEVELOPMENT OF COMPOSITES BASED ON GREEN POLYMERS: POLYLACTIC ACID MATRIX REINFORCED WITH KERATIN, BY THREE DIMENSION PRINTING. Ana L. Hernández-Zea, Ana L. Martinez-Hernández, Cynthia G. Flores-Hernández, Armando Almendarez-Camarillo, Carlos Velasco-Santos	100
421	THERMAL, MECHANICAL AND MORPHOLOGICAL CHARACTERIZATION OF POLYETHYLENE/CARBON FIBER COMPOSITES PREPARED BY THERMOCOMPRESSION Zenen Zepeda Rodríguez, Rubén González Núñez, Gustavo Castellanos López1, Milton Vázquez Lepe	101
449	MULTIFUNCTIONAL BIONANOCOMPOSITES WITH SHAPE MEMORY EFFECT Laura Peponi, Valentina Sessini, Marina P. Arrieta, Daniel López	102

6. Polymer engineering, processing and rheology

28	SÍNTESIS Y CARACTERIZACIÓN DE POLIURETANOS ALIFÁTICOS FOTO-ENTRECRUZABLES BASADOS EN POLICAPROLACTONA Ángel Marcos-Fernández, Rubén Seoane Rivero, Koldo Gondra, Pilar Bilbao	103
85	KINETIC STUDY AND MATHEMATICAL MODELING IN ATRP Iván Zapata-González, Enrique Saldívar-Guerra, Robin A. Hutchinson	104
129	FREE-RADICAL POLYMERIZATION IN A MULTIZONE AUTOCLAVE REACTOR Ramiro Infante Martínez, Enrique Saldívar Guerra, Luis Villarreal Cárdenas	105
131	DETERMINATION OF MOLECULAR WEIGHT DISTRIBUTIONS OF DIFFERENT TYPES OF POLYETHYLENE FROM A SIMPLE REPTATION MODEL Miguel A. Fernández Estrada, Javier Gudiño Rivera, Rubén Saldívar Guerrero, Rubén H. López Bañuelos	106
143	ENZYMATIC HYDROLYSIS OF THE GALACTOMANNAN FROM DELONIX REGIA SEED EFFECT ON SOLUBILITY AND VISCOSITY Wilbert Rodríguez Canto, Manuel Aguilar Vega, Luis Chel Guerrero	107
203	SYNTHESIS OF POLY(BUTHYL METHACRYLATE) NANOPARTICLES IN NANOEMULSIONS PREPARED BY PHASE INVERSION TEMPERATURE TECHNIQUE Arturo Gómez, A Flores, Lourdes A. Pérez Carrillo, Martín Rabelero, Rosaura Hernández, Abraham G. Alvarado	108
286	ASSOCIATION OF CHEMICAL MODIFICATIONS IN XANTHAN PRUNI Paula Michele Abentroht Klaić, Yasser da Siveira Krüger, Claire Tondo Vendruscolo, Ligia Furlan, Patrícia Diaz Oliveira, Angelita da Silveira Moreira	109
290	CONTROLLED ACRYLIC ACID POLYMERIZATION BY COMBINING REDOX INITIATION AND CHAIN TRANSFER Gerardo Cáceres Montenegro, Carolina G. Gutierrez, Roque J. Minari, Jorge R. Vega, Luis M. Gugliotta	110
316	ROBUST STATE ESTIMATION OF POLYMERIZATION PROCESSES Jhovany Tupaz, Mariano Asteasuain, Mabel Sánchez	111



324	FORCING RADICAL COPOLYMERIZATION REACTIONS TO DESIGN THE PROPERTIES OF MULTICOMPONENT POLYMER SYSTEMS C.F. Jasso-Gastinel, A.H. Arnez-Prado, F.J. Rivera-Gálvez, L.O. Sahagún-Aguilar, F.J. Aranda-García, M.A. López-Manchado, M.E. Hernández-Hernández, L.J. González-Ortiz	112
352	MATHEMATICAL MODEL FOR THE SYNTHESIS OF THERMOSETTING POLYMERS BASED ON EPOXY RESINS Emilio Berkenwald, Marisa Spontón, Verónica Nicolau, Diana Estenoz	113
375	SENSITIVITY ANALYSIS FOR A SYSTEM OF TERPOLYMERIZATION Oscar Meza Díaz, Juan Carlos Tapia Picazo	114
387	COMPARISON OF RHEOLOGICAL PROPERTIES AND IZOD IMPACT RESISTANCE OF PPE/HIPS/SBS BLENDS AND ABS Erika I. López Martínez, Juan A. Arteaga-Bustillos, Mónica E. Mendoza-Duarte, Alejandro Vega-Ríos, Claudia A. Hernández-Escobar, Sergio G. Flores-Gallardo	115
388	EFFECT THE DEPOLYMERIZATION OF THERMOPLASTIC STARCH (TPS) FILMS OBTAINED BY EXTRUSION TWIN SCREW Mayela Casas, Francisco Rodríguez, Gustavo Soria, Juan Contreras	116
422	PROCESSING AND CHARACTERIZATION OF POLYETHYLENE TEREPHTHALATE AND HIGH DENSITY POLYETHYLENE COMPOSITES WITH AGAVE FIBERS Erendira E. Covarrubias Flores, Rubén González Núñez, Milton O. Vázquez Lepe	117
437	ANÁLISIS DE UN SISTEMA DE OBTENCIÓN DE FIBRA DE CARBÓN DE BAJA PUREZA Daniel Alcalá Sánchez, Juan Carlos Tapia Picazo	118

7. Polymeric membranes and their applications

51	MIXED MATRIX MEMBRANES BASED ON POLYSULFONE AND MODIFIED CLINOPTILOLITE ZEOLITE: STUDY OF THERMAL AND GAS PERMEATION PROPERTIES Gema C. Hernández Silva, Griselda Castruita de León, Sandra P. García Rodríguez, H. Iván Meléndez Ortiz	119
60	CONDUCTIVE MEMBRANES BASED ON COMPOSITE POLYMERS FOR ENERGY APPLICATIONS Vicente Compañ Moreno	120
134	GAS SEPARATION PROPERTIES OF UNSUPPORTED CMC MEMBRANES FROM BLENDS OF HIGH TEMPERATURE RIGID AROMATIC POLYMERS José Manuel Pérez Francisco, José Luis Santiago García, María Isabel Loría Bastarrachea, Manuel Aguilar Vega	121
139	BIODIESEL PRODUCTION FROM SOYBEAN OIL BY CROSSLINKED PVA/PAMPS BLENDS CATALYTIC MEMBRANES Maria Ortencia González-Díaz, Zazil Corzo-González, Maria I. Loria-Bastarrachea, Manuel Aguilar-Vega	122
167	SYNTHESIS OF NEW CROSSLINKED FLUORINE-CONTAINING POLYNORBORNENE DICARBOXIMIDE Ivette Aranda-Suárez, Arlette A. Santiago, Mercedes Gabriela Téllez Arias, Joel Vargas	123



194	ANTIFOULING ASYMMETRIC MEMBRANES: EFFECT OF COAGULATION BATH IN S-PPS FORMATION AND PROPERTIES Marcial Yam, José Santiago ¹ , María Loría, Santiago Duarte, Francisco Ruiz, Manuel Aguilar	124
311	EFFECT OF ADDING FERROUS SOLUTIONS ON CHEMICAL AND THERMAL STABILITY OF CHITOSAN MEMBRANES Juan Carlos Castro Alcántara, Mariana Cerda Zorrilla, José Antonio Azamar Barrios	125

8. Modern synthetic methods of polymers

11	ADMET POLYMERIZATION USING GREEN CHEMISTRY Taylor W. Gaines, Kathryn R. Williams, Kenneth B. Wagener, Giovanni Rojas	126
32	SYNTHESIS AND CHARACTERIZATION OF SILICON-CONTAINING AROMATIC POLY(AZOMETHINE)S. A STUDY OF MOLECULAR FLEXIBILITY Claudio A. Terraza, Luis H. Tagle, Rene A. Hauyon, Patricio A. Sobarzo, Pablo A. Ortiz, Alain Tundidor-Camba, Carmen M. González-Henríquez	127
65	A ROUTE TO PRECISE SUPRAMACROMOLECULAR CONSTRUCTS: QUANTITATIVE MOLECULAR FISSION AND FUSION George R. Newkome	128
71	PHOTOCURING KINETICS OF A TERNARY ACRYLATE-THIOL-OXETANE SYSTEM Ricardo Acosta Ortiz, Darío Trujillo Arriaga, Omar Acosta Berlanga, Aida Esmeralda García Valdéz	129
73	ETHYLENE POLYMERIZATION WITH MONOMETALIC ZIRCONOCENE HYDRIDE CATALYSTS María Teresa Córdova, Maricela García, Odilia Pérez	130
228	Síntesis y caracterización de polimetacrilato de 4-(2-tiofenil) bencilo Felipe Gallardo, Juan Pablo Soto, Juliet Aristizabal, Juan Carlos Ahumada, Cindy Escalona, Víctor Rojas	131
357	CONTROLLED SYNTHESIS OF α,ω -TELECHELIC PDMS M. Soledad Lencina, Vivina Hanazumi, Leonardo Redondo, Camila Müller, Daniel Vega, Mario Ninago, Andrés Ciolino, Marcelo Villar	132

9. Modern Methods of Analysis and Characterization of Polymers and Theoretical studies

14	ANALYSIS OF LOW MOLECULAR WEIGHT POLYMERS USING LATEST ADVANCED MULTI-DETECTOR GPC SYSTEMS Mark R. Pothecar ¹ , Edna Alvarez	133
66	NaNANOSTRUCTURING AND SURFACE FUNCTIONALIZATION OF POLYMERS BY GASEOUS PLASMA TREATMENT FOR BIOMEDICAL APPLICATIONS Alenka Vesel, Ita Junkar, Karin Stana Kleinschek, Miran Mozetič	134
122	PARTICLE SIZE DISTRIBUTION BY CAPILLARY HYDRODYNAMIC FRACTIONATION: A NEW APPROACH BASED ON MULTI-WAVELENGTH UV DETECTION Luis A. Clementi, Miren Aguirre, José R. Leiza, Luis M. Gugliotta, Jorge R. Vega	135
124	ON-LINE MONITORING OF THE SYNTHESIS OF N,N-DIMETHYLACRYLAMIDE HYDROGELS BY UV-SPECTROMETRY Valeria, S. Garcia ¹ , Luis A. Clementi ^{1,2} , Carolina G. Gutierrez ¹ , Luciana Vera-Candioti ³ , Veronica V.G. Gonzalez, Luis M. Gugliotta	136



132	THERMAL BEHAVIOR AND MORPHOLOGICAL CHARACTERIZATION OF LDPE/LLDPE AND LDPE/MLLDPE BINARY BLENDS Dinorah I. Rodríguez Otamendi, Javier Gudiño Rivera, Rubén Saldívar Guerrero	137
146	EXPERIMENTAL AND NUMERICAL STUDY OF ETHANOL DIFFUSION IN POLYOXYMETHYLENE INJECTION-MOLDED PARTS Diana Amaya, Jorge Medina, Camilo Cruz	138
292	ESR SPECTROSCOPY IN THE IDENTIFICATION OF FREE RADICALS GENERATED BY DIFFERENT CURING MODES IN A DENTAL RESIN CEMENT Bruno Luiz Santana Vicentin, Eduardo Di Mauro	139
310	MICRO-RAMAN ANALYSIS OF THE ALPHA RADIATION EFFECT ON THE POLY ALLYL DIGLYCOL CARBONATE. Mariana Cerda Zorrilla, Juan Carlos Castro Alcántara, José Antonio Azamar Barrios, Guillermo C. Espinosa García	140
418	INESTABILIDADES ELÁSTICAS DE FILMS METÁLICOS SOBRE SUSTRATOS POLIMÉRICOS Diana C. Agudelo, Daniel A. Vega, Marcelo A. Villar	141
441	MICRO AND NANO MOLECULARLY IMPRINTED POLYMERS (MIPs) FOR TO PRECONCENTRATED ORGANIC TARGET MOLECULES AND FOR TO BE USED AS RECEPTORS IN ELISA TEST Eduardo Pereira, César Cáceres, Yadiris García, Ewa Moczko, Bernabé L. Rivas, Sergey A. Piletsky	142

10. General topics on Polymers

86	CONDUCTIVIDAD IONICA EN POLÍMEROS COMPOSITOS CONTENIENDO SALES DE LITIO BASADOS EN LÍQUIDOS IÓNICOS SOPORTADOS Abel Garcia-Bernabé, Eduardo García-Verdugo, Santiago V. Luis, Vicente Compañ	143
117	BLEACHING ON PLASTICIZED PVC FORMULATIONS EXPOSED TO NATURAL WEATHERING González-Falcón Elizabeth, Sánchez-Peña M. Judith, Arellano Martín, González-Ortiz Luis J.	144
184	THE EFFECT OF ADDITION OF VEGETABLE OIL IN THE HYDROPHOBIC BEHAVIOR OF WATERBORNE POLYURETHANE Gabriela Miranda, Wesley Monteiro, Cláudia dos Santos, Rosane Ligabue	145
242	PREPARATION AND CHARACTERIZATION OF POLYMER POLOXAMER P-407 FUNCTIONALIZED WITH ESTERS DERIVED OF CITRIC ACID José Eduardo Hernández Torres, Ernesto Rivera Becerril, Gerardo Pérez Hernández	146
253	MODIFICATION OF THE DEGREE OF CRYSTALLINITY OF POLY-(R)3-HYDROXYBUTYRATE POWDER BY MEANS OF PLASMA TREATMENT Samuel V.O. da Silva, Tobias Hartmann, Renata A. Simão, Lothar Kroll	147
303	EFFECT OF PLASMA TREATMENT ON HYDROPHOBICITY OF PAPER Jennifer Flórez Cristancho, Renata Antoun Simão	148
309	PLASMA SPUTTERING OF Cu ON POLYETHYLENE M. R. Mejía-Cuero, E. Colín-Orozco, M. G. Olayo-González, G. J. Cruz-Cruz, R. Valdivia-Barrientos, J. C. Palacios-González, I. Martínez-Cienfuegos	149



440	PREPARATION OF GRAPHENE OXIDE BY HUMMERS METHOD WITH A NEW EXFOLIATION TECHNIQUE	150
	Luis A. Macclesh del pino Perez, Tomas Lozano, Ana Beatriz Morales Cepeda, Luisiana Morales-Zamudio	
444	FORMACIÓN INICIAL DE LA CADENA DE POLYINDOFENOL USANDO PERÓXIDO DE HIDRÓGENO (H ₂ O ₂) PARA OXIDAR PARAFENILENDIAMINA (C ₆ H ₈ N ₂)	151
	Rosaura Vanessa Albino-Andrade, Juan Horacio Pacheco-Sánchez	
451	BIODEGRADABLE POLYURETHANES BASED ON PCL AND COUMARIN WITH PHOTOREVERSIBLE BEHAVIOUR	152
	Castor Salgado, Marina P. Arrieta, Marta Fernández-García, Laura Peponi, Daniel	



COLLAGEN/PVA/SC ELECTROSPUN SCAFFOLD FOR 3D CELL CULTURE

Luis H. Delgado Rangel ¹, Julia Hernández Vargas ¹, J. Betzabe González Campos ^{1*}, Zaira Y. García Carvajal ², Judit Aviña Verduzco ¹ and José María Ponce-Ortega ^{1#}

1. Instituto de Investigaciones Químico Biológicas, # Posgrado en Ingeniería Química, Universidad Michoacana de San Nicolás de Hidalgo, Ciudad Universitaria, 58030, Morelia Mich., México. betzabe.gonzalez@yahoo.com.mx
2. Centro de Investigación y Asistencia en Tecnología y Diseño del Estado de Jalisco, Av. Normalistas NO. 800, Col Colinas de la Normal, 44270, Guadalajara Jal., México.

Introduction

Tissue engineering involves the fabrication of three-dimensional scaffolds to support cellular growth and proliferation. The goal: generation of 'neotissues' that the body can adapt to carry out a physiological function¹. One of the most common techniques for obtaining 3D composite biomaterials with suitable architecture to this end is the electrospinning process, which promotes the formation of nanometric fibers with suitable porosity, providing a high surface-volume ratio and a three-dimensional arrangement that resembles cell growth and proliferation in natural conditions.

Research has been focused on the development of biomaterials capable of imitating the complex fibrillar architecture. Collagen based biomaterials have been used for the production of scaffolds, exploring different combinations with other biopolymers in order to improve tissue function and their mechanical, physical and chemical properties².

Experimental Part

3-D collagen based composite scaffolds were produced by electrospinning technique, using different combinations and concentrations of collagen, chondroitin sulfate, hyaluronic acid and poly (vinyl alcohol). Electrospinning parameters such as flow rate, needle-collector distance and voltage were determined for all mixtures and conditions. The characterization of the electrospun composites was carried out by FTIR and FESEM analysis.

Results and Discussions

Of all combinations, the best nanofibers with the fewest beads were obtained from a mixture made from 25% collagen (3.2% w/v in 1,1,1,3,3,3-hexafluoro-2-propanol), 37.5% of poly (vinyl alcohol) (PVA) (8% w/v in water) and 37.5% of chondroitin sulfate (CS) (2.5% w/v in water). The electrospinning was performed at 25 ° C, 20 kV, 1 mL/hr and 12 cm needle-collector distance using a collector plate.

Figures 1 and 2 show FESEM and FTIR results respectively, nanofibers structure and FTIR interactions between polymers are highlighted. It is important to note that the addition of SC to collagen/PVA mixture highly improves solution electrospinnability and it also can enhance cell attachment. Macroscopically, this nanofiber mat is amenable to handling macroscopically. IR analysis suggest ether formation because of interactions between OH-groups of PVA and C=O groups of collagen.

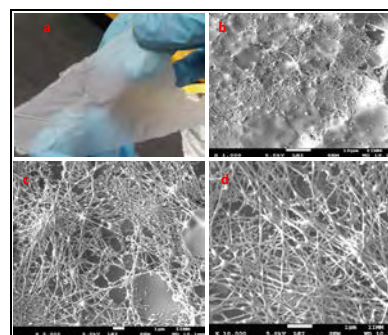


Figure 1. SEM images at different scales of the collagen-PVA-SC fiber.

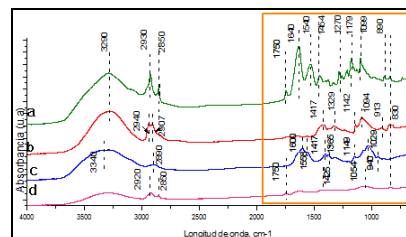


Figure 2. IR spectrum for pure collagen (a), pure PVA (b), pure CS (c) and the compound collagen-PVA-CS (d).

Conclusions

It was possible to obtain nanofibers from polymers commonly used for application as cellular scaffolds; the best results of the tested combinations and concentrations were obtained by using 25% of collagen, 37.5% of PVA and 37.5% of SC. The addition of SC, however, the electrospinnability of solutions is a strong limitation to overcome. It is necessary to improve the conditions of electrospinning process to obtain higher quality nanofibers.

Acknowledgment: CONACyT for financial support to 150767, 261425 and 234073 projects.

References

1. J. Lannitti, D. Reneker, T. Ma, D. Tomasko, D. Farson, *Material Science and Engineering C* 2007, 27, 504.
2. Jamil A. Matthews, Gary E. Wnek, David G. Simpson, Gary L. Bowlin, *Biomacromolecules* 2002, 3, 232.

TEMPLATING DOUBLE AND TRIPLE CRYSTALLINE MORPHOLOGIES IN BIODEGRADABLE COPOLYMERS AND TERPOLYMERS

Alejandro J. Müller^{1,2}

1. *POLYMAT and Polymer Science and Technology Department, Faculty of Chemistry, University of the Basque Country UPV/EHU, Donostia-San Sebastián, Spain (alejandrojesus.muller@ehu.es).*
2. *IKERBASQUE, Basque Foundation for Science, Bilbao, Spain*

Multiple crystalline diblock and triblock copolymers and terpolymers are fascinating multiphasic materials. When they are miscible or weakly segregated in the melt, the crystallization event drives the structure formation and overwrites any previous melt microdomain structure. The first block to crystallize can therefore create a superstructural “template”, within which the other components must self-assemble.^{1,2,3}

In this work double crystalline and triple crystalline diblock and triblock copolymers and terpolymers based on biodegradable or biocompatible building blocks are studied. Amongst the materials studied, two terpolymers with identical PEO and PCL block lengths and two different PLLA block lengths were analysed. The triple crystalline nature of these terpolymers was confirmed by Wide Angle X-Ray scattering (WAXS). The different blocks crystallize in sequence: the PLLA block crystallizes first, then the PCL block, and finally the PEO block.

The crystallization process takes place from a homogenous melt as indicated by Small Angle X-Ray Scattering (SAXS) experiments. As PLLA content in the terpolymer increases, the crystallization and melting enthalpies and temperatures of both PEO and PCL blocks decrease. Polarized light optical microscopy (PLOM) observations performed as a function of temperature, demonstrated that the PLLA block templates the morphology of the terpolymer, as it forms spherulites upon cooling from the melt. The PCL and PEO blocks crystallized upon cooling inside the interlamellar regions of the previously formed PLLA block spherulites. Therefore, unique triple crystalline mixed spherulitic superstructures can be formed.

Figure 1 shows the development of the superstructural morphology as one triblock terpolymer is cooled from the melt. Subscripts indicate composition in wt% and superscript the number average molecular weight of the entire PEO₂₃PCL₃₄PLLA₄₃^{19.9} triblock terpolymer. The first exotherm observed upon cooling from the melt (between 70 and 80 °C) corresponds to the crystallization of the PLLA block. As this block crystallizes, spherulites that contain PLLA lamellae separated by PLLA, PCL and PEO mixed amorphous chains within interlamellar regions are formed. Such spherulites constitute a template within which, in a sequential fashion, the PCL block and then the PEO block are forced to crystallize upon cooling. Hence, when the second block crystallizes (i.e., the PCL block, see exotherm just below 40 °C), double crystalline spherulites are formed. Upon

further cooling, the third block crystallizes (i.e., the PEO block, see exotherm at approximately 20 °C) and unique triple crystalline spherulites are finally formed.³

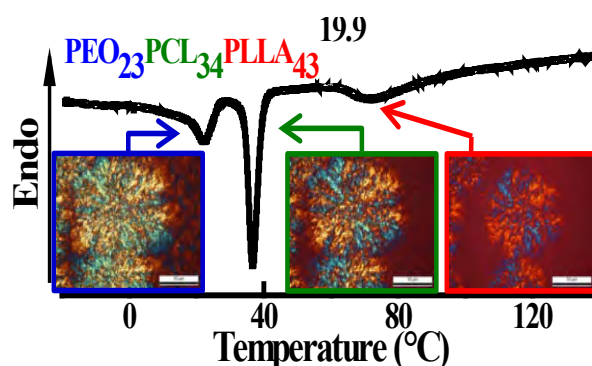


Figure 1. DSC cooling scan for the PEO₂₃PCL₃₄PLLA₄₃^{19.9} triblock terpolymer and corresponding superstructural morphologies.

WAXS studies were also performed to assign the corresponding block crystallization during cooling.³ Spherulites transform from single crystalline (i.e., containing only PLLA lamellae) to double crystalline (i.e., containing PLLA and PCL lamellae) and finally to triple crystalline (all three blocks crystallize) entities upon cooling from the melt.

References

1. Michell, R. M.; Müller, A. J. *Prog. Polym. Sci.*, **2016**, 54-55, 183.
2. Castillo, R. V.; Müller, A. J. *Prog. Polym. Sci.*, **2009**, 34, 516.
3. Zhao J.; Pahovnik D.; Gnanou Y.; Hadjichristidis N. *Polym. Chem.*, **2014**, 5, 3750.
3. Palacios, J. K.; Mugica, Agurtzane; Zubitur, M.; Iturrospe, A.; Arbe, A.; Guoming, L.; Wang, D.; Zhao, J.; Hadjichristidis, N.; Müller, A. J. *RSC Advances*, **2016**, 6, 4739.

PICKERING SILICA-BASED STYRENE EMULSION POLYMERIZATION KINETICS: UNTANGLING MECHANISMS

Benoit Fouconnier¹, Francisco López-Serrano^{2*}

1. Facultad de Ciencias Químicas, Universidad Veracruzana, Av. Universidad Km 7.5, Col. Santa Isabel, Coatzacoalcos, Veracruz, C. P. 96535, MÉXICO. broger@uv.mx
2. Departamento de Ingeniería Química, Facultad de Química, Universidad Nacional Autónoma de México. Ciudad Universitaria, Cd. Mx., 04510, MÉXICO. lopezserrano@unam.mx

Introduction

Recent developments of fabrication routes for nanocomposite materials have promoted the use of finely divided solids as stabilizers instead of surfactants.¹ Solid nanoparticles act as emulsifiers and stabilize droplets due to their adsorption at the water-oil interface. These surfactant-free dispersed systems are the so-called Pickering emulsions, which differ from conventional emulsions due to their high stability against coalescence.² For these reasons, Pickering emulsions are used for the synthesis of core-shell nanocomposite particles. Their preparation is simple, sophisticated instrumentation is not required, commercial solid dispersions or solutions can be used without further treatments, and the produced latex is surfactant-free.³ Due to the importance of this process, a step towards the understanding of some mechanistic events is taken in this work.

Experimental Part

The poly(styrene) particles were synthesized in a batch reactor at 80°C, using a styrene (St) in water emulsion (with a dispersed phase mass fraction of 0.15) stabilized by a SiO₂ (Bindzil 830) nanoparticles (SnP) and hexadecyltrimethylammonium bromide (CTAB) mixture, with 2.1 wt% SnP, relative to water, and a [CTAB]/[SiO₂] ratio of 0.013. A three-bladed metal overhead turbine stirrer at 250 rpm was used. The reactor was purged with nitrogen during 15 min. The reactions were initiated using three (0.5, 1 and 2 wt% relative to St) ammonium persulfate (APS) concentrations. Conversion was determined by gravimetry and particle size by dynamic light scattering (Zetasizer Nano-ZS2000).

Results and Discussions

Figure 1 shows the time-conversion evolutions. As expected, the higher the APS concentration the faster the reaction rate. When no surface modification is performed (open circles), for the same amount of APS (1 %), a lower reaction rate is achieved. The polymerization process is better controlled when the SnP are surface modified. Two nucleation rate periods exist (not shown) and particle nucleation occurs along the reaction. The modified SiO₂ nanoparticles participate in the growing polymer particles nucleation and stabilization mechanisms, providing affinity with silica nanoparticles due the presence of CTAB tails onto the silica particles. Therefore, leading to the formation of smaller particles, in comparison with the bare SiO₂ experiments. The inset in this

figure shows that a pseudo-bulk system is found and a severe gel-effect is observed. With the surface modified SiO₂ the particle radical entrance occurs in a more controlled fashion, as seen in the inset with a lower radical per particle number but with a smaller particle size (not shown) yielding a faster reaction rate. Contrary, the non-modified SiO₂ presented a catastrophic coagulation process, probably due to a salting-out effect.

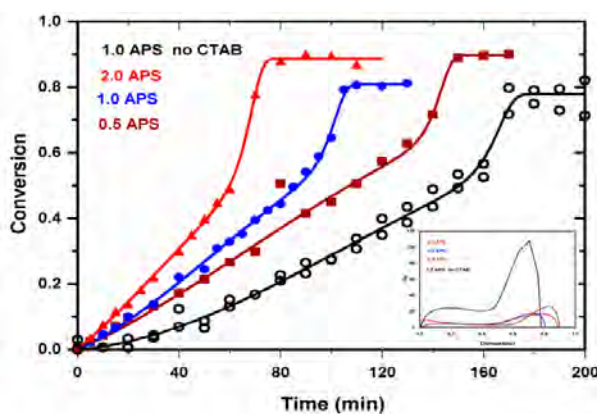


Figure 1. Experimental conversion against time data for the surface modified SiO₂ at different APS concentrations. Inset: Inferred average number of radicals per particle. For comparison one experiment with un-modified SiO₂ is presented in black.

Conclusions

It was found that the modified SiO₂ nanoparticles promote the entry of radicals in a more controlled fashion. An anomalous behavior occurs when SiO₂ are not surface modified, yielding a chaotic nucleation. A pseudo-bulk behavior was detected in all studied systems.

Acknowledgment: This work was financially supported by: DGAPA-PAPIIT project IN113215, CONACyT grant CB-2014-240160 and UNAM-UV interchange program. Bindzil was kindly supplied by Silicatos y Derivados S.A. de C. V.

References

1. Teo, G. H.; Ng, Y. H.; Zetterlund, P. B.; Thickett, S. C. *Polymer* 2015, 63, 1.
2. Arditty, S.; Whitby, C.P.; Binks, B.P.; Schmitt, V.; Leal-Calderon, F. *Eur. Phys. J. E.* 2003, 11, 273.
3. Zou, S.; Hu, Y.; Wang, C. *Macromol. Rapid Commun.* 2014, 35 1414



ZIRCONOCENE ALUMINOHYDRIDE IMMOBILIZED ON ORGANIC SUPPORTS FOR THE SYNTHESIS OF POLYETHYLENE

Alba N. Estrada-Ramirez¹, Odilia Perez¹, Rene D. Peralta², Maricela Garcia-Zamora¹, Victor E. Comparán¹, Gladys Y. Cortez-Mazatán²

Centro de Investigación en Química Aplicada, CIQA, Blvd Enrique Reyna N° 140, 25294, Saltillo, Coahuila

1. *Departamento de Síntesis de Polímeros, ciga2005_alba_estrada@hotmail.com, Odilia.perez@ciqa.edu.mx*
2. *Departamento de Procesos de Polimerización, rene.peralta@ciqa.edu.mx*

Introduction

Polyethylene (PE) synthesized with supported metallocene catalysts, is obtained at high catalytic activity (CA), however, fine particles of PE are observed, due to the leaching of the catalyst during the polymerization.¹ Desorption of the catalysts has been tried to avoid, using different methods and supporting materials. In this work, we report the synthesis of high density polyethylene (HDPE) and linear low density polyethylene (LLDPE), using five organic supports based in particles of P(St-DVB) and functionalized particles with acrylic acid (AA) P(St-DVB-AA) of 100 nm, prepared by miniemulsion.² Organic supports contain chains of polyethylene oxide (PEO) of polymerizable surfactants (TP) (Noigen RN50 and HBC 30). Organic supports were modified with MAO to form agglomerates (secondary particles)² (Fig. 1), to immobilize the aluminohydride (*i*-PrCp)₂ZrH₃AlH₂; the systems were activated at different MAO/Zr ratios. Polymers and copolymers were characterized by DSC, GPC, WAXD, ¹³C RMN and morphology by TEM.

Experimental Part

Catalytic systems and synthesis of HDPE and LLDPE with (organic support/MAO)/(i-PrCp)₂ZrH₃AlH₂

Zirconocene aluminohydride (*i*-PrCp)₂ZrH₃AlH₂ was synthesized from (*i*-PrCp)₂ZrCl₂ and LiAlH₄, and immobilized on organic particles. After its activation at different MAO/Zr ratios (500, 1100 and 2500), the ethylene polymerization was carried out in a “slurry” process using a semi-batch reactor of 600 mL. The reaction conditions were set at T = 70 °C, 42 psi of ethylene pressure, 500 rpm, and 200 mL of isooctane as solvent were used.

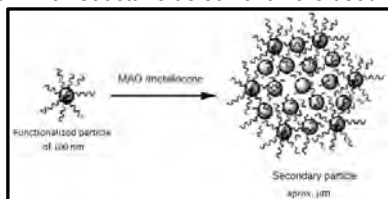


Figure 1. Schematic representation of the secondary particles formation with MAO and metallocene catalyst.²

Results and Discussions

Table 1 shows the characteristics of the five organic supports used to synthesize HDPE and LLDPE. The CA obtained was higher than 2100 Kg PE/mol Zr h for HDPE and 2100 and 1900 Kg PE/mol Zr h for the LLDPE with 1-hexene and 1-octene respectively. Polymers showed typical fusion and crystallization temperatures (*T_f*, *T_c*) of HDPE and LLDPE, and the alpha-olefins incorporation determined by nuclear magnetic resonance (NMR) was low, between 0.3-1%, but sufficient to change the physical characteristics of the polymers.

Table 1. Organic supports used in the synthesis of HDPE and LLDPE

Organic supports	AA %	TP	Al %	Zr %
S1 P(St-DVB)	-	HBC 30	18.5	2.29
S2 P(St-DVB-AA)	3	HBC 30	16.5	1.75
S3 P(St-DVB)	-	NRN 50	17.5	1.59
S4 P(St-DVB-AA)	3	NRN 50	21.9	1.06
S5 P(St-DVB-AA)	4	HBC 30	19.7	1.89

Conclusions

Zirconocene aluminohydride was immobilized in five organic supports based in particles of P(St-DVB) and P(St-DVB-AA) of 100 nm, where the catalytic systems showed high CA in the synthesis of HDPE and LLDPE.

Acknowledgment: The authors thank to CONACYT Mexico for financial support, Project 167901 and the doctoral fellowship of Alba Nidia Estrada. Also thank to Guadalupe Méndez Padilla, M^a.Teresa Rodriguez, Blanca Huerta, and Miriam Lozano for characterizations.

References

- 1.- Bijal K. B.; Bong Ch. S.; J. Mater. Chem., 2010, 20, 7150–7157
- 2.- Yong-J. J., Nikolay N., M. Klapper,; Polymer Bulletin 2003, 50, 343-350



SEMICONDUCTORES POLIMERICOS DEL TIPO PUSH/PULL EN BASE A TIOFENO Y BENZODIOXAZOL

Juan Carlos Ahumada¹, Juan Pablo Soto¹, Juliet Andrea Aristizabal¹

1. Pontificia Universidad Católica de Valparaíso, Avenida Universidad 330, Campus Curauma, Valparaíso, Chile juan.ahumada.c@mail.pucv.cl

Introducción.

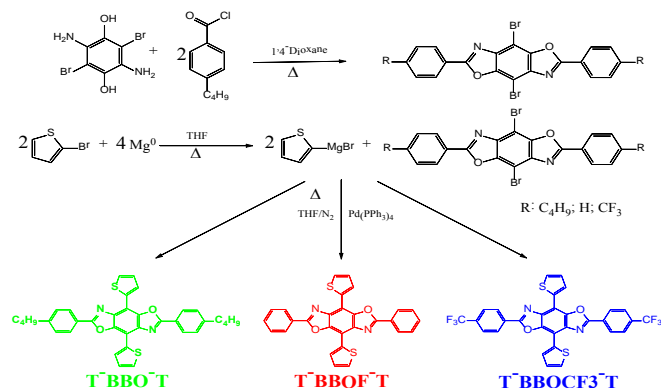
Durante los últimos años los polímeros conjugados han tenido un gran auge por su aplicación en la fabricación de diversos dispositivos electrónicos. Este interés radica en el bajo costo de fabricación de estos materiales, peso ligero, flexibilidad mecánica y por la modulación de las propiedades químicas de ellos mediante cambio en su estructura [1]. En la actualidad la investigación de este tipo de sistemas orgánicos está enfocado en obtener nuevos materiales con bajo *bandgap*, siendo los que han obtenido mejores resultados aquellos que incorporan, dentro de la cadena polimérica, distintos fragmentos con diferentes densidades electrónicas, conocidos como sistemas del tipo push/pull [2]. En este trabajo se presenta la síntesis y caracterización (RMN, Masas) de tres distintos monómeros en base a tiofeno y benzodioxazol, como también la electropolimerización, estudio morfológico (SEM), espectroscópico (Raman) y propiedades ópticas (UV-Vis) de los polímeros depositados.

Parte experimental.

La síntesis de los monómeros se realizó mediante un acoplamiento de Kumada, la que se describe en el esquema 1. A su vez la polimerización de los monómeros se llevó a cabo en una celda de tres compartimientos utilizando platino como electrodo de trabajo, Ag/Ag⁺ como electrodo de referencia, como contra electrodo un alambre de platino, como solvente CH₂Cl₂ y el electrolito de soporte fue TBAPF₆. Por último la caracterización morfológica de los polímeros se realizó sobre una superficie de vidrio conductor como FTO y mediante microscopía electrónica de barrido.

Resultados y Discusión.

En la figura 1 se puede apreciar los perfiles voltamperométricos de la electropolimerización de los monómeros.



Esquema 1. Síntesis de derivados de benzodioxazol-tiofeno

En ella se observan los perfiles obtenidos para los tres compuestos observándose un cambio en la forma de éstos relacionado con la diferencia en la distribución de densidad electrónica de los monómeros. Además se observa para cada sistema un aumento de la corriente a medida que aumenta el número de ciclos, lo que indica la formación de un del polímero conductor sobre la superficie del electrodo. En cuanto a los procesos anódicos se aprecian tres, los que se atribuyen a la oxidación del monómero (0.9 V) y a los fragmentos de tiofeno (0.4 V) y benzodioxazol (0.6 V).

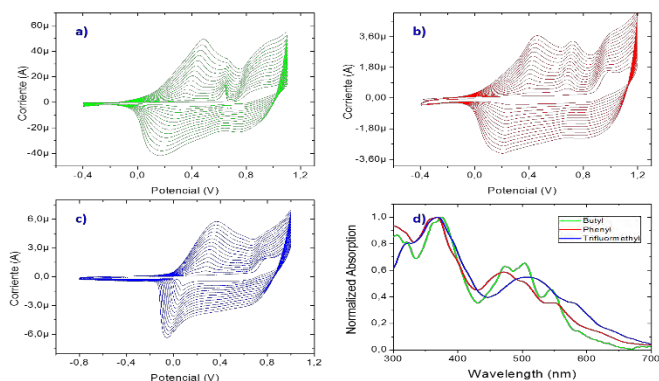


Figura 1. Voltamperogramas cíclicos de los polímeros de a) T-BBO-T; b) T-BBOF-T; c) T-BBOCF3-T y d) espectro UV-Vis de cada uno de los polímeros.

En las micrografías se observa los 3 depósitos poliméricos, en los que se observa homogeneidad en toda la superficie del electrodo, además de rugosidad y un crecimiento tridimensional.

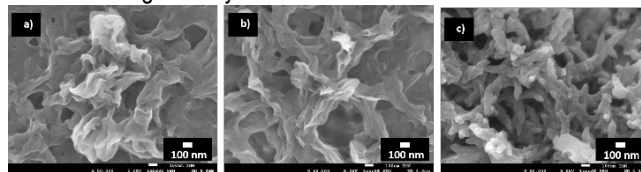


Figura 2. Micrografía SEM de los polímeros de a) T-BBO-T; b) T-BBOF-T; c) T-BBOCF3-T.

Conclusión. Es posible obtener polímeros del tipo *push/pull* en base a tiofeno/benzodioxazol los que presentan una buena conductividad y propiedades ópticas, siendo el mejor de estos tres el que contiene el grupo trifluorometil.

Agradecimientos: Becas Coniyt 21140238, DI 37382/2015 PUCV, DI 039.340/2016 PUCV.

Referencias.

- Chu TY, Lu JP, Beaupre S, J Am Chem Soc. 2011; 133; 4250.
- Iain McCulloch; Raja Shahid; Accounts Chem Res. 2012; 45; 714.

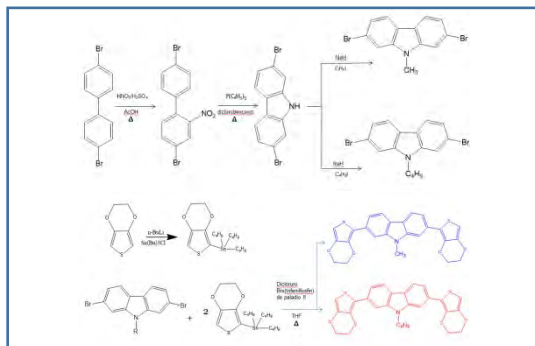
Polímeros Conductores: Síntesis, Caracterización y Electropolimerización de Copolímeros de Carbazol y Etilendioxitiofeno

Cindy Escalona, Juan Soto, Simon Le Page, Juan Ahumada, Felipe Gallardo, Juliet Aristizabal

Pontificia Universidad Católica de Valparaíso, Avda. Universidad 330, Curauma, Valparaíso Chile, cindy.escalona.g@mail.pucv.cl

Introducción Diversas investigaciones han propuesto que la formación de un polímero conductor con fragmentos donador-aceptor (D-A), fomenta la distribución electrónica en el polímero resultante¹, viéndose reflejado en un aumento en el rango de absorción de la radiación² lo que lo hace altamente atractivo como material en la fabricación de fotoceldas solares³. Además, al realizar la copolimerización se logra que propiedades como la alta conductividad, solubilidad y estabilidad de los respectivos homopolímeros se combinen e idealmente se potencien.

Experimental La síntesis comienza con la formación del fragmento 2,7-dibromocabrazol a partir del compuesto disponible comercialmente 4,4'-dibromobifenilo. Posteriormente se procede a la sustitución nucleofílica con yoduro de metilo y de butilo. Paralelamente, se hace la reacción entre tributilo de estaño con etilendioxitiofeno, para finalmente por un acoplamiento tipo Stille llevar a cabo la formación de 3,4-di(etilendioxitiofeno)-2,7-metilcarbazol (EMC) y 3,4-di(etilendioxitiofeno)-2,7-butilcarbazol (EBC). El detalle de la síntesis se muestra en el esquema 1.



Esquema 1. Ruta de síntesis de 3,4-di(etilendioxitiofeno)-2,7-butilcarbazol .

La caracterización se llevó a cabo por RMN de ¹H y ¹³C. Las unidades sintetizadas fueron electropolimerizadas a través de voltamperometría cíclica usando una celda de tres compartimentos, bajo las siguientes condiciones: concentración de los monómeros 1x10⁻³M, acetonitrilo como solvente, TBAPF₆ 0.1M como electrolito soporte, platino (0.2cm²) como electrodo de trabajo, alambre de platino como electrodo auxiliar y Ag/AgCl como electrodo de referencia, velocidad de barrido 1.0 V/s a 25°C.

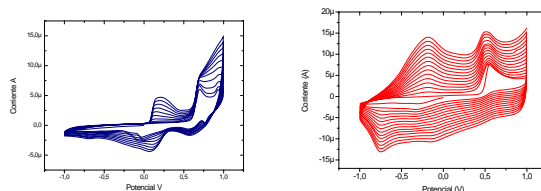


Figura 2. Voltamperograma de EMC y EBC.

Resultados y discusiones En la figura 2 es posible apreciar el perfil del proceso de electropolimerización, identificando en ambos casos un aumento de la corriente a medida que aumenta el número de ciclos así, como también, se observa dos procesos de oxidación y al menos dos de reducción. Esto da cuenta de la formación de un depósito de naturaleza conductora sobre la superficie del electrodo.

El análisis de las respuestas electroquímicas de ambos depósitos, y la comparación con los perfiles anteriores muestra que existe un pico de oxidación del monómero a 0.7V y del polímero a 0.25V para EMC, mientras que en caso de EBC el pico de oxidación del monómero se encuentra a 0.5V y del polímero a -0.25V. Esto implica que la cadena alquílica tiene un gran efecto en las propiedades electroquímica del material, lo que puede deberse al diferente ordenamiento de las macromoléculas, lo que concuerda con los datos de microscopia de barrido electrónico obtenidos para ambos depósitos.

Conclusiones Es posible realizar la síntesis de copolímeros que contengan unidades alternadas de 3,4-etilendioxitiofeno y carbazol, a partir del diseño de la unidad monomérica y su posterior electropolimerización. Los depósitos obtenidos tiene naturaleza conductora y son dopantes tipo p. Finalmente la modificación de la cadena alquílica en la unidad de carbazol afecta las propiedades del depósito así como su mecanismo de nucleación y crecimiento.

Acknowledgment: Becas Conicyt 21140976, DI 37382/2015 PUCV, DI 039.340/2016 PUCV.

References

1. Luyao Lu, Tianyue Zheng, Qinghe Wu, Alexander M. Schneider, Chem. Rev. 2015, 115, 12666–12731.
2. Dhanabalan, A.; van Duren, J. K. J.; van Hal, P. A.; van Dongen, J. L. J.; Janssen, R. A. J. Cells. Adv. Funct. Mater. 2001, 11, 255–262.
3. Stuart, A. C.; Tumbleston, J. R.; Zhou, H.; Li, W.; Liu, S.; Ade, H.; You, W. J. Am. Chem. Soc. 2013, 135, 1806–1815.

MAGNETOHYPERTERMIA IN A VEGETABLE OIL BASED POLYMER

C. Meiorin¹, D. Muraca², D.G. Actis³, P. Mendoza Zélis³, M.I. Aranguren¹, M. Knobel⁴, M.A Mosiewicki¹

1. Instituto de Investigaciones en Ciencia y Tecnología de Materiales (INTEMA), Universidad Nacional de Mar del Plata–CONICET, J. B. Justo 4302, 7600 Mar del Plata, Argentina
2. Instituto de Física Gleb Wataghin (IFGW), Universidade Estadual de Campinas, Campinas- SP, Brazil
3. Instituto de Física La Plata (IFLP-CONICET), Universidad Nacional de La Plata, Argentina
4. Brazilian Nanotechnology National Laboratory (LNNano/CNPEM), Campinas-SP, Brazil
email: mirna@fi.mdp.edu.ar

Introduction

The development of polymeric nanocomposites obtained from renewable raw materials has become an important area of research due to their potential applications in different scientific and industrial fields and the environmental advantages when compared to synthetic polymers.

Tung oil is extracted from the seeds of the tung tree and it is a highly unsaturated oil that can be polymerized with styrene in the presence of a cationic initiator ¹. Previous works have reported that some of the compositions display shape memory properties (SMP) ¹. The load of these systems with nano-magnetite (NM) can increase their applications. The magnetite nanoparticles can absorb electromagnetic energy from an external high-frequency field and release it as heat, which under specific conditions, can be used to trigger the SMP of the nanocomposites ².

The aim of this work is to study the influence of NM concentration on a polymeric matrix based on tung oil and styrene.

Experimental Part

Magnetite nanoparticles were produced by means of coprecipitation method from an aqueous Fe³⁺/Fe²⁺ solution using excess of a concentrated solution of NH₄OH and coated with oleic acid. The resulting MN have a mean size of 9.8 nm ³.

Nanocomposites preparation. Styrene was added and mixed with tung oil (weight ratio of 50/50) and this step was followed by the addition of the initiator (boron trifluoride diethyl etherate). Then, a selected percent of oleic acid-coated magnetite was added and this mixture was put into an ultrasonic device to obtain a good dispersion of MN and finally, poured into the mold ³. The reactants were heated at 60°C for 12h and then at 100°C for 12h.

Nanocomposites characterization:

Thermogravimetric analysis were performed using a TGA-DTGA Q500 TA instrument at 10°C/min under air atmosphere.

The static magnetic properties were studied using a SQUID magnetometer (Quantum Design, MPMS XL). Both isothermal magnetization curves as well as zero field cooling and field cooling (ZFC/FC) measurements were performed.

Specific absorption rate (SAR) data from magnetic hyperthermia experiments were obtained from magnetocalorimetric tests using a resonant R–L–C circuit Huttinger radiofrequency (rf) field generator. The SAR values are calculated as

$$SAR = \frac{dT}{dt} \frac{c}{NM}$$

where T is temperature, t is time, c is the specific heat capacity of the sample and NM is the nanoparticle concentration.

Results and Discussions

The isothermal magnetization and FC/ZFC tests showed that all the nanocomposites present superparamagnetic behavior at room temperature. The maximum blocking temperature (T_{Bmax}) increases as the content of NM increases in the material with values of 100, 126, 122, 160 and 180 K for samples with 1.5, 3, 5, 7 and 10 wt.% of NM, respectively. This behavior can be attributed to possible interactions among the particles.

Figure 1 shows SAR values as a function of NM content. As was expected, the specific absorption rate increases with the content of NM in the samples.

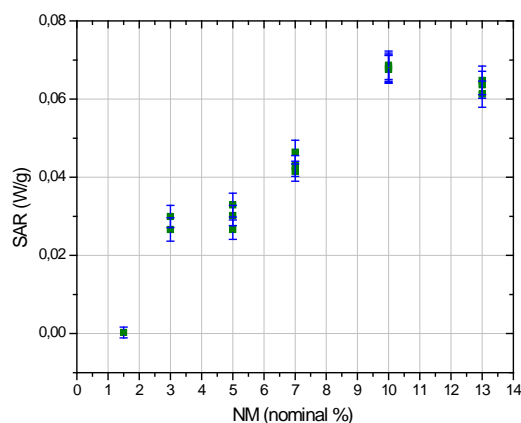


Figure 1. SAR as a function of NM content

Conclusions

Hyperthermia can be possible in the nanocomposites based on tung oil for contents above 1 wt.% of magnetite.

Acknowledgments: The authors gratefully acknowledge to CONICET, ANPCyT, UNMDP (Argentina) and FAPESP, CNPq (Brazil).

References

1. Meiorin, C.; Aranguren, M. I.; Mosiewicki, M. A. *Polym. Int.* 2012, 61, 735.
2. McBain, S.C.; Yiu, H.H.P.; Dobson, J. *Int J. Nanomedicine* 2008, 3, 169.
3. Meiorin, C.; Muraca, D.; Pirota, K.R.; Aranguren, M.I.; Mosiewicki, M.A. *European Polymer Journal* 2014, 53 (1), 90.



INFLUENCE OF ELECTROSPINNING PROCESS PARAMETERS ON THE STRUCTURE AND MORPHOLOGY OF SMART POLYMER FIBERS MADE OF POLY(VINYLIDENE FLUORIDE)

Anthony Moulins¹, Mitasha Swain¹, Nicole Demarquette¹, Ricardo Zednik¹

1. *École de Technologie Supérieure, Université du Québec, 1100 Rue Notre-Dame Ouest, H3C 1K3, Montréal, Canada* nicoler.demarquette@etsmtl.ca
ricardo.zednik@etsmtl.ca

Introduction

Although electrospinning is an established technique¹, it was not until the 1980s that it attracted the attention of the scientific community with the advent of nanotechnology. This technique has been shown to be useful for preparing porous membranes formed of PVDF fibers². PVDF is of particular interest, because its crystalline β -phase has good piezoelectric properties³. In the present study, we investigate electrospun poly(vinylidene fluoride) (PVDF) to analyze its crystalline structure and changes in fiber morphology as a function of varying manufacturing parameters. The influences of the electrostatic field E (10 to 25kV), the distance between the needle and the collector d (15 to 20 cm) and the polymeric flow rate Q_v (1 to 5 mL·h⁻¹) on the morphology of the meshes obtained were evaluated by scanning electron microscopy (SEM) and X-ray-diffraction (XRD) techniques.

Methods

20%wt PVDF ($M_w \approx 275\,000\text{ g}\cdot\text{mol}^{-1}$, $M_n \approx 107\,000\text{ g}\cdot\text{mol}^{-1}$) was dissolved at 90°C in dimethylformamide (DMF) and acetone solutions of varying concentrations, ranging from 100%wt DMF to 70%wt DMF (remainder acetone). The homogeneous polymer solution was loaded into a 10 mL polypropylene syringe. A fifteen minute holding time prior to electrospinning was observed to reduce air bubbles.

During the electrospinning process, the solution was ejected through a disposable stainless steel needle using a syringe pump, while applying a positive voltage to the needle tip. A grounded metal target was employed to collect the electrospun fibers, which formed a randomly oriented non-woven membrane structure.

The morphology of these manufactured membranes was studied using an Hitachi S3600N scanning electron microscope. In order to reduce surface charging during imaging, a thin conductive layer of gold ($20\pm 2\text{nm}$) was applied to the samples. The X-ray diffraction structural analysis of the PVDF membrane was performed using a PW3040 X'Pert PRO diffractometer.

Results

Figure 1 shows a representative non-woven membrane produced from electrospun PVDF fibers. Although the individual fibers display minor surface roughness, they are not porous. No appreciable defects, such as pearls, crazing, or fiber branching were observed. In addition, the large diffraction peak at $2\theta = 20.4^\circ$ shown in Figure 2 is consistent with the the (110) planes associated with the orthorhombic body centered PVDF β -phase. This suggests that the crystallized polymer chains are highly

textured and run parallel to the fiber length and perpendicular to the membrane thickness.

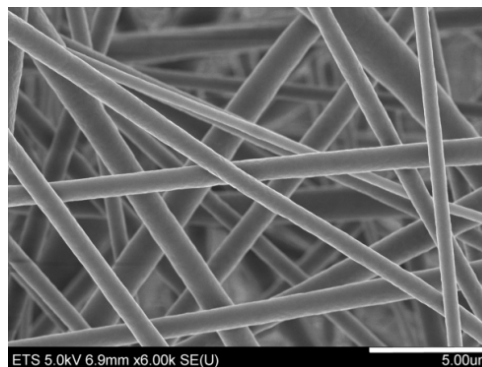


Figure 1. SEM micrograph of PVDF nanofibers produced from solution 2 with a flow rate of 1 mL·hr⁻¹ and a field of 1 kV·cm⁻¹.

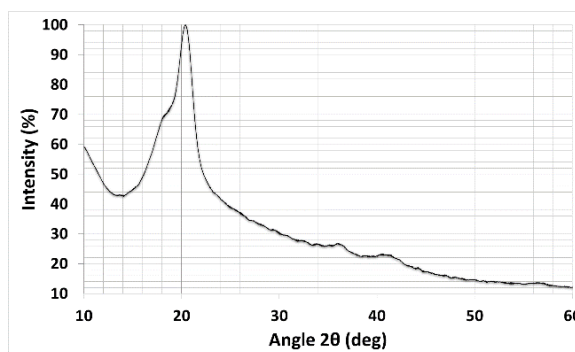


Figure 2. XRD spectrum of an electrospun PVDF membrane.

Conclusions

The process parameters determined in this study enable the production of non-woven PVDF membranes with a prevailing crystalline β -phase using the electrospinning technique. The strong electrostatic field and mechanical stresses associated with the electrospinning technique likely promote the formation of the metastable β -phase. We also found that a voltage increase or flow rate decrease causes a reduction of the fiber diameter, which is useful for customizing the membrane morphology.

References

1. G.Taylor. Electrically driven jets. *Proc Royal Soc.* A313, 453 (1969).
2. Zhao, Z. *et al.* Preparation and properties of electrospun poly(vinylidene fluoride) membranes. *J. Appl. Polym. Sci.* 97, 466 (2005).
3. Kawai, H. The Piezoelectricity of Poly (vinylidene fluoride). *Jpn. J. Appl. Phys.* 8, 975 (1969).

LAYER-by-LAYER HYBRID GRAPHENE OXIDE PDADMAC MULTILAYERED FILMS

Layza Arizmendi ¹, Raquel Ledezma ¹, Alberto Rodríguez ¹, Sergio Moya ² and Ronald Ziolo

1. Centro de Investigación en Química Aplicada, Depto. Materiales Avanzados. Blvd. Enrique Reyna Herosillo 140, C.P. 25294, Saltillo, Coahuila, México.
2. CICbiomaGUNE, Paseo Miramón 182 C, 20009, San Sebastián, Gipuzkoa, España.

Introduction

The design, assembly and management of nanoscale multilayer assemblies is emerging as one of the most important challenges of scientific, technical and industrial research. The layer by layer technique (LBL) allows for the nanoscale fabrication of hybrid nanomaterial assemblies of biological, physical and chemical interest. The base of this technique is the sequential adsorption of polyelectrolytes on a charged surface to form multilayer polymer films and eventual devices by the sequential deposition or use of varied and multiple components [1]. Graphene oxide (GO) is of important scientific, technical and industrial interest since to can be functionalized to form new platforms for materials development and can also be reduced to form a more conducting form of GO closer to that of grapheme [2]. The combination of GO and the LBL assembly technique can form multilayer hybrid materials that can be integrated into chemically, biologically, electronically and optically active devices for extended applications. The scope of the present work extends to the preparation, characterization and further study of GO multilayered polyelectrolytes films and their eventual role in hierarchical devices.

Experimental Part

For the LBL assembly GO dispersions were prepared using 0.01 mg GO/mL of Millipore purified water and placing in a sonication bath for 15 min right before use. Branched polyethylenimine (average Mw 25,000) (PEI), poly (dimethyldiallyl ammonium chloride) (PDADMAC), PDADMAC+s and poly (sodium4-styrenesulfonate) (PSS) were prepared using 1 mg/mL of Millipore purified water; for the PDADMAC+s after polymer addition, NaCl was added to make a 0.5 M solution. All the above solutions, including water used for washings, were adjusted to pH 10 by the addition of NaOH concentrated solution. The assembly was done on top of a gold coated quartz crystal. Between layer applications the quartz crystal was rinsed with water for several minutes [3]. A quartz crystal micro balance (QCM) q-sense was used for LBL film formation and confocal Raman microscopy (Renishaw, 532 nm) for measurements.

Results and Discussions

Comparison of figures 1A and 2A shows different results in frequencies (Hz); 1A indicates 500 Hz, when the PDADMAC solution is used alone and 2A illustrates an increase to 1000 Hz when NaCl its added to PDADMAC. Figures 1B and 2B correspond

to the Raman spectra with D and G bands located at 1350 and 1600 cm⁻¹ characteristic of GO [4]. DC conductivity values for the PDADMAC and PDADMAC+s films were 3.2 and 2.7 S/cm, respectively.

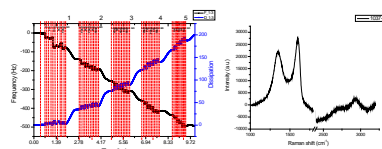


Figure 1. A) QCM curve (left) and B) Raman Shifts (right) for PEI [PDADMAC/PSS/PDADMAC/PSS/PDADMAC/GO].

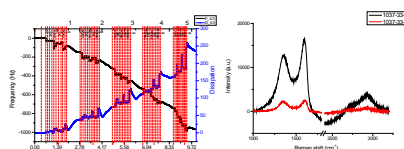


Figure 2. A) QCM curve (left) and B) Raman Shifts (right) for PEI [PDADMAC+s/PSS/PDADMAC+s/PSS/PDADMAC+s/GO].

Conclusions

Multilayered GO sheets were assembled using the LBL technique with intercalating layers of PDADMAC and PSS to form hybrid multilayered films and the improvement in frequency with NaCl addition. QCM-D measurements show the formation with continuous growth films and CRM shows D and G bands characteristic for GO.

Acknowledgment: The authors would like to thank the European Commission Project HIGRAPHEN (FP7-PEOPLE-2013-IRSES) Project ID 612704. “Hierarchical functionalization and assembly of Graphene for multiple device fabrication” and Gilberto Francisco Hurtado López for help in the electric conductivity measurements.

References

1. G. Decher; Science (1997), 277(5330), 1232-1237.
2. R. F. Ziolo, C. Avila and L. Arizmendi; Graphene, Carbon Nanotubes and other BCN Materials, Ch. 4 in Isotopes in Nanoparticles: Fundamentals & Applications; J. Llop, V. Gomez, P. N. Gibson, Eds., Pan Stanford Publishing Pte. Ltd. 2016.
3. J. J. Iturri, S. Stahl, R. Richter, S. E. Moya; Macromol. (2010), 43(21), 9063-9070.
4. O. García, R. Ledezma, E. Saldívar, L. Yate, S. Moya, R. F. Ziolo; Polymer (2014), 55, 2347-2355.

PROPIEDADES REOLÓGICAS TRANSITORIAS DE MATERIALES COMPUESTOS A BASE DE POLIPROPILENO REFORZADO CON NANO-ARCILLAS DE PALIGORSKITA

Carlos Gamboa Sosa ¹, César Martín Barrera ¹, Genaro Soberanis Monforte ², P.I. González-Chi ¹

1. Centro de Investigación Científica de Yucatán, Calle 43 No. 130, Chuburná de Hidalgo, 97205, Mérida, México. ivan@cicy.mx
2. Universidad Tecnológica Metropolitana, Calle 115 No. 404, Santa Rosa, 97279, Mérida, México.

Introducción

La reología es comúnmente usada para el estudio de materiales compuestos nano-reforzados (MCN) ya que sus propiedades dependen de la estructura y morfología de la fase dispersa, la interacción entre los componentes (partícula-partícula y partícula-polímero) y las condiciones de procesamiento.^{1,2} Las pruebas reológicas transitorias a tasa de corte constante, usualmente presentan un pico al inicio de los ensayos llamado pico del sobre-esfuerzo (*overshoot*) cuya amplitud depende del grado de ordenamiento y movimiento de las partículas en un sistema;³ por tanto, los cambios en el valor de su respuesta podría reflejar los cambios en la estructura de un MCN. El presente trabajo busca establecer una metodología a través de pruebas reológicas transitorias como herramienta para determinar el grado de disgregación y distribución de nano-arcillas de paligorskita en una matriz polimérica de polipropileno.

Parte Experimental

MCN a base de una matriz de polipropileno Valtec Indelpro/polipropileno maleado Eastman G-3015 y arcilla de paligorskita de la región sureste del estado de Yucatán, se utilizaron tres tipos: sin tratamiento (ST), purificada (PUR) y silanizada (SIL) variando el contenido en 0.5, 1 y 2 % en peso (la superficie de la arcilla se trató con el silano marca Aldrich 3-aminopropiltrimetoxisilano). Los materiales compuestos fueron obtenidos en un extrusor modular doble husillo ZSK30 marca Werner & Pfleiderer configurado con niveles de esfuerzo cortante en el procesamiento: medios (M), altos (H) y esfuerzos altos asistido con un cabezal sónico marca Sonotrol a 20 kHz (S).

La caracterización reológica se hizo con barridos de corte transitorio empleando un reómetro rotacional AR-2000 marca TA Instruments con la geometría de platos paralelos $\varnothing = 25$ mm. Se utilizaron probetas circulares de 25 mm de diámetro y 2 mm de espesor; la temperatura de fundido fue de 180 °C, gap de 950 μ m y una tasa de corte de 1 s⁻¹. Micrografías TEM fueron obtenidas con un microscopio electrónico de transmisión marca FEI, el voltaje utilizado fue de 300 kV.

Resultados y Discusión

La Fig. 1 compara el valor máximo del pico del sobre-esfuerzo (VMPS) de los MCN con diferentes tipos de arcilla de paligorskita: ST, PUR y SIL. Se observa la gran influencia de las condiciones de procesamiento sobre la respuesta reológica. El aumento en el

VMPS para las muestras S respecto a las muestras H podría estar indicando que el uso de sonicación favorece la dispersión. La Fig. 2 presenta el VMPS de los MCN con distintos contenidos de arcilla: 0.5, 1 y 2 % en peso. Se observa una clara disminución en sus propiedades con el aumento del contenido de nano-refuerzo, que podría significar que se favorece la formación de aglomerados.

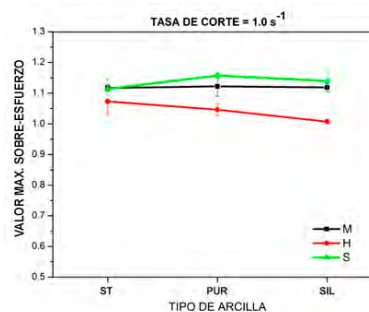


Figura 1. VMPS de MCN con 0.5 % de arcilla ST, PUR y SIL.

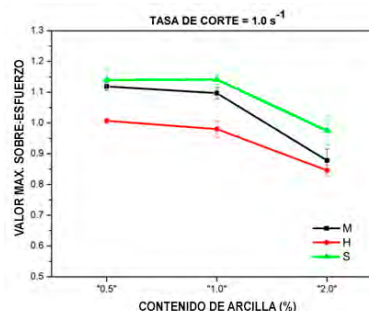


Figura 2. VMPS de MCN con 0.5, 1 y 2 % de arcilla SIL.

Conclusiones

El grado de disgregación y distribución en los MCN está relacionado con el VMPS por lo que este parámetro reológico podría ser utilizado para determinar la micro-estructura interna del material compuesto.

Referencias

1. Jahromi, Q. Const. and Build. Mat. 2009, 23, 2894.
2. Zuo, M.; Zheng, Q. Sci. in Ch. Series B: Chem. 2008, 51, 1.
3. Lertwimolnun, W.; Vergnes, B. Polymer, 2005, 46, 3462.



Nanopartículas de Talco en films orientados por Roll-casting

Ma. Gabriela Passaretti ¹, Daniel A. Vega ², Marcelo A. Villar ¹

1. *Planta Piloto de Ingeniería Química, PLAPIQUI (UNS-CONICET), Departamento de Ingeniería Química, UNS, Camino “La Carrindanga” Km 7, (8000) Bahía Blanca, Argentina. mypassaretti@plapiqui.edu.ar*
2. *Instituto de Física del Sur, IFISUR (UNS-CONICET), Departamento de Física, Universidad Nacional del Sur, Alem 1253, (8000) Bahía Blanca, Argentina.*

Introducción

Los nanocompuestos poliméricos (NCP) son materiales de gran potencial debido a la mejora en sus propiedades finales. La incorporación de nanopartículas a estructuras ordenadas de copolímeros bloques proporciona control sobre la distribución y la orientación de las partículas, esta incorporación podría permitir el desarrollo de nanomateriales con propiedades mejoradas, tanto mecánicas como ópticas, eléctricas, de barrera. El agregado de nanopartículas (NPs) puede llevarse a cabo en fundido, en solución o en una combinación de ambos. En este trabajo se utilizó el procesamiento en solución de un copolímero tribloque comercial de poli(estireno-*b*-butadieno-*b*-estireno) (SBS) con partículas minerales de talco y posteriormente la aplicación de una técnica de alineación denominada roll-casting (RC). La técnica de RC permite obtener films con estructuras organizadas macroscópicamente.

Experimental

Se utilizó un copolímero tribloque comercial SBS de *Sigma-Aldrich* ($M_w=140.000$ g/mol), cumeno de *Sigma-Aldrich*, y NPs de talco (*Dolomita SAIC – Argentina*) como material de carga. Se prepararon soluciones de SBS con distintas concentraciones de NPs y el solvente se evaporó lentamente en el equipo de RC durante 5-6 horas. El film resultante, fue sometido a un tratamiento a temperatura, bajo vacío, para la eliminación del solvente remanente. Finalmente se realizaron tratamientos térmicos para mejorar la orientación. Para la caracterización de los films se tomaron imágenes con un microscopio electrónico de barrido (SEM, *LEO EVO 40-XVP*) a las muestras frenteadas con un crio-microtómo sin y con ataque químico para poder observar con mayor claridad las NPs de talco. Además, se realizaron mediciones de difracción de rayos X de bajo ángulo (SAXS) utilizando una cámara *Kratky 1D* y ensayos de tracción en una máquina de ensayos universal *Instron 3369*.

Resultados y Discusión

A partir de las curvas de SAXS se determinó la existencia de un empaquetamiento hexagonal correspondiente a cilindros de poliestireno (PS) en una matriz de polibutadieno (PB) aún a altos porcentajes de talco. Midiendo el módulo elástico paralelo y perpendicular a los cilindros se determinó la orientación macroscópica de los cilindros de PS, siendo la relación de estos módulos (E_{\parallel}/E_{\perp}) un indicativo del grado de ordenamiento macroscópico en los films (Fig. 1). Además, se observó que es posible modificar la permeabilidad al oxígeno mediante la orientación macroscópica o por el

agregado de nanopartículas. Las imágenes de SEM muestran que las nanopartículas de talco tuvieron una orientación preferencial en la dirección de flujo (Fig. 2).

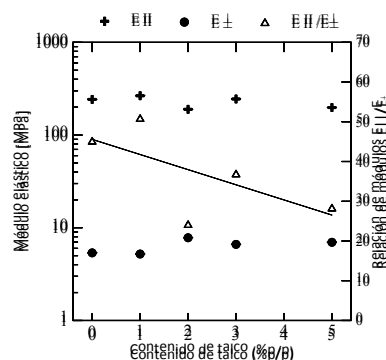


Figura 1. Módulos elásticos paralelo y perpendicular al flujo y relación de ambos.

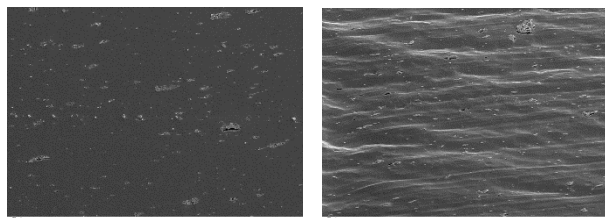


Figura 2. Micrografía SEM de la muestra SBS-RCT-5% con la dirección de los cilindros paralela al frenteo.

Conclusiones

Los resultados de SAXS para los films obtenidos por RC muestran un buen alineamiento de los cilindros de PS en la matriz de PB demostrando que esta técnica es eficiente para el ordenamiento macroscópico inclusive con el agregado de 5% de carga. Los resultados de ensayos de tracción para ambos casos, con y sin carga, mostraron que los films obtenidos por RC son altamente anisotrópicos mientras que los obtenidos por simple cast son isotrópicos. Mediante SEM se corroboró lo observado en SAXS y ensayos mecánicos.

Agradecimientos: Al CONICET, la ANPCyT y la UNS.

Referencias

1. Albalak, R.; Thomas, E. *J. of Polymer Sci.* 1994, 32, Part B, 341.
2. Villar, M.; Rueda, E.; Thomas, E. *Polymer* 2002, 43, 5139.

CARBON NANOTUBES FUNCTIONALIZATION: IN SEARCH OF NANOCOMPOSITES PROPERTIES IMPROVEMENT

J. A. Torres-Avalos¹, F. López-Serrano², S. M. Nuño-Donlucas¹

1. Departamento de Ingeniería Química, Universidad de Guadalajara, Boul. M. García Barragán #1451, Guadalajara, Jal 44430, México jq.josue.torres@gmail.com
2. Departamento de Ingeniería Química, Facultad de Química, Universidad Nacional Autónoma de México, Ciudad Universitaria, Cd. Mx., 04510, México. lopezserrano@unam.mx

Introduction

Carbon nanotubes (CNTs), discovered in 1991 by Iijima, have awakened huge interest designing polymeric nanocomposites. CNTs provide extraordinary properties such as: extreme strength (even higher than steel), good conductivity, flexibility, etc¹. However, a huge challenge has to be overcome in order to use them, due to their great tendency to form agglomerates. Most of the present efforts are focused on the CNTs dispersion as reinforcements in polymeric matrices². To achieve this, covalent functionalization can be used, which consists in attaching chemical moieties to the CNTs. These moieties are used as a covalent linkage to polymeric chains to promote CNTs dispersion³.

Experimental Part

CNTs were obtained by chemical vapor deposition purified with steam and partially oxidized by treatment with HNO₃ reflux. These CNTs reacted with oxalyl chloride [(COCl)₂]. The acyl chloride CNTs were further reacted with methacrylic acid (MAA) attaching an acrylic group on CNTs surface. These functionalized CNTs were used as a chemical linker. This chemical route is presented in the upper section of Figure 1. Finally, the functionalized CNTs were added to a MAA/butyl acrylate (BuA) emulsion copolymerization system stabilized with sodium dodecyl sulfate. After polymerization, the nanocomposites were precipitated, filtered, washed, dialyzed and dried. Characterization included: FTIR, QLS, DSC, TGA and ¹H-NMR analysis.

Results and Discussions

The lower section of Figure 1 shows the FTIR spectra of the compounds obtained from the different steps of the chemical route employed to functionalize the CNTs. The red curve is the FTIR spectrum of CNTs after steam purification (CNTs purified); the black curve depicts the CNTs after HNO₃ treatment (CNTs-COOH); the blue curve corresponds to the CNTs treated with HNO₃ and COCl₂ (CNTs COCl), while the green curve is the product of the chemical reaction between MMA and CNTs COCl (CNT COCl-MMA). A simple inspection of the spectral contributions detected in all these spectra validates that functionalization reactions of the CNTs occurred.

QLS results show that two populations of particles are present in the nanocomposites lattices. The average diameter of the first was ca. 30 nm and the second was ca. 180 nm. DSC results show that a random copolymer of MMA-BuA was obtained. There is no clear tendency of the CNTs effect on the glass transition

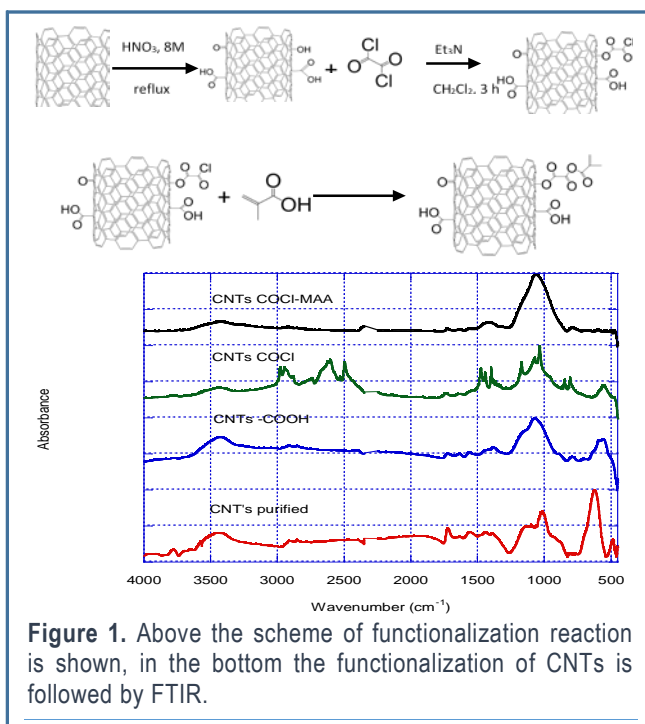


Figure 1. Above the scheme of functionalization reaction is shown, in the bottom the functionalization of CNTs is followed by FTIR.

temperature of the polymeric matrix of the MMA-BuA/CNTs nanocomposites. The nanocomposite MAA/BuA/CNTs (20/80/1 wt. %) does not show a Tg, while (40/60/1) presents one Tg at 40°C, almost the same as the one observed in the copolymer MMA/BuA (40/60) without CNTs.

Conclusions

CNTs were chemically functionalized and attached to MMA monomer before copolymerization reaction. An improvement in the nanocomposites thermal properties was achieved respect to the ones observed for pure MMA/BuA copolymer.

Acknowledgment: FLS gratefully acknowledges support by DGAPA-UNAM project PAPIIT IN113215 and the interchange program between UdeG and UNAM.

References

1. Chang, Ch-Ch., Hsu I-K., Aykoi, M., Hung, W-H., Chen, Ch-Ch., Cronin, S, ACSNANO, 2010, 4, 5095.
2. Ajayan, P., Tour, J. *Nature* 2007, 447, 1066.
3. Silva-Jara, J. M.; Manríquez-González, R., López-Dellamary, F. A. Puig, J.E., Nuño-Donlucas. S.M., *J MACROMOL SCI A*, 2015, 52, 732.

FLUORESCENCE EMISSION COLOR CHANGES OF ACRYLONITRILE DERIVATIVES DUE TO NANOCRYSTALS, MORPHOLOGY. SYNTHESIS, STRUCTURE, AND OPTICAL PROPERTIES

M. Judith Percino¹, Margarita Cerón¹, Oscar Rodríguez¹, Guillermo Soriano-Moro¹, Enrique Pérez-Gutierrez², José Bonilla-Cruz³

1. Benemérita Universidad Autónoma de Puebla, Complejo de Ciencias, ICUAP, Edif. 103H, 22 Sur y San Claudio, Puebla, Puebla, México, C.P. 72570 judith.percino@correo.buap.mx
2. Centro de Investigaciones en Óptica, CIO, Loma del Bosque 115, Colonia Lomas del Campestre, León, Guanajuato, México, C.P. 37150
3. Centro de Investigación en Materiales Avanzados S.C. (CIMAV-Unidad Monterrey), Av. Alianza Norte 22, Autopista Monterrey-Aeropuerto Km 10, PIIT, Apodaca-Nuevo León, México, C.P. 66600

Introduction

Solid state lighting (SSL) of organic chromophores has attracted much attention due to their potential applications in devices such as light-emitting diodes, photovoltaic devices, and sensors. Tuning and controlling the wavelength of emission of an organic material is crucial in order to identify the appropriate application, and the optical properties of different dyes in the solid state strongly depend on the molecular structure and intermolecular interactions. Recently, organic chromophores that exhibit quenching of fluorescence in the solid state have been reported, and this phenomenon is termed aggregation-caused quenching (ACQ). In contrast, when the emission of fluorescence depended on the presence of the solid state, the process was termed aggregation-induced emission (AIE) or aggregation-induced emission enhancement (AIEE).

Experimental Part

The studied compounds were characterized by H1-NMR, EI, FT-IR, UV-Vis spectroscopy, fluorescence, cyclic voltammetry (CV), single crystal and powder X-ray diffraction, DSC and SEM.

Results and Discussions

Herein, we report results from optical characterization (absorption and emission) of α,β -unsaturated acrylonitrile with structures of electron donor D- π -A acrylonitrile derivatives. The investigation reveals differences in the characteristic emission such as an enhancement in fluorescence in solvent as well as in the solid state. Their photophysical properties have been investigated and compared with between them in order to evaluate the effect of the substituents, which afforded a dye that exhibited emission in solution and in the crystal form, depending on the habit and size of crystal formed, i.e. nanocrystals. The differences in solid-state photoluminescence indicated variations in the morphology of the crystals and organic films, as well as the crystal habit and size.

Conclusions

H1-NMR, EI, FT-IR, UV-Vis spectroscopy, fluorescence, CV, single-crystal/ powder X-RD, DSC and SEM. The morphology and size of crystals exhibit an enhanced emission compared to the same concentration dilute solution in a good solvent. The complexity of this problem is well captured by the fact that despite many studies, this problem has not been fully solved, but predictions may be possible using the experimental and theoretical approaches in organic solid state chemistry that take into account the nanoparticle properties. We think that the phenomenon observed clearly carry out to the crystallization grow microcrystal or nanocrystals when it is used for nanoscale electronic devices and correlated to the electron conduction.

Acknowledgment: The authors wish to express their gratitude to VIEP-BUAP (projects PEZM-NAT16-G, SOMJ-NAT16-I, CASM-NAT16-I, CERM-NAT16-I), PROMEP-SEP/103.5/13/2110 (Thematic network of collaboration) and CONACyT (projects 183833 and 157552), as well as to F. E. Longoria Rodriguez (CIMAV-MTY) for technical assistance with XRD.

References

1. Burroughes, J. H.; Bradley, D. D. C.; Brown, A. R.; Marks, R. N.; MacKay, K.; Friend, R. H.; Burns, P. L.; Holmes, A. B. *Nature* 1990, 347, 539–541.
2. Yamaguchi, Y.; Ochi, T.; Miyamura, S.; Tanaka, T.; Kobayashi, S.; Wakamiya, T.; Matsubara, Y.; Yoshida, Z.-I. *J. Am. Chem. Soc.* 2006, 128, 4504–4505.
3. Zhang, H. Y.; Zhang, Z. L.; Ye, K. Q.; Zhang, J. Y.; Wang, Y. *Adv. Mater.* 2006, 18, 2369–2372.
4. Percino, M. J.; Chapela, V. M.; Ceron, M.; Soriano-Moro, G.; Castro, M. E.; Melendez, F. J. *J. Mol. Struct.* 2013, 1034, 238



SYNTHESIS OF NANOCOMPOSITES WITH STAR SHAPED POLY(ϵ -CAPROLACTONE)-CO-POLY(ETHYLENE GLYCOL) AS POLYMERIC MATRIX

Leonardo Ramses Cajero Zul¹, Sergio Manuel Nuño Donlucas²

1. Departamento de Ingeniería Química Universidad Guadalajara, Boul. M. García Barragán #1451, Guadalajara, Jal. 44430 Mexico, lcajero@yahoo.com.mx
2. Departamento de Ingeniería Química Universidad Guadalajara, Boul. M. García Barragán #1451, Guadalajara, Jal. 44430 Mexico, gigio@cencar.udg.mx

Introduction

Now day, environmental concerns and a shortage of petroleum resources have driven efforts aimed at bulk production of biodegradable polymers such as aliphatic polyesters, polysaccharides, unsaturated polyesters, poly(vinyl alcohol), and modified polyolefins¹. Among them, poly(ϵ -caprolactone) (PCL) has received much attention as a new aliphatic polyester being developed for a wide range of application due its thermoplastic, biodegradable and biocompatible properties². On the other hand, poly(ethylene glycol) (PEG) is employed extensively in pharmaceutical and biomedical areas³. As a new anisotropic unidirectional nanomaterial, carbon nanotubes (CNTs) is a new reinforcement for polymeric nanostructure materials, because its extraordinary high elastic module, force and resilience⁴.

Experimental Part

Synthesis of CNTs was carried out by the technique of chemical vapor deposition (CVD) using Fe as catalyst. The CVD process was carried out at room temperature under local atmospheric pressure for 8 hr and at 900 °C. The CNTs were purified with steam at 600 °C for 3 hr. For insertion of the carboxyl and hydroxyl groups on CNTs surface, 0.5 g of CNTs were maintained under reflux in a Soxhlet with 75 mL of nitric acid 7 M for 6 h. The solid was separated by centrifugation and washed with water.

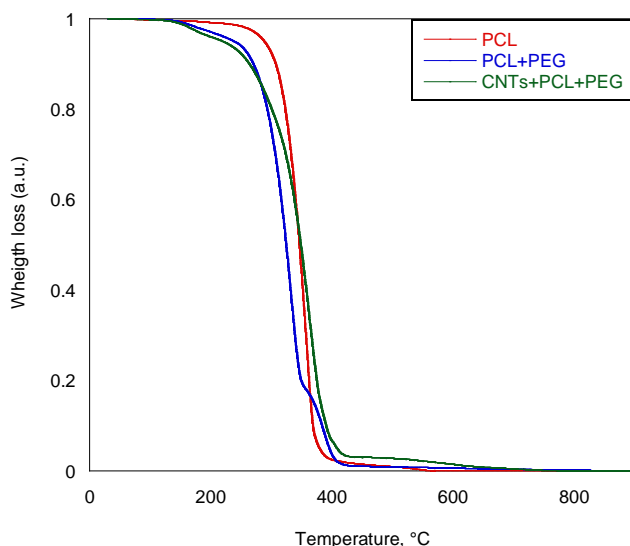


Figure 1. Evolution of sample weight in function of temperature change.

Synthesis of star shape PCL was made at 110 °C under nitrogen bubbling with stirring during 1 h using pentaerythritol as initiator and stannous octoate as catalyst. The PCL synthesized was purified and dried in a rotary evaporator for 30 min and finally into a vacuum oven during 24 h at 50 °C. A prepolymer of star-shaped PCL-oxalyl chloride (OxCl) was synthesized by a reaction between hydroxyl end groups of star-shaped PCL and OxCl. The prepolymer reacts with PEG to get the star shape PCL-PEG copolymer. Nanocomposites was made adding functionalized CNTs (prepared by the treatment of CNTs -containing hydroxyl and carboxyl groups- with OxCl) to the prepolymer at the same time that it reacts with PEG. Nanocomposites were characterized with TGA, DSC, and FTIR.

Results and Discussions

Figure 1 shows TGA thermograms of pure star shape PCL (red line), star shape PCL+PEG copolymer prepared at molar rate [1/1] (blue line) and a nanocomposite CNTs+PCL+PEG prepared at molar rate [1/1/1] (green line). TGA curves depicts that the thermal degradation of star shape PCL begins at 300 °C. On the other hand, thermal degradation of star shape PCL-PEG copolymer begins at 200 °C. For the nanocomposite, the degradation also start at ca. 200 °C, but as the temperature increase, is evident that show a better thermal stability that observed for pure PCL-PEG copolymer, and pure PCL. In fact, the presence of functionalized CNTs improvement the thermal stability of all nanocomposites studied.

Conclusions

The CNTs increase the stability of the CNTs+PCL+PEG nanocomposites.

Acknowledgment: The Mexico National Council for Science and Technology (CONACyT) provided the financial support for this work (CB-2008-101369).

References

1. Albertson, P. A., Ed. Partition of cell particles and macromolecules, 3rd ed.; Wiley: New York, 1986.
2. Dong, C.M., Qiu, Y.K., Gu, Z.W., Feng, X.D., Macromolecules, 34 (2001) 4691-4696.
3. J. Li and W. J. Kao, "Synthesis of Polyethylene Glycol (PEG) Derivatives and PEGylated - Peptide Biopolymer Conjugates," pp. 1055–1067, 2003.
4. Potschke, P.; Abdel-Goad, M.; Alig, I.; Dudkin, S.; Lellinger, D. Polymer 2004, 45, 8863–8870.



EFFECT OF NUCLEATION ON THE CRYSTALLIZATION OF POLY (LACTIC ACID)/POLY (PROPYLENE) BLENDS

Dulce K. Contreras García¹, Yovana García Morais¹, Sergio Barrientos Ramírez¹, Georgina Montes de Oca Ramírez²

1. Universidad Anáhuac México Norte, Facultad de Ingeniería CADIT, Av. Universidad Anáhuac, núm. 46 Col. Lomas Anáhuac Huixquilucan, Edo. de México, C.P. 52786, México. sergio.barrientos@anahuac.mx
2. CIATEQ A.C. Unidad Lerma, Circuito de la Industria Poniente No. 11 Lote 11 Mz 3, Parque Industrial Ex Hacienda Doña Rosa, 52004 Lerma de Villada, México

Introduction

Poly (lactic acid) (PLA) is a biodegradable polyester that is produced from renewable resources. However its inherent brittleness and low impact resistance represent an important limitation to its usage. The main purpose of this investigation is to study the effect of nucleation of incorporation of a compatibilizer in PLA/PP blends on the crystalline content. Differential scanning calorimetry was used to study the thermal properties (such as Tg and Tm) and isothermal cold crystallization behavior of PLA/PP.

Experimental Part

Mixtures of PLA/PP (50/50 w/w) with and without compatibilizer (5% w/w) were prepared on a twin-screw extruder.

Isothermal crystallization was performed using a differential scanning calorimeter (DSC) TA Q10 system. The sample was heating from 30 to 180 °C at 20°C/min and maintaining it at 180°C for 5 min. Subsequently, it was cooled to 30 °C at 20 °C/min

Results and Discussions

Figure 1 shows the DSC thermograms of PLA and PP homopolymers to determine transitions separately. Figure 2 shows the DSC thermograms of PLA/PP mixtures with 1 and 5 % compatibilizer. It can be seen that only the sample with 5 % compatibilizer has a recrystallization at 73 °C, suggesting that the block copolymer was used as a compatibilizer has an effect of nucleating agent. In addition, the presence of the compatibilizer reduces the degree of crystallinity of polypropylene in the blend. PLA is known that causes a decrease in the crystallinity of PP, but this phenomenon is only observed at high concentrations of compatibilizer, indicating that the compatibilizer has effect in the separate phases of the immiscible segments.

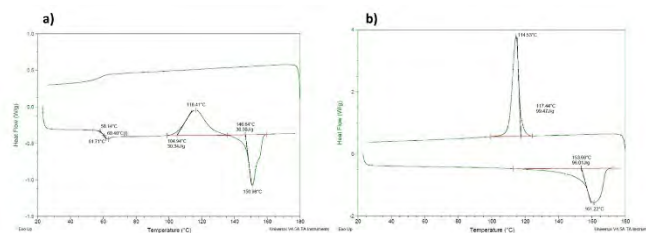


Figure 1. DSC thermograms for a) PLA and b) Polypropylene homopolymers.

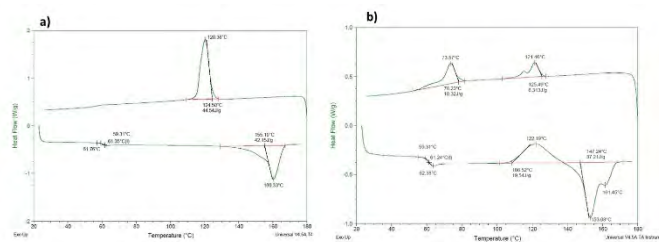


Figure 2. DSC thermograms for PLA/PP blends a) without compatibilizer and b) with compatibilizer

Conclusions

The presence of high concentrations of compatibilizer in the PLA/PP mixtures reduces the crystallinity of PP and has an effect as a nucleating agent of PLA.

References

1. Liao, Rougu; et. al. J. Appli. Polym. Sci., 2007, 104, 310-317.
2. Ploypetchara, Nain; et al, Energy Procedia, 2004, 56, 201-210.

Well-defined nanoparticles from polymer electrolytes PSSNa via RAFT polymerization

Claude St Thomas¹, Enrique J. Jimenez Regalado², Alexis Vélez de la Fuente², Judith Cardoso Martinez³, Ramiro Guerrero Santos², Hortensia Maldonado-Textle², Judith Cabello Romero²

1. Catedrático CONACYT, CIQA, Centro de Investigación en Química Aplicada, Blvd Enrique Reyna # 140, C.P. 25294, Saltillo, Coahuila, México Claude.stthomas@ciqa.edu.mx
2. Centro de Investigación en Química Aplicada, Blvd Enrique Reyna # 140, C.P. 25294, Saltillo, Coahuila, México
3. Departamento de física, CBI, Universidad Autónoma Metropolitana-I, Apartado Postal 55-534, México, CDMX. 09340

Introduction

In last decades, polymer electrolytes are gained great interest due to their wide range applications. Electrochemical remains the most known applications¹. However, with the introduction of reversible deactivation radical polymerization (RDRP) a lot of attentions were focused in polymer electrolytes as macroagent to obtain amphiphilic block copolymers. Armes and coworkers² are reported and described the effect of anionic or cationic in the synthesis of well-defined nanoparticles. Also, Charleux et al³ are reported the preparation of Poly (sodium 4-styrene sulfonate) PSSNa as macroagent Nitroxide Mediated Polymerization (NMP). In this work, we reported the preparation of well-defined nanoparticles from water-soluble PSSNa macroagent obtained via RAFT polymerization.

Experimental Part

Polymerization of PSSNa was performed at 75°C via RAFT polymerization. In a reactor, 11 g of SSNa (55 mmol), 0.062 g of ACPA (0.2 mmol), 0.122 g of DMAT (0.4 mmol) and 35 g of water (1.95 mol) were added. Mixture was heated at 75°C under constant agitation (ca. 300 rpm). High conversion was reached and polymer was obtained by precipitation in cold acetone. Synthesis of Latex: In a reactor, 0.52 g of PSSNa (0.005 mol), 0.0095 g of ACPA, 3.1 g of styrene (0.030 mmol) and 10 g of water (0.55 mol) were added. Polymerization was carried out at 75°C and stable latex was obtained and characterized by NMR, DLS, SEM and TEM.

Results and Discussions:

Macroagent PSSNa was synthesized via RAFT polymerization using molar ratio [SSNa]/[DMAT]/[ACPA] = 130/1/0.5. Polymer was obtained by precipitation in cold acetone and dried under vacuum during 24 hours at 50°C. The molecular weight ($M_w = 9,500$ g/mol) was measured by viscosimeter. Once obtained, macroagent was used in PISA. Stable latex with different average diameter was acquired. Latex with molar ratios [MA]/[S] = 50, 750 and 1000 were characterized by TEM. As observed in Fig 1., sample of L2 was withdrawn and dilute in deuterated water. At 7.6 ppm was appeared protons of aromatic group PSSNa closed to sodium-sulfonate and 6.7 ppm was detected protons of aromatic group closed to

backbone of polymer. PS was not detected due to his insolubility in water media.

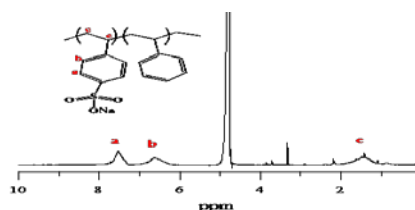


Fig. 1. ¹H NMR of amphiphilic triblock copolymer PSSNa-*b*-PS-*b*-PSSNa

In the Fig 2, TEM micrographies were presented. As observed, latex acquired a micelle morphology (F2 a). When the concentration of PS increases, nanorods were observed (Fig 2b and c). Despite authors are reported mutual repulsion between ionic groups.



Fig. 2. TEM micrographies of latex PSSNa-*b*-PS-*b*-PSSNa with different concentration of PS.

Conclusions

Well-defined amphiphilic triblock copolymer PSSNa-*b*-PS-*b*-PSSNa were prepared via PISA and characterized. DLS, TEM and SEM analysis demonstrate formation of nanometric particles while NMR analysis confirm the structure of latex in water media.

Acknowledgment

Thanks are given to CONACYT for nomination of CST as Research Fellow and CIQA for financial support (internship project). Also, to Enrique Diaz-Barriga, Jesus Garcia-Cepeda and Guadalupe Telles-Padilla for TEM, SEM and NMR analysis.

References

1. Editorial, *Electrochimica Acta*, **2011**, 57, 4-13.
2. Semsarilar, M.; Ladmiral, V.; Blanazs, A. and Armes, S P. *Langmuir*, **2012**, 28, 914-922
3. Brusseau, S. ; Charleux, B. *Polym Chem.* **2010**, 1, 720-729

EFFECT OF THE COMPOSITION IN STATIC AND DYNAMIC MECHANICAL PROPERTIES OF POLYMERS SYNTHESIZED IN TWO STAGES. SYSTEMS: STYRENE – BUTYL ACRYLATE / BUTYL ACRYLATE AND STYRENE – METHYL METHACRYLATE / BUTYL ACRYLATE

Francisco J. Rivera Gálvez¹, María E. Hernández¹, Carlos F. Jasso-Gastinel¹.

1. Chemical Engineering Department, Universidad de Guadalajara, Blvd. Gral. Marcelino García Barragán #1421, 44430, Guadalajara, Jalisco, carlos.jasso@cucei.udg.mx

Introduction.

Since decades ago, scientists have focused their efforts on optimization of polymer properties using physical and/or chemical blending of the components. The materials synthesized in two or more stages have been of particular interest for the synergism that may occur by interaction. Particle size, morphology, chains composition and interaction between phases are the key parameters to improve the mechanical performance of structured materials. In this work, materials were synthesized in two – stages forming copolymeric seeds of different character to be combined with poly (butyl acrylate) in the second stage to follow mechanical behavior of the materials while varying seed composition.

Experimental Part.

Monomers were polymerized by emulsion in a batch reactor in two stages (TS) with sodium dodecyl sulphate as initiator at 72 °C. First, on a weight per cent basis, random copolymers of styrene - methyl methacrylate (S-MMA) of 90/10, 80/20 and 70/30 or styrene – butyl acrylate (S-BA) 90/10 and 80/20 compositions were formed; in the second stage, butyl acrylate was polymerized using as seed one of the above copolymers to obtain global polymeric compositions of 70/30 or 60/40 (S-MMA)/BA or (S-BA)/BA. Polymer latexes were then dried at room temperature in an aerated chamber. Material samples were obtained by compressing molding at predetermined temperature and pressure. Static and mechanodynamic tests were respectively performed on a Universal Testing Machine (United FM) and Dynamo – Mechanical Analyzer (TA model Q800, using the three-point bending deformation for a temperature sweep mode at 1.5 °C/min), following ASTM D 638 (static) at 5 mm/min crosshead speed and 23 °C, and ASTM D 5023 (dynamic)..

Results and Discussions.

Polymers with S-BA seed show relatively harder and tougher behavior than the ones with S-MMA seed, in addition to a small increase in strain, due to a better interaction between phases. That is shown in Table 1. In Figure 2, the higher moduli of S-BA/BA

compared to S-MMA/BA materials up to 50 °C confirms the results obtained with static tests; nevertheless, beyond that temperature the materials with higher BA global content show moduli decay at lower temperature, denoted by the storage modulus vertical decrease and the loss modulus peak (T_g) whose position varied with seed composition.

Table 1. Stress-strain properties of several TS materials with 70 wt % of copolymeric seed, where the number inside each parenthesis indicates S content within the seed.

Material	Young's Modulus (MPa)	Toughness (MPa)	Strain (%)
TS-(S90-MMA)/BA 70	642	38	3.6
TS-(S80-MMA)/BA 70	605	39	3.6
TS-(S90-BA)/BA 70	729	141	7.4
TS-(S80-BA)/BA 70	710	133	6.6

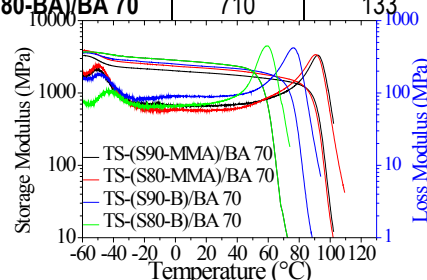


Figure 2. Storage and Loss Modulus as a function of temperature and frequency of 1 Hz for several TS materials. For material codes see Table 1.

Conclusions.

The mechanical performance of the polymeric materials prepared in two-stages can be benefited (moduli, deformation capacity and toughness) using a copolymeric seed that includes the component that is used for during the second stage. That is a consequence of the phase interaction that is promoted with such approach.



SYNTHESIS AND CHARACTERIZATION OF TiO₂ / ZnO NANOFIBERS FROM PVAC ELECTROSPUN MICROFIBER PRECURSORS

Sandra Milena Camargo Silva¹ Efrén Muñoz Prieto¹, Edwin Gomez Pachon¹, Ricardo Vera Graziano²

²Grupo de Investigaciones DANUM, Universidad Pedagógica y Tecnológica de Colombia, Tunja, Colombia

¹Instituto de Investigaciones en Materiales, UNAM, PO Box 70-360, Cd. Universitaria, CDMX, México, 04510

graziano@unam.mx

Introduction

The synthesis and characterization of TiO₂ / ZnO nanofibers obtained after calcination of microfibers made of poly(vinyl acetate) with titanium isopropoxide and Zn nanopowder is reported here.

Experimental

The precursor fibers were prepared by solution electrospinning, as described elsewhere.¹ The polymer was dissolved first in N,N dimethyl formamide at room temperature. Titanium isopropoxide (IV) was dissolved in acetic and mixed with the Zn nanopowder. The colloidal suspension was added to the polymer solution. The precursor fibers were transformed in TiO₂ / ZnO nanofibers by calcination at 500° C.

Results and Discussions

The precursor fibers form a porous random mesh made of long microfibers as observed by SEM.

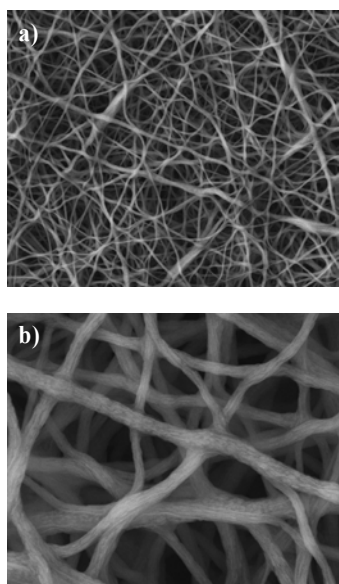


Figure 1. SEM micrographs of TiO₂ / ZnO nanofibers: (a) 10000X (b) 50000X.

This morphology is also observed in the TiO₂ / ZnO nanofibers after calcinations but the mean diameter of the fibers was reduced to 200 nm (Figure 1). The nanofibers have a high surface

area/volume ratio and show better mechanical properties compared to other known forms of the same material.² The XRD and EDS data showed that the TiO₂ / ZnO nanofibers are made of oriented crystalline structures of TiO₂ (anatase) and ZnO (Figures 2 and 3).

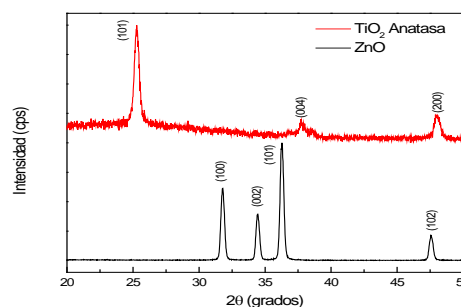


Figure 2. XRD spectra of TiO₂ / ZnO nanofibers.

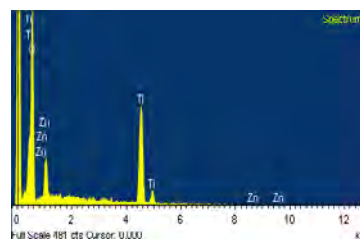


Figure 3. FESEM-EDS data on calcinated nanofibers

Conclusions

The precursor fibers were conveniently made by electrospinning. The TiO₂ / ZnO nanofibers morphology and properties show characteristics that make them potentially useful in the field of renewable energy, in particular for solar cell applications.

Acknowledgments:

To the grant of Project PAPIIT IN108116, UNAM and the technical support of Novelo-Peralta O, Romero-Ibarra JE, Canseco-Martínez MA, and Tejada Cruz A.

References

- Gómez-Pachón EY; Sánchez-Arévalo FM; Sabina FJ, Maciel-Cerda A; Montiel-Campos R; Batina N; Morales-Reyes I; Vera-Graziano R. J Mater. Sci. 2013, 48:8308–8319.
- Kanjwal MA, *et al.* Macromol. Res. 2010. vol. 18. no. 3, p. 233-240.

SYNTHESIS OF FLUORINATED RANDOM COPOLYMER (P₃FM-*co*-P₁₃FM) BY RAFT AND IT'S CHAIN EXTENTION WITH MMA IN sc(CO₂). MORPHOLOGY OF DISPERSED MICROSPHERES

Yañez-Macias Roberto¹; Guerrero-Santos Ramiro¹, Maldonado-Textle Hortensia¹, Cabello-Romero Judith Nazareth¹, Garza-Cepeda Jesús Angel², Torres-Lubián José Román¹

1. Departamento de Síntesis de Polímeros, Centro de Investigación en Química Aplicada, Blvd. Enrique Reyna 140, Saltillo Coah., C.P. 25296, México.
2. Laboratorio de Microscopía Electrónica, Centro de Investigación en Química Aplicada, Blvd. Enrique Reyna 140, Saltillo Coah., C.P. 25296, México.

Introduction

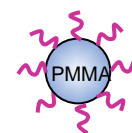
In recent years, there has been growing interest in the preparation of polymer particles using this reversible deactivation technique. In particular, dispersion RAFT polymerization is a versatile tool to prepare monodisperse microspheres that can be applied to a range of applications including electronics, coatings, support materials for biochemical analysis.¹ Supercritical carbon dioxide (scCO₂) has emerged as a viable “green” alternative to conventional organic solvents due it is abundant, inexpensive, non-flammable, and non-toxic, while at supercritical conditions (T_c = 31.1 °C, P_c = 7.38 MPa).² Additionally, scCO₂ is a thermodynamically good solvent only for relatively non-polar low molecular weight compounds or fluorinated poly(meth)acrylates. RAFT-mediated polymerizations have been shown to work in supercritical fluids, so the combination of scCO₂ and RAFT has allowed the formation of microparticles with defined molecular weights and polydispersities.

Experimental Part

The random copolymer polytrifluoroethyl methacrylate (CF₃) –co-polytridecafluorooctyl methacrylate (CF₁₃)(PF₃M-*co*-PF₁₃M) was synthesized by RAFT methodology using 4-cyanopentanoic acid dithiobenzoate (CPAD) as transfer agent, AIBN as initiator in dioxane at 70°C. Chain extension of fluorinated macro-RAFT was carried out in scCO₂ using AIBN as source of radicals. The reactions were performed at 65°C and 27.6 MPa for 20 h in a 30 ml autoclave. Molar mass and composition of random copolymer used a Macro-RAFT and the block copolymer of (PF₃M-*co*-PF₁₃M)-*b*-PMMA was determined by NMR (M_n = 17,000 g/mol). (Scheme 1)

Results and Discussions

Fluorinated macro-CTA was analyzed by ¹H NMR using CDCl₃ as solvent. The signals and chemical shifts observed are consistent with the proposed structure, given a composition of 74% mol of CF₃ and 26 % mol of CF₁₃ co-monomers. Because its CO₂-philic nature, this fluorinated macro-CTA was used as stabiliser for MMA copolymerization in scCO₂. After 20 h of reaction an overall conversion of 14.0 % was obtained. The molar composition of the resulting block copolymer was 61% PF₃M-*co*-PF₁₃M and 39% for PMMA.



Scheme 1. Strategy for synthesis of PMMA spheres using fluorinated macro-RAFT:

The characterization by SEM of (PF₃M-*co*-PF₁₃M)-*b*-PMMA is displayed in Fig.1 and shows spherical particles of around 150 nm. DSC studies are necessary to confirm the synthesis of diblock copolymer.

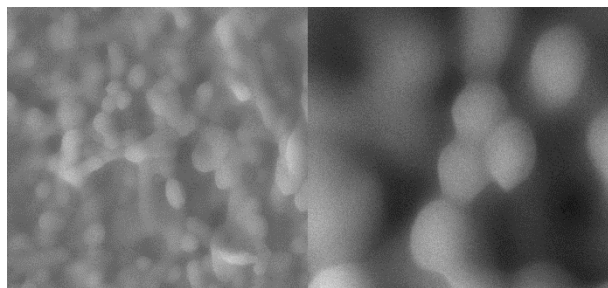


Figure 1. SEM images of spheres obtained by chain extension of fluorinated macro-CTA with MMA

Conclusions

Random fluorinated copolymer with targeted molar mass was synthesized efficiently by RAFT polymerization. This macro-RAFT acted as stabilizer of PMMA due its affinity with scCO₂ allowing the formation of microspheres due the self-assembly of diblock copolymer in scCO₂.

Acknowledgment:

References

1. Zong, M., Thurecht K., and Howdle S.M., *Chem. Commun.* 2008, 45, 5942-5944.
2. Hojjati, B. and Charpentier P.A., *Polymer* 2010, 51, 5345-5351

BIOSYNTHESIS OF SILVER NANOPARTICLES AND ITS USE IN POLYMER SOLAR CELLS

Edgar J. López-Naranjo¹, I. Paz Hernández-Rosales², Luis J. González-Ortiz³, Damaris Velázquez-Páez², Alejandro Manzano-Ramírez⁴

1. Departamento de Ingeniería de Proyectos, CUCEI, Universidad de Guadalajara, José Guadalupe Zuno No.48, 45100, Guadalajara, México. edgar.lopezn@academicos.udg.mx
2. Universidad Autónoma de Nayarit, Ciudad de la Cultura Amado Nervo, 63190, Tepic, México.
3. División de Ciencias Básicas, CUCEI, Universidad de Guadalajara, Blvd. Marcelino García Barragán No.1421, 44430, Guadalajara, México.
4. CINVESTAV-IPN Unidad Querétaro, Libramiento Norponiente No.2000, 76230, Querétaro, México

Introduction

Polymer solar cells (PSCs) have attracted a lot of interest due to their low cost, flexibility, lightweight and ease of processing.¹ Although power conversion efficiencies (PCEs) over 10% have been reported, further improvement is necessary to overcome inorganic devices.² Recently, metallic nanoparticles (MNPs) have been incorporated into different layers of PSCs to increase light harvesting and the PCEs of PSCs.³ Synthesis of MNPs commonly involve the use of toxic compounds as stabilizing agents. Thus, a greener approach is essential to promote both, performance and safety. Green or biochemistry routes, where biological entities like microorganisms or plant extracts are used to obtain MNPs have lately received vast attention.^{4,5} Therefore, the aim of the present work is to synthesize silver nanoparticles (AgNPs) using an aqueous extract obtained from *Agave tequilana* Weber cultivar azul (ATE) as stabilizing agent and to evaluate the performance of P3HT:AgNPs films to be used as active layer in PSCs.

Experimental Part

Materials: Silver nitrate (AgNO₃, 99.99%), poly3-hexylthiophene-2,5-diyl (P3HT), dichlorobenzene (anhydrous 99%), *Agave tequilana* Weber cultivar azul extracted from Tequila, Jalisco (20°88'11.1" N 103°83'14.5" O).

Synthesis of AgNPs: Different ratios of ATE, 6mM AgNO₃ solution and distilled water were used as indicated in Table 1. This mixture was autoclaved at 120°C for 5 min.

Film elaboration: P3HT was dissolved in DCB (15 mg/ml) and stirred for 1 h at room temperature, AgNPs were then added. Active layers were obtained via dip coating.

Characterization: Samples were characterized via UV-vis, SEM, and electrically using a Keithley 4200-SCS source measure unit.

Results and Discussions

Color evolution of samples detected via physical inspection of laboratory jars before and after being autoclaved (Fig. 1a, A and B) indicates that a reduction reaction took place. SEM results show that AgNPs were obtained using ATE (Fig. 1b) Finally, UV-vis absorbance spectra between 380 to 800 nm indicates the presence of nanoparticles in sample 2 (Fig. 1c).

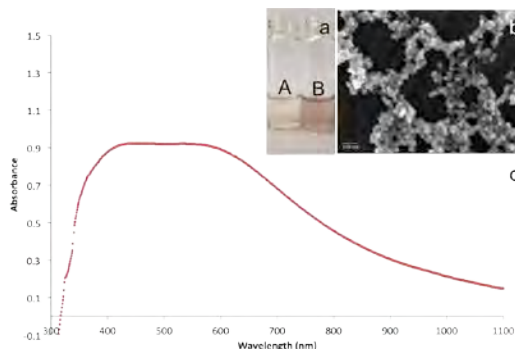


Figure 1.

- (a) Color change in sample 2, before (A) and after (B) being autoclaved (b) SEM micrograph of synthesized AgNPs using ATE, (c) UV-vis spectra of synthesized AgNPs

Table 1. Synthesis conditions of AgNPs

Sample	ATE:AgNO ₃ ratio
1	1:4
2	1:3
3	1:1
4	3:1

Conclusions

Results demonstrate that it is possible to obtain AgNPs using a plant extract as stabilizing agent, providing an eco-friendly, simple and low cost synthesis route.

Acknowledgment: To José Eleazar Urbina-Sánchez for his technical support.

References

1. Xian-Hao, L.; Li-Xin, H.; Jin-Feng, W.; Bin, L.; Zheng-Sen, Y.; Li-Qian, M.; Shao-Peng, Y.; Guang-Sheng, F. *Sol Energy* 2014, 110, 627.
2. Wenfei, S.; Jianguo T.; Die, W.; Renqiang, Y.; Weichao, C.; Xichang, B.; Yao, W.; Jiqing, J.; Yanxin, W.; Zhen, H.; Linjun, H.; Jixian, L.; Wei, W.; Pinghui, W.; Belfiore, L.A. *Mat Sci Eng* 2016, Part B, 61.
3. Morvillo, P.; Del Mauro, A.d.G.; Nenna, G.; Diana, R.; Ricciardi, R.; Minarini, C. *Energy Procedia* 2014, 60, 13.
4. Jagpat, U.B.; Bapat, V.A. *Ind Crop Prod* 2013, 46, 132.
5. Mulvihill, M.J.; Beach, E.S.; Zimmerman, J.B.; Anastas, P.T. *Annu Rev Environ Resour* 2011, 36, 271.

SERS SUBSTRATES FOR ACETONE DETECTION

Iván Alziri Estrada-Moreno, Elsa Anabel Mercado-Gardea, Mónica Elvira Mendoza-Duarte, Sergio Gabriel Flores-Gallardo, Alejandro Vega-Rios, Rocío Domínguez-Cruz, Velia Carolina Osuna-Galindo, Pedro Piza-Ruiz, Alfredo Márquez-Lucero

1. Centro de Investigación en Materiales Avanzados, S.C., Miguel de Cervantes 120, 31109, Chihuahua, Chih, México
ivan.estrada@cimav.edu.mx

Introduction

Raman is a very versatile molecular spectroscopic technique, which is sensitive, rapid, and accurate, having the disadvantage of no detections at low concentrations. By Surface-Enhanced Raman Spectroscopy (SERS) ¹ this can be improved with the additions of metallic nanoparticles (Au, Ag, Cu, etc.) to the surface of the material. Employing SERS to measure acetone can help to detect it in air. Acetone is well known that can be harmful to human beings or it can be used as a biomarker in some illness. ² This work presents the results on synthesizing Polystyrene/Ag nanoparticles to be evaluated as a detector of acetone by raman spectroscopy.

Experimental Part

First, the PS spheres were obtained by emulsion polymerization. After that, the Ag particles were synthesized by a three step procedure. TEM-SEM images were acquired with scanning electron microscope, Jeol JSM 7401-F, at an accelerating voltage of 25kV. SERS measurements were performed with a Raman confocal microscopy spectrometer of 632.5 nm, Horiba Lab RAM HR vis 633. Raman spectra were collected with a droplet of rhodamine or acetone at certain concentration. The spectra region was 200–3000 cm^{-1} .

Results and Discussions

Figure 1 shows the TEM images of the polystyrene spheres obtained. An average size of approximately 66 nm, but there are some bigger spheres and aggregates. The use of polystyrene is because it shows some affinity to acetone and it could help to adsorb acetone in the surface. The insert in Figure 1 shows the solution PS/NPs Ag when was dried.

The raman spectra obtained when the acetone is sprayed over the surface PS/NPs AG is plotted on Figure 2. As the peak of C-C bond located at 785 cm^{-1} is intense it is monitored. As the amount of acetone in an air mixture is increased the peak experiments an increment.

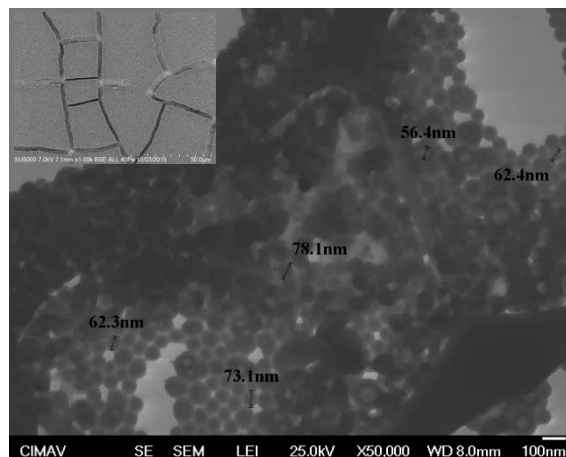


Figure 1. SEM image of Polystyrene particles obtained. In the insert we show the surface of the PS/NPs Ag material.

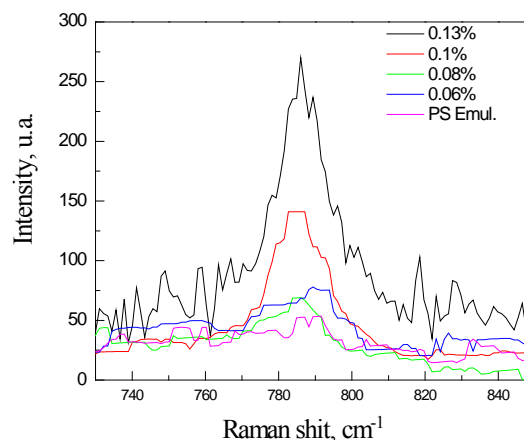


Figure 2. SERS spectra of acetone on the surface of PS/NPs Ag.

Conclusions

This results shown that PS/NPs Ag can be employed to detect acetone in air in concentrations low as 0.6 % by means or Raman spectroscopy. Which is a reliable and fast technic.

References

- Schlücker, S. *Angewandte Chemie - International Edition* 2014, 53, 4756.
- Wang, Z. & Wang, C. *Journal of breath research* 2013, 7, 3.

Graphene Based Materials Functionalized with Natural Polymeric Biomolecules

Velasco-Santos C.¹*, Jiménez-Cervantes-A E.², Bustos-Ramírez K.¹, Rodríguez-Gonzalez C.², Lopez-Marin L.M.,², Martínez-Hernández A.L.¹

¹División de Estudios de Posgrado e Investigación, Instituto Tecnológico de Querétaro, Av. Tecnológico s/n, 76000, Querétaro, México. *Corresponding author email: cylaura@gmail.com; ²Centro de Física Aplicada y Tecnología Avanzada UNAM, Juriquilla Querétaro 76230, Querétaro, México.

Introduction

The use of 2D nanocarbon materials as scaffolds for the functionalization with different molecules has been rising as a result of their outstanding properties. This work describes the synthesis of graphene and its derivatives, particularly graphene oxide (GO) and reduced graphene oxide (rGO). Both GO and rGO represent a tunable alternative for applications with polymer biomolecules due to the oxygenated moieties, which allow interactions either in a covalent or non-covalent way. From here, other discussed topics are the biofunctionalization with keratin (KE) and chitosan (CS). The non-covalent functionalization is based primarily on secondary interactions like van der Waals forces, electrostatics interactions or π - π stacking formed between KE or CS with graphenic materials. On the other hand covalent functionalization with KE and CS is mainly based on the reaction amongst the functional groups present in those biomolecules and the graphenic materials. As a result of the functionalization, different applications has been proposed in our group for these novel materials. Some of them are presented here.

Experimental Part

Functionalization with KE and CS.

Functionalization of Graphene materials: rGO and GO with polymeric molecules was achieved using redox reaction with $KMnO_4$, malic acid and H_2SO_4 .^{1,2} Non covalent reactions were achieved in Keratin by stirring a mixture of rGO with KE for 3 h at room temperature (KE/rGO-1:1). For Grafting CS similar system was used but in different temperatures.³

Characterization

The characterization here presented is focused to morphological images of grafted polymer biomolecules using Electron Transmission Microscopy (TEM) and the quantification of the attached molecules, also the interactions of polymer in graphene materials was analyzed by Raman and Infrared spectroscopies. Dynamical Mechanical Analysis of composites obtained with grafted materials were also obtained using tension clamps using 1 Hz of frequency.

Results and Discussions

Figure 1 and 2 show the images obtained by TEM of KE and CS, attached to graphene materials respectively. Details of polymer

grafting obtained by spectroscopies, quantification of grafted polymer, and possible applications as bacteria support and in polymer composites⁴ are also presented in this work.

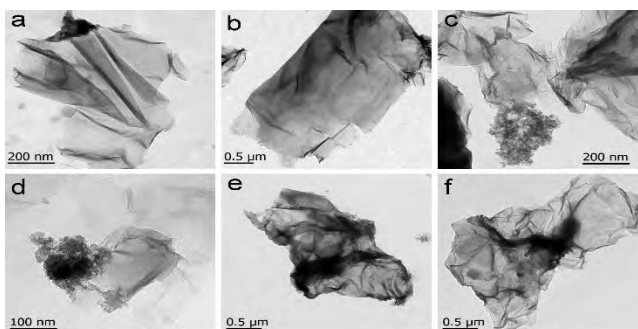


Figure 1. TEM images of (a) GO, (b) rGO, (c-d) KE/GO-1 and (e-f) KE/rGO-1:1.

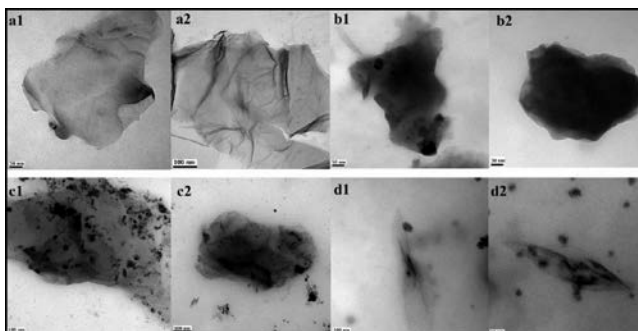


Figure 2. TEM images of: (a) GO, (b) CsGO temperature 1 (55-60°C), (c) CsGO temperature 2 (75-80°C) and (d) CGO temperature 3 (95-100°C).

Conclusions

Natural Polymers as keratin and chitosan, modified the behavior of graphene materials, allowing in this way diversifying their possible applications in composites or templates..

References

1. Jiménez-Cervantes-A. E. et al., *J. of Alloys and Comp.* 2015, 643, S137.
2. Rodríguez-Gonzalez C. et. al. *Digest J. of Nanomater and Biostruc.*, 2012, 8, 127.
3. Bustos-Ramírez K., et al., *Materials* 2013, 6, 911.
4. Rodríguez-Gonzalez et al. . *Ind. & Eng. Chem. Res.* 2012, 51, 3619

SAFER ALTERNATIVES TO OBTAIN GRAPHENE OXIDE.

Eliana Higueta¹, Yuliana Franco², Omar Gutiérrez³

1. Instituto Tecnológico Metropolitano, Street 54a # 30-01, 050001, Medellín, Colombia. elianahigueta94850@correo.itm.edu.co
2. Instituto Tecnológico Metropolitano, Street 54a # 30-01, 050001, Medellín, Colombia.
3. Instituto Tecnológico Metropolitano, Street 54a # 30-01, 050001, Medellín, Colombia.

Introduction

Polymer nanocomposites based on carbon nanostructures have been used for improved mechanical, thermal, electrical, and gas barrier properties of polymers.¹ The discovery of graphene with its combination of extraordinary physical properties and ability to be dispersed in various polymer matrices has created a new class of polymer nanocomposites. On account of the recent emergence of using graphene oxide (GO) to prepare graphene-based materials for composites and other applications, in this work, we propose four novel alternative ways to the Hummer's method² that prevents or reduces the use of NaNO_3 , KMnO_4 , H_2O_2 , BaCl_2 ; in order to obtain graphene oxide by using safer and cheaper synthesis avoiding the use of hazardous species.

Experimental Part

Starting from commercial graphite (FTDT-0197 Quimicos JM S.A), the graphite oxide (GO) was prepared by using four different paths by stirring 5 g of graphite during 1.5 h into: (1) 125 mL of concentrated H_2SO_4 (sln1), (2) 125 mL of concentrated H_2SO_4 (sln2), (3) 100 mL of concentrated HCl (sln3) and (4) 100 mL of concentrated H_2SO_4 (sln4). Then, were added carefully 15 g of KMnO_4 to the sln4 (at 10°C) respectively. In the next step, were added: 500 mL of H_2O_2 (5%) to the sln1, 100 mL of HNO_3 to the solutions sln2 and sln3, and 500 mL of H_2O_2 (5%) to the sln4. These four systems were stirred during 48 hours except for the sln4, which at 12 h was washed with 400 mL of HCl (16%) and abundant deionized water. After that, the four solutions were washed with ammonia and centrifuged (10000 rpm, 10°C , 30 min) until a neutral pH was achieved. The GO's obtained were dried overnight in an oven at 100°C . With the dried GO's thermogravimetric studies were carried out (TA Instruments Q600) at a heating rate of 20 Kmin^{-1} . FTIR spectra (SHIMADZU IRTracer-100) were recorded for raw graphite and the GO's. In order to obtain an exfoliated graphene oxide (TrGO), thermal reductions were carried out using a fixed bed reactor in nitrogen atmosphere (60 mL/min) and a tubular furnace operating at 600°C . 0.5 g of GO were loaded into the reactor. DRX analysis (Siemens D5000) for graphite, GO and TrGO were recorded.

Results and Discussions

The FTIR spectra obtained for graphite and for GO1, GO2 GO3 and GO4 (from solutions sln1, sln2, sln3, y sln4 respectively), show in the GO's the presence of bands associated to functional groups: OH, COOH, COC, CO. This suggest that the four paths work. Nevertheless, the thermogravimetric tests revealed mass losses about 12 %wt for GO1, GO2 and GO3, while a mass loss of 50 %wt was observed for GO4. This difference is attributed to the remarkable oxidizing effect of KMnO_4 even enhanced in

presence of acid solution (H_2SO_4). On the other hand, the other methods do not employ KMnO_4 avoiding violent effervescence during the addition of both KMnO_4 and the H_2O_2 required to reduce the residual permanganate and manganese dioxide to colorless soluble manganese sulfate.³ In addition, another important contribution is the reduction of time consuming by using centrifugation instead of sedimentation for days.

Fig. 1 shows the DRX patterns for graphite, GO4 and TrGO4.

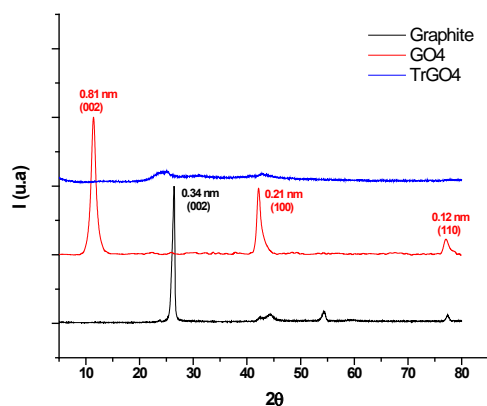


Figure 1. DRX patterns for graphite, GO4 and TrGO4.

From this figure it can be seen that the characteristic peak (plane 002, interplanar distance 0.34 nm) of graphite, appears in GO4 at lower 2θ angles, indicating a separation (0.81 nm) in the sheets of (002) plane.⁴ This peak does not appear for TrGO4, suggesting an exfoliated structure typical of graphene nanosheets.

Conclusions

The implemented methods allow to obtain graphene, nevertheless the fourth method offers a higher oxidation level because the presence of KMnO_4 .

References

1. Meng, L. & Park, S. Preparation and Characterization of Reduced Graphene Nanosheets via Pre-exfoliation of Graphite Flakes. *Bull. Korean Chem. Soc.* **33**, 209–214 (2012).
2. Sun, L. & Fugetsu, B. Mass production of graphene oxide from expanded graphite. *Mater. Lett.* **109**, 207–210 (2013).
3. William S. Hummers, J. & Offeman, R. E. Preparation of Graphitic Oxide. *J. Am. Chem. Soc.* **80**, 1339 (1958).
4. Naebe, M. *et al.* Mechanical Property and Structure of Covalent Functionalised Graphene/Epoxy Nanocomposites. *Sci. Rep.* **4**, 4375 (2014).

EXFOLIACIÓN DE GRAFENO EN FASE LÍQUIDA: PRIMERA ETAPA EN LA PRODUCCIÓN DE NANOCOMPUESTOS EPOXI/GRAFENO

Leonel Ignacio Silva, Juan Pablo Tomba, Carmen Cristina Riccardi*

INTEMA, Facultad de Ingeniería, Universidad Nacional de Mar del Plata, CONICET, Mar del Plata, Argentina.

criccard@fi.mdp.edu.ar

Introducción

El primer reto en la producción de nanocompuestos es tener un control óptimo en la exfoliación del grafeno y su introducción en la matriz polimérica.¹ Con el fin de evitar la aglomeración de las láminas de grafeno son muchos los métodos presentados en la bibliografía, de los cuales la gran mayoría requiere de muchas etapas laboriosas para lograr tal fin.² En este trabajo se presenta un método novedoso que implica la exfoliación de grafito utilizando como fase líquida el prepolímero diglicidil éter de 1,4-butanoediol (DGEBD) tal que permita obtener una dispersión estable. La utilización de este reactivo diluyente persigue dos objetivos: lograr la exfoliación del grafeno aprovechando su baja viscosidad en relación a otros prepolímeros epoxi y finalmente obtener sistemas que presenten una concentración y dispersión adecuada en los nanocompuestos DGEBA/DGEBD-grafeno. En este trabajo nos centraremos en el primer objetivo, comparando los resultados con fases líquidas de uso común como lo son el DMF y NMP. Estos resultados preliminares apuntan a desarrollar un material que combine las propiedades altamente competentes del grafeno, con las virtudes químicas de las resinas epoxi y con el creciente potencial tecnológico de un material final nanoestructurado.

Parte experimental

Se utilizó grafito comercial Sigma-Aldrich y como fase líquida DMF (C_3H_7NO), NMP (C_5H_9NO) y DGEBD (diglicidil éter de 1,4-butanoediol). La exfoliación del grafito se realizó con una batea ultrasónica Elma-Elmasonic P60H: frecuencia:37kHz, potencia: 100%, ondas:Sweep. El baño de agua se mantuvo a $T \leq 30^\circ C$. La tensión superficial (γ) se calculó utilizando un Goniómetro Ramé Hart con el método "pendant drop". Los espectros de absorción UV-VIS fueron adquiridos con un espectrofotómetro Shimatzu PC 160^a PLUS UV-VIS.

Resultados y discusiones

En la Fig. 1 se presentan las dispersiones estables obtenidas de grafeno en cada uno de los solventes utilizados, luego de 12h de sonicación. Con los valores experimentales de coef. de absorción, α , (ver Tabla 1) y aplicando la ley de Beer se obtuvieron las curvas de concentración, C de grafeno vs. tiempo de sonicación (ver Fig.2). En promedio se observa un incremento aprox. de 200% cuando se triplica la C inicial de grafito (de C3 a C9). Se obtuvo alta C. de grafeno utilizando como fase líquida el DGEBD, de lo cual no hay referencias en la bibliografía. Esto

último es un resultado auspicioso en la futura producción de nanocompuestos epoxy/grafeno.

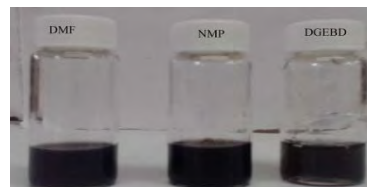


Figure 1. Dispersiones estables de grafeno en NMP, DMF y DGEBD.

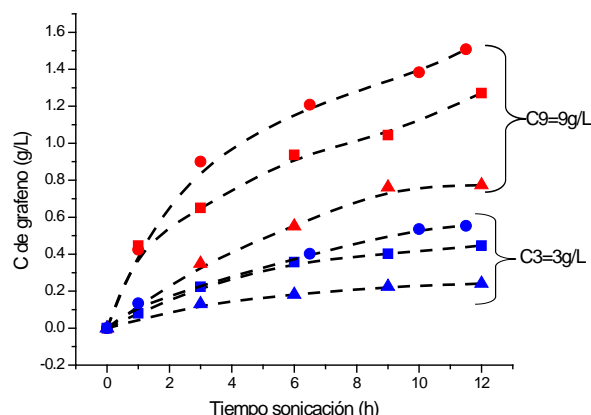


Figure 2. C de grafeno vs. tiempo de sonicación. (●) NMP, (■) DMF y (▲) DGEBD. $C_0 = C$. inicial de grafito.

Table 1. Tensión superficial (γ), coef. de absorción (α) y C. final de grafeno (C9)

Solvente	γ (mJ/m ²)	α (L/gm)	C9 (g/L)
DMF	37	1120.3	1.5
NMP	42	2241.3	1.3
DGEBD	43	2362.8	0.8

Conclusions

El DGEBD puede ser utilizado para obtener grafeno utilizando el método de exfoliación en fase líquida ya que: 1) se obtuvieron dispersiones estables, 2) su valor de γ lo define como "buen solvente" y 3) las concentraciones finales de grafeno son del orden a las obtenidas con solventes de uso común.

References

- Kim, H., *Macromolecules*, **43**, 6515-6530, 2010
- Hernandez, Y., *Nat. Nanotechnol.*, **3**, 563-568, 2008.

ORDENAMIENTO EN FILMS DELGADOS DE COPOLÍMERO BLOQUE BAJO CO₂ SUPERCRÍTICO

Anabella A. Abate¹, Cristian M. Piqueras², Marcelo A. Villar², Daniel A. Vega¹

¹Instituto de Física del Sur, (IFISUR, UNS-CONICET), Universidad Nacional del Sur, Av. Alem 1253, (8000) Bahía Blanca, Argentina dvega@uns.edu.ar

²Planta Piloto de Ingeniería Química (PLAPIQUI; UNS-CONICET), Camino “La Carrindanga” Km 7, (8000) Bahía Blanca, Argentina.

Introducción

El desarrollo de patrones nanométricos basados en el autoensamblado es considerado en la actualidad como una de las rutas más prometedoras para reemplazar tecnologías litográficas de alta resolución, tales como litografía con rayos X, haces de electrones o por interferencia. En particular, los copolímeros bloque han recibido gran atención no sólo debido a la escala de sus dominios (nanómetros) y su diversidad de propiedades (velocidad de ataque químico diferencial, permitividad dieléctrica controlada, etc.), sino a la gran simplicidad que tienen para sintonizar tanto el tamaño como la forma de sus dominios, simplemente modificando la composición, masa molar o su arquitectura. En la actualidad este tipo de materiales está siendo ampliamente utilizado en una gran diversidad de aplicaciones que van desde el desarrollo de máscaras para litografía y aplicaciones fotónicas o fonónicas al desarrollo de nano-objetos, materiales porosos y membranas moleculares para filtración de virus y screening de ADN.^{1,2,3}

En este trabajo se estudia el ordenamiento de monocapas y bicapas copolímeros tribloque asimétricos en base poli(estireno-*b*-butadieno-*b*-estireno) (SBS) con microestructura cilíndrica en un medio de dióxido de carbono supercrítico (scCO₂).

Esquema Experimental

Se utilizó un copolímero tribloque SBS de Sigma-Aldrich con una masa molar promedio en peso (Mw) de 140.000 g/mol. Las muestras se prepararon sobre sustratos de silicio por el método de *spin-coating* y se sometieron a una atmósfera de dióxido de carbono a 40 °C y 80 bar, condiciones en las cuales el ambiente se encuentra en estado supercrítico. La caracterización del film se realizó mediante microscopía de fuerza atómica (AFM) en modo *tapping* en un microscopio Innova-Bruker.

Resultados y discusión

En la Fig. 1a se muestra una imagen de AFM (fase) de una monocapa de copolímero antes del tratamiento en scCO₂. En este caso el patrón muestra una estructura desordenada, con los cilindros de PS (fase minoritaria) orientados en dirección paralela a la superficie del sustrato de silicio. Luego de 2 hs de tratamiento, se observa que el copolímero se reorientó en dominios cilíndricos verticales perpendiculares al sustrato de silicio (Fig. 1b).

Este comportamiento puede atribuirse al efecto “plastificante” del scCO₂ en los polímeros sintéticos, en el cual el scCO₂ se disuelve y difunde a través de las moléculas provocando un hinchamiento (*swelling*) del material. Este hinchamiento viene acompañado de la ruptura de las interacciones entre cadenas del copolímero, lo cual incrementa la movilidad de las cadenas varios órdenes de magnitud respecto del polímero en su estado original y permite al sistema reorientar sus dominios de modo de minimizar su energía.

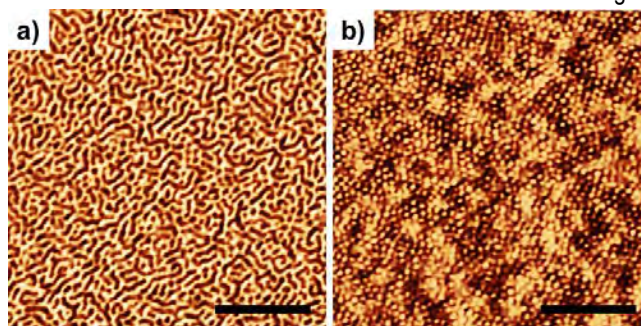


Figura 1. Imagen AFM (fase) de una monocapa de SBS sobre sustrato de Si a) condición inicial, b) luego de 2 hs en scCO₂. La escala corresponde a 500nm.

Conclusiones

Para la mayoría de las aplicaciones tecnológicas basadas en autoensamblado molecular la presencia de diferentes tipos de defectos limita fuertemente su aplicabilidad. En este trabajo se ha observado que tratamientos térmicos suaves scCO₂ permitirían tanto acelerar notoriamente la velocidad de ordenamiento y remoción de defectos como controlar la orientación de las nanoestructuras con respecto al sustrato.

Referencias

1. C. M. Piqueras, V. Puccia, D. A. Vega, M. A. Volpe. Applied Catalysis B: Environmental, 2016, 185, 265.
2. N. A. García, R. L. Davis, S. Y. Kim, P. M. Chaikin, R.A. Register, D. A. Vega. RSC Advances, 2014, 38412.
3. E. A. Matsumoto, D. A. Vega, A. D. Pezzutti, N. A. García, P. M. Chaikin, R. A. Register, PNAS (Proc. Natl. Acad. Sci. USA) 2015, 112, 12639.

TRANSFORMING PHYTOCHEMICAL WASTE FROM COLOMBIAN SUGARCANE MILLS INTO POLYMERS WITH ADDED-VALUE

Lina M. Delgado¹, Constain H. Salamanca², Guillermo L. Montoya², Giovanni Rojas¹

1. Universidad Icesi, Facultad de Ciencias Naturales, Departamento de Ciencias Químicas, Calle 18 No 122-135, Cali, Colombia grojas@icesi.edu.co.
2. Universidad Icesi, Facultad de Ciencias Naturales, Departamento de Ciencias Farmacéuticas, Calle 18 No 122-135, Cali, Colombia.

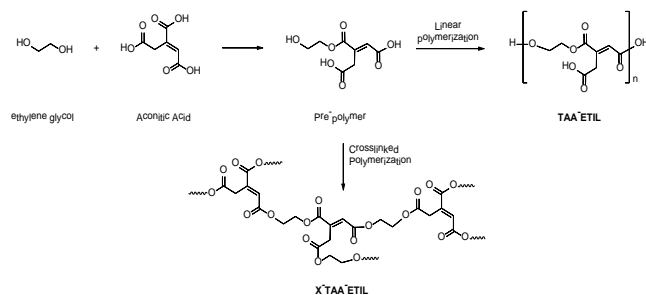
Introduction

Sugarcane is the major source of jobs and wealth in the southwest of Colombia, producing more than two million tons of high quality sugar per year.¹ Although the business is prospering, investigating new products and materials arisen from the sugar industry is just natural. Our interdisciplinary work led to the discovery of new organic products (phytochemicals) such as aconitic acid along the industrial sugar extraction process, which is comparable with other sugarcane industries around the world, for example South Africa and Australia.²

In this work we employed different routes for the synthesis of polymeric materials from aconitic acid, yielding a variety of materials with tunable physical and chemical properties. Traditional wet chemistry, using solvents produced a set of tailor-made linear, branched and cross-linked polymers. Additionally, we present a set of more environmental friendly materials obtained from “green chemistry techniques” that avoid the use of organic solvents and employ clean-power-sources.

Experimental Part

Polyesters from aconitic acid and ethylene glycol were obtained via microwave polymerization at various reaction times 5, 15, 30 and 60 minutes. In comparison, traditional wet chemistry was also used for the controlled polymerization employing a reported methodology.³



Scheme 1. Products obtained from both synthetic route

Results and Discussions

The use of microwave irradiation has a number of advantages over conventional heating methods, usually polymerization is achieved at significantly shorter reaction times, preventing side reactions and homogeneous heating is obtained⁴

Table 1. Reaction conditions, name of products and Solubility of the obtained polymers.

Monomers	Time	Cross-linked	Lineal	Name	Solubility
	5 min	X		X-TAA-ETIL5	Partially soluble ^{1,2}
	15 min	X		X-TAA-ETIL15	Partially soluble ^{1,2}
	30 min	X		X-TAA-ETIL30	Insoluble
	60 min	X		X-TAA-ETIL60	Insoluble
	1h		X	TAA-ETIL1H	Soluble ³
	24h		X	TAA-ETIL24H	Soluble ³
	48h		X	TAA-ETIL48H	Soluble ³

All materials were analyzed by FTIR and DSC to follow the reaction progress and identified his thermal behavior.

Thermal analysis of polymers obtained via microwave irradiation showed the presence of a glass transition, suggesting that all materials are cross-linked and amorphous. Although polymers obtained via wet chemistry are expected to be linear structures also showed glass transition. Regardless the absence of a melting transition, solubility of polymers in organic polar solvents suggested that they are linear structures. We currently are performing more analysis to verify their primary structure.

Conclusions

Synthesis of polyesters from *trans*-aconitic acid and ethylene glycol was performed using two synthetic routes, the first mediated microwave irradiation and the second best known as wet or traditional chemistry, yielding crosslinking and linear polyesters respectively.

We are currently working on the primary structure characterization of the linear polymer which in essence are linear models of the microwave obtained crosslinked polymers.

References

1. Montoya, G., Londoño, J., Cortes, P., Izquierdo, O., *Journal of Agricultural and Food Chemistry*, **2014**, 8314-8318.
2. Rein, P., *Cane Sugar Engineering*, **2007**, Verlag, Berlin, 465pp
3. Zuluaga, F., Valderruten, N. E., & Wagener, K. (1999). The ambient temperature synthesis and characterization of bile acid polymers. *Polymer Bulletin*, 41-46.
4. Sinnwell, S., & Ritter, H. (2007). Recent Advances in Microwave-Assisted Polymer Synthesis. *Aust. Journal of Chemistry*, 729-743.

CASE STUDY: REINFORCED DROP-IN BIOPLASTIC COMPOSED OF GREEN HDPE, CELLULOSE AND LIGNIN

Marco Aurelio De Paoli¹, Renan Gadioli¹, Walter R Waldman²

1. *Polymer Processing Laboratory, Chemistry Institute, Unicamp, Campinas, Brasil mdepaoli@iqm.unicamp.br*
2. *Department of Physics, Chemistry and Mathematics, UFSCar, Sorocaba, Brasil.*

The polymer industry used renewable resources until the middle of the last century to obtain monomers and additives. The second part of the 20th Century saw a tendency to use petrochemicals to substitute these raw materials. This trend reversed with the pressure to reduce the dependence on petrochemicals and to preserve the environment, and the future will see a growing use of renewable resources by the polymer industry.

In the area of polymer additives, these resources presently include: monomers, biocides, pigments, dyes, plasticizers, lubricants, reinforcing agents and anti-oxidants.

This key lecture will focus on the use of cellulose fibers as reinforcing agent and lignin as primary anti-oxidant for green high-density polyethylene (HDPE l'm Green, Braskem).

Drop-in bioplastics are non-biodegradable materials, derived from renewable raw materials offering identical technical properties to their fossil fuel based counterparts.¹

Acknowledgment: Authors acknowledge financial support from FAPESP under grant Nr. 2010/17804-7 and Green HDPE sample from Braskem.

Reference

1. FA Oroski, FC Alves, JV Bomtempo, "Bioplastics Tipping Point: drop-in or non drop-in ?", *Journal of Business Chemistry* 2014, 11, 43 -50.



THE OPTIMIZATION OF LACCASE IMMOBILIZATION CONDITIONS ONTO TWO DIFFERENT POLYMERIC MICROSPHERES BY RESPONSE SURFACE METHODOLOGY

Myleidi Vera ¹, Bernabé L. Rivas ¹

1. University of Concepción, Casilla 160-C, 4030000, Concepción, Chile. mylevera@udec.cl

Introduction

Laccases (E.C. 1.10.3.2) are extracellular enzymes able to catalyze the oxidation of a wide range of recalcitrant compounds because of their high specificity, activity and selectivity. However, the use of free enzymes for practical applications may be hampered by their low stability, high sensibility and easy losses of its activity. Many of these problems can be overcome using enzymatic immobilization.¹ Laccase has been successfully immobilized onto different supports, but the polymeric microspheres is mostly preferred, due to its high surface to volume ratio and the easy of synthesis. In general, the supports can react with amine or with aldehyde and carboxylic acid groups in the enzyme.² However, in order to optimize the enzymatic immobilization process, is important to determine the best support and the laccase immobilization conditions. In this work, polymeric microspheres with oxirane and hydrazide groups were synthesized by dispersion polymerization. Then, these spheres were used as support for laccase immobilization and some factors were optimized using the Box-Behnken design (BBD). Finally, the immobilized enzymes onto each support, were compared among themselves and with the free enzymes.

Experimental Part

Synthesis of monodisperse polymeric microspheres

Microspheres with oxirane groups were synthesized using dispersion polymerization. For this purpose, glycidyl methacrylate reacted in methanol for 8 h at 65 °C, using magnetic stirring. The hydrazide-functionalized microspheres were obtained dispersing the poly(glycidyl methacrylate) P(GMA) microspheres in hydrazine hydrate overnight. The microspheres were analyzed prior to and after the reaction by SEM and FTIR.

Immobilization of laccase onto microspheres

For immobilization of *Trametes versicolor* laccase onto two types of supports, the response surface methodology was used and BBD with 3-factors, 3-levels was employed for the optimization study. The factors were pH, contact time and amount of enzyme. The immobilization was analyzed by UV-Vis spectroscopy.

Results and Discussions

The P(GMA) microspheres were successfully obtained, and some of them were modified for replace oxirane group for hydrazide

group as is show in the Fig. 1. Furthermore, for SEM was possible to verify the average size (2.96 μm) and the polydispersity (0.013).

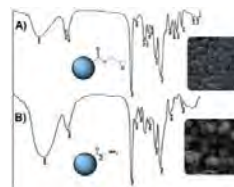


Figure 1. IR and SEM of A) P(GMA) microspheres and B) P(GMA) hydrazide-functionalized microspheres.

The enzyme immobilization was carried out according to the conditions given for the statistical design. The response surface methodology gave the best conditions for each support, such as is shown in Fig. 2. The optimization shows that the best support for *Trametes versicolor* immobilization is the P(GMA) microspheres, and the better conditions are: pH = 4.26, contact time = 1.3 h, and amount of enzyme = 11.05 μg/μL, with these conditions, the maximum immobilization efficiency was 83.4 %.

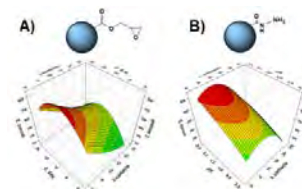


Figure 2. Response surface of immobilization efficiency for each support.

Conclusions

Based on the optimization study it was possible determine that P(GMA) microspheres are the best support for enzyme immobilization and the better conditions generate an immobilization efficiency of 83.4 %.

Acknowledgment: Myleidi Vera wish to thank to CONICYT 2015 PhD national scholarship folio: 21150178 for financial support.

References

- Prasetyo, E.; Semlitsch, S.; Nyanhongo G.; Lemmouchi, Y.; Guebitz, G. *Chemosphere* 2016, 144, 652.
- Dogan, T.; Bayram, E.; Uzun, L.; Senel, S.; Denizli, A. *J. Appl. Polym. Sci.* 2015, 132, 41981.

MONODISPERSE MICROSPHERES OF GLYCIDYL METHACRYLATE AS POLYMERIC SUPPORT FOR LACCASE IMMOBILIZATION

Myleidi Vera¹, Bernabé L. Rivas¹

1. University of Concepción, Casilla 160-C, 4030000, Concepción, Chile. mylevera@udec.cl

Introduction

Laccases are enzymes able to catalyze the oxidation of a wide variety of substrates with higher redox potentials; for that reason, these are used for degradation of a variety of contaminant compounds. However, the immobilization of this enzyme is more cost-effective, it offers the possibility of the adaptability to engineering design and reuse in large scale than free enzymes.¹ Therefore, a continuous interest has been centered in the enzymatic immobilization, and laccase enzymes have been immobilized on various supports but monodisperse spheres are mostly preferred, due to its maximum surface to volume ratio. Thereby, solid spheres in the micron range could be optimal due its higher outer surface area available for enzyme immobilization.²

In this work, microspheres of poly(glycidyl methacrylate), P(GMA), were synthesized by dispersion polymerization, and used for covalent immobilization of *Trametes versicolor* laccase based on the substitution reaction between epoxy groups in the support and amino groups of the enzyme. The influence of several parameter such as temperature, pH, contact time, etc. on the enzymatic activity were evaluated for both free and immobilized enzymes using ABTS as substrate.

Experimental Part

Synthesis of monodisperse microspheres of P(GMA)

Monodisperse microspheres of P(GMA) were synthesized using dispersion polymerization. For this purpose, glycidyl methacrylate in methanol media reacted with magnetic stirring for 8 h at 65 °C, in a nitrogen atmosphere. The microspheres obtained were analyzed by SEM and FTIR.

Immobilization of laccase onto microspheres

For the immobilization of *Trametes versicolor* laccase, approximately 10 mg of P(GMA) microspheres were immersed in a laccase solution at 4.26 pH value. The reaction was carry out in a shaker at room temperature for 1 h. Finally, the microspheres were washed 3 times with buffer solution and stored at 4 °C. The immobilization was analyzed by UV-Vis spectroscopy.

Activity studies for free and immobilized laccase

The activity of both free and immobilized laccases was determinate spectrophotometrically at 420 nm, using ABTS as the substrate.

Finally, studies of effect of pH and temperature were carry out in a wide pH (2-6) and temperature (20-70 °C) range.

Results and Discussions

The P(GMA) microspheres obtained by dispersion polymerization had a low polydispersity (0.013) and an average size of 2.96 µm as is show in the Fig. 1. These microspheres features make them the ideal solid support for laccase immobilization.

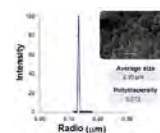


Figure 1. Monodisperse microspheres of P(GMA), size range and polydispersity.

Once synthesized the microspheres, *Trametes versicolor* laccases were covalently attached by nucleophilic attack of amino groups of enzyme to the epoxy groups of the P(GMA) microspheres as shown in Scheme 1. The immobilization efficiency obtained was of 84 %. Furthermore, immobilized enzymes shows better properties of stability and resistance to pH and temperature than free enzymes.



Scheme 1. Reaction of enzyme with the oxirane group in P(GMA) microspheres

Conclusions

Dispersion polymerization is great strategy in order to obtain polymeric spheres in the micron range with high monodispersity. Furthermore, the spheres obtained by this method are ideal for enzyme immobilization of *Trametes versicolor*. Finally, the immobilized enzymes onto these support have better properties than free enzymes.

Acknowledgment: Myleidi Vera wish to thank to CONICYT 2015 PhD national scholarship folio: 21150178 for financial support.

References

1. Pang, S.; Wu, Y.; Zhang, X.; Li, B.; Ouyang, J.; Ding, M. *Process Biochem* 2016, 51, 229.
2. Ammann, E.; Gasser, C.; Hommes, G.; Corvini, P. *Environ Biotechnol* 2014, 98, 1397.

EFFECT OF CHITOSAN-BASED EDIBLE COATINGS WITH NATURAL COMPOUNDS ON THE MICROBIAL PRESERVATION OF MINIMALLY PROCESSED STRAWBERRIES

Bárbara Tomadoni¹, Mirna A. Mosiewicki², Mariana Pereda², Alejandra Ponce¹

1. GIA, CONICET, UNMdP, Av. Juan B. Justo 4302, 7600, Mar del Plata, Argentina. bmtomadoni@fi.mdp.edu.ar

2. INTEMA, CONICET, UNMdP, Av. Juan B. Justo 4302, 7600, Mar del Plata, Argentina.

Introduction

Strawberry (*Fragaria ananassa*) is a non-climacteric fruit with a very short postharvest life, susceptible to physiological disorders, mechanical damages, infections caused by pathogens and mainly deterioration by fungi. One strategy to extend the shelf-life of fresh-cut fruits are edible coatings derived from biopolymers, such as chitosan (CH) which has been proven to have good antifungal properties for food protection. Active ingredients can be incorporated into the edible coatings to enhance both safety and nutritional quality of the product. Hence, the objective of the present study was to evaluate the effect of the incorporation of vanillin (V) and geraniol (G) into chitosan-based edible coatings on fresh-cut strawberry microbial quality.

Experimental Part

CH film-forming solutions were prepared according to Pereda *et al.*¹, and glycerol (Gly) content was added to achieve a Gly/CH ratio of 0.28. For the composite solutions, V and G were applied at 2 and 4 times MIC (Minimum Inhibitory Concentration) which was previously determined by Tomadoni *et al.*². V was dissolved in ethanol before being incorporated in the CH solution. On the other hand, G was applied directly into the CH solution and stable emulsions were formed by using an UltraTurrax. Strawberries treatment consisted in a washing step (immersion in tap water for 2 min), followed by destemming and cutting in halves. Subsequently, strawberry halves were immersed in the different film-forming solutions for 2 min at 20 °C and then the remaining liquid was allowed to drain. Samples were stored for 7 d under refrigerated conditions (5 °C). At 0, 2, 5 and 7 days, mesophilic bacteria (MES, 34 °C, 24 h) and yeast and moulds counts (YM, 25 °C, 5 d) were evaluated according to Ponce *et al.*³.

Results and Discussions

The effects of CH-based edible coatings on the native microflora of strawberries are shown in Fig. 1. No significant differences were found on MES between the treated and the control samples throughout storage time (Fig. 1a). With regards to YM counts, every treatment was effective in reducing YM at day 0 (2 log reductions compared to untreated samples) (Fig. 1b). Control samples showed an increase in YM with storage time, while every coating showed a reduction of about 2 log, particularly CH+G4MIC which turned out to be the most effective (YM <2 log by the end of storage) (Fig. 1b).

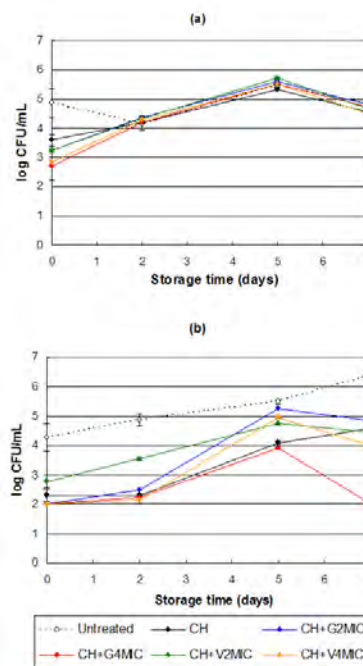


Figure 1. Native microflora evolution in fresh-cut strawberries treated with CH-based edible coatings enriched with vanillin and geraniol: (a) mesophilic bacteria; (b) yeast and molds.

Conclusions

Results showed that the incorporation of vanillin into chitosan-based edible coatings was not able to improve its antimicrobial properties; however, G4MIC was able to enhance the microbial quality of the fresh-cut fruits compared to both untreated samples and CH-pure coatings. Further studies are being performed to assess the effects on nutritional and sensorial quality. At the same time, physical and structural properties of the films will be analyzed.

Acknowledgment: CONICET, ANPCyT, UNMdP

References

- Pereda, M.; Aranguren, M.I.; Marcovich, N.E. *J. Appl. Polymer* 2008, 107(2), 1080.
- Tomadoni, B.; Cassni, L.; Moreira, M.R.; Ponce, A. *LWT- Food Sci. Technol.* 2015, 64(2), 554.
- Ponce, A.G.; Agüero, M.V.; Roura, S.I.; del Valle, C.E. *J. Food Sci.* 2008, 73, 257.



ESTUDIO DE LA DEGRADACIÓN DE BOLSAS CON ADITIVO PRO-OXIDANTE IRRADIADAS CON RADIACIÓN GAMMA MEDIANTE PROPIEDADES MECÁNICAS

Jenny Aguilar ¹, Maribel Luna ², Vladimir Valle ¹, Miguel Aldás ¹

1. Escuela Politécnica Nacional, Departamento de Ciencia de Alimentos y Biotecnología, Ladón de Guevara E11-253, Quito, Ecuador. miguel.aldas@epn.edu.ec
2. Escuela Politécnica Nacional, Departamento de Ciencias Nucleares, Ladón de Guevara E11-253, Quito, Ecuador

Introducción

El consumo de plástico en el mundo ha incrementado en las últimas décadas, sobre todo en los “productos denominados de un solo uso” como las bolsas plásticas de supermercado; las cuales luego de desechadas, se disponen en rellenos sanitarios y botaderos, pudiendo permanecer intactas por años¹. Por este motivo, los aditivos pro-oxidantes fueron desarrollados para acelerar la rotura de las cadenas de polímeros como el polietileno. Existen investigaciones que respaldan su eficacia mientras otras indican que la activación del aditivo necesita obligatoriamente factores como el calor, la radiación ultravioleta y la sollicitación mecánica^{2,3}. Algunos autores han estudiado el efecto de la radiación ionizante en el comportamiento del polietileno, por lo cual este trabajo tiene como objetivo determinar el efecto de la radiación gamma en la activación del aditivo pro-oxidante de bolsas de supermercado^{4,5}.

Parte Experimental

Se analizó el efecto de la fuente de Co-60 a dosis de 5 y 10 kGy sobre las propiedades mecánicas de bolsas con aditivo pro-oxidante de dos casas comerciales diferentes (muestras A1 y A2), junto a una degradación acelerada en cámara de arco de Xe. Además, se analizó una bolsa plástica sin aditivo como patrón de referencia (muestra N1). La degradación acelerada se llevó a cabo en la cámara de arco de xenón Q-SUN Xe-1-S bajo norma ASTM D5071 ciclo 1. Para la determinación del porcentaje de elongación de las probetas se siguió la norma ASTM D 882. Se usó un equipo de ensayos universales INSTRON 1011. Los ensayos se realizaron a una velocidad de elongación constante de 500 mm/min, con una celda de carga de 0,5 kN.

Resultados y Discusión

La Fig. 1 indica el aumento en el porcentaje de elongación promedio de probetas de las bolsas A1, A2 y N1 irradiadas en fuente de Co-60 a las dosis de 5 y 10 kGy. La desviación estándar de este grupo de probetas indica una dispersión grande en las mediciones. Se puede observar que después de la irradiación de las probetas, el porcentaje de elongación de las mismas aumenta, tanto en las bolsas con aditivo pro-oxidante como las que no contienen este aditivo. La bolsa sin aditivo (N1) tuvo el mayor incremento en esta propiedad respecto a las bolsas con aditivo pro-oxidante, contrario a lo esperado según Ferreto, Oliveira, Lima, Parra y Lugão (2012), cuyo estudio indica que el porcentaje de elongación a la rotura de PE sin aditivo pro-

oxidante, a 5 y 10 kGy, disminuye al ser irradiados con radiación gamma¹⁰.

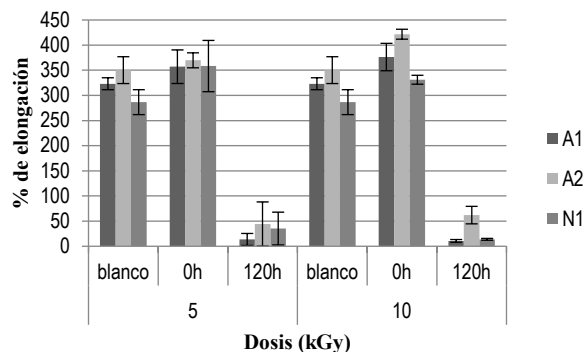


Figura 1. Variación en el porcentaje de elongación a la rotura de las bolsas (A1, A2 y N1) sometidas a radiación en fuente de Co60 a 5 y 10 kGy y a 120 h de degradación acelerada en cámara de arco de Xe

Al final del experimento, el % de elongación de las probetas cayó a valores alrededor del 50% incluso en las probetas sin aditivo pro-oxidante.

Conclusiones

La aplicación de radiación gamma provocó que el PEAD sin aditivo pro-oxidante, tenga una degradación comparable al PEAD con este aditivo. Se determinó que, si bien las propiedades mecánicas de las muestras decaen en gran medida, éstas todavía no se encuentran totalmente degradadas.

Referencias

1. Castillo M. *Consultoría Para La Realización de Un Estudio de Caracterización de Residuos Sólidos Urbanos Domésticos Y Asimilables a Domésticos Para El Distrito Metropolitano de Quito*. Quito; 2010.
2. Muniyasamy S, Corti A, Chiellini E. *Oxo-Biodegradation of Full Carbon Backbone Polymers*. Alemania: LAP LAMBERT; 2012.
3. Quiroz F, Cadena F, Sinche L, Chango I, Aldás M. Estudio de la degradación en polímeros oxo-biodegradables. *Rev politécnica*. 2009;30(1):180-192.
4. Bardi MAG, Kodama Y, Giovedi C, Rosa DS, Machado LDB. Effect of ionizing radiation on mechanical and thermal properties of low-density polyethylene containing pro-degradant agents. *Int Nucl Atl Conf*. 2009;12.
5. Moez a A, Aly SS, Elshaer YH. Effect of gamma radiation on low density polyethylene (LDPE) films: optical, dielectric and FTIR studies. *Spectrochim Acta A Mol Biomol Spectrosc*. 2012;93:203-207.



ESTUDIO DE LA DEGRADACIÓN DE BOLSAS CON ADITIVO PRO-OXIDANTE IRRADIADAS CON RADIACIÓN GAMMA MEDIANTE ESPECTROFOTOMETRÍA DE INFRARROJO

Jenny Aguilar ¹, Maribel Luna ², Vladimir Valle ¹, Miguel Aldás ¹

1. Escuela Politécnica Nacional, Departamento de Ciencia de Alimentos y Biotecnología, Ladón de Guevara E11-253, Quito, Ecuador. miguel.aldas@epn.edu.ec

2. Escuela Politécnica Nacional, Departamento de Ciencias Nucleares, Ladón de Guevara E11-253, Quito, Ecuador

Introducción

Algunos estudios académicos y de empresas privadas buscan determinar formulaciones y condiciones óptimas de bolsas plásticas aditivadas, que faciliten su degradación en tiempos más cortos respecto a plásticos comunes^{1,2}. Una de las técnicas utilizadas para el seguimiento de la degradación es registrar el incremento de grupos funcionales propios de la degradación como grupos carbonilos en las cadenas poliméricas. Por otro lado, la radiación ionizante es un tipo de energía que tiene la capacidad de excitar los átomos de la material y romper enlaces, por lo que en este trabajo se decidió utilizarla como un catalizador para la activación del aditivo pro-oxidante y la correspondiente degradación del polímero^{3,4}.

Parte experimental

Se utilizaron bolsas de PEAD, las cuales contienen aditivos pro-oxidantes en su formulación (Muestras A1 y A2). Además, se utilizó una muestra que no contenía aditivo pro-oxidante para comparación (Muestra N1). La irradiación se realizó en la fuente de Co-60 a dos dosis absorbidas: 5 y 10 kGy. Después, se sometió las probetas irradiadas a una degradación acelerada en una cámara de arco de xenón bajo norma ASTM D5071 ciclo 1. Las muestras de las bolsas plásticas permanecieron dentro de la cámara de Xe durante 1 000 h. Se analizó la degradación por medio de espectroscopía infrarroja por transformadas de Fourier (FTIR), en el espectrofotómetro marca PERKIN ELMER modelo Spectrum One. El ensayo se hizo por transmitancia. A partir de los espectros obtenidos se calculó el índice de carbonilo, como se indica en la Ecuación 1, relacionando las áreas de los picos entre 1 800 a 1 600 cm⁻¹ (área de grupos carbonilos) respecto al área de referencia de 2 096 a 1 978 cm⁻¹.

$$I_{CO} = \frac{\text{Área entre } 1800 \text{ a } 1600 \text{ cm}^{-1}}{\text{Área entre } 2096 \text{ a } 1978 \text{ cm}^{-1}} \quad \text{Ec.(1)}$$

Discusión de resultados

La figura 1 muestra que después de irradiadas en la fuente de Co60 (0 h), las probetas exhiben un leve incremento del índice de carbonilo. Esto indica que la radiación ionizante ioniza las moléculas de polietileno (PE) y permite que el aditivo pro-oxidante reaccione y produzca roturas en la cadena, y por ende la formación de nuevos grupos radicales. El efecto de degradación acelerada de la cámara de Xe produce un incremento del índice

de carbonilo hasta 2,6924 en la bolsa sin aditivo y 2,6379 en la bolsa con aditivo A1 con una dosis de 5 kGy. Además, se puede notar que, a las 750 h disminuye el índice de carbonilo para volver a aumentar a las 1 000 h de exposición. Esta aleatoriedad en la formación de radicales carbonilo se puede deber a la posterior formación de grupos hidroxilos (lo que hace que la tendencia de la curva descienda) y la nueva formación de nuevos grupos carbonilo en otras regiones de la cadena polimérica (lo que incrementa el índice de carbonilo).

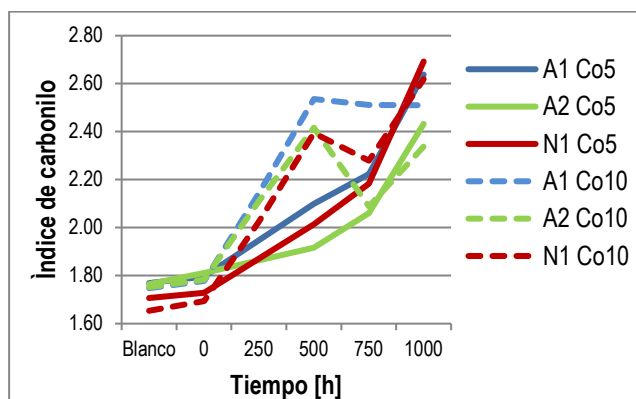


Figura 1. Variación en el índice de carbonilo de muestras irradiadas en fuente de Co-60 y degradadas en cámara de Xe

Conclusiones

La radiación ionizante de la fuente de Co-60, a dosis bajas, inicia un proceso degradativo en bolsas plásticas de PEAD con y sin aditivo pro-oxidante. Las bolsas plásticas irradiadas y que no contienen aditivo pro-oxidante, sufren una degradación mayor a aquellas que sí contienen este aditivo.

Referencias

- Muniyasamy, S., Corti, A., y Chiellini, E. (2012). Oxo-biodegradation of Full Carbon Backbone Polymers. Alemania: LAP LAMBERT.
- Quiroz, F., Cadena, F., Sinche, L., Chango, I., y Aldás, M. (2009). Estudio de la degradación en polímeros oxo-biodegradables. Revista Politécnica, 30(1), 180–192.
- Drobny, J. G. (2013). Ionizing radiation and polymers: principles, technology, and applications. Oxford: Elsevier Inc.
- Makuuchi, K., y Cheng, S. (2012). Radiation processing of polymer materials and its industrial applications. New Jersey: Jhon Wiley y Sons.



STRESS TRANSFER QUANTIFICATION IN GELATIN-NANOFIBRILLATED CELLULOSE COMPOSITES BY RAMAN SPECTROSCOPY

Franck Quero¹, Stephen J. Eichhorn², Javier Enrione³

1. Department of Materials Science, Faculty of Physical Sciences and Mathematics, Universidad de Chile, Beauchef 851, 8370456 Santiago, Chile. fquero@ing.uchile.cl
2. College of Engineering, University of Exeter, Exeter EX4 4QL, United Kingdom.
3. Biopolymer Research and Engineering Lab (BiopREL), School of Nutrition and Dietetics, Faculty of Medicine, Universidad de los Andes, Av. Monseñor Álvaro del Portillo 12.455, 7620001 Las Condes, Santiago, Chile.

Introduction

Currently there is no information available in the literature about the micromechanical interaction or stress transfer between gelatin and nanofibrillated cellulose (NFC). A relevant method to quantify the micromechanical interaction between cellulose and a surrounding polymer matrix is Raman spectroscopy. This method consists in following the shift towards a lower wavenumber of a Raman band belonging to cellulose initially located at $\sim 1095\text{ cm}^{-1}$ upon external tensile deformation.¹ Recently, it has been demonstrated that stress transfer from gelatin to bacterial cellulose can be quantified by Raman spectroscopy.²

Experimental Part

Gelatin-NFC composite films were fabricated by adding never-dried NFC into a 7 w/v % solution of bovine or salmon gelatin. The pH was then adjusted to 7. The suspension was subsequently sonicated and poured into polystyrene Petri dishes and subsequently obtained by solvent casting at 5°C . A Renishaw Raman spectrometer (RM 1000 system), having a 785 nm wavelength laser, was utilized. Composite films having dimensions of $\sim 20 \times 9 \times 0.3\text{ mm}$ containing 15 wt.% NFC were deformed in tensile mode using a deformation rig. A Raman spectrum was obtained at each 0.2 % increment. The positions of the Raman band located at $\sim 1095\text{ cm}^{-1}$ were plotted as a function of tensile strain and stress. In order to quantify the micromechanical interaction, the data were fitted with linear fits and the slope reported, expressed in $\text{cm}^{-1}\%$ and $\text{cm}^{-1}\text{ GPa}^{-1}$, is a measure of the micromechanical interaction between gelatin and NFC. Experiments were repeated in triplicate.

Results and Discussions

Figure 1 reports typical detailed shifts in the position of the Raman band initially located at $\sim 1095\text{ cm}^{-1}$ as a function of stress for bovine and salmon gelatin-NFC composites. Stress transfer, although it was lower compared to stress transfer from bovine gelatin to bacterial cellulose, was found to occur from gelatin to NFC. As a function of stress, a significant difference was observed for the composites materials prepared using bovine or salmon gelatin at pH 7 as shown in Figure 1. Values of -27 ± 3

$\text{cm}^{-1}\text{ GPa}^{-1}$ and $-18 \pm 2\text{ cm}^{-1}\text{ GPa}^{-1}$ were obtained respectively for bovine and salmon gelatin-NFC 15 wt.% composite films. This may be attributed to a “softer” interface that may form in these conditions between salmon gelatin and NFC compared to bovine gelatin and NFC.

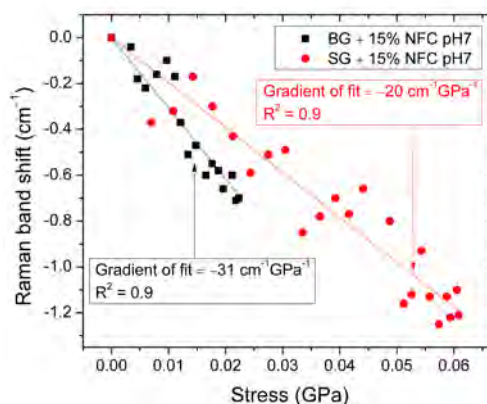


Figure 1. Typical shifts in the position of the Raman band initially located at $\sim 1095\text{ cm}^{-1}$ as a function of stress for bovine and salmon gelatin-NFC 15 wt.% composite films.

Conclusions

In this study, Raman spectroscopy was found to be a relevant analytical tool to quantify the stress transfer between gelatin obtained from two sources and NFC. Stress transfer from gelatin to NFC was found to occur. Stress transfer from bovine gelatin to NFC was found to be more efficient compared to the stress transfer from salmon gelatin to NFC when the pH of the suspension was 7. Data from other characterization techniques including SEM, UV-Vis, DSC, DMA will be also presented.

Acknowledgment: Fondecyt proyect N°3140036

References

1. S. J. Eichhorn, J. Sirichaisit, R. J. J. Young, R. J. J. Mater. Sci., **36**, 3129–3135 (2001).
2. F. Quero, A. Coveney, A. E. Lewandowska, R. M. Richardson, P. Díaz-Calderón, K. -Y. Lee, S. J. Eichhorn, A. M. Alam, J. Enrione, Biomacromolecules **16**, 1784–1793 (2015).



EXPLORATORY STUDIES ON POLI(3-HYDROXYBUTYRATE) SOIL DEGRADATION AND ASSESSMENT OF LOSS MASS RATE

Matheus Marques Torres¹, Mariane Igansi Alves¹, Karine Laste Macagnan¹, Luciana Bicca Dode¹, Claire Tondo Vendruscolo¹, Angelita da Silveira Moreira¹, Yasser da Silveira Kruger¹, Patrícia Diaz de Oliveira¹

1. Universidade Federal de Pelotas, Campus Universitário Capão do Leão, S/N, CEP 96010-900 Caixa Postal 354, Pelotas, RS, Brasil. matheus.torres@ufpel.edu.br

Introduction

Nowadays, popularization of production and use of plastic is well visible worldwide. However, despite this profitable dependence of industry, it is also known the difficulty that plastics derived from fossil fuels can bring at the time of disposal. Polymers produced from renewable resources, such as those extracted from bacteria, are a less intrusive alternative to the environment¹. Polyhydroxybutyrate [P(3HB)] is a microbial polyester and possess characteristics that allows the substitution of petrochemical plastics² as polypropylene. It is completely biodegradable, and the speed of degradation depends on environmental characteristics as microbiota, temperature and humidity. The aim of this study was to evaluate the degradation rate in soil of P(3HB) synthesized by *Ralstonia solanacearum* [P(3HB)-RS].

Experimental Part

The production and the extraction was made according to Macagnan¹. The commercial P(3HB) Biocycle® (PHB Industrial S.A.) was used as control. The samples were produced by solubilizing up 1g in 40 mL of chloroform for 30 min at 58 °C for further evaporation in Petry plate with 9 cm of diameter to film formation. The soil was obtained in the local market to fill the earth cells. Eight trays for plant germination, containing 15 cells each, were used. Four treatments were used: (1) sterilized soil, (2) sterilized soil with addition of inoculum *R. solanacearum*, (3) sterilized soil with addition of inoculum *Bacillus megaterium* and (4) natural soil without treatment. For the preparation of inoculum, fresh cells of each bacterium were prepared according Macagnan¹, with 200 mL of volume. The obtained films were cut, weighed and separated into polyester bags. Samples, in triplicate, were then buried in the soil to be removed at the intervals of 20 and 40 days.

Results and Discussions

The table 1 illustrates the degree of degradation of P(3HB). Degradation rate was higher in P(3HB)-RS, in both periods. In treatment 4, the biopolymer degradation rate was higher due to the presence of the native microbiota, observing the loss of almost half of the original weight in 40 days, for the P(3HB)-RS. Among the sterilized soils, the highest rate of degradation was observed in treatment 3, and the mass loss of P(3HB)-RS and control P(3HB) had doubled between the times of 20 and 40 days. Bacteria *R. solanacearum* and *B. megaterium* accumulate P(3HB) and possess necessary enzymes for its degradation. However, the control P(3HB) mass loss, between treatments 1 and 2, in both times, the rates are very close,

showing that the bacteria *R. solanacearum* did not degraded this biopolymer.

Table 1. Average of degradation of P(3HB) in 20 and 40 days.

Samples	Time (days)	Treatments (%)			
		1	2	3	4
[P(3HB)-RS]	20	3,59	7,25	12,50	19,21
	40	10,24	12,02	33,75	49,24
Control P(3HB)	20	2,54	2,64	6,39	3,69
	40	7,08	7,87	12,26	18,58

1- sterilized soil, 2- sterilized soil with addition of inoculum *R. solanacearum*, 3- sterilized soil with addition of inoculum *Bacillus megaterium* and 4- natural soil without treatment.

The degradation rate found for P(3HB) control in treatment 4 was relatable to Casarin et al.³ and Araújo et al.⁴, where degradation time is close, but in some cases, a little longer than the observed in the present study.

Conclusions

Despite having the study not yet finished, with 40 days degradation data, it is possible to state that the P(3HB)-RS may be considered an attractive material from an ecological point of view, since degradation rate exceeds the currently commercially available P(3HB). We can also inferred that the *R. solanacearum* and *B. megaterium* are potential degradative bacteria for P(3HB). Moreover, degradation by *B. megaterium* is more effective and can require more studies to elucidate the production of enzymes, and the degradation mechanism.

Acknowledgment: To Profa. Dra. Eugenia Jacira Bolacel Braga from Botanical Depart. of UFPel, for lending us the greenhouse and CNPq for scholarship.

References

1. Macagnan, K. L. Dissertação de mestrado. Biotecnologia, UFPel (2014).
2. Cordova, L.; Meza, C.; Gonzalez, G.; Gonzalez R. Revista Internacional de Contaminación Ambiental, 2013, 77-115.
3. Casarin, S. A.; Agnelli, J. A. M.; Malmonge, S. M.; Rosário, F. Polímeros Ciência e Tecnologia, vol.23, n.1, p.115-122, 2013.
4. Araújo, R. de J.; Conceição, I. D. da; Carvalho, L. H. de; Alves, T. S.; Barbosa, R.. Polímeros Ciência e Tecnologia, vol.25, n.5, p.483-491, 2015.



CALCIUM RELEASE EVALUATION DURING SILK FIBROIN DIALYSIS

Luisa Storelli dos Reis^{1,2}, Giovana Maria Genevro³, Mariana Agostini de Moraes¹, Pedro de Alcântara Pessoa Filho²

1. Universidade Federal de São Paulo, Rua São Nicolau, 210, 09913-030, Diadema, Brazil. mamoraes@unifesp.br

2. Escola Politécnica, Universidade de São Paulo, Av. Prof. Lineu Prestes, 580, Bloco 18, 05434-070, São Paulo, Brazil.

3. Universidade Estadual de Campinas, Av. Albert Einstein, 500, 13083-852, Campinas, Brazil.

Introduction

Bombyx mori silkworm cocoons consist of two proteins, fibroin and sericin. Fibroin is the protein that forms the core of the silk fibers while sericin bonds the silk fibroin cores together into a single silk strand.^{1,2} Silk fibroin (SF) has been mainly studied due to its biocompatibility and biodegradability properties, which makes it a biomaterial option for tissue engineering.³ Fibroin presents two different molecular conformations: silk I and silk II. Silk I is the metastable and water-soluble form while silk II is water-insoluble and thermodynamically stable. In order to obtain the SF solution, the sericin must first be removed from the fibroin.⁴ Then, the SF fibers can be dissolved in concentrated aqueous solutions of salts.¹ The SF salt solution has strong ionic force that solvates the fibroin fibers. However, in order to produce fibroin materials, the salts removal through dialysis is necessary. During dialysis, the ionic force of the solution weakens because salt is removed, so the SF solution becomes metastable (hydrogel can be formed).⁵ Thus, the study of fibroin dialysis is essential since it influences directly the materials produced with fibroin solution.

Experimental Part

First, sericin was removed from the fibroin. Then, a calcium chloride/ethanol aqueous solution with a molar ratio 1: 8: 2 (calcium chloride: water: ethanol) was prepared and the fibers were dissolved at 85°C (10 g of fibers in 100 mL of solvent) during 1h and 30min. Finally, the fibroin solution was dialyzed against ultrapure water (10 mL of SF solution in 150 mL of water), according to previously published procedure.⁵ The dialysis process lasted 3 days and the dialysis water was changed at 24 h interval. The dialysis water conductivity was measured and then submitted to a calcium (Ca) analysis by atomic absorption spectroscopy (AAS). The aqueous fibroin solution obtained after the dialysis process had its viscosity properties investigated.

Results and Discussions

Table 1 shows the conductivity measurements of dialysis water (by dialysis day) in comparison to ultrapure water. Fig. 1 presents the calcium concentration in dialysis water due to Ca release. The results were gathered from 5 replicates. As expected, the water conductivity value after dialysis is higher due to Ca diffusion from SF solution to water. Also, Ca concentration is proportional to water conductivity. It can be observed that the calcium concentration (and conductivity) lowered with every water change since the calcium concentration gradient is higher on the first day

of dialysis and this gradient lowers everyday due to water change. When the dialysis process is over, there is still a residual Ca concentration in the prepared SF solution. With viscosity properties investigation, it was observed that the aqueous SF solution has a dynamic viscosity of 2.5 cP at 26°C and is a newtonian fluid.

Table 1. Conductivity measurements of dialysis water at 25°C

Water	Pure	Day 1	Day 2	Day 3
Conductivity (mS/cm)	0,001	18.13±4.17	3.60±1.30	0.53±0.19

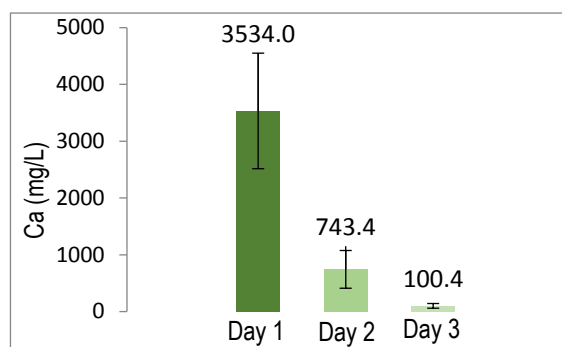


Figure 1. Calcium concentration in dialysis water.

Conclusions

After the dialysis process, there is still a residual calcium concentration left in the SF aqueous solution. The remaining salt helps to solvate the fibroin fibers and interferes with the properties of consequent hydrogel formation.

Acknowledgment: IQ/USP, CNPq

References

- Sashina, E., Bochek, A., Novoselov, N., Kirichenko, D. Russ. J. Appl. Chem. 2006, 79, 6.
- Gong, Z., Huang, L., Yang, Y., Chena, X., Shao, Z. Chem. Commun. 2009.
- Altman, G., Diaz, F., Jakuba, C., Calabro, T., Horan, R., Chen, J., Lu, H., Richmond, J., Kaplan, D. Biomaterials. 2003, 24.
- Vepari, C.; Kaplan, D. Prog. Polym. Sci. 2007, 32.
- Nogueira, G., Moraes, M., Rodas, A., Higa, O., Beppu, M. Mat. Sci. Eng. C. 2011, 31.



FORMULACIÓN Y EVALUACIÓN DE UN HIDROGEL A BASE DE CARRAGENINA, COMO RECUBRIMIENTO DE FERTILIZANTES NPK DE LIBERACIÓN CONTROLADA

Katherine Ávila Viatela¹, Angie Cifuentes Cetina²

1. Universidad de Bogotá Jorge Tadeo Lozano, Carrera 4 # 22-61, Apartado Aéreo 34185, Bogotá D.C., Colombia. johanak.avilav@utadeo.edu.co, angier.cifuentesc@utadeo.edu.co

Introduction

A pesar de que la implementación de los fertilizantes es necesaria para apoyar la producción agrícola y satisfacer la demanda de alimentos, su uso es ineficiente, ya que no todos los nutrientes aplicados son absorbidos por el cultivo (Stewart, 2007). Esto no solo ocasiona reducciones en el rendimiento del cultivo y pérdida de la fertilidad del suelo, sino también genera contaminación ambiental dado que el exceso de nutrientes que no son absorbidos llegan a cuerpos de agua por lixiviación o a la atmósfera por volatilización (Ongley, 1997).

Hoy en día una estrategia clave es desarrollar prácticas de manejo que aumenten la eficiencia del uso de nutrientes y la retención de humedad del suelo, que se reflejen en incrementos en la productividad, en un aumento de la relación beneficio/costo para el agricultor y en la disminución del impacto negativo a nivel ambiental. Por lo tanto el objetivo de este trabajo es formular, sintetizar y evaluar fisicoquímicamente un hidrogel a base de carragenina *kappa* II, que pueda ser utilizado como recubrimiento de fertilizantes NPK para garantizar la liberación lenta y continua de nutrientes al ambiente y que tenga el potencial de aumentar la eficiencia del uso del fertilizante y la retención de humedad del suelo.

Experimental Part

Se formuló un hidrogel con concentración del 3% a partir de carragenina, glicerol y agua, se puso en calentamiento la solución y luego se colocó en un molde agregando el fertilizante NPK, se dejó en el refrigerador por 30 min y luego al gel se le realizaron pruebas de IR, SEM, viscosidad y cinéticas en pHs (4,5-5,5-6,5) y soluciones salinas de NaCl, KCl y CaCl (10 mMol) para ver cómo se daba el proceso de hinchamiento a través del tiempo.

Results and Discussions

La figura 2 muestra la microestructura de hidrogeles a base de carragenina. En la parte (a) se observa a escala micrométrica, la morfología de la superficie externa, la cual presenta cavidades con un alto grado de homogeneidad y rugosidad del orden de 20 μm , se presenta además una estructura compacta, observándose intersticios entre "escamas" con espacios.

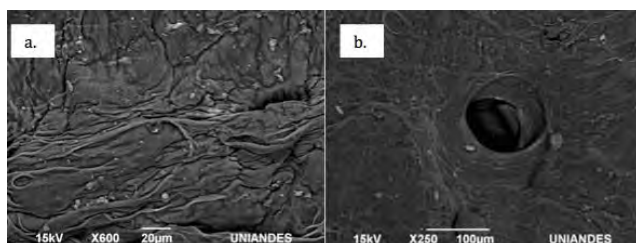


Figure 2. Micrografía MEB del hidrogel a base de carragenina a. sin fertilizante, b. con fertilizante

En la parte (b), si bien los microporos y mesoporos no son visibles, las fotografías presentan las formas y localización de los macroporos sobre la superficie de la muestra.

A partir del estudio cinético se pueden apreciar tres fases de absorción en las curvas que se presentan en la figura 3: una primera fase de retención rápida del agua en el hidrogel, el tiempo de contacto es de 10 min para el pH 4,5; una segunda fase en donde el agua ingresa al interior de la porosidad del hidrogel y el tiempo de contacto es de 10 a 30 min. En el caso de los pH 5,5 y 6,5 se puede observar que el tiempo de retención y de contacto es el mismo (1 - 20 min). Por último se presenta una tercera fase, en donde se alcanza el equilibrio y la absorción por el hidrogel es menor debido a que los poros están saturados, esta etapa se alcanza después de 20 min para los pH 5,5 y 6,5 y para el pH 4,5 a los 30 min.

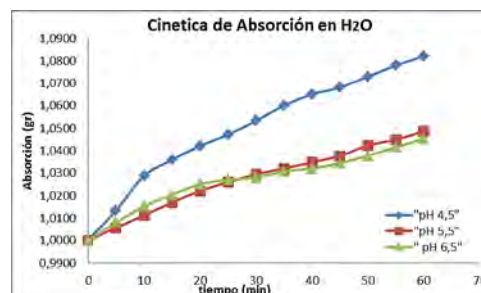


Figure 3. Cinética de absorción de agua a diferentes pH en agua.

Conclusions

Los experimentos de hinchamiento en los hidrogeles con fertilizante y sus respectivas cinéticas indican que las macroesferas preparadas a partir de carragenina son excelentes candidatos para ser utilizados como fertilizantes de liberación controlada, siendo amigable para el medio ambiente. A partir de la formulación del co-polimero de carragenina y fertilizante NPK, se obtuvieron óptimos resultados respecto a sus propiedades fisicoquímicas en espectroscopia FT-IR y SEM, además del tamaño del gel logrando mejor efecto de liberación controlada, estas conclusiones podrían servir para la aplicación en la agricultura y en un estudio a macroescala con un cultivo que se realizará en el futuro.

Acknowledgment:

Los autores agradecen al proyecto financiado por Colciencias en el marco de la "Vicerrectoría de Investigaciones de la Universidad de Bogotá Jorge Tadeo Lozano", Bogotá, Colombia.

References

- Ongley, E. D. *Lucha contra la contaminación agrícola de los recursos hídricos* Food & Agriculture Org. (1997). (No. 55).
- Stewart, W. M. Consideraciones en el uso eficiente de nutrientes. *Informaciones Agronómicas*, (2007). 67, 1-7.



ADSORPTION CAPACITY OF METHYLENE BLUE BY XANTHAN BIOPOLYMER

Miguel Oliveira¹, Ligia Furlan¹, Yasser Krüger³, Anderson Correa¹, Paula Klaic^{1,2}, Angelita Moreira¹, Patrícia Oliveira¹, Claire Vendruscolo¹.

1. Universidade federal de Pelotas, Campus Universitário, Caixa Postal 354, CEP 96010-900 Pelotas, RS, Brazil. ligia.furlan@gmail.com
2. Instituto Federal de Educação Ciência e Tecnologia do Rio Grande do Sul, Campus Farroupilha, rua São Vicente, 785, CEP 95180-000, Farroupilha, RS, Brazil.
3. Instituto Federal de Educação Ciência e Tecnologia, Campus Pelotas, Praça Vinte de Setembro, 455, CEP 96.015-360, Pelotas, RS, Brazil

Introduction

In recent years, many studies have been conducted with a view to finding new alternative materials and methods to reduce these discharges on the environment, such as adsorption processes, flocculation, chemical oxidation, photo degradation and biodegradation.^{1,3} Xanthan gum is an extracellular biopolymer produced by bacteria of the genus *Xanthomonas* and ionic exchange can be a useful strategy for changing or enhancing its rheological properties. In order to obtain a chemically modified xanthan with controlled counter ion type and concentration, the counter ions naturally incorporated to polymer during fermentation process must be removed, thus changing the carboxylate groups to the –COOH form.² The aim of this work is to study the adsorption of methylene blue, a cationic dye, by xanthan biopolymer obtained from by *Xanthomonas arboricola* pv *pruni* strain 101, in order to serve as a model for the removal of acidic and basic dyes contained in industrial effluents.

Experimental Part

Xanthan *pruni* was produced by culturing *X. arboricola* pv *pruni* strain 101 in a 10 L bioreactor according to the methodology described in the literature.² To evaluate the mass of the adsorbed dye, we prepared samples with 100, 200 and 300 mg of xanthan, each containing 50 mL of dye at a concentration of 10 mg L⁻¹. These samples were placed in Erlenmeyer flasks, sealed and shaken in a thermostatted bath for 3 h at a speed of 100 rpm at 25 °C. Next, aliquots of supernatant from each bottle were centrifuged and analyzed by UV-Vis at a wavelength of 665 nm. The concentration of dye in the supernatant was determined using a calibration curve of the dye. The time for the system to reach equilibrium was determined by placing 50 mL of dye solution ($C_0 = 10 \text{ mg L}^{-1}$) in contact with 100 mg of xanthan. The samples were collected at predetermined intervals and centrifuged, and the dye concentration was then determined. The solutions were kept in contact with the adsorbent to reach equilibrium adsorption.

Results and Discussions

Fig 1 presents the curve of the final concentration of adsorbate in the liquid phase (C_t) versus time (in minutes). We observed that the amount of dye adsorbed reached its maximum value at approximately 91%.

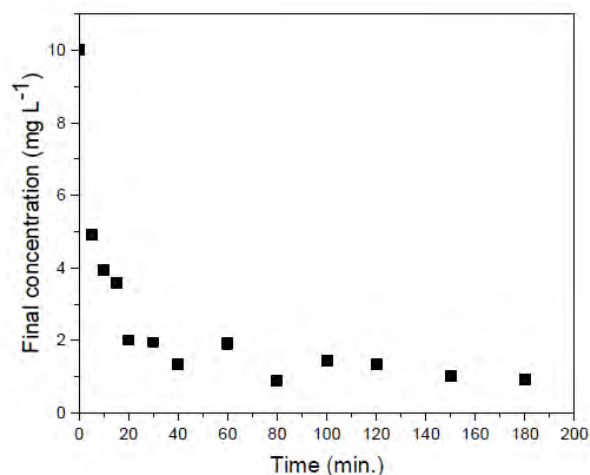


Figure 1. Kinetics of adsorption of the methylene blue dye.

With respect to the adsorbent weight we noted that a weight of 100 mg of biopolymer provided an maximum amount adsorbed of about 25 mg g⁻¹ (mass of adsorbed solute/gram of adsorbent), where the adsorption equilibrium is achieved in time period as high as 100 min, we have shown that the adsorption on activated xanthan is rapid.

Conclusions

The adsorption equilibrium was reached at approximately, 100 min and the removal percentage of the dye was 86%, using 100 mg of biopolymer and initial concentration of the methylene blue dye, 10 mg L⁻¹.

Acknowledgment: The authors acknowledge CNPq for supporting this research.

References

1. Oliveira, M.P.; Furlan,.; Zambiasi, R.C., Proc. 51º. Congresso Brasileiro de Química, Brasil, 2011,
2. Klaic, P.M.A.; Vendruscolo, C.T.; Furlan, L.; Moreira, A. da S. Food Hydrocolloids 2016, 56, 118-126.
3. Oliveira, M.P.; Corrêa, A. G.; Moschen, J.S.; Nascimento, L.M.R.; Furlan, L.; Klaic, P. M. A.; Moreira, A.S.; Oliveira, P.D.; Vendruscolo, C. T. Anais do 13º Congresso Brasileiro de Polímeros, Natal, RN, Brasil, 2015.



EVALUATION OF NATURAL RUBBER WITH FILLERS FROM PYROLYTIC CARBON BLACK POST INDUSTRIAL WASTE

William Urrego Yepes ¹, Leyla Yamile Jaramillo Zapata ¹, Juan Carlos Posada Correa ¹, Daniel Santiago Tobón ¹

¹. Instituto Tecnológico Metropolitano (ITM), Calle 73 #76A-354, 050034, Medellín, Colombia, williamurrego@itm.edu.co

Introduction

Currently there are different kinds of postindustrial wastes of high generation, which are considered as a serious environmental problem, due to the high cost of their appropriate disposal¹. The present work evaluates the effect of a byproduct normally treated by pyrolysis, as fillers in natural rubber compounds. This waste is the pyrolytic carbon black (CBp), obtained from scrap tire rubber. According to previous studies, it has been found that the addition of CBp may improve mechanical properties of the natural rubber composites in order to replace conventional carbon black (CB)^{2,3}. With the present study we want to evaluate the effect of adding pyrolytic carbon black on mechanical and rheological properties of a composite material made from natural rubber, to finally make a comparison with a carbon black 550 due to materials size similarities.

Experimental Part

Natural rubber (NR) and CBp composites were mixed in a torque rheometer Haake Rheodrive 7 PolyLab OS internal mixer according to the ASTM D3184 standard. Composites with CB (M1), CBp (M2) and CB 50%/ CBp 50% (M3) were prepared; 20phr and 40phr of fillers were used and the vulcanization process was evaluated by rotorless rheometry according to ASTM D5289 standard. Specimens for tensile tests (ASTM D412), tear strength (ASTM D624) and hardness (ASTM D2240) were compression molded. Five replicates were tested for each condition.

Results and Discussions

From N₂ physisorption analysis it is observed that the surface area of the CB 550 is similar to CBp. The addition of different CB do not generate significant difference in the mixing process, which was evaluated by torque rheometry. The stress-strain curve (Figure 1) shows that the effect of CBp is similar to CB 550 when 20phr is added, while by adding 40phr, more reinforcing power of CB 550 is obtained. The other mechanical properties (see table 1) have the same trend as that presented in 40phr composites. Properties for M1 composites are the best ones, followed by M2 and M3 composites. The addition of different carbon blacks generates changes in vulcanization time (t_{100}), this time increases proportionally depending on the phr filler used.

Figure 1. Stress-strain curves of NR/CBp and/or CB composites

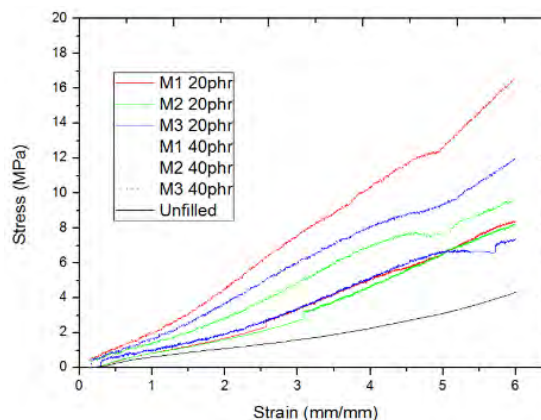


Table 1. Properties obtained for NR/CBp and/or CB composites.

	M _h - M _L (dNm)	t ₁₀₀ (min)	Hardness (ShoreA)	Modulus 100% (MPa)	Tensile strength 600% (MPa)	Tear Strength (N/mm)
Unfilled NR	9,10	14,62	46,00	0,62	4,34	22,30
M1 (20phr)	11,35	19,13	51,20	0,85	8,36	46,22
M2 (20phr)	10,08	20,27	49,40	0,84	8,25	33,53
M3 (20phr)	10,59	20,32	51,00	0,95	7,37	35,20
M1 (40phr)	16,74	19,40	61,60	1,98	16,57	50,29
M2 (40phr)	12,48	21,32	56,00	1,43	9,59	44,51
M3 (40phr)	14,40	19,67	58,60	1,57	12,05	40,20

Conclusions

It was found great differences in performance of composites with 40phr of CBp and conventional CB, while by adding 20 phr the effect was little evident. Carbonaceous residues on the CBp surface could reduce surface activity and dispersability of this filler in the matrix. Only hardness is slightly affected with the addition of CBp in NR.

Acknowledgment: Authors acknowledge to Instituto Tecnológico Metropolitano-ITM, Colciencias and Universidad Pontificia Bolivariana-UPB for supporting present research work (Project 115071552230).

References

1. A. Du, Z. Zhang and M. Wu, *Mater. Exp. Pol. L.* 2009, 3, 5, 295–301.
2. C. J. Norris, M. Hale and M. Bennett, *Plas.Rubb. and Comp.* 2014, 43, 8, 245–256.
3. F. Cataldo. *Macromol. Mater. Eng.* 2005, 290, 463–467.



REINFORCEMENT OF RECYCLED HIGH DENSITY POLYETHYLENE WITH ALDER SAWDUST (ALNUS ACUMINATA)

Katherine Méndez¹, Guillermo Jiménez¹

1. Laboratorio de polímeros POLIUNA, Universidad Nacional de Costa Rica, Campus Omar Dengo, 1st avenue 9th street, 40101, Heredia, Costa Rica.

Introduction

Research of wood-plastic composites has gained widespread attention in recent years because their relative low weight compared to their high mechanical properties and resistance to severe environmental conditions.¹ The main problem encountered when wood is used comes from the opposite nature of the hydrophobic polymer matrix and the hydrophilic vegetal fillers.² Several strategies to increase interactions between cellulose fibers and polymer matrices were recently reviewed, such as chemical modifications with silane coupling agents.³ The aim of this work is to prepare composites with recycled HDPE and alder sawdust, to evaluate the effect of filler concentration in the material mechanical properties, as well as the impact of the silane treatment in the sawdust used.

Experimental Part

Wood-plastic composites were prepared in a Brabender, mixing recycled HDPE and alder sawdust at 5, 10 and 20 % m/m during 10 minutes at 220°C and 40 rpm. For each different concentration it was used sawdust without any treatment and also sawdust modified with tris(2-methoxyethoxy)vinylsilane applied at a concentration of 4% by weight, with 0.5% of benzoyl peroxide as catalyst. These composites were tested for flexion and tensile stress, according to ASTM D790-10 and ASTM D638-10. Besides they were submitted to DCS and TGA analysis to compare their thermal stabilities.

Results and Discussions

Table 1 compares the tensile and flexural modulus for the composites prepared. Increasing the amount of sawdust increases both modulus. This table also illustrates the increment in both modulus when the sawdust was treated with tris(2-methoxyethoxy)vinylsilane. This behavior shows an improvement in the mechanical properties of the composites as the amount of sawdust is raised, and also demonstrates the effectivity of tris(2-methoxyethoxy)vinylsilane as a coupling agent between the HDPE and the fibers. The Si—O bonds from the silane, act as a bridge between the cellulose and the recycled HDPE.

The TGA analysis indicate that thermal stability decreases slightly when sawdust concentration increases. The decomposition temperatures were 420.40°C for the HDPE-R 100% material, 412.13, 401.54 and 363.79°C for the mixes with 5, 10 and 20% of sawdust without chemical treatment and 412.48, 405.00 and 400.11°C for the mixes with 5, 10 and 20% of sawdust treated.

This could be good if the purpose of the composite is to be degraded more easily. The same behavior is displayed in the melting points obtained from the DSC analysis. Melting points temperatures were 134.98°C for the HDPE-R 100% material, 134.48, 134.39 and 134.20°C for the mixes with 5, 10 and 20% of sawdust without chemical treatment and 134.50, 134.46 and 134.37°C for the mixes with 5, 10 and 20% of sawdust treated. The melting point is a colligative property, thus, it was expected lower melting points when amount of fibers increase. In both analysis, the temperatures are lower for the composites made with untreated sawdust, which evidences again that tris(2-methoxyethoxy)vinylsilane was an excellent coupling agent.

Table 1. Tensile and flexural modulus registered for the composites prepared

Sample	Tensile modulus (MPa)	Flexural modulus (MPa)
HDPE-R 100%	315,73	605,36
HDPE-R + 5% sawdust	311,76	1054,90
HDPE-R + 10% sawdust	386,06	1508,34
HDPE-R + 20% sawdust	586,98	1944,62
HDPE-R + 5% sawdust silanized	327,49	1208,64
HDPE-R + 10% sawdust silanized	391,09	1564,02
HDPE-R + 20% sawdust silanized	514,70	2223,34

Conclusions

The work shows that recycled HDPE could be reinforced with alder sawdust. The incorporation of the fibers enhanced the mechanical properties, and the treatment fibers demonstrate a better adhesion in the matrix.

Acknowledgment: POLIUNA

References

- Herrera, P.; Aguilar, M. *J. Appl. Polym. Sci.* 1997, 65, 197.
- Robin, J.; Breton, Y. *J. Reinf. Plast. Compos.* 2001, 20, 1253.
- Abdelmouleh, M.; Boufi, S.; Belgacem, A.; Dufresne, A. *Compos. Sci. Technol.* 2007, 67, 1627.



USE OF INDUSTRIAL WASTE IN ASPHALT MASSES

Hélio Wiebeck¹ Jorge Coelho², Antônio Lúcio Duarte Ferreira² Fábio José Esper³, Janaina Aline Galvão Barros⁴

1. Departamento de Engenharia Metalúrgica e de Materiais - Escola Politécnica da Universidade de São Paulo, São Paulo/SP
hwiebeck@up.br

2. Único Asfalto.

3. Centro Universitário Estácio Radial de São Paulo/S.P.

4. Instituto de Pesquisa Energéticas e Nucleares

Introduction

Brazilian pavements are basically old and the eminent growth of traffic and more and more intense vehicle loads have accelerated the deterioration process of flexible pavements, in which the use of rehabilitation techniques using conventional materials no more reach an appropriate mechanical behaviour. This is an ascent problem due to the terrestrial transport system in Brazil is essentially supported on highways. Many alternatives to improve the properties of the bituminous layers has been studied as addition some aggregates as recycled rubber (waste tire), rice husk ash, steel slag, recycled aggregates from construction and demolition waste, and other additives.

UNICO company introduces industrial waste in order to allow the asphalt produced is obtained with better chemical and mechanical performance as well as a more affordable price. The results showed that, in relation to conventional mixtures, produced with conventional bitumen, asphalt UNICO considerably improved the elastic behaviour of the resulting mixture, increasing their resistance to fatigue and permanent deformation, as well their capacity to delay cracking propagation.

Experimental Part

UNICO bitumen asphaltic is a special mixture that provides better chemical and mechanical properties (table 1).

Table 1. UNICO asphaltic bitumen composition

UNICO - Asphalt Composition – in mass (%)	
Asphaltic Bitumen	5,5%
Aggregates (40% crushed bedrock and 60% dust of crushed bedrock)*	94,5%

* crushed bedrock smaller than 12.5 mm and dust of crushed bedrock smaller than 4.8mm.

Bitumen has been widely used in pavement construction due to its special viscoelastic characteristics and excellent performance. The use of crumb rubber (CR) recycled from waste tires using an ambient grinding process was evaluated in two asphalt formulation (conventional asphaltic bitumen and UNICO asphaltic bitumen) (table 2.)

Table 2. Differences between conventional and UNICO asphaltic composition

Conventional asphaltic bitumen	UNICO Asphaltic bitumen
crushed bedrock smaller than 25mm and bigger than 19mm	crushed bedrock in smaller dimension

Results and Discussions

Results show that size of crushed bedrock affect directly on pattern quantity of bitumen asphaltic necessary (figure 1)

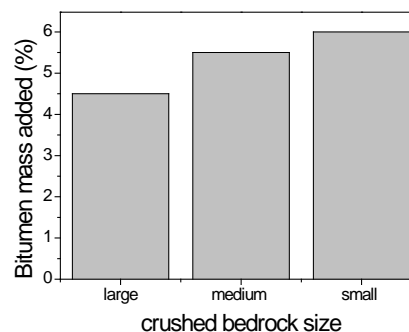


Figure 1. Bitumen as bonding agent added.

In spite the use of waste tire rubbers as bitumen modifiers can contribute to alleviate pollution problems derived from discarding scrap tires, the addition of ground tire rubber to bitumen enhance mechanical properties, which improves its resistance to both rutting and fatigue cracking.

The performance of crumb rubber has been changed over the years because each company has a different process of granulate tire rubber besides of different metallic contaminants, synthetic fiber reinforcement in the rubber composition and as mentioned Cristiano Costa Moreira, director of Solocap company (MG - Brazil), the crude oil composition in the tires production has been changing over the years. (table 3)

Table 3. Relative viscosity of crude oil in the tires manufacturing.

Years	1969	1996	2010
Relative viscosity	170	190	220

Conclusions

The results showed that it is possible to disperse tire rubber in asphalt. The addition of recycled tire rubber in asphalt mixtures could improve engineering properties of asphalt mixtures, and the rubber content has a significant effect on the performance of resistance.

References

- X. Lu, U. Isacson, Constr. Build. Mater. 16 (2002) 15.
- M. Garcia-Morales, P. Partal, F.J. Navarro, F. Martinez-Boza, C. Gallegos, Polym. Eng. Sci. 47 (2007) 181.
- Amash, A.; Zugenmaier, P. Polymer 41 (2000) 1589.
- Monea, Rosa M.J. Estudo da Viabilidade de incorporação de borracha moída de pneu em asfaltos para impermeabilização na construção civil. 2006. 48fls. Dissertação de Mestrado. Universidade de São Paulo, SP.



THE INFLUENCE OF ALKALI CONCENTRATION, TEMPERATURE AND TIME ON HEMICELLOSES EXTRACTION FROM CURAUÁ FIBERS

Mariana Roldi de Oliveira¹, Sandra Maria da Luz²

1,2. Laboratório de Tecnologias em Biomassas - Universidade de Brasília - UnB, Faculdade do Gama, Setor Leste, 72.444-240, Brasília, DF, Brazil. 1. mroldi.arq@gmail.com, 2. sandraluz@unb.br

Introduction

The growing environmental awareness and the looking for materials of low impact cause the desire of society to expand the use of natural resources, mainly the new polymers. Biomasses of plant origin are made of three major components: cellulose, hemicellulose and lignina¹. The hemicellulose is an amorphous or semi crystalline polymer that can be extract from plants. Thus, this research aims to investigate the influence of the variables as alkali concentration, temperature and time on the yield of hemicellulose extraction from curauá fibers in order to optimize the extraction process of this polymer.

Experimental Part

The methodology was adapted from Bahcegul et al², using 10 g of fibers immersed in 200 mL of distilled water at room temperature for 1 hour. After filtration, the material was placed under stirring in 100 mL of alkaline KOH solution. The pH of the liquor obtained was adjusted to 4.8 using acetic acid and by centrifuged at 1000 rpm for 5 minutes at 20°C. Then, the liquor was precipitated in a acetic acid/ ethanol solution 1:10 for 24 hours at room temperature and the hemicellulose obtained was taken to an oven at 60°C for 75 hours and weighed. It was evaluated the influence of three parameters of the methodology from a 2³ factorial design, using duplicated tests. The factorial design and testing are presented in Tables 1 and 2, respectively.

Table 1. 2³ Factorial design.

Level	Concentration (% m/v)	Temperature (°C)	Time (h)
-	10	Room temp.	3
+	20	50°C	5

Table 2. Design matrix.

Sample	Concentration (% m/v)	Temperature (°C)	Time (h)
1	10	Room temp.	3
2	20	Room temp.	3
3	10	50	3
4	20	50	3
5	10	Room temp.	5
6	20	Room temp.	5
7	10	50	5
8	20	50	5

Results and Discussions

The yields of hemicellulose varied as shown in Table 3. Fractions of cellulose may be present depending on the alkaline solution

content used for extraction, since curauá has only 9.9% of hemicellulose³.

Table 3. Yields of hemicellulose obtained (dry basis).

Sample	Yields (g)		Average (g)	Yields (%)
1	1.49	1.43	1.460 ± 0.03	16.03
2	1.35	1.95	1.650 ± 0.30	18.11
3	1.43	1.16	1.295 ± 0.14	14.22
4	1.40	1.39	1.395 ± 0.01	15.31
5	1.24	1.16	1.200 ± 0.04	13.17
6	1.89	1.46	1.675 ± 0.22	18.39
7	1.31	1.60	1.455 ± 0.15	15.97
8	1.88	1.92	1.900 ± 0.02	20.86

The value of effects varied as shown in Table 4, with standard error of 0.106. In order to make the variables and their interactions to be considered with significant of 95% confident interval, the effects values must be greater than 0.243. It was observed that only the concentration has a significant effect on the yield of the hemicelluloses extraction.

Table 4. Values of effects and their significance.

Sample	Effect	T8 95%.s*	Significant
Average	1.504	> 0.243	Yes
C	0.303	> 0.243	Yes
T	0.015	< 0.243	No
t	0.108	< 0.243	No
CT	-0.030	< 0.243	No
Ct	0.158	< 0.243	No
Tt	0.225	< 0.243	No
CTt	0.015	< 0.243	No

C=Alkali Concentration; T= Temperature; t= Time

*95% probability points of Student's t distribution with 8 degrees of freedom multiplied by standard error.

Conclusions

We concluded that only the concentration is a significant factor, obtaining higher yields on its upper level (20%). Other factors, as well as their interactions, did not present significant influence.

References

1. Yang, H.; Yan, R.; Chen, H.; Lee, D. F.; & Zheng, C. Fuel 2007, 86, 1781.
2. Bahcegul E.; Toraman, H. E.; Ozkan, N.; Bakir, U. Bioresource technology 2011, 103, 440.
3. Spinacé, M. A. S.; Lambert, C. S.; Femoselli, K. K. G.; Paoli, M. A. Carbohydrate Polymers 2008, 77, 47.



EDIBLE FILM DEVELOPMENT ARRACACHA STARCH BASED

Viviane de S. Silva¹, Renan Primo¹, Jose I. Velasco⁴, Farayde M. Fakhouri^{2,3,4}, Rafael A. de Oliveira¹

1. Faculty of Agricultural Engineering, UNICAMP, Av. Cândido Rondon, 501, Barão Geraldo, Campinas, SP, Brazil. viviane.silva@feagri.unicamp.br vibenhur@yahoo.com.br
2. Faculty of Chemical Engineering, UNICAMP, Av. Albert Einstein, 500 - CEP 13083-852 - Campinas - SP - Brazil
3. Faculty of Food Engineering, Rodovia Dourados, Itahum, University City, Dourados, MS, Brazil
4. Univerty Politècnica de Catalunya, Campus Nord, Calle Jordi Girona, Barcelona, Espanha

Introduction

The films prepared from renewable materials have proved of great commercial value because are biodegradable and, consequently, protect the environment. ¹This can be made with various polymers ², including starch. Arracacha root is rich in carbohydrates, and its starch in presence of water, produces clear pastes under heating allowing its use in products that require this property, in this case, edible films. These films can be obtained from different types of materials. The most used materials are polysaccharides, proteins and lipids. ² This material must be transparent, non-toxic, odorless and flavorless; and starch can promote these characteristics. In this context, the aim of this study was to develop and evaluate arracacha starch based edible films with glycerol addition.

Experimental Part

The film production was performed by casting technique whereby central composite design (Table 1), with of macromolecule (3, 4 and 5%) and plasticizer glycerol concentration (10, 15 and 20% in relation to macromolecule) as independent variables and water solubility ⁴ and water vapor permeability (WVP) as responses.⁵ Tukey test was used to determine differences between the properties of arracacha starch films for 95% of confidence level.

Results and Discussions

By the consistency and aspect of films, it can be observed that its visual characteristics were similar to materials from oil derivatives (Fig. 1). The addition of plasticizer affects the solubility of starch films because it interacts with film matrix, increasing the free space between the chains, facilitating the water inlet in film and, consequently, intensifying its solubility. This can be observed in treatment 1 (Table 1) in which occurred reduction of the solubility in low glycerol content. Based on results obtained during analysis, the treatment 3 (Table 1) showed a lower water vapor permeability. Probably, this value was influenced by the increase in macromolecule concentration, although increment glycerol (20%) in same concentration of starch (5%) induced instability of films materials, causing rupture. This fact determines that it is an infeasible concentration for film production. The increase concentration of glycerol caused enhanced solubility that was

lower than 15%, demonstrating the water resistance of obtained filmogenic material.

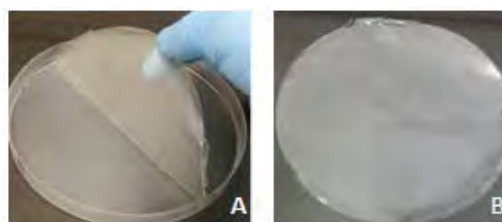


Figure 1. Film removed of Petri dish (A) and after its removal (B)

Table 1. Solubility and water vapor permeability (WVP)

Treatment	Concentration %	Solubility (%)	WVP (gmm/m ² dkPa)
1	3S10G	13.09	4.50
2	3S20G	15.13	3.41
3	5S10G	14.73	2.42
4	5S20G	18.19	-
5	4S15G	22.13	4.16
6	4S15G	22.14	3.92
7	4S15G	22.30	3.74

S:starch; G: glycerol

Conclusions

It is possible to of create edible films with arracacha starch, with homogeneous visual characteristics, transparent, easy handling and with suitable properties for application in other products as edible coatings.

Acknowledgement: CNPq, FEAGRI, FEQ

References

1. Bourbon, A. I., Pinheiro, A.C.; Cerqueira, M.A.; Rocha, C.M.R.; Avides, M.C.; Quintas, M.A.C.; Vicente, A.A.. Journal of Food Engineering. Amsterdam. 2011, 106, 2, 111-118.
2. Falguera, V.; Quintero, J.P.; Jiménez,A.; Muñoz,J.A.; Ibarz, A. Trends in Food Science & Technology. 2011, 22, 292-303.
3. ASTM, E 96-95, 1995, 10.



WATERBORNE ACRYLIC/CASEIN LATEXES AND THEIR APPLICATION AS ECOFRIENDLY COATING

Matías L. Picchio¹, Mario C.G. Passeggi (Jr.)², María J. Barandiaran³, Roque J. Minari¹, Luis M. Gugliotta¹

1. INTEC (CONICET-UNL), Güemes 3450, 3000, Santa Fe, Argentina. lgug@intec.edu.ar

2. IFIS (CONICET-UNL), Güemes 3450, 3000, Santa Fe, Argentina.

3. POLYMAT (UPV/EHU), Avenida Tolosa 72, 20018, Donostia-San Sebastián, Spain.

Introduction

Acrylic/casein hybrid latexes have gained increasingly industrial interest in recent years because of their promising properties as binders for coatings.¹ Since the highly hydrophilic character of casein, hybrid films present some shortcoming such as poor water resistance which limits their further application.² It is expected that increasing compatibility between polymer and protein phases, by covalently bonding both components, will result in superior properties of the hybrid films. In this regard, the chemical modification of casein appears as a promising route to favor the grafting of acrylic polymers and overcome the weak characteristic of the hybrid materials. The aim of this work is to evaluate the incorporation of vinyl groups onto casein, and to analyze the effect of the number of functionalities on the polymer/protein compatibility and the coating properties of the materials.

Experimental Work

Casein containing methacrylic groups was obtained via amine-epoxy reaction using glycidyl methacrylate as functional monomer. Reaction was carried out in aqueous media at 50°C during 4 h. The resulting methacrylated caseins (MC), with varied vinyl functionalities (from 2 up to 40), were used in the surfactant-free emulsion polymerization of butyl acrylate/methyl methacrylate, with tert-butyl hydroperoxide as initiator. Polymerizations were carried out at 80°C for 3 h. The amount of casein grafted to the acrylic polymer (CDG) was determined by UV spectroscopy following a previous report.³ Water resistance of the hybrid materials was determined by immersing film specimens in such medium during 7 days. Tensile tests of films, with dumbbell shape, were carried out with an elongation rate of 25 mm/min in a universal testing machine.

Results and Discussions

As it can be seen from Fig. 1, the incorporation of 40 methacrylic groups onto casein notably increased the amount of protein grafted to the acrylic polymer from 20% up to 74%, thus improving the compatibility of the hybrid system. Also it is noted that while films prepared with native casein disintegrated immediately after immersion, those synthesized from MC containing 10 or more vinyl groups resisted the test during 7 days without presenting damage. On the other hand, Fig 2 shows that hybrid films obtained with MC presented higher tensile strength and deformation capability than native casein based films. However, the increase of casein methacrylation degree deteriorated the elongation at break of the materials, probably due to increasingly crosslinking levels were reached.

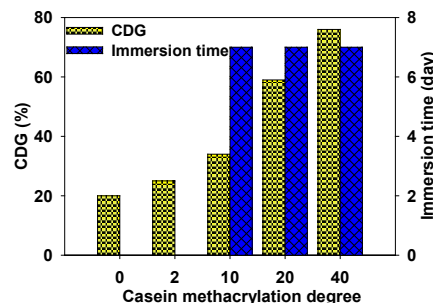


Figure 1. Influence of casein methacrylation degree on CDG and water resistance of the hybrid films.

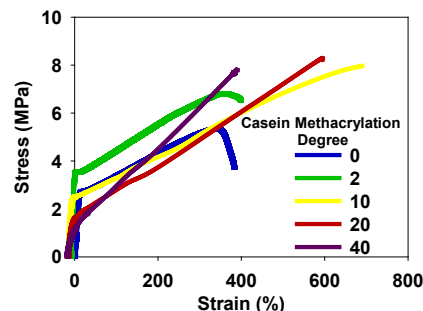


Figure 2. Effect of the casein methacrylation degree on mechanical properties of the hybrid films.

Conclusions

Casein methacrylation approach showed to be a successful alternative to overcome the poor water resistance of the hybrid acrylic/casein materials. Coating performance of the formulated latexes demonstrates that they are promising for the development of a new generation of bio-based binders.

Acknowledgment: The financial support received from CONICET, UNL, ANPCyT, the Secretary of Science, Technology and Innovation of Santa Fe State, and the Secretary of University Policies from the Education Ministry (all of Argentina) is gratefully acknowledged.

References

- Xu, Q.; Fan, Q.; Ma, J.; Yan, Z. *Prog. Org. Coat.* 2016, 99, 223.
- Picchio, M.L.; Passeggi (Jr), M.C.G.; Barandiaran, M.J.; Gugliotta, L.M.; Minari, R.J. *Prog. Org. Coat.* 2015, 88, 8.
- Picchio, M.L.; Minari, R.J.; Gonzalez, V.D.G.; Passeggi (Jr); M.C.G.; Vega, J.R.; Barandiaran, M.J.; Gugliotta, L.M. *Macromol. Symp.* 2014, 344, 76.



REMOCIÓN DE ÓXIDOS DE METALES MEDIANTE EL USO DE HIDROGELES BIODEGRADABLES

Agustín Martínez-Ruvalcaba¹, Emilo Cruz-Barba¹, Juan Carlos Sánchez¹, Leticia Cázares¹, Syeni Agredano²

1. Departamento de Ingeniería Química, CUCEI, Universidad de Guadalajara, Blvd. Marcelino García Barragán #1421, C. P. 44430, Guadalajara, Jalisco, México. agustin.martinez@academico.udg.mx
2. Departamento de Ingeniería Química y Bioquímica, Instituto Tecnológico de Tepic, Avenida Tecnológico #2595, C. P. 63175, Tepic, Nayarit, México.

Introducción

En esta trabajo se pretende elaborar una serie de mezclas de hidrogeles de carboximetilcelulosa sódica-ácido cítrico diferentes concentraciones, para analizar su eficacia en la remoción de óxidos en placas metálicas a tiempos controlados. Esta propuesta es diseñada debido a que en la actualidad la industria no cuenta con métodos ecológicamente viables que rehabiliten superficies metálicas corroídas, sino que solamente cuenta con algunas técnicas que previenen la misma tales como recubrir con resinas o neutralizadores de óxidos en sus equipos. Es importante conocer métodos correctivos y no solo preventivos en cuanto a temas de oxidación para así ampliar la vida útil de los materiales y obtener mejores rendimientos tanto en los equipos como en las estructuras metálicas. El ácido cítrico es una excelente agente quelante, que además se utiliza para eliminar incrustaciones de cal de las calderas y evaporadores. Puede ser utilizado para ablandar el agua, lo que lo hace útil en jabones y detergentes para la ropa. Algunos limpiadores son formulados con ácido cítrico para mejorar la disolución y la remoción de óxido y otros desechos de las superficies metálicas. El ácido cítrico tiende a reaccionar con metales pesados, tales como Cd, Cu, Cr, Fe (II), Fe (III), Ni, Pb para formar complejos solubles en agua^{1,2}.

Métodos Experimentales

Hidrogeles de Carboximetilcelulosa-Ácido Cítrico

Se prepararon soluciones de ácido cítrico a concentraciones de 5%, 10% y 40% (en peso) a las que posteriormente se añadió la carboximetilcelulosa sódica (CMC), con el objetivo de que en dichas soluciones ácidas, el biopolímero alcanzara concentraciones de 0.5%, 1.0%, 2.0% y 2.5%. (todas ellas en porcentaje peso).

Tratamiento a las Placas Metálicas

Las placas metálicas fueron adquiridas en una herrería local de la ciudad de Guadalajara, estas placas fueron cortadas con unas dimensiones de ancho de 2 cm y con un largo de 5 cm. Se aplica una capa de aproximadamente 2 mm de espesor por ambos lados de la placa y se coloca la placa recubierta de hidrogel en una caja Petri de vidrio para evitar cualquier pérdida de materia por evaporación.

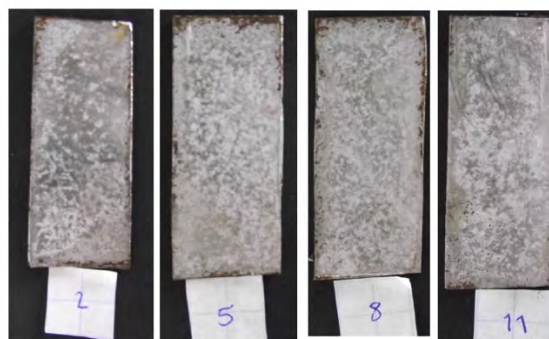


Figura 1. Placas tratadas con gel de CMC-ácido cítrico (al 10%)

Resultados y Discusiones

Se observó que los hidrogeles preparados a concentraciones ácidas del 5% no alcanzan el desempeño requerido para limpiar las placas metálicas. A la concentración de ácido cítrico de 40% en gel de CMC entre 1.0% y 2.5% es totalmente desfavorable para la remoción y limpieza de óxido en las placas metálicas, debido a que presenta un comportamiento constante de depositar una capa granulosa y verde sobre las placas. Así mismo se encontró que las concentraciones que mejor desempeño tuvieron fueron aquellas preparadas a 2.0% y 2.5 % peso CMC cargadas con ácido cítrico al 10%, los resultados arrojan que a esta concentración de ácido cítrico presenta un desempeño eficaz y favorable en el proceso de limpieza y remoción de óxido en placas metálicas. Otro factor observado es que a mayor grado de porcentaje peso de CMC el desempeño del hidrogel limpiador aumenta.

Conclusiones

El desarrollo de hidrogeles biodegradables a base de CMC y ácido cítrico es una solución adecuada para el proceso de recuperación de superficies metálicas corroídas. Es importante mencionar que estos hidrogeles no han sido sumergidos en alguna solución sino que esta alternativa puede ser usada a modo de pasta, lo cual genera un impacto económico menor en el uso de los recursos destinados a la rehabilitación de superficies metálicas que han sufrido un proceso de corrosión.

Referencias

1. Peppas N.A. *Advanced Materials*. 2006, 18, 1345.
2. Amer S. www.pollutionengineering.com 2012, January 2012, 27.

HYDROGELS OF PEG/PVA: METRIBUZIN RESEARCH

 José Luis Gadea P.¹, Fidel Benjamín Alarcón H.¹, María del Carmen Fuentes A.¹, Angeluz Olvera V.¹

1. *Escuela de Estudios Superiores de Xalostoc. Universidad Autónoma del Estado de Morelos. Av. Nicolás Bravo S/N, Parque Industrial de Cuautla, Ayala, Morelos. C.P. 62715. gadea.joseluis@gmail.com*

Introduction

Adsorption of penetrants into glassy polymers and release of active ingredients from the swollen matrices has been extensively studied, but those materials is not completely sensitive to degradation by the action of bacterial enzymes, turning into potential pollutant. Herbicides are chemical compounds capable of killing or inhibiting the growth of certain plants and they have been frequently detected in natural waters¹. Poly(ethylene glycol), PEG, and Poly(vinyl alcohol), PVA, Hydrogels compounds has been a matter of rehearsal for their physical and chemical properties in a different way²⁻³. Thus the interaction of both polymers has not been studied enough. In this work we report of hydrogels based on chemical crosslinking of PVA by PEG chemically modified at its ends with acyl chloride groups, susceptible to degradation via hydrolysis. The use of these hydrogels and his biodegradation properties, so this materials can be used for absorption of organic compounds because its temperature and pH response sensibility.

Experimental Part

In order to get modified PEG needed, it's used the poly(ethylene glycol) bis (Carboxymethyl) ether (Mn: 600 g/mol) modifying the endings chains by adding thionyl chloride and Dichloromethane under anhidric conditions. The PVA is the result of acid hydrolysis from poly(vinyl acetate) (Mn: 100,000 g/mol). Hydrogel of PEG/PVA were synthesized from the chemical crosslinked from both polymers, previously modified in N.N Dimethylformamide, following three rinses, the first in a buffer solution at pH 7.0, the second rinse with distilled water and the third in a Methanol 50 % solution. All performed at room temperature for 24 hours each one. After this the hydrogel is cut into disc and dried at room temperature to get its constant weight. The Metribuzin load is performing by swelling xerogel adding distilled water from 150 and 300 ppm for 48 hours in order to get the total swelling of hydrogel material. Once it get loaded proceed to get drying at room temperature measuring its weight until it gets even. The final value of metribuzin concentration in the gel is measuring by spectrophotometric UV- Vis (Spectrophotometer Cintra 3030) with a maximum length at 293 nm absorption set.

Results and Discussions

For maximum Metribuzin load in hydrogel by following UV-Vis measurements initially every 10 min and finally every 30 min and then every hour. See fig. 1 were loaded and unloaded xerogel shows. The releasing of Metribuzin was by distilled water at room

temperature. See fig. 2 were the Metribuzin concentration gradually raise in the media when Hydrogel swell releasing this. Maximum concentration reached was 130 ppm in 70 min approximately for hydrogels loaded at 150 ppm, meanwhile for hydrogels initial loaded Metribuzin of 300 ppm get reach its superior equilibrium at 120 min whit maximum concentration of 196 ppm.

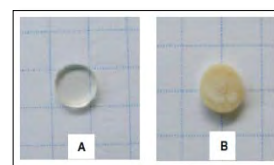


Figure 1. A. Xerogel and B. Xerogel loaded.

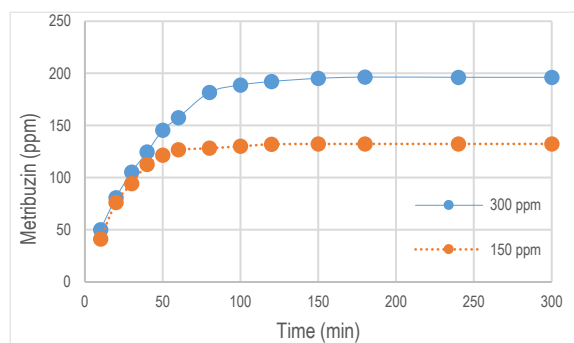


Figure 2. Maximum concentration of metribuzin.

Conclusions

Maximum concentration reached from Metrobuzin in to hydrogels highly stands in the initial load compound. The aspect hydrophilic performed by hydrogels networks makes more easy the fixation of Metribuzin in a water media at room temperature.

Acknowledgment: Proyecto Prodep 2015: UAEMOR-PTC-347

References

1. Honorio M., Vaz de Liz J., Peralta M. Felix de Sena R., Humberto J. Environmental Protection J. 2013, 4, 564-569
2. Cesteros, L.C.; González-Teresa, R.; Katime, I. Eur. Polym J. 2009, 45, 674.
3. Gadea J.L., Cesteros L. C., Katime I., Eur. Polym. J. 2013, 49, 3582-3589.

ADSORPTION OF HRP ON AGAVE-FIBER/HDPE FOAMED COMPOSITES AND ITS POSSIBLE USE IN THE DEGRADATION OF A TEXTILE DYE

Valeria Figueroa Velarde ², Mayra García Sánchez ¹, Luis Carlos Rosales Rivera ¹, Pedro Ortega Gudiño ¹, Orfil González Reynoso ¹, Jorge Ramón Robledo Ortiz ²

1. Departamento de Ingeniería Química, Universidad de Guadalajara, Blvd. M. G. Barragán 1451, 44100, Guadalajara, Jalisco, México. lcr33@hotmail.com
2. Departamento de Madera Celulosa y Papel, Universidad de Guadalajara, Carretera a Nogales, km 15.5 AP5293, Zapopan, 45020, Jalisco, México.

Introduction

Enzymatic degradation is an efficient approach that can convert toxic wastes into products that are innocuous to the environment, avoiding the need to completely degrade or remove them.^{1,2} Peroxidases have ideal biocatalyzing characteristics including temperature and pH resistance, high stability and a wide range of substrates that can be used, besides its low cost of production.³ In this work, horseradish peroxidase (HRP) was physically adsorbed on foamed composites of high density polyethylene (HDPE) and agave fiber. Adsorption conditions were optimized measuring the enzymatic activity at different values of concentration, time, pH and temperature.

Experimental Part

Foamed HDPE pellets were produced by extrusion using a twin screw counter-rotating extruder Model ZSE27 (Leistritz), equipped with a down-line pelletizer and using a screw speed of 40 rpm. Pellets of HDPE were mixed with 5% (w/w) agave fiber and 1% (w/w) ACA as foaming agent with 0.2% (w/w) zinc oxide as catalyst. All experiments were carried out using a shaker incubator model LSI-3016A (LabTech). Adsorption of the HRP enzyme was done using different concentrations in 50 mM acetate buffer at pH 5. pH studies were done using acetate buffer (pH 4.0-5.0), PBS buffer (5.5-7.0) and Tris buffer (7.5-9.0).

Results and Discussions

Fig. 1 depicts the activity comparison between immobilized HRP vs. in solution, changing the pH value in the immobilization procedure. Activity was detected in the whole range of pH studied, due to the different HRP isoenzymes present in the work. The highest values were obtained using acetate buffer in the immobilization protocol, while the PBS buffer gave the highest values in solution experiments.

Temperature experiments are depicted in Fig. 2; a typical bell shape activity response is observed for the HRP in solution, while activity for the immobilized enzyme is more stable at temperatures above 65°C.

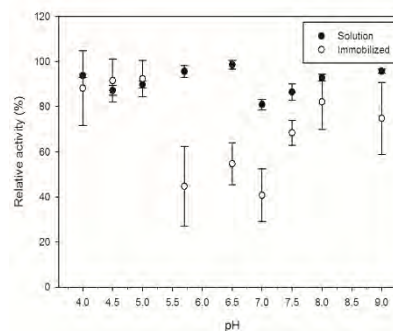


Figure 1. Activity response varying pH values, using HRP immobilized vs. in solution.

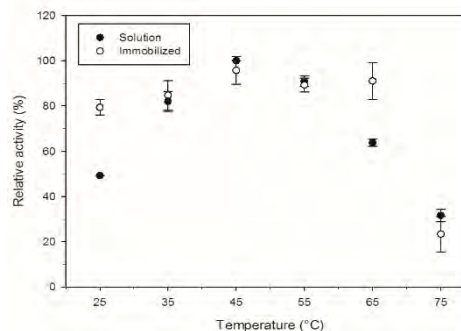


Figure 2. Effect of temperature on the activity of HRP, immobilized vs. in solution.

Conclusions

The use of a foamed composite that incorporates agave fiber is an interesting platform for the immobilization of enzymes. It was possible to optimize several conditions of the HRP physical adsorption and this platform can be used for the degradation of a textile dye.

Acknowledgment: CONACYT, CUCEI, UdeG

References

1. Boucherit N., Abouseoud M., Adour L., J. Environ. Sci. 2013, 25, 1235.
2. Ulson de Souza S. M. A. G., Forgiarini E., Ulson de Souza A. A., Hazard J. Mater. 2007, 147, 1073.
3. Fernandes K. F., Lima, H. Pinho C. S., Collins C. H., Process Biochem. 2003, 38, 1379.

CASTOR OIL POLYURETHANE/CELLULOSE DERIVATIVES AND POLYACRYLIC ACID

Mario A. Gómez Jiménez^{1*}, Rosa E. Zavala Arce¹, J.L. Rivera Armenta², Ana Ma. Mendoza Martínez², Nancy P. Díaz Zavala², Norma A. Rangel Vazquez³

1. División de Estudios de Posgrado e Investigación, Instituto Tecnológico de Toluca, Av. Tecnológico s/n. Colonia Agrícola Buenavista, 52149, Metepec, Edo. De México, México, maalgomez@hotmail.com
2. Instituto Tecnológico de Ciudad Madero, J. Rosas y J. Urueta s/n Col. Los Mangos, 89440, Ciudad Madero, Tamaulipas, México
3. Instituto Tecnológico de Aguascalientes, Av. Adolfo López Mateos Ote. No. 1801, Fracc. Bona Gens, 20256, Aguascalientes, Aguascalientes, México

Introduction

Crosslinked polymer networks are held together by permanent entanglements with only accidental covalent bonds between the polymers. The three conditions for eligibility of an IPN are: (1) the two polymers are synthesized and/or crosslinked in the presence of the other, (2) the two polymers have similar kinetics, and (3) the two polymers are not dramatically phase separated. An interpenetrating polymer network (IPN) is a material containing two (or more) polymer networks, which are combined and at least one of them is synthesized and/or crosslinked in the immediate presence of the other. IPNs offer the possibility of combining in network form which otherwise are non-compatible polymers with opposite properties^{1,2}. The present study is concerned with IPN's synthesis made of PU based on castor oil/cellulose derivatives and PAA. IPN's were prepared by sequential method. Microstructure, thermal and mechanical properties of three PU/PAA ratios (75/25, 50/50, 25/75) are reported here.

Experimental Part

The IPNs were synthesized by sequential method. PU synthesis was carried out adding castor oil, cellulose derivatives and 2,4-TDI to the reactor previously mixed at room temperature. Acrylic acid was heated at 60°C, followed by crosslinking agent addition. Afterwards, the acrylic acid solution was added to PU-prepolymer and mixed for 20 minutes. Stoichiometric amount of initiator to acrylic acid was added at this stage and continuing heating to initiate polymerization. All reagents were used as they were received from suppliers.

Fourier transform infrared (FTIR) spectroscopy was carried out at room conditions using a Perkin Elmer tral range, with 4cm⁻¹ resolution, using an attenuated total reflectance (ATR) accessory under 16 scans. Differential scanning calorimetry (DSC) was carried out on a TA Instrument 2010 calorimeter.

Results and Discussions

Fig. 1 shows IR spectra for IPN including HEC with 3 PU/PAA ratios. Bands corresponding to urethane ($-\text{CH}_2$ a 2926 - 2907cm⁻¹,

$-\text{CH}_3$ a 2851 - 2841cm⁻¹ y C=O a 1725 - 1701cm⁻¹) can be observed. Incorporation of acrylic acid was confirmed by the presence of a peak at 1691cm⁻¹ attributed to carbonyl of acrylic acid units (also $-\text{CH}_3$ 2911cm⁻¹) network.

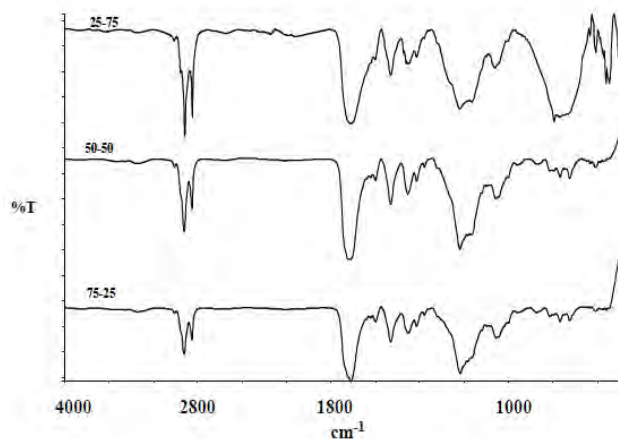


Fig. 1 FT-IR spectra of IPNs, HEC 1w% (3w% ACVA, 2.5w%NNMBA)

Conclusions

It was possible to prepare IPNs PU based in castor oil CA and HEC/PAA, varying the crosslinker agent concentration, catalyst and PU/PAA ratio in 3 levels. By FTIR was possible to detect characteristic signals of PU, PAA, but was not clear to prove presence of CA. By means of DSC analysis two Tg's were detected for the samples, corresponding to PU and PAA networks, which suggest phase separation in a macroscopic level.

References

1. Pissis, P., G. Georgoussis, V.A. Bershtein, E. Neagu and A.A. Fainleb, "Dielectric studies in homogeneous and hetero-geneous polyurethane/polycyanurate interpenetrating polymer networks," *Journal of Non-Crystalline Solids*, 2002, **305**, 150–158.
2. Sperling, L.H., *Interpenetrating polymer networks and related materials*, 1981, Plenum Press.



ADSORCIÓN DE TARTRACINA EN UN SISTEMA CONTINUO CON UN CRIOGEL Q-C-EDGE: EFECTO DE ALTURA DE LECHO Y FLUJO DE ALIMENTACIÓN

A. García-Gonzalez¹, P. Ávila-Pérez^{2,1}, B. García-Gaitan¹, J. L. García-Rivas¹, J. Sánchez-Jaime¹, R. E. Zavala-Arce^{1*}

1. Instituto Tecnológico de Toluca, Av. Tecnológico s/n. Fraccionamiento La Virgen Metepec, Edo. De México, México C.P. 52149, rzavala@toluca.tecnm.mx

2. Instituto Nacional de Investigaciones Nucleares, Carretera México Toluca s/n, La Marquesa, Ocoyoacac, Estado de México, México

Introducción

El desarrollo de la bioadsorción usando polímeros naturales como el Quitosano (Q) y la Celulosa (C) para la remoción de colorantes se ha venido desarrollando como alternativa para la decoloración de agua (Guibal et al., 2013).

El trabajo aquí presentado se enfoca en probar las capacidades de sorción del colorante tartracina disuelto en agua por un criogel sintetizado por congelamiento descongelamiento (Lozinsky et al., 2003) a partir de los polímeros mencionados en un sistema continuo, probando diferentes caudales y tamaños de lecho, con la finalidad de observar el efecto en los tiempos de ruptura y saturación de la columna.

Parte Experimental

La síntesis del criogel Q-C-EGDE se realizó disolviendo quitosano grado industrial en una disolución de ácido acético 0.4 M, a la cual se le agregó celulosa en proporción Q:C 1.8:1, la solución con la celulosa en suspensión se goteó sobre nitrógeno líquido.

Las esferas generadas se secaron por el proceso de liofilización, el cual generó el material poroso para utilizarlo en la adsorción, llevándolo posteriormente a entrecruzamiento con etilenglicol diglicidil éter (EGDE).

El montaje del sistema de adsorción en flujo continuo consistió en usar parámetros de diseño para dimensionar el diámetro y altura de la columna siendo estas de diámetro interno de 2.5 cm. alimentadas con un flujo ascendente, las alturas seleccionadas fueron de 3 y 6 cm y los flujos de alimentación de 3 y 6 mL/min.; los experimentos se llevaron a cabo a temperatura ambiente.

Se recolectaron muestras cada minuto la primera hora y cada 15 minutos el tiempo restante, siendo criterio de paro de la columna el 90 % de la saturación de la columna; la concentración del efluente se midió usando espectrofotometría UV-Vis.

Adams-Bohart, Thomas y Dosis-respuesta para columnas de adsorción que describen el comportamiento de las curvas de ruptura del experimento en flujo continuo.

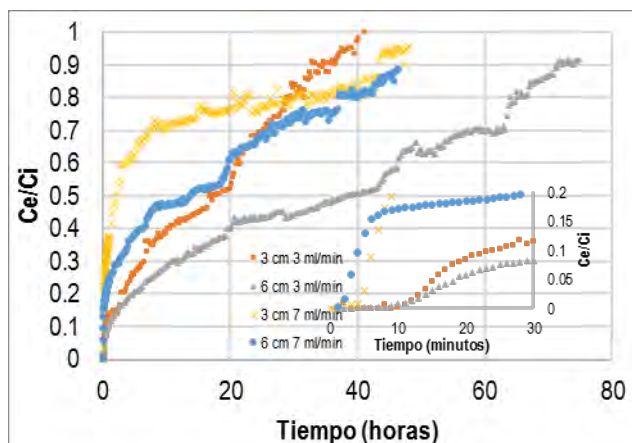


Figura 1. Comparación de las curvas de ruptura para 3 y 6 cm y caudales de 3 y 7 ml/min

Los datos obtenidos fueron ajustados a los modelos matemáticos de

Resultados y Discusiones

En la figura 1 se puede observar la comparación de las curvas de ruptura de los experimentos llevados a cabo para la adsorción en flujo continuo, observando que el aumento caudal reduce los tiempos de ruptura y saturación del proceso de adsorción.

Conclusiones

Los estudios realizados en columna de lecho fijo, muestran las capacidades de sorción del criogel Q-C-EGDE en sistema en continuo, en el cual la altura del lecho constituyó un incremento en los tiempos de saturación al igual que en los tiempos de ruptura, mientras que, al aumentar los flujos, estos tiempos disminuyeron considerablemente.

Agradecimientos: Al TecNM (5892.19-P), ININ, CONACYT

Referencias

- Guibal Eric, Cambe Simon, Bayle Sandrine, Taulemesse Jean-Marie, Vincent Thierry, (2013), Silver/chitosan/cellulose fibers foam composites: From synthesis to antibacterial properties, Journal of Colloid and Interface Science, 393, p 411-420.
- Lozinsky V. I., Galaev I. Yu., Plieva Fatima M., Savina Irina N., Jungvid Hans, Mattiasson Bo, (2003), Polymeric cryogels as promising materials of biotechnological interest, Trends of Biotechnology, Vol. 21 No.10, pp 445-451.

CARROT PROCESSING WASTE AS RAW MATERIAL FOR EDIBLE FILM PRODUCTION

Caio G Otoni^{1,2}, Marcos V Lorevice², Márcia R de Moura³, Marcos D Ferreira², Luiz HC Mattoso^{1,2}

1. PPG-CEM/UFSCar, Rod. Washington Luis km 235, 13565-905, São Carlos, Brazil. cgotoni@gmail.com;

2. Embrapa, Rua XV de Novembro 1452, 13560-970, São Carlos, Brazil;

3. UNESP/FEIS, Av. Brasil 56, 15385-000, Ilha Solteira, Brazil.

Introduction

As consumers increasingly seek for environmentally friendly materials instead of their non-biodegradable, non-renewable counterparts, biopolymers arouse a growing interest from the scientific community. A major drawback, though, is their costs typically higher than synthetic polymers. The use of underutilized food processing waste alongside food-grade polymers denotes a feasible strategy to reduce edible film production costs and to provide unique sensory, antioxidant, and nutritional properties.¹ Carrot is an inexpensive vegetable rich in phenolic compounds, carotenoids, vitamins, minerals, and fibers. Carrot processing waste was used to produce edible films featuring original properties but still meeting the mechanical, barrier and thermal requirements for food packaging applications.

Experimental Part

Carrots (26.2 ± 1.6 cm long and 4.2 ± 0.6 thick; Fig. 1a) were sanitized for 10 min in a 200 ppm chlorine solution (Fig. 1b), peeled (Fig. 1d), cut into 1 cm cubes (Fig. 1e), washed in a 3 ppm chlorine solution, and centrifuged (Fig. 1f). Stems and petioles (Fig. 1c) were discarded while peels and uneven pieces (typically regarded as waste; Fig. 1d) were blended into fine particles.

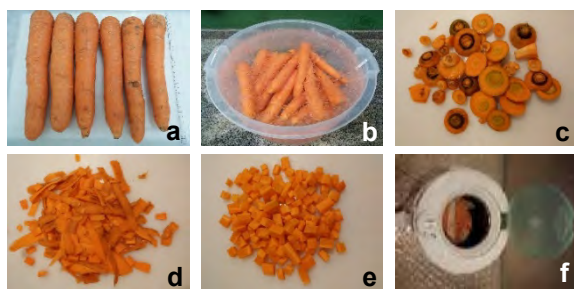


Figure 1. Illustration of carrot minimal processing into cubes.

Carrot waste particles were either spread at a constant thickness onto a flat surface and dried at room temperature for 24 h or added by 35, 45 and 55% (w/w) of hydroxypropyl methylcellulose (HPMC) Methocel® E4M (Dow Chemical, USA) and cast likewise.

Once conditioned at 50% RH for at least 48 h, the films were characterized as to their mechanical properties – through tensile testing in accordance with ASTM D882-12, water barrier properties,² and thermal degradation up to 600 °C at 10 °C/min.

Results and Discussions

Carrot waste particles did not lead to a cohesive layer detachable from the casting surface. HPMC was then added as a binding

agent and successfully led to free-standing thin films, whose mechanical and barrier properties are summarized in Table 1.

Table 1. Tensile strength (TS), elastic modulus (EM), elongation at break (EB) and water vapor permeability (WVP) of carrot waste-based edible films added by HPMC Methocel® E4M.

HPMC (%)	TS (MPa)	EM (GPa)	EB (%)	WVP (g mm/kPa h m ²)
0	-	-	-	-
35	2.5 ± 0.3	0.19 ± 0.02	1.7 ± 0.2	5.73 ± 0.62
45	3.5 ± 0.3	0.22 ± 0.02	1.8 ± 0.3	3.63 ± 0.21
55	7.9 ± 0.7	0.38 ± 0.03	3.0 ± 0.7	4.35 ± 0.24

Increased HPMC contents led to stiffer, more resistant and extensible films. Films comprising higher carrot waste contents allowed greater moisture permeation due to the plasticizing role that low M_w sugars and organic acids play in polymer matrices.¹

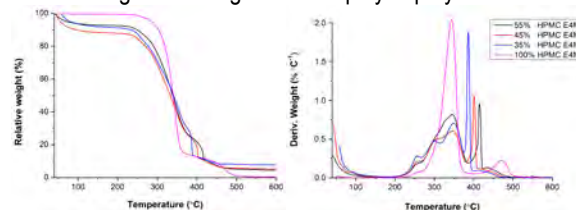


Figure 2. Thermal degradation profile of carrot waste-based films.

Fig. 2 shows that the thermal degradation profiles of all waste-containing films were similar, but poorer than that of pure HPMC films. Concerning yield, the minimal processing of 1 kg of carrot produced 462 g of reusable waste, which allowed the production of 13 m² of ~120- μ m-thick free-standing film.

Conclusions

Free-standing edible films featuring remarkable orange color and carrot flavor were produced by the combination of previously underutilized carrot processing waste and film-forming polysaccharide. Future studies are necessary to achieve films with physical properties comparable to those of synthetic polymers.

Acknowledgment: São Paulo Research Foundation (FAPESP, grant #2014/23098-9).

References

- Otoni, C. G.; Moura, M. R.; Aouada, F. A.; Camilloto, G. P.; Cruz, R. S.; Lorevice, M. V.; Soares, N. F. F.; Mattoso, L. H. C. *Food Hydrocolloids* 2014, 41, 188-194.
- McHugh, T. H.; Avena-Bustillos, R. J.; Krochta, J. M. *Journal of Food Science* 1993, 58, 899-903.

MICROBIOLOGICAL DETERIORATION OF POLYURETHANE/POLY(2-(DIETHYLAMINO)ETHYL METHACRYLATE) HYBRID MATERIALS

Paula Faccia¹, Francisco Pardini², Claudio Gervasi², Javier Amalvy^{2,3,4}, María Teresa Del Panno¹

1. CINDEFI (CCT CONICET La Plata – UNLP), Av. 50 N° 227, La Plata Argentina.
2. CIDEPIINT (CCT CONICET La Plata – CIC), Av. 52 entre 121 y 122, La Plata, Argentina.
3. INIFTA CCT CONICET La Plata – UNLP, Diag. 113 y 64, La Plata, Argentina.
4. CITEMA (UTN-FRLP), Av. 60 y 124, Berisso, Argentina.

*jamalvy@inifta.unlp.edu.ar

Introduction

Polymer biodeterioration depends on its composition and physicochemical characteristics, where small variations in the chemical structure can result in big differences in terms of biodegradability.¹ Polyurethane/acrylic hybrid systems (PU/A) have been prepared by polymerization of 2-(diethylamino)ethyl methacrylate (DEA), a stimuli-sensitive polymer, for control delivery system of active principles such as insecticide, agrochemical, or preserving food additives.² The aim of this work is to study the microbial degradation of PU/A hybrid systems.

Experimental Part

Films of PU/DEA hybrid materials (with 10 and 90% wt. of DEA) were placed into individual flasks containing 20 mL of soil suspension (20 % wt.) in mineral medium (MM) and incubated at 25°C for 1 month. After this, films were transferred into a new flask with 20 ml of MM, and incubated under the same conditions for 1 month. This step was repeated four times. Structural changes in the polymer produced by the degradation bacterial consortium were studied after the final step. FTIR-ATR spectra were obtained by recording 120 scans between 4000 and 750 cm^{-1} at a resolution of 4 cm^{-1} using an ATR accessory. Contact angle (CA) tests were performed by the sessile drop method using a Goniometer with an automated dispensing system. Weight loss (WL) was calculated after washing and drying the film at 60 °C until constant weight and the equilibrium swelling degree (SD_{eq}) by immersing the samples in distilled water at 25°C until reaching the swelling equilibrium.²

Results and Discussions

The PU spectrum after degradation is shown in Fig. 1. Variations in the intensities of the band assigned to the stretching vibration of N-H, O-H and C=O are observed. These changes can be associated with the ester bond hydrolysis and formation of urea groups.³ Hybrid films spectra show more significant changes as the decrease intensity of the peak assigned to the C-H vibration of methylene groups adjacent to the N atom of the DEA moiety; an increase of the absorbance's intensity of the band assigned to free N-H groups stretching vibration; and a decrease in the intensity of bands assigned to the vibration of the C-N bond. These changes can be attributed to the cleavages of the C-N bond of the DEA moiety.

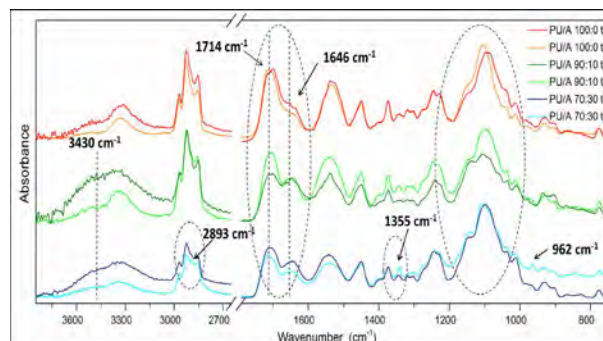


Figure 1. ATR-FTIR spectra of PU/A films before (t_0) and after (t_f) microbial deterioration.

Table 1 shows the result of WL, SD_{eq} , and CA from the samples before and after microbial deterioration. In hybrid systems are observed an increase of the SD_{eq} and a decrease of the CA. These changes are more significant for PU/A 70:30 system and can be attributed to the break of C-N bond followed by the splitting of the amine group of the DEA. The PU film shows less weight increase than hybrid films.

Table 1. Values of WL, SD_{eq} , and CA for samples, before (t_0) and after (t_f) microbial deterioration.

Sample	WL (%)	SD_{eq} (%)		CA (°)	
		t_0	t_f	t_0	t_f
PU/A 100:0	6.0	14.5	6.5	76	62
PU/A 90:10	7.4	18.3	28.4	62	44
PU/A 70:30	9.3	19.6	75.2	72	32

Conclusions

The extent of changes observed in hybrid films by the microbial deterioration are related to the DEA proportion in the polymer and they differ with those observed in PU film suggesting a different polymer degradation mechanism. PU deterioration begins by the breakdown of the polymer backbone, while in the hybrid systems it begins with the rupture of C-N bond of the amino group.

Acknowledgment: CONICET, CIC and ANPCyT (PICT 2014 – 1785).

References

1. Gu, J.D. *Int. Biodeter. Biodegr.* 2003, 52, 69.
2. Pardini, F.; Pardini, O.; Amalvy, J. *J. Appl. Polym. Sci.* 2013, 39799.
3. Shah A, Hasan F, Akhter J, Hameed A, Ahmed S. *Ann. Microbiol.* 2008, 58, 381.



SYNTHESIS AND CHARACTERIZATION OF CHITOSAN CRYOGELS

Anete Jessica Arcos-Arévalo¹, Rosa Elvira Zavala-Arce¹, Pedro Ávila-Pérez^{2,1}, Beatriz García-Gaitán¹, José Luis García-Rivas¹, María de la Luz Jiménez-Núñez¹

1. *Tecnológico Nacional de México/Instituto Tecnológico de Toluca. Avenida Tecnológico S/N Col. Agrícola Bella Vista, Metepec, México, México. C.P. 52149. rzavala@toluca.tecnm.mx*
2. *Dirección de Investigación Tecnológica, Instituto Nacional de Investigaciones Nucleares (ININ). Carretera México-Toluca S/N La Marquesa, Ocoyoacac, México, México. C.P.*

Introduction

In an effort to remove ions such as Cu^{2+} , F^- , Cd^{2+} , among others, as well as other substances like dyes, a diversity of techniques has been studied, being adsorption one of the most versatile due to its high efficiency, sludge minimization and regeneration of the sorbent material^{1,2}. In recent years, biopolymers such as chitosan have proved to be effective for fluoride removal. Chitosan is a biodegradable and biocompatible material, non-toxic, obtained from natural sources and is an ecological low cost material³. Chitosan shows a limited swelling in water, which restricts access towards its functional groups (amino and hydroxyl groups)⁴. Chemical and physical modifications improve the readiness of contact sites on chitosan, as the addition of ions such as Al^{3+} and Fe^{3+} to enhance the removal of some ions or the cryogels preparation which provide an adequate structure since they have macropores and microchannels, furthermore by adding a crosslinking agent to the cryogels is possible to obtain a more stable and resistant material against interaction with aqueous solutions, thus providing a better contact surface that can contribute to an efficiency increase during the adsorption process. The aim of this work was to synthesize chitosan's cryogels crosslinked with ethylene glycol diglycidyl ether (E) and its modification with Fe^{3+} , in order to use them in the removal of ions from aqueous solutions.

Experimental Part

QE cryogel was synthesized by preparing a chitosan solution (Q) with acetic acid, which is crosslinked with ethylene glycol diglycidyl ether (E) at 1% of weight in relation with chitosan's weight, with constant stirring for 6 h under inert atmosphere. The obtained solution was subjected to a cryogenic process, removing the water with a lyophilization process. The cryogels were washed with acetic acid at 1.5%, and deionized water till neutral pH. The QEFc cryogel is obtained by modifying the QE cryogel with FeCl_3 (0.1 M) with constant stirring 24 h, at 25 °C, the obtained cryogels were washed with ethanol and deionized water till neutral pH. Both cryogels were characterized by BET method to determine the specific surface area of cryogels, Fourier-transformer infrared spectrometer (FTIR) to identify the presence of certain functional groups, X-ray photoelectron spectrometer (XPS) to further verify the existence of study species in the materials, and scanning electron microscope (SEM) to observe the morphology of the synthesized materials and point of zero charge (PZC).

Results and Discussions

Figure 1 shows the formation of macroporous materials, in the results of EDS elemental analysis of both cryogels, it is observed that elements are carbon, oxygen, nitrogen, iron.

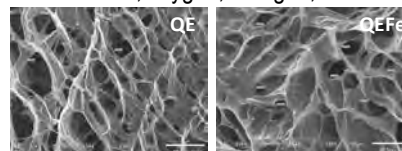


Figure 1. Cryogels QE and QEFc

The specific surface area of cryogels was determined by the BET method, the obtained specific surface area for the QE and QEFc cryogels was 36.67 and 29.17 m^2g^{-1} respectively. Figure 2 showing the cryogels's PZC, when the solution's pH is lower than the solid's pH the total charge will be positive, if the solution's pH is greater than the PZC then the surface will be negatively charged, the QEFc cryogel showed a lower PZC than the QE cryogel, which can indicate that the amount of total acids is greater than the basic groups.

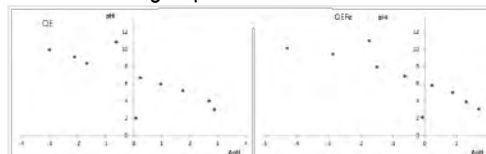


Figure 2. PZC, Cryogels QE and QEFc

The FTIR analysis allowed to identify characteristic bands of the main functional groups, which serve for various ions's removal. The XPS showed interactions of iron and oxygen in the QEFc cryogel, as well as with the amino group.

Conclusions

The obtained cryogels are porous materials that can provide a better contact surface between the functional groups of chitosan and different ions in aqueous solutions, so these materials are a suitable alternative for removal ions in water.

Acknowledgment: To DGEST, CONACYT and ININ.

References

1. Swain, S. K., T. Patnaik, P.C. Patnaik, Usha Jha, R.K. Dey.. *Chem. Eng. J.* 215–216, 2013.
2. Sujana, M.G., A. Mishra and B.C. Acharya. *Ap. Surf. Sci.* 270, 2013.
3. Huang, R., B. Yang, Q. Liu, K. Ding. *J. Flu. Chem.*, 141, 2012.
4. Kumar Reddy, D. H., S.-M. Lee. *Adv. Col. Int. Sci.* 201–202, 2013.

EFFECTO DE DOS TAMAÑOS DE PERLAS DE QUITOSANO-CELULOSA-ENTRECRUZADO CON ETILENGLICOL DIGLICIDIL ÉTER (Q-C-EDGE) EN LA ADSORCIÓN DE ROJO No. 2

Adriana Olivares Castro¹, Rosa Elvira Zavala-Arce¹, María de la Luz Jiménez Nuñez¹, Celso Hernández-Tenorio¹, Beatriz García-Gaitán¹, Mario Alejandro Gómez-Jiménez¹

1. Instituto Tecnológico de Toluca, Av. Tecnológico s/n. Colonia Agrícola Bellavista. C.P. 52149, Metepec, Edo. De México.
www.ittoluca.edu.mx

Introducción

La contaminación química del agua es causada por numerosas sustancias, que son vertidas en ella, por los sectores industriales. El descubrimiento de colorantes artificiales ha tenido un alto impacto por su amplio espectro de aplicaciones en los sectores productivos. Los colorantes tipo azo son, generalmente tóxicos y cancerígenos, al ser descargados a cuerpos de agua ha desencadenado un efecto negativo sobre la salud humana y también reduce la diversidad acuática. Una aplicación que está tomando fuerza en la actualidad es el empleo de los hidrogeles como tratamiento de aguas residuales, removiendo sustancias contaminantes que no se logran eliminar con tratamientos químicos y físicos. En este trabajo se evaluó la adsorción del colorante Rojo No.2 (R-2) utilizando esferas de hidrogel de quitosano y celulosa entrecruzadas con etilenglicol diglicidil éter.

Parte Experimental

Se sintetizó un hidrogel de Q-C y se entrecruza utilizando 0.1 ml de etilenglicol diglicidil éter (EDGE), en una solución de 7:25 hidrogel-agua desionizada. Los tamaños de perlas obtenidos en promedio fueron de 2.1 y 2.9 mm. Los experimentos se realizaron por triplicado. Las cinéticas se llevaron a cabo utilizando soluciones de R-2 de 170 mgL⁻¹ de concentración inicial y 30 mg de hidrogel a 200 rpm a temperaturas de 10, 30 y 50° C en tiempos de 0.25 a 90 horas. A partir de estos resultados se llevaron a cabo las isothermas a 72 horas, a las mismas temperaturas y velocidades de agitación empezando con una concentración de 150 mg/L con incrementos de 50 hasta 500 mg/L Las concentraciones se determinaron usando el espectrofotómetro UV-VIS.

Resultados y Discusión

En la figura 1. Se muestran los resultados de las cinéticas de adsorción realizadas a pH de 3, comparando dos tamaños de perlas de hidrogel Q-C-EDGE.

Los resultados de las isothermas se muestran en la figura número 2.

Las capacidades máximas de sorción obtenidas por los diámetros 2.9 y 2.1 fueron: 687 y 667 mgg⁻¹ respectivamente, valores

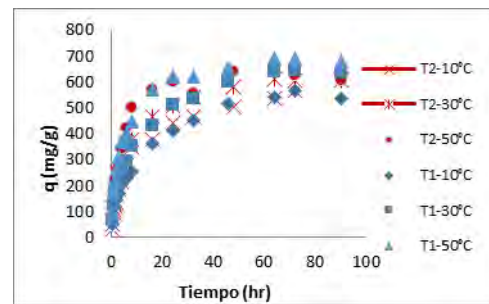


Figura 1. Cinéticas de sorción de R-2 con perlas de tamaño 2.1 mm (T2) y 2.9 mm (T1) a diferentes temperaturas

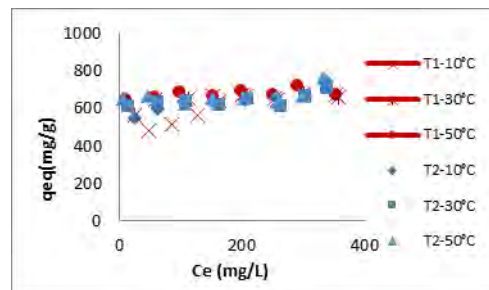


Figura 2. Comparación de las Isothermas con perlas de tamaño 2.1 mm (T2) y 2.9 mm (T1)

superiores a los reportados con películas de quitosano (105 mgg⁻¹)¹ y con hojas de Jacinto (70 mgg⁻¹)².

Conclusiones

La capacidad de adsorción del R-2 mostrada por el Q-C-EDGE es alta comparada con otros biomateriales, la variación de tamaño de perla y temperatura no mostraron un efecto considerable en la capacidad de adsorción.

Referencias

1. Rego, T.V.; Cadaval, T.R.S.; Dotto, G.L.; Pinto, L.A.A., Journal of Colloid and Interface Science 2013, 411, 29.
2. Guerrero-Coronilla; Morales-Barrera; Cristian-Urbina. Journal of Environmental Management 2015, 105.

BIODEGRADABLE POLYMERIC PLA/GO COMPOSITES WITH ENHANCED THERMO MECHANICAL PROPERTIES

Mónica Elvira Mendoza Duarte*, Iván Alziri Estrada Moreno, Daniel Lardizábal Gutiérrez, Sergio Gabriel Flores Gallardo, Erasto Armando Zaragoza Contreras, Erika Ivonne López Martínez, Alejandro Vega Rios.

Centro de Investigación en Materiales Avanzados, S.C., Ave. Miguel de Cervantes #120, 31136, Chihuahua, Chih., México.

*monica.mendoza@cimav.edu.mx

Introduction

PLA mixed with particles can experiment a modification in its properties.¹ Among the fillers that offer many different characteristics is graphite. The graphite is a material consisting of a sheet like structure (graphene), which has excellent properties. By a chemical treatment of the graphite as the Hummer's method,² graphite oxide (GO) can be obtained. GO presents numerous oxygenated functional groups that can be used to covalently bind it to polymers. The aim of this work is to investigate the effect of the inclusion of expanded graphite (EG) and graphite oxide (GO) with different oxidation grades into a poly-lactide (PLA) matrix on the thermo-mechanical properties of the composite.

Experimental Part

Poly (L,L – lactide) (2002D) –PLA-, supplied by NatureWorks LLC, was employed as the polymer matrix. Expanded graphite (EG) Grafoil TG-679 supplied by Graftech International was employed as filler particle. Graphite Oxide (GO) at two different oxidation times was obtained by the Hummer's method². For the incorporation of GE and GO in the PLA matrix the graphite was milled by a high energy ball miller. The PLA/GE and PLA/GO were obtained by melt blending in an internal mixing chamber at a graphite concentration of 0.1 wt%. The mixing temperature was 190°C under a mixing velocity program: 2min 30 rpm, 10 min 90 rpm, employing blades type CAM. The obtained composites were ground and later molded by hot press compression to obtain films for characterization.

Films were characterized by DMA in a tension film geometry. A temperature ramp was done from 20 to 140°C at a 0.1% applied strain and 1 Hz of frequency. After that films were heated a constant temperature of 110°C during 30 min to observe the variation of Elastic modulus due to the crystallization of the matrix.

Results and Discussions

The storage modulus (E') of the neat PLA at 25°C is 2.67×10^9 Pa with the filler addition this module is increased in up to 28% when it is the graphite with longer oxidation time GO(3), Figure 1. In the rubbery zone, it is observed the presence of cold crystallization, that is greater for the composites with GO particles, this suggests that the cold crystallization is favored by the oxidation of the graphite. This can be attributed to separation of the graphene layers due to oxidation. Also it is interesting the fact that the E' value for the

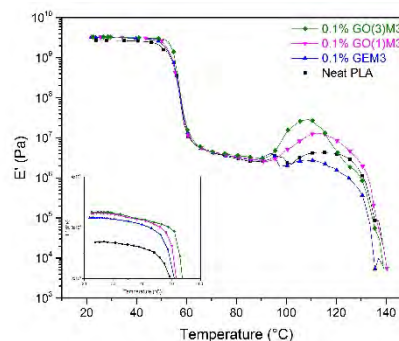


Figure 1. Temperature Ramp of PLA/GE/GO composites

PLA/GO composites starts to drop at a temperature slight higher than the neat PLA.

Figure 2 shows that during cold crystallization the E' is improved depending on the oxidation of the graphite.

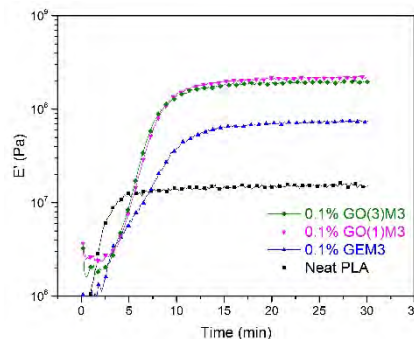


Figure 2. Time Sweep of PLA/GE/GO composites

Conclusions

The thermo-mechanical properties of the composites were improved with the addition GO. Additionally it was found that the crystallization velocity depends on the oxidation of the graphite suggesting that the functional groups obstaculize de cristal formation.

References

1. Dubois Ph, Murariu. JEC Composites Magazine. No/45 October 2008
2. Hummers and Offeman; Journal of American Chemical Society (1958).



EFFECT OF ACIDITY ON THE CATALYTIC ACTIVITY OF HZSM-5 ZEOLITES FOR ITS APPLICATION IN CHEMICAL RECYCLING OF POLYPROPYLENE PLASTIC WASTES

Yuliana Franco¹, Eliana Higueta², Omar Gutiérrez³

1. Instituto Tecnológico Metropolitano, Street 54a # 30-01, 050001, Medellín, Colombia. yuliana.franco18@gmail.com.
2. Instituto Tecnológico Metropolitano, Street 54a # 30-01, 050001, Medellín, Colombia.
3. Instituto Tecnológico Metropolitano, Street 54a # 30-01, 050001, Medellín, Colombia.

Introduction

Pyrolysis is a chemical recycling technique that has become one of the most attractive method for waste polymer treatment allowing the recovery and valorization of its degradation products.¹ For instance, if 1 kg of PE is pyrolyzed in order to obtain a hypothetical mix of 10%-petroleum gas, 30%-gasoline, 40%-diesel and 20%-wax, based on the calorific value of those commercial fuels, the net energy gained is estimated in 42 MJ/kg.² In this sense, this study deals with the modification of catalytic activity of HZSM-5 zeolites by means ionic exchange in order to determine its effect over the catalytic pyrolysis of PP, by using for this, non-isothermal pyrolysis in order to get information related to the kinetics of the thermodegradation reactions. This analysis gives useful information for the future design of industrial reactors.³

Experimental Part

Starting from HZSM-5 zeolite (HSZ-822, Tosoh Corporation) with Si/Al ratio of 23.8 and particle size of 10 mm, by using NH_4NO_3 solutions with different concentrations (5.0, 1.0 and 0.2 M), three modified HZSM-5 zeolites were respectively achieved: ZSM-5_5M, ZSM-5_1M y ZSM-5_0.2. Then, by using commercial PP wastes (disposable cups) and the four zeolites considered, thermogravimetric studies were carried out (STD 600) with heating rates (β) of 10, 15 and 20 Kmin^{-1} ; in nitrogen atmosphere (100 mL/min) with percentages of 0, 15, 30 and 45 wt.% of zeolite. For the determination of the activation energy (E_a) profile we used the isoconversional method of Friedman.⁴

Results and Discussions

The results (Fig. 1) show that values higher than 30 % wt of HZSM-5 does not significantly reduce the energy associated with the PP thermodegradation.

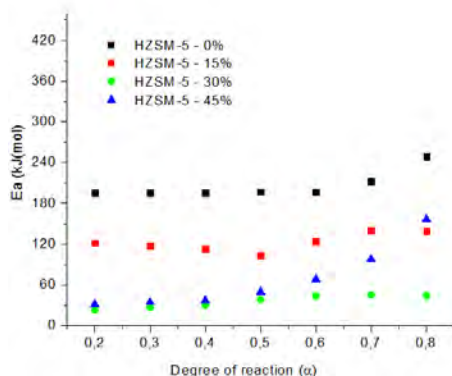


Figure 1. E_a vs. α for the different HZSM-5 catalyst weight.

Additionally, the results indicated (Fig. 2) that with the ionic exchange is possible to alter the zeolite's acidity, being useful in order to control the product distributions obtained through chemical recycling of polypropylene wastes.

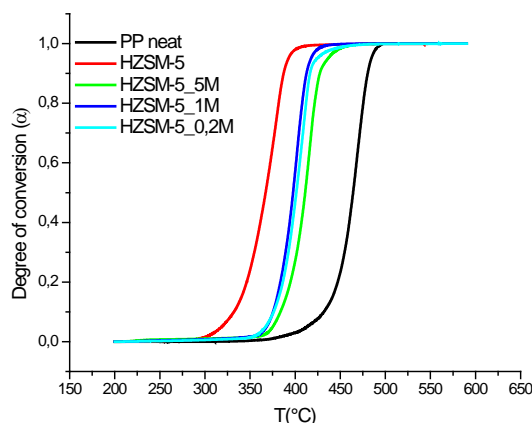


Figure 2. $\alpha(T)$ for all HZSM-5 zeolites (30 wt%., $\beta=20\text{Kmin}^{-1}$).

Conclusions

The ionic exchange treatment allowed to modulate the acidity of HZSM-5 zeolite. This result offers a great potential in terms of the control over the yield and selectivity of hydrocarbons that can be obtained with valorization or chemical recycling of plastic wastes.

Acknowledgment: Laboratorio de Ciencias Térmicas, Instituto Tecnológico Metropolitano.

References

1. Al-Salem, S. M., Lettieri, P. & Baeyens, J. *Prog. Energy Combust. Sci.* **36**, 103–129 (2010).
2. Feng, G. *Pyrolysis of Waste Plastics into Fuels*. (University of Canterbury, 2010).
3. Font, R. *Thermochim. Acta* **591**, 81–95 (2014).
4. Papageorgiou, G. Z., Achilias, D. S., Nianias, N. P., Trikalitis, P. & Bikiaris, D. N. *Thermochim. Acta* **565**, 82–94 (2013).



BIODEGRADATION UNDER COMPOSTING CONDITIONS OF PCL-BASED POLYURETHANES PRODUCED BY ENZYMATIC POLYMERIZATION

Marina P. Arrieta¹, Karla A. Barrera-Rivera², Daniel Lopez¹, Antonio Martínez-Richa², Laura Peponi¹

1. Instituto de Ciencia y Tecnología de Polímeros, ICTP-CSIC, calle Juan de la Cierva 3, 28006 Madrid, Spain

lpeponi@ictp.csic.es

2. Departamento de Química, Universidad de Guanajuato, Noria alta s/n, Guanajuato, Gto. 36050. MEXICO,

Introduction

As a consequence of the increasing environmental concern, biodegradable materials are gaining interest in several industrial sectors. Poly(ϵ -caprolactone) (PCL) is a biodegradable polymer interesting for the developed of biodegradable poly(urethanes). Moreover, enzymatic polymerizations offers a great opportunity for using non petrochemical renewable resources as starting substrates of functional polymeric materials and thus contributes to global sustainability without depletion of scarce resources. Therefore, enzymatic polymerization has a large potential as an environmentally friendly synthetic process of polymeric materials, providing a good example to achieve “green polymer chemistry”.

Enzyme-catalyzed polymerization may become a versatile method for the production of sustainable polyurethanes, as lipase, for example, is a renewable catalyst with high catalytic activities. The most prominent advantage of using a hydrolytic enzymes for the production of polymers is the reversible polymerization-degradation reaction that allows chemical recycling¹.

Experimental Part

Oligomeric PCL diol was synthesized using biocatalysis with immobilized *Yarrowia lipolytica* lipase (YLL) and diethyleneglycol as initiator. Two different linear poly ester-urethanes were prepared from synthesized PCL diol with HDI, named PU0, and with amino acid chain extenders, L-lysine ethyl ester dihydrochloride¹, named PU2. The obtained materials were disintegrated under composting conditions following the ISO-20200 standard². Samples were recovered from the disintegration container at different times. Morphological analysis was further carried out to all degraded samples by visual appearance and scanning electron microscopy (SEM).

Results and Discussions

The degradation of both PU were studied under composting conditions and checked at different times. The observations showed that both PUs increased their opacity during composting and they were totally disintegrated after 50 days (Fig. 1). SEM analysis (Fig. 2) showed that the structural disintegration was higher for PU2 than for PU0.

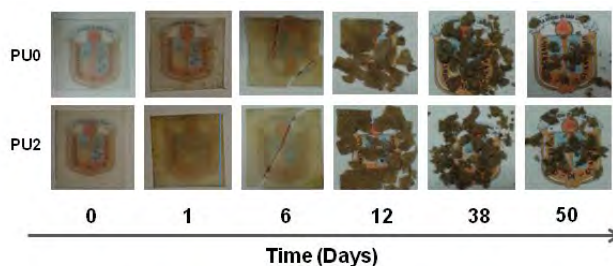


Figure 1. Visual appearance of PU films at different disintegration times under composting

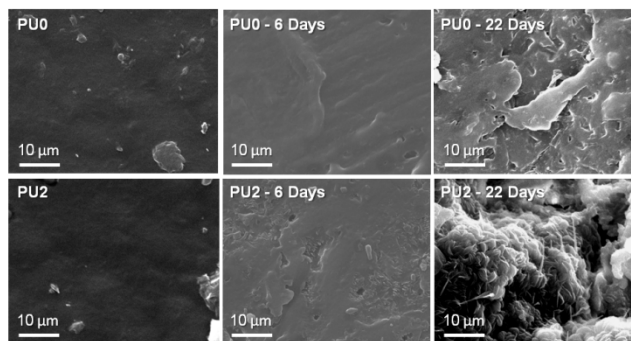


Figure 2. SEM observations at different disintegration times under composting for both PUs.

Conclusions

Both PUs were successfully disintegrated under composting conditions in less than two month, showing their biodegradable character.

Acknowledgment: We are indebted to the MINECO for the MAT2013-48059-C2-1-R. LP and MPA acknowledge MINECO for the “Ramon y Cajal” (RYC-2014-15595) and “Juan de la Cierva” (FJCI-2014-20630) contracts.

References

1. Barrera-Rivera, K.A., Marcos-Fernández, A., Martínez Richa, A. *ACS Symposium Series*, 2015, 1192, 27-40.
2. UNE-EN ISO 20200-2006.

DEVELOPMENT OF BIORESORBABLE ELECTROSPUN SMALL-DIAMETER VASCULAR GRAFTS

Florencia Montini-Ballarín¹, Pablo C. Caracciolo¹, Gustavo A. Abraham¹

1. Instituto de Investigaciones en Ciencia y Tecnología de Materiales, INTEMA (UNMdP-CONICET), Av. Juan B. Justo 4302, B7608FDQ, Mar del Plata, Argentina. gabraham@fi.mdp.edu.ar

Introduction

To this day, the development of small-diameter vascular grafts (SDVG, < 6 mm) with an appropriate biomechanical response still presents a big challenge. The availability of an off-the-shelf conduit, without long *in vitro* culture periods, with proper biological and mechanical properties for coronary bypass surgery is the main challenge of vascular tissue engineering.¹ In this work, we developed a bilayered nanofibrous bioresorbable electrospun conduit from poly(L-lactic acid) (PLLA) / segmented poly(ester urethane) (SPU) blends, by mimicking the collagen-to-elastin ratio of media and adventitia layers in native tissues. The influence of the different electrospinning parameters into the fiber formation, fiber morphology and fiber mean diameter for PLLA, SPU and two PLLA/SPU blends were studied. *In vitro* hydrolytic degradation and mechanical behaviour were exhaustively investigated. Surface modification of inner layer with heparin and lysozyme was performed to introduce antithrombogenic properties and to reduce the risk of infection after implantation, respectively.

Experimental Part

SDVG were prepared by electrospinning technique. SPU was synthesized from polyester macrodiol, aliphatic diisocyanate and a diester-diphenol chain extender.² PLLA/SPU solutions 90:10 and 50:50 were sequentially electrospun to form an outer and inner layer, respectively. Tubular structures were fully characterized in terms of physico-chemical, morphological, thermal and surface properties. A complete mechanical characterization was performed by uniaxial tension, suture, dynamical compliance and burst pressure tests.³ *In vitro* studies of platelet adhesion and cytotoxicity by MTT test analyzing mesenchymal stem cells proliferation were performed on SDVG before and after surface modification.

Results and Discussions

Electrospinning parameters and solution intrinsic properties were optimized for PLLA, SPU, and their blends. Bead-free uniform nanofibers were obtained. A bilayered SDVG was successfully produced by sequential electrospinning of blends (Fig. 1). *In vitro* degradation studies suggested that degradation time would match the required for regeneration process. The biomimetic mechanical response displayed a behavior in the range of natural vessels (Fig. 2). Surface modification by ester and urethane groups were explored. Both routes displayed good heparinization density. Surface-modified SDVG did not induce cytotoxicity on MSC and presented a reduction in platelet adhesion.

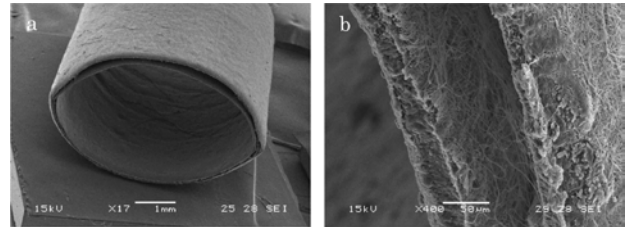


Figure 1. SEM micrographs showing the bilayered nanofibrous structure

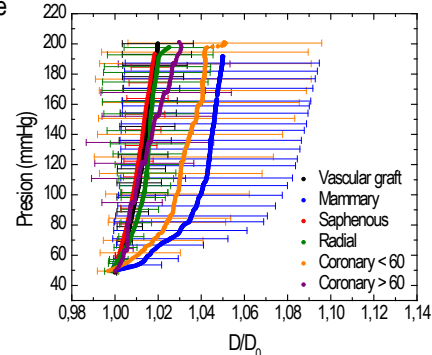


Figure 2. Comparison of P vs D curves among vascular graft, coronary, radial, mammary and saphenous vessels.

Conclusions

Bioresorbable SDVG presented a J-shaped response when subjected to internal pressure as a cause of both nanofibrous layered structure and composition. Compliance values were in the order of native coronary arteries and very close to the bypass gold standard-saphenous vein. Studies with human umbilical vein endothelial cells (HUVECs) on dynamic bioreactor are in progress.

Acknowledgment: CONICET, ANPCyT, UTNBA (Argentina), UDELAR (Uruguay), USC and UPM (Spain).

References

- Hasan, A.; Memic, A.; Annabi, N.; Hossain, M.; Paul, A.; Dockmeci, M.R.; Dehghani, F.; Khademhosseini, A. *Acta Biomater.* 2014, 10, 11.
- Caracciolo, P.C.; Thomas, V.; Vohra, Y.; Buffa, F.; Abraham, G.A. *J. Mater. Sci. Mater. Med.* 2009, 20, 2129.
- Montini-Ballarín, F.; Calvo, D.; Caracciolo, P.C.; Rojo, F.; Frontini, P.M.; Abraham, G.A.; Guinea-Totuerro, G. *J. Mech. Behavior Biomed. Mater.* 2016, 60, 220.

ON THE FRICTION AND WEAR CHARACTERISTICS OF POLY(METHYLMETHACRYLATE)/ BIPHASIC CALCIUM PHOSPHATE COATINGS UNDER LUBRICATED CONDITION

L. Daniel Aguilera¹, Karla J. Moreno^{1*}, J. Santos García¹, Julio de Jesús Aguirre^{1,2}, Griselda Castruita de León³, Héctor Iván Meléndez Ortiz³

1. Instituto Tecnológico de Celaya/TNM, Ave. Tecnológico S/N, 38010 A.P.57, Celaya, México. karla.moreno@itcelaya.edu.mx

2. Universidad Politécnica Juventino Rosas C.P. 38253, Guanajuato, México

3. CONACYT-Centro de Investigación en Química Aplicada, Blvd. Enrique Reyna 140, 25294, Saltillo, Coahuila, México.

Introduction

Biphasic calcium phosphates (BCPs) composed of hydroxyapatite (HA) and β -tricalcium phosphate (β -TCP) are widely recognized for their excellent biocompatibility properties due to similitude to bone mineral¹. The present work focused on the friction and wear of poly(methylmethacrylate)/ biphasic calcium phosphate (PMMA/BCP) coatings on stainless under lubricated condition and investigated the influence of BCP concentration as previous study in order to consider it as coating for load bearing implants to enhance the service life of the artificial replacements.

Experimental Part

BCP powder was obtained previously by a precipitation method², posteriorly; BCP with different concentration was added during PMMA polymerization by free radical from its monomer methyl methacrylate (MMA) obtaining a homogenous solution with BCP concentrations of 0.10 wt. %, 0.25 wt. %, 0.35 wt. %, 0.50 wt. % with respect to amount of MMA used. Cylindrical stainless substrates were immersed in PMMA/BCP solutions; the samples were dried at 90°C during 4 h. The wear tests were carried out on a Tribometer applying the pin on disk method³ with 2N of load, simulated body fluid was used as lubricant. The wear mechanism was observed by an optical microscope.

Results and Discussions

Figure 1 exhibit the variation of kinetic friction coefficients (μ_k) with the sliding distance for PMMA/BCP coatings at different BCP concentration. PMMA/BCP coating showed the higher friction coefficient values at 0.35wt.% of BCP concentration while the lowest values of μ_k were obtained for the maximum and minimum content of BCP, 0.10wt.% and 0.50wt.%, respectively; however, it can be note that behavior of friction coefficient more stable was for PMMA/BCP coating at 0.10wt.%. The inset of figure 1 shows the influence of BCP concentration on the volume loss and wear rate finding the lowest values for PMMA/BCP coating with 0.35wt.%. Figure 2 exhibit the wear track (WT) for PMMA/BCP with 0.10wt.% and 0.25wt.% as representatives. It can be observed the lightly decrease in the wear track width (WTW) with the increase of BCP concentration, the grooves present inside the WT, which are parallel to sliding direction (SD), are characteristic of abrasive wear.

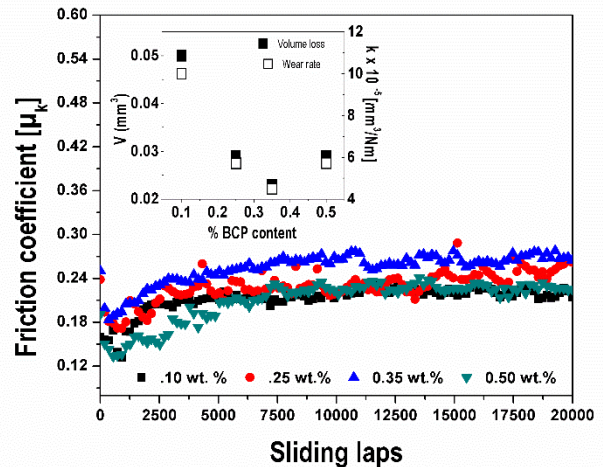


Figure 1. Variation of friction coefficients of PMMA/BCP coating.

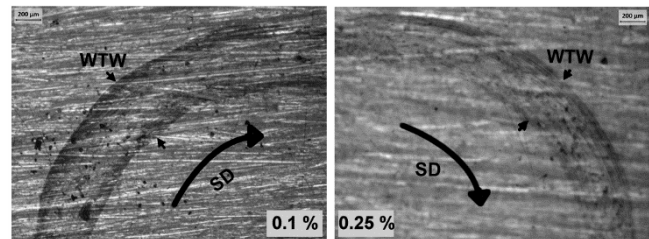


Figure 2. Micrographs of wear track for PMMA/BCP produced after pin on disk test under lubricated condition.

Conclusions

The results suggest that PMMA/BCP coating with 0.35 wt.% exhibited better characteristic tribological doing it more suitable as protective coating in future medical applications such as bearing implants.

Acknowledgment: The authors gratefully the financial support of TNM.

References

1. Lei, N.; Dong, C.; Jun F.; *et. al.* Biochem. Eng. J. 2016, 98, 29.
2. Carolina H.N. Master in Chemistry Science Dissertation, ITC, 2010.
3. ASTM Standard G99-05:2005, Standard Test Method for Wear Testing with a Pin-on-Disk Apparatus.

IMPROVED THERMAL PROPERTIES OF NEW CYANOACRYLATE POLYMERS CONTAINING 6-HYDROXYHEXYL ACRYLATE

Gabriel Estan-Cerezo^{1,2}, Diego A. Alonso², José Miguel Martín-Martínez¹

1. Adhesion and Adhesives Laboratory, University of Alicante, 03080 Alicante, Spain. jm.martin@ua.es
2. Organic Chemistry Department and Institute of Organic Synthesis, University of Alicante, 03080 Alicante, Spain.

Introduction

Cyanoacrylate adhesives are used in revealing fingerprints and cyanoacrylate polymers have been recently used in drug delivery systems because of their ability to degrade with time. The performance of the cyanoacrylate polymers are limited by their poor stability at high temperature. In order to improve the thermal stability, the addition of different compounds to cyanoacrylates has been proposed, including ethyleneglycol diacrylate [1], methyl methacrylate [2], and methyl vinyl ketone [3], among other. Although most of these additives improved the thermal stability of cyanoacrylate polymers, the adhesion property decreased. Therefore, in this study the addition of a novel acrylate – 6-hydroxyhexyl acrylate (HHA) – is proposed for improving the thermal stability of ethyl cyanoacrylate (ECN) without reducing its adhesion.

Experimental

Ethyl cyanoacrylate (ECN) was provided by Adhbio S.L. (Elche, Spain). 6-hydroxyhexyl acrylate (HHA) was synthesized by reacting 1,6-hexanediol and acryloyl chloride [4]. Three mixtures containing 0, 5.7, and 10 v/v% of HHA in ECN were prepared and stored in opaque glass vials. Polymerization of ECN and ECN+HHA mixtures was carried out by drop-wise addition of 1 v/v% aqueous (ultrapure water) triethylamine solution.

The chemical structure and tacticity of the polymers were analyzed by ¹H- and ¹³C-NMR. Differential Scanning Calorimetry (DSC) was used for analyzing the structure and thermal stability of ECN and ECN+HHA polymers. The thermal stability of the polymers was determined by Thermal Gravimetric Analysis (TGA). Finally, the adhesion properties of ECN and ECN+HHA mixtures were obtained by using single lap-shear test, a pulling rate of 100 mm/min was used.

Results and Discussion

Immediate adhesive strength of flexible PVC/ECN+HHA mixture/flexible PVC joints (Table 1) increases when HHA is added, more noticeably by adding 10 v/v% of HHA.

Table 1. Immediate adhesion of flexible PVC/ECN+HHA mixture/flexible PVC joints.

Mixture	Shear strength (kPa)	Locus of failure
ECN	121 ± 28	CA*
ECN+5% HHA	130 ± 31	CA
ECN+10% HHA	268 ± 43	CA

* CA = Cohesive failure of the adhesive.

Table 2 shows that in the first DSC heating run, the enthalpy of post-polymerization of ECN is reduced by adding HHA, i.e. the addition of HHA enhances the extent of polymerization of the ECN monomer. Table 2b shows that in the second DSC heating run, the addition of HHA causes a decrease in the T_g value, indicating an improved polymer toughness and flexibility.

The thermal stability of the polymers obtained from the just prepared mixtures was also studied by TGA. Between 125 and 200°C, the highest

is the HHA loading, the lowest is the polymer stability (Figure 6), but the thermal stability is improved at temperatures above 225 °C. Therefore, at low temperature the occluded HHA between the polymer matrix is released by heating giving low molecular weight species, whereas the major thermal stability at higher temperature is due to the formation of few larger polymer chains of ECN. On the other hand, the ECN+10%HHA polymer prepared from the mixture stored for 192 days shows lower thermal stability at low temperature (70-100°C) than for ECN polymer, probably due to the formation of oligomers caused by the nucleophilic reactivity of the HHA. Furthermore, after 192 days of storage, the thermal stability of ECN+10%HHA polymer increases noticeably and the decomposition temperature is produced around 300°C likely due to the formation of bigger polymer chains and cross-linked structure induced by reaction between ECN and HHA.

Table 2. Some parameters obtained from DSC experiments.

Polymer	ΔH _{post-pol} (J/g)	T _g (°C)
ECN	26	130
ECN+5% HHA	19	122
ECN+10% HHA	8	107

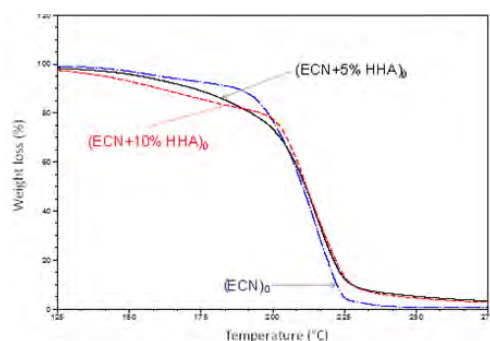


Figure 1. Variation of the weight loss as a function of the temperature for ECN+HHA polymers. Under script “o” means polymers prepared by using the just prepared mixtures.

Conclusions

Addition of HHA increases the toughness and thermal stability of ECN polymers. The higher is the amount of HHA added, the higher is the thermal stability and adhesion of ECN+HHA polymers.

References

1. Samatha, P.; Thimma Reddy, T.; Srinivas, P.N.; Krishnamurti, Polym. Plast. Technol. Eng. 2000, 39, 381.
2. Han, M.G.; Kim, S. Polymer 2009, 50, 1270.
3. Maruyama, K.; Tsushima, Y.; Kuramochi, T.; Ibonai, M.; Nagasawa, K. Int. J. Adhes. Adhes. 1989, 9, 143.
4. Alconcel, S.N.S.; Kim, S.H.; Tao, L.; Maynard H.D. Macromol. Rapid Commun. 2013, 34, 983.



CASTOR OIL BASED POLYURETHANE / TITANIUM COMPOSITE FOAMS

Fernando J. Aguilar-Perez¹, Rossana F. Vargas-Coronado¹, Juan V. Cauich-Rodríguez¹, Juan J. Pavon-Palacio², José A. Rodríguez-Ortiz³, Yadir Torres-Hernández³

1. Centro de Investigación Científica de Yucatán, Calle 43 # 130, Colonia Chuburná de Hidalgo, CP 97200, Mérida, Yucatán, México. *jvcr@cicy.mx*
2. Grupo de Biomateriales Avanzados y Medicina Regenerativa, BAMR, Universidad de Antioquia, Calle 67 No. 53–108, AA 1226, Medellín, Antioquia, Colombia.
3. Escuelas de Ingeniería, Dpto. de Ingeniería y Ciencia de Materiales y del Transporte, Universidad de Sevilla, Sevilla, España.

Introduction

Biocompatible polyurethanes (PU) foams based on Castor oil (CO) have been suggested for bone regeneration.¹ However, one of the main drawbacks is the difference in the mechanical properties between the bone and the PU foams. Therefore, it is possible to improve their mechanical performance by using biocompatible fillers such as titanium (Ti). This metallic biomaterial is a good alternative for bone tissue replacement as a consequence of its balance of mechanical, physical-chemical, and biofunctional properties.² Considering this, the aim of this study was to obtain composites foams made of CO based PU and Ti powder and to perform a physical-chemical and mechanical characterization to determine their suitability for bone regeneration purposes.

Experimental Part

CO based polyurethane composites foams were prepared by simultaneous polymerization and foaming. For this, castor oil, Tin (II) 2-ethylhexanoate and Ti powder (for 1, 3 and 5 wt.%) were mechanically stirred at 60 °C. After this, isophorone diisocyanate (IPDI) was added dropwise into the castor oil/Ti mixture and the reaction kept for 10 min in order to obtain a prepolymer. Then, 1,4-butanediol and deionized water were used as a chain extender and as foaming agent respectively. After 2 min of stirring, the polymer was placed in an oven at 120 °C for 1 h. Composites were characterized by Fourier transform infrared spectroscopy (FTIR) using attenuated total reflectance (ATR), X-ray diffraction (XRD) and scanning electron microscopy (SEM). Compressive mechanical test were performed using 1 cm² (base) x 2 cm (height) prism. Density and porosity were determined using Archimedes principle.

Results and Discussions

Preliminary observation showed that the foam height decreased when the amount of Ti increased and that a more intense grey color was developed. Pores with interconnections were confirmed, registered and measured by SEM (Fig. 1a). The FTIR spectra of unfilled PU and PU/Ti composite foams are shown in Figure 1b. The PU synthesis was confirmed by FTIR spectra as the characteristic bands of PU at 3356, 2923 and 1741 cm⁻¹, for N-H, C-H and C=O respectively were observed. X-ray reflections at 2θ = 40.2° confirmed the presence of Ti in composites' foams as this peak increased with Ti concentration (Fig. 1c). Density and

porosity of foams (see Table I) agree with values reported in literature.³ Compressive modulus and strength tend to increase with Ti concentration as observed in Table I.

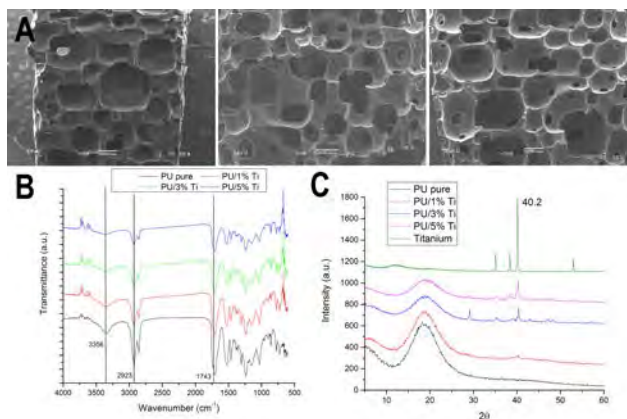


Figure 1. a) SEM images of PU/Ti composites with 1, 3 and 5 wt.%; b) and c) FTIR and XRD of composite foams.

Table I. Compressive mechanical properties of PU and composites' foams.

Foam	E (kPa)	σ_{max} (kPa)	Density (kg/m ³)	Porosity %
PU	4.7 ± 0.9	16.4 ± 2.9	128 ± 7	87
PU/1% Ti	8 ± 4.7	39.2 ± 0.7	171 ± 12	83
PU/3% Ti	16.3 ± 3.3	68.7 ± 6.6	196 ± 16	82
PU/5% Ti	14 ± 2.3	86.4 ± 10.6	240 ± 14	80

Conclusions

Composite foams exhibited properties that depended on Ti concentration. Density of foams increased when Ti increase but porosity was reduced. Both compressive strength and modulus of composite foams tend to increase with Ti concentration. These properties are lower than trabecular bone.

Acknowledgment: CONACYT 248378 Project. Daniel Aguilar for DRX technical assistance (projects FOMIX-Yucatán 2008-108160 and CONACYT LAB-2009-01 No. 123913). PhD scholarship 389314 from CONACYT.

References

1. Cangemi JM, et al. *Polimeros: Ciencia e Tecnologia* 2008. 18(3):201-6.
2. Demetrio da Silva V, et al. *Polym Bull* 2013. 70(6):1819-33.
3. Wang L, et al. *Biomed Mater* 2009. 4(2):025003.

POLYETHYLENE GLYCOL DIGLYCIDYL ETHER CROSSLINKED CHITOSAN AS BIOMATERIAL

M. G. Chuc-Gamboa ¹, J. A. Tec-Sánchez ¹, R. Vargas-Coronado ¹, J. V. Cauch-Rodríguez ¹, J.M. Cervantes-Uc ¹,
M.P. Gutierrez-Amador ²

1. Centro de Investigación Científica de Yucatán, Calle 43 # 130, Colonia Chuburna de Hidalgo, CP 97200, Mérida, Yucatán, México. jvcr@cicy.mx
2. Escuela Superior de Apan, Universidad Autónoma del Estado de Hidalgo. Carretera Apan-Calpulalpan km 8. C. P. 43920, Apan, Hidalgo, México.

Introduction

Chitosan (CHT) is a natural polycationic saccharide with many applications as biomaterial and as scaffold for tissue engineering purposes.¹ Its applications range from wound dressing and controlled drug release to soft and hard tissue replacement.² However, as a natural polymer its properties depend on source, degree of deacetylation, degree of crosslinking, etc. In this regard, glutaraldehyde (GA) is one of the most common crosslinking agents with the problem of residual aldehyde groups that can lead to calcification or even toxicity. With this in mind, we are proposing the use of polyethylene glycol diglycidyl ether (PEGDE) as a crosslinking agent to stabilize the polymeric network. This study belong to a project that will made use of this scaffold for bone tissue engineering using dental pulp stem cells. Therefore, characterization of the PEGDE crosslinked chitosan is presented.

Experimental Part

Chitosan of medium molecular weight and degree of deacetylation of 70-80% (Aldrich) was dissolved in acetic acid aqueous solution (0.4 M) and then crosslinked with either GA or PEGDE at various concentrations. Films obtained after solvent casting were neutralized with 5 wt.% NaOH, washed with distilled water and dried at room temperature. The crosslinked films were characterized by FTIR, UV, DSC, TGA, WAXS, SAXS and SEM. Swelling behavior on distilled water was also followed up to 7 days.

Results and Discussions

The FTIR spectra (Fig. 1) of CHT-PEGDE films showed a broad band at 3355 cm⁻¹ attributed to OH and NH and the band at 1648 cm⁻¹, attributed to amide I (C=O stretching) without appreciable changes after crosslinking. CHT-GA films showed higher UV absorption than CHT-PEGDE films. Evidence of crosslinking was provided by TGA as the decomposition temperature was lower than the pristine CHT. From swelling measurements, water absorptions were 221.6% (CHT), 72.0% (CHT-GA), 168.2% (CHT-PEGDE 1), 159.1% (CHT-PEGDE 2), 110.1% (CHT-PEGDE 3) respectively. As shown in Fig 2, the SAXS spectra of chitosan crosslinked films exhibited its characteristic crystalline peaks at 12° and 20°. In addition, this technique allows the identification of diffraction peaks at 3°, 5°, 9°, 11° and 14°, which do not appear in WAXS diffractogram but assigned to both hydrated

and anhydrous crystalline structures.

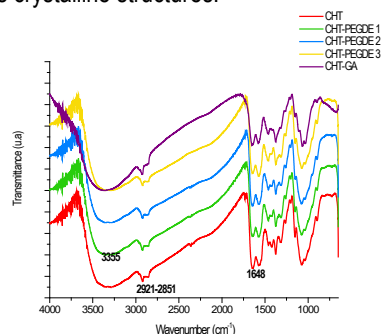


Figure 1. FTIR spectra of Chitosan (CHT), glutaraldehyde crosslinked chitosan (CHT-GA), PEGDE crosslinked chitosan (CHT-PEGDE) at 0.114 mM (1), 0.228 mM (2) y 0.342 mM (3).

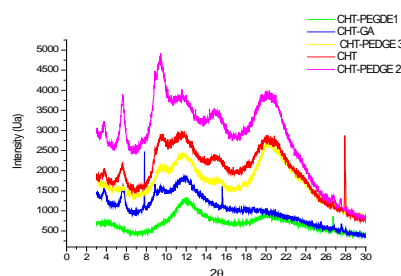


Figure 2. SAXS spectra of Chitosan (CHT), glutaraldehyde crosslinked chitosan (CHT-GA), PEGDE crosslinked chitosan (CHT-PEGDE) at 0.114 mM (1), 0.228 mM (2) y 0.342 mM (3).

Conclusions

The results achieved up to now, demonstrate that PEGDE can be used as an alternative crosslinking agent for chitosan. SEM micrographs showed different rugosities depending on the crosslinker type. Biocompatibility studies are being conducted in order to assess their adhesion and proliferation of DPSC.

Acknowledgments: CONACYT 248378 Project. Daniel Aguilar for DRX technical assistance (projects FOMIX-Yucatán 2008-108160 and CONACYT LAB-2009-01 No. 123913). Ing. Bt. Jessica Arlete Porcallo Rojas for SEM micrographs.

References

1. Rafferty R, O'Brien FJ, Cryan SA. *Molecules* 2013. 15:5611.
2. Saravanan S, Leena RS, Selvamurugan N. *Int J Biol Macromol* 2016. 141:30115.



AN ALTERNATIVE FOR THE TREATMENT OF CHAGAS DISEASE: HYDROGELS FOR BENZNIDAZOLE CONTROLLED RELEASE

Valeria S. Garcia, Verónica D. Gonzalez, Luis M. Gugliotta

INTEC (CONICET - UNL), Güemes 3450, 300, Santa Fe, Argentina. lgug@intec.unl.edu.ar

Introduction

Chagas' disease is an illness that affects 8 to 10 million people.¹ Benznidazole (Bz) is the drug most widely used drug for treating Chagas. Between 4% and 20% of adult patients treated with Bz have shown side effects.^{2,3} Here we propose the use of patches formed from hydrogels for Bz controlled release. The use of hydrogels to this purpose not only allows the controlled drug administration, but also reduces the frequency and magnitude of Bz dose; which reduces the occurrence of side effects and increases comfort in the administration. In the present work, the following variables were studied in order to find the best conditions for the release of Bz from *N,N*-dimethylacrylamide (DMA) hydrogels: i) the release time; ii) the hydrogel thickness (5 and 1 mm); iii) the strategy the Bz load (during the synthesis and after synthesis); and iv) the release medium (pH 5 and pH 7).

Experimental Part

Synthesis: DMA hydrogels crosslinked with *N,N*-methylene-bis-acrylamide (BIS) were synthesized by solution free-radical polymerization at 37 °C for 4 h into syringes (12 mm in diameter). The mass fraction of DMA in water was 10 wt% and the ratio of BIS/DMA was 2 mol%. Upon reaction completion, hydrogels were cut into discs (1 and 5 mm thickness), washed and dried to constant weight. To assess the effect of drug loading, a group of hydrogels were synthesized in the presence of Bz.

Release Studies: Bz loading into the DMA hydrogels was carried out by the swelling equilibrium method. The release of Bz was realized by placing the xerogel loaded into 10 mL of pH 5 or pH 7 buffer at 37°C. At periodic intervals, 1 mL of solution containing drug were withdrawn and 1 mL of buffer was added to keep constant the final volume.

Results and Discussions

The effect of the following variables on the Bz release was studied:

Release time: at 5 hours practically all loaded Bz was released from the hydrogels (Fig. 1.a). This behavior could be due to: i) drug becomes trapped on the surface of the matrix during the loading process and is released immediately upon activation in a release medium; and ii) migration of drug to surface during drying. To explain the latter behavior, loaded hydrogels were tested without previous drying. Under this last conditions, 60% of the Bz was released from hydrogel; while 71% of Bz was released from xerogel (Fig. 1.b). The high percentage of Bz released from hydrogels, may be attributed to surface adhesion of the drug to the hydrogel surface.

Hydrogels thickness: 71% of Bz was released from xerogel with 1 mm thickness, while only 33% of Bz was released from the

xerogel of 5 mm thickness (Fig. 1.c). Drug release depends on two processes which occur simultaneously, water absorption and drug diffusion out of the hydrated polymer. Thus, the increase in the hydrogel thickness, affects the release pattern.

Bz load strategy: 71% of Bz was released from xerogel loaded after synthesis, while only 39% of Bz was released from xerogel synthesized in the presence of Bz (Fig.1.d). In the loading with synthesis, the Bz may react with the monomer and could not be released from the matrix. Furthermore, the polymerization conditions may affect the integrity and efficiency of the drug.

Release medium: no significant differences were observed for the Bz release at pH 5 (68%) and pH 7 buffer (71%). The change in buffer solution had no effect on the water uptake of the DMA hydrogels because of their non-ionic character (Fig. 1.e).

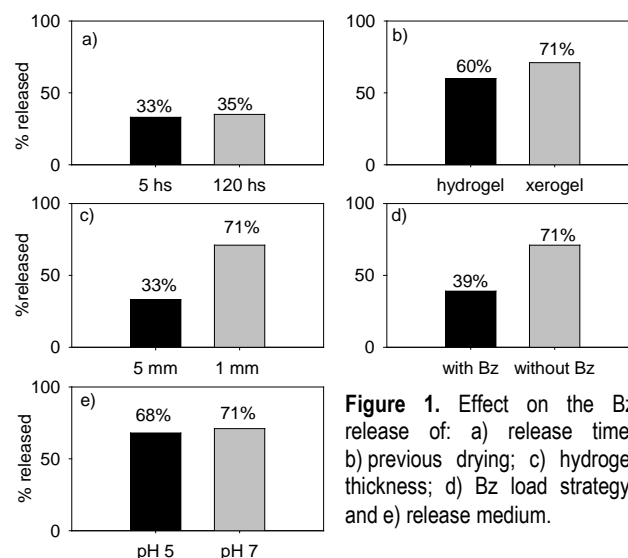


Figure 1. Effect on the Bz release of: a) release time; b) previous drying; c) hydrogel thickness; d) Bz load strategy; and e) release medium.

Conclusions

From these preliminary results, DMA hydrogels could be possibly used in the transdermal treatment of patients with Chagas disease. However, further work is required to establish the utility of this system through long-term pharmacokinetic studies.

Acknowledgment: To CONICET and UNL for their financial support. To Maprimet S.A. for the donation of Bz.

References

1. Organización Panamericana de la Salud 2006.
2. Castro J., Montalto M., Bartel L. Hum. Exp. Toxicol. 2006, 25,471.
3. Sosa Estani S., Segura E. Curr. Opin. Infect. Dis. 2006, 19, 583.



POLYURETHANES BASED ON METFORMINE AND ATORVASTATIN FOR THE CONTROL OF METABOLIC SYNDROME

Guido Zapata-Catzin ¹, Marcos Bonilla-Hernández ¹, Rossana Vargas-Coronado ¹, Juan V. Cauich-Rodríguez ¹, Stefania Zeppetelli ², Assunta Borzacchiello ²

1. Centro de Investigación Científica de Yucatán, Calle 43 # 130, Colonia Chuburna de Hidalgo, CP 97200, Mérida, Yucatán, México. *jvcr@cicy.mx*
2. Institute for Polymers, Composite and Biomaterials (IPCB) National, Research Council of Italy Mostra d'Oltremare pad. 20, Viale J.F. Kennedy 54, 80125 Napoli, Italia.

Introduction

Biodegradable segmented polyurethanes (SPUs) represent a promising class of polymers for various biomedical applications including soft and hard tissue replacement.¹ However, their potential can be extended to drug delivery applications.² In this study, polyurethanes with metformin (Met) or atorvastatin (Atv) as chain extenders were synthesized. These new polymers were physicochemically characterized and cultured with fibroblast to assess their potential biomedical applications.

Experimental Part

SPUs were synthesized by the reaction of poly (ϵ -caprolactone) diol with an excess of 4,4'-methylene-bis-cyclohexyl diisocyanate and then chain extended with either Met or Atv. SPUs were characterized by Fourier transform infrared spectroscopy (FTIR), thermogravimetric analysis (TGA) and differential scanning calorimetry (DSC). Biocompatibility was assessed using L929 fibroblasts in contact with polyurethane extracts (obtained according to ISO 10993-5) by means of the Alamar Blue assay.

Results and Discussions

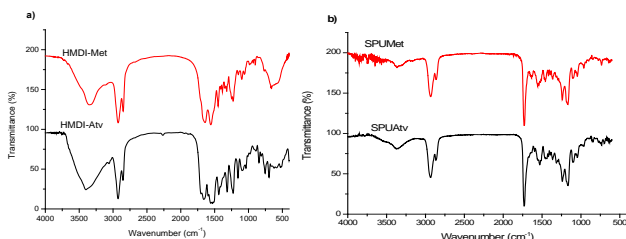


Figure 1. FTIR spectra of a) HMDI-Met and HMDI-Atv. b) SPUMet and SPUAtv.

Model polymers made of HMDI-Met (Figure 1a top), N-H stretching was observed at 3350 cm^{-1} , C=O at 1641 cm^{-1} and C-N at 1560 cm^{-1} . In model polymers made of HMDI-Atv (Figure 1a bottom), N-H was located at 3403 cm^{-1} , C=O at 1660 cm^{-1} and C-N was masked by absorption at 1596, 1553, 1527 and 1510 cm^{-1} probably due to aromatic C=C. The corresponding SPUMet (Figure 1b top) showed peaks at 3365 cm^{-1} (N-H), 1729 cm^{-1} (C=O for ester) and 1635 cm^{-1} (C=O for ureas) and 1557 cm^{-1} (C-N). SPUAtv (Figure 1b bottom) showed absorption at 3366 cm^{-1} (N-H), 1731 cm^{-1} (C=O for ester) and 1595 cm^{-1} (C=C).

The thermal properties of these SPUs are summarized in Table 1.

Table 1. Thermal properties of SPUMet and SPUAtv.

Sample	PCL:HDMI:ATV	% Hard segment	% Soft segment	DSC ($^{\circ}\text{C}$)		TGA ($^{\circ}\text{C}$)	
				T_m^a	First decomposition (T_d1)	Second decomposition (T_d2)	
SPUAtv	1:2.2:1	35.135	64.864	52.41	277	445	
SPUMet	1:2.5:1.5	31.137	68.863	52.10	332	461	

^a T_m =melting temperature for PCL, T_d is decomposition temperature.

SPUs were semicrystalline polymers ($T_m=52^{\circ}\text{C}$) as shown by DSC while thermal stability depended on the type of chain extender. In general, SPUAtv tend to be less thermally stable than SPUMet.

Both SPUAtv and SPUMet extracts, obtained from polyurethanes without triethylamine, showed positive effects on cell viability of L929 fibroblasts up to day 5 (see Figure 2).

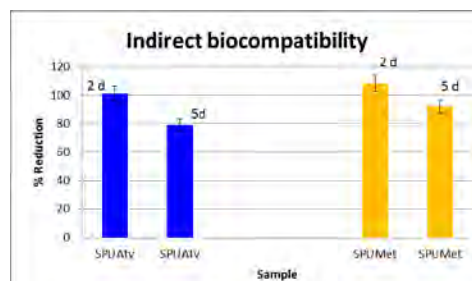


Figure 2. a) Alamar Blue Assay of SPUAtv and SPU extracts.

Conclusions

Polyurethanes containing atorvastatin or metformine are good candidates for medical applications as they exhibited good biocompatibility with fibroblasts. These polymers will be further studied in terms of degradation behavior and drug release.

Acknowledgment: CONACYT 248378 Project.

References

1. Guelcher SA. Tissue Eng Part B Rev 2008. 14(1):3-17.
2. Cheng JY, Hou TY, Shih MF, Talsma H, Hennink WE. Int J Pharm 2013. 450:145-162.



ANTIBACTERIAL GLASS IONOMER CEMENT MODIFIED WITH PROPOLIS

B. Maldonado-Gallegos¹, D. Aguilar-Pérez¹, J. V. Cauich-Rodríguez¹,
 S. E. Hernández-Solis², F. Aguilar-Ayala²

1. Centro de Investigación Científica de Yucatán, Calle 43 # 130, Colonia Chuburna de Hidalgo, CP 97200, Mérida, Yucatán, México. jvcr@cicy.mx
2. Facultad de Odontología, (UADY) Calle 61 A No492 A. x Avenida Itzáes y 90 Col. Centro, CP 97000, Mérida, Yucatán.

Introduction

Glass ionomer cements (GICs) are an important resource in adhesive dentistry due to their chelating capability to bony tissue. GICs are composed of calcium fluoroaluminosilicate glass and an aqueous solution of polyacrylic, itaconic and tartaric acids.¹ These materials exhibit good biocompatibility and fluoride release, despite their notable shortage in both compressive and flexural strength.² Current improvements in GICs seek to increase their mechanical performance and to provide antibacterial properties without affect the inherent properties of the material.³ In order to provide antibacterial properties, several additives have been used for instance: Chlorhexidine (CHX), Quaternary Ammonium Salts (QAS), modified polymers, etc.⁴ but in some cases their mechanical performance is also altered. Thus, the aim of this study was modify a GIC with propolis (PGIC) due to their well-known antibacterial, anti-inflammatory and antimicrobial.⁵ properties and to evaluate the changes in fluoride release and mechanical properties (bending and compressive strength).

Experimental Part

Fuji IX GIC (Tokyo, Japan) powder was used as the solid part of the formulation while the liquid part was modified with 25 y 50 μ L of ethanolic propolis (20% w/v). The PGIC was cured for 24 h and then place in distilled water. The fluoride release was measured with a fluoride ion electrode (Orion® 9609 BN) every 24 h for 30 days. For compressive test, the ISO 9917-1 standard was slightly modified as cylindrical samples (7 mm high and 4 mm diameter) were tested on a Shimadzu machine (AG1-100) with a 5 kN load cell at a loading rate of 1 mm/min. Rectangular samples (length 25 mm, 1.75 mm width and 2 mm of thickness) were used for three points bending test and tested at 1 mm/min following the 9917-2 ISO standard. The minimum inhibitory concentration (MIC) of propolis was determined against *Streptococcus mutans* (ATCC 25175). For antimicrobial activity both broth (MTT for PGIC extracts) and agar diffusion method were used.

Results and Discussions

Both GIC and PGIC showed a burst release of fluoride within the first 24 h and then it decreased and maintained a continuous release up to 30 days (Figure 1) in agreement with previous studies.⁶ However, compressive and bending strength was reduced as the amount of propolis was increased (see Table I) but were within the same range as those reported by Xie et al.⁷ The MIC of water:ethanol (85:15) solution of propolis was 2.5% (25 mg/ml). The inhibition halo in the agar diffusion test was less than 0.5 mm but similar to those reported by Topcuoglu et al.⁸

However, by using broth diffusion method (direct contact of *S. mutans* with extracts) antimicrobial activity was observed.

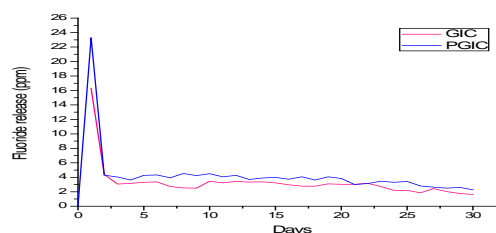


Figure 1. Effect of fluoride release on GIC and PGIC.

Table I. Mechanical properties of GIC and PGIC (24 h)

	Compression			Bending		
	E (MPa)	ϵ_{Max} (%)	σ_{Max} (MPa)	E (GPa)	ϵ_{Max} (%)	σ_{Max} (MPa)
GIC	82.4 ± 8.8	2.48 ± 0.2	211 ± 8.8	19.70 ± 6.40	0.10 ± 0.02	11.10 ± 1.71
PGIC 25 μ l	15.9 ± 6.3	2.54 ± 0.3	90.83 ± 10.6	7.12 ± 2.51	0.29 ± 0.09	7.78 ± 1.41
PGIC 50 μ l	20.0 ± 8.5	3.12 ± 0.2	64.68 ± 10.8	3.53 ± 1.76	0.42 ± 0.16	6.25 ± 1.85

E= Elastic Modulus σ_{Max} = Maximum strength, ϵ_{Max} = Deformation at maximum strength.

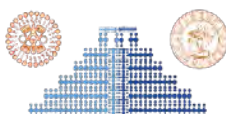
Conclusions

Propolis addition to a commercial GIC doesn't modify fluoride release but tend to reduce compressive and bending strength. The lowering on mechanical properties can be compensated by improvements in *S. mutans* antibacterial properties.

Acknowledgment: Rossana Vargas Coronado for technical assistance. CONACYT project 248378.

References

1. Pameijer CH. Int J Dent 2012. (3):752861.
2. Tascón J. Rev Panam Salud Publica 2005. 17(2):110–5.
3. Holla G, Yeluri R, Munshi AK. Contemp Clin Dent 2012. 3(3):288–93.
4. Botelho M. Caries Res 2003. 37:108–114
5. Santos VR. Altern Med 2012. 131–69.
6. Delgado Muñoz CR, Ramírez Ortega JP, Yamamoto Nagano A. Rev Odontológica Mex 2014. 18(2): 84–88.
7. Xie D, Brantley WA, Culbertson BM, Wang G. Dent Mater 2000. 16(2):129–138.
8. Topcuoglu N, Ozan F, Ozyurt M, and Kulekci G. Eur J Dent 2012. 6(4):428–433.



PLASMA POLYMERIZED ϵ -CAPROLACTONE BIOFILMS

Roberto Olayo-Valles¹, José Antonio Lopez-Barrera², Jesús Olayo-Lortia³, Omar E. Uribe-Juárez⁴, Ernesto J. Espinosa-Santamaría¹, Juan-Carlos Ruiz⁵, Juan Morales-Corona¹

1. Departamento de Física, Universidad Autónoma Metropolitana - Iztapalapa, Mexico City, Mexico rolyo@xanum.uam.mx
2. Academia de Física, Colegio de Ciencia y Tecnología, Universidad Autónoma de la Ciudad de México, Unidad Cuauhtepec, Mexico City, Mexico
3. Departamento de Biología de la Reproducción, Universidad Autónoma Metropolitana - Iztapalapa, Mexico City, Mexico
4. Departamento de Ingeniería Eléctrica, Universidad Autónoma Metropolitana - Iztapalapa, Mexico City, Mexico
5. Departamento de Ingeniería de Procesos e Hidráulica, Universidad Autónoma Metropolitana - Iztapalapa, Mexico City, Mexico

Introduction

Polycaprolactone (PCL) is a biocompatible and biodegradable polymer extensively used in tissue engineering, drug delivery and other biomedical applications because of its biocompatibility and slow rate of biodegradation in comparison with other widely used aliphatic polyesters such as polylactide (PLA), poly(lactide-co-glycolide) (PLGA). PCL, however, is also less hydrophilic than PLA and PLGA which limits direct application in tissue engineering applications. To increase interactions between PCL based materials and cells, the surface has been modified by plasma treatment which introduces new oxygen functionalities on the surface.^{1,2} In this work, we demonstrate that films prepared by the plasma polymerization of ϵ -caprolactone show improved cell adhesion compared to PCL.

Experimental Part

Films of plasma polymerized ϵ -caprolactone (PPCL) were prepared in a low pressure (7×10^{-2} Torr) plasma reactor. The films were deposited on glass slides placed between two electrodes connected to a rf power supply. In all cases the frequency was 13.5 MHz and the reaction time 90 min. Films were prepared at different power amplitudes between 20 W and 100 W. The films were characterized by FTIR, XPS, AFM and water contact angle.

The possible use of PPCL films for tissue engineering applications was evaluated by preparing beta cell cultures on the different samples as well as commercial PCL. The PCL samples were prepared by spin coating on glass slides from a solution of PCL in toluene. The cultures were monitored for 5 days at the end of which cell viability was evaluated using a calcein/ethidium homodimer assay and fluorescence microscopy.

Results and Discussions

FTIR characterization of all the PPCL films show strong bands at 3350 cm^{-1} due to the presence of OH groups. In contrast, the C=O band around 1741 cm^{-1} was weak. This indicates that carbonyl groups present in the monomer do not survive the plasma polymerization process.

This result was confirmed by XPS which clearly shows a decrease in COOC groups with increasing input power in the PPCL films.

XPS also shows the presence of OH groups in PPCL in higher proportion to that found in PCL films. The proportion of OH groups decreases as the power amplitude during synthesis was increased.

Viability of beta cells cultivated for 5 days on the different samples was evaluated by staining the cells with a calcein/ethidium homodimer assay and observing the samples in a fluorescence microscopy. The assay stains live cells green and dead cells red. All PPCL films outperformed PCL films in promoting cell adhesion. Within PPCL films, those that were synthesized at lower power amplitudes promoted better cell adhesion (Fig. 1).

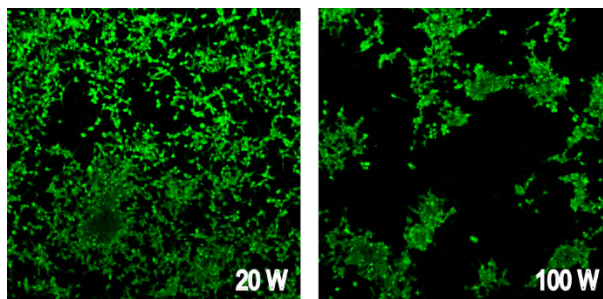


Figure 1. Fluorescence microscopy images of stained beta cells after 5 days in culture on PPCL films synthesized at 20 W (left) and 100 W (right).

Conclusions

PPCL films were demonstrated to be biocompatible and compare favorably in their interactions with cells compared with PCL. This is due to a very different surface chemistry which, in the case of PPCL, is rich in OH groups (confirmed by FTIR and XPS). The subsurface structure of the films is also quite different from PCL and will affect whether and how these materials degrade.

References

1. Jacobs, T.; De Geyter, N.; Morent, R.; Desmet, T.; Dubruel, P.; Leys, C. *Surf. Coatings Technol.* 2011, 205, S543.
2. Martins, A.; Pinho, E. D.; Faria, S.; Pashkuleva, I.; Marques, A. P.; Reis, R. L.; Neves, N. M. *Small* 2009, 5, 1195.

HYDROGEN PEROXIDE PLASMA TO INCREASING THE POLYANILINE ADHESION ON METALLIC SUBSTRATES FOR MEDICAL APPLICATION

Lidia Ma. Gómez^{1,3}, Ma. Guadalupe Olayo¹, Maribel González-Torres^{1,3}, Francisco González-Salgado^{1,4}, Rafael Basurto², Elena Colín⁵, J. Cuauhtémoc Palacios⁵, Guillermo J. Cruz^{1*}

1. *Departamento de Física, 2 Departamento de Química, Instituto Nacional de Investigaciones Nucleares, Carretera México-Toluca s/n, La Marquesa, Ocoyoacac, Edo. Mex. C. P. 52750, México.*guillermo.cruz@inin.gob.mx, guillermoj.cruz@hotmail.com*
3. *Posgrado en Ciencia de Materiales, Universidad Autónoma del Estado de México, Paseo Tollocan y Colón, Toluca, Edo. Mex. C. P. 52000, México.*
4. *Departamento de Posgrado, Instituto Tecnológico de Toluca, Av. Tecnológico s/n, Col. La Virgen, Metepec, Edo. Mex. C. P. 52140, México.*
5. *Facultad de Ingeniería, Universidad Autónoma del Estado de México Cerro de Coatepec, s/n Ciudad Universitaria, Toluca, Edo. Mex., CP 50130, México.*

Introduction

Polyaniline (PAn) has been used as coatings on metals against corrosion, however, in contact with fluids there is coating detachment due to the poor adhesion on the surface, which has been made by electrochemistry. In this work, plasmas of H₂O₂ is used to erode and oxidize the metallic surface on which PAn is synthesized improving the bond between polyaniline and metal. Some polyanilines have proven to be biocompatible with blood cells [1], so they are studied as coatings on metallic implants for the human circulatory system.

Experimental Part

Stainless steel springs and sheets were coated with PAn synthesized by plasma at 10⁻¹ mbar and 20 W during 10 min in a vacuum tubular glass reactor. The substrates were stainless steel (SS) springs and sheets treated previously with H₂O₂ plasma to erode, clean and sensitize the surface. The resistance of PAn coatings was evaluated by immersion in PBS solutions (in mM: NaCl=24, Na₂HPO₄=10, KH₂PO₄=3) at 37°C during two months in static and dynamic fluids, simulating the average velocity (43 cm/s) of an artery diameter of 17 mm, that corresponds to a cardiovascular system of a typical adult human of 70 kg.

Results and Discussions

PAn coatings followed the morphology of the substrate, are homogeneous and showed good adhesion (Figure 1a). The oxygen of H₂O₂ looks that forms oxygen bridges in the polymer. After 2 months of using static and dynamic PBS fluids at 37°C, PAn remained adhered to the metal with some slight cracks on the SS plain surface. PAn coatings in dynamic fluids had detachment of superficial layers, however the interior layers remained attached. PAn coatings with H₂O had contact angles between 82.4° and 88.0° and with PBS were between 88.3° and 88.9°. Figure 2 shows the atomic energy states of PAn coatings studied through the detailed energy spectra of C1s orbitals. The structure has states that correspond to fragmentation and oxidation of the monomers, unreacted anilines, resonant structures and oxygen bridges.

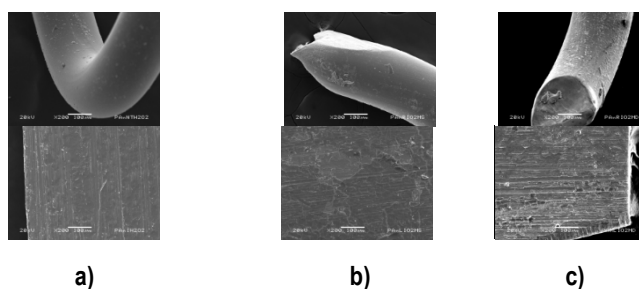


Figure 1. Surface of PAn coatings on stainless steel spring (top) and sheet (bottom) a) without immersion and after 2 months immersed in PBS solution in b) static and c) dynamic fluids.

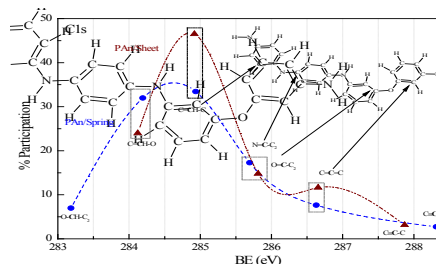


Figure 2. Energy distribution of C1s orbital of PAn coatings.

Conclusions

PAn coatings were synthesized on SS surfaces using hydrogen peroxide plasmas to increase the adherence between polymers and metals. After 2 months of submersion in PBS solutions the coatings remained adhered to the metallic surfaces with slight peeling or fractures only on the superficial layers. The chemical structure of the coatings has chemical states that suggest some fragmentation of aniline rings, crosslinking and oxygen bridges which can be the reason of the adhesion increase.

Acknowledgment: CONACYT for the financial support to this work of this work through the projects 154757 and FC-152. and to Jorge Perez for the support in the SEM analyses.

References

1. Chen Y.; Kang E. T.; Neoh K. G.; Wang P.; Tan K. L. *Synthetic Metals* 2000, 110, 47.



HEPARIN ABSORPTION IN POROUS PPy/I AND ITS RELEASE IN KR SOLUTIONS

Maribel González-Torres^{1,2}, Guillermo J. Cruz Cruz¹, Lidia Ma. Gómez Jiménez^{1,2}, Francisco González Salgado^{1,3}, Rosario Ramírez Segundo, Fernando G. Flores Nava⁴, Rafael Basurto Sánchez¹, Ma. Guadalupe Olayo González^{1*}

1. Departamento de Física, Instituto Nacional de Investigaciones Nucleares. Carretera México-Toluca s/n, La Marquesa, Ocoyoacac, Edo. Mex. CP 52750, México. *guadalupe.olayo@hotmail.com
2. Posgrado en Ciencia de Materiales, Universidad Autónoma del Estado de México Paseo Tollocan y Colón, Toluca, Edo. Mex., CP 52000, México.
3. Departamento de Posgrado, Instituto Tecnológico de Toluca, Av. Tecnológico s/n, Col. La Virgen, Metepec, Edo. Mex., CP 52140, México.
4. Tecnológico de Estudios Superiores de Jocotitlán. Carretera Toluca-Atlacomulco Km. 44.8, Ejido de San Juan y San Agustín, Jocotitlán, Edo. Mex., CP 50700, México.

Introduction

When the body is injured, platelets are responsible for repairing the damage by thrombin activation causing the growth of scars^{1,2}. Heparin is a drug that prevents the formation and growth of thrombus. In this work, plasma polypyrrole is studied as a possible carrier and dispenser of Heparin in polymer-drug mixtures as coatings for metallic implants in the circulatory system to avoid some rejection reactions. The polymer is evaluated before and after the drug absorption.

Experimental Part

Polypyrrole doped with iodine (PPy/I) was synthesized by plasma in RF resistive glow discharges in a tubular glass reactor. The polymers were obtained as films and after that pores were induced by lyophilization. For the Heparin (Aldrich) absorption, the porous polymers were immersed in water-Heparin solutions for 16 h evaporating the solvent at room temperature. The mass ratio for the Heparin:PPy/I samples was 1:10. The release was evaluated in static and dynamic fluids. For the static fluids, 5 mg of PPy/I-Heparin mixture were collocated within 10 mL of Krebs-Ringer (KR) solution, 1.5 mL of the medium was tested at 5-10 min. The release in dynamic fluids was done by incubating 5 mg of the PPy/I-Heparin mixture into 10 mL of water or KR solution. At 10 min intervals, 1.5 mL of the release medium was removed for UV-Vis analysis and replaced with an equal volume of fresh medium. XPS analyses were made to analyze the mixture surface, the morphologic analyses were done by SEM.

Results and Discussions

Fig. 1 a) and b) show PPy/I before and after Heparin absorption with Heparin-polymer ratio 1:10. The pores disappeared maybe because Heparin was absorbed into the pores and once filled covers the polymer surface. Fig.2 shows the concentration of Heparin (C, µg/mL) vs time of contact (t, min) released in KR solution using static and dynamic fluids. The process has a rapid release of Heparin in the first 60 min, which can be the outer layer of the mixture that rapidly dissolves in the medium. The other part of Heparin was released at a slower velocity suggesting a different mechanism that could be due to the drug release from the pores.

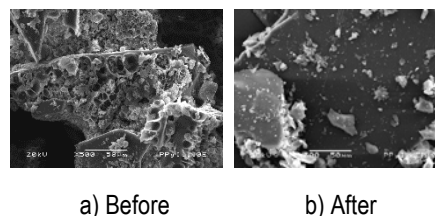


Figure 1. Surface of PPy/I before and after Heparin absorption.

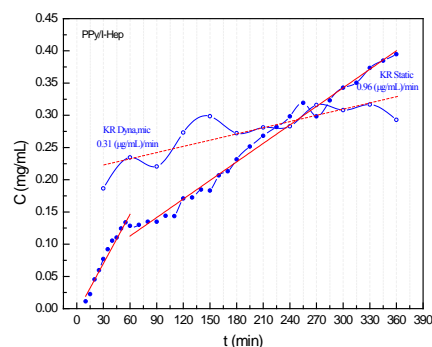


Figure 2. Heparin release in Krebs Ringer solution as a function of the contact time.

Conclusions

Heparin was absorbed into porous polypyrrole first filling the pores and later coating the surface. The Heparin release was done in two different rates in static fluids, first the outer layer dissolved increasing rapidly the concentration in KR solutions to later reduce the rate due to the drug release of the pores.

Acknowledgment: The authors acknowledge CONACYT for the partial financial support to this work whit the projects 154757 and FC-152 and to Jorge Pérez for the SEM analyses.

References

1. Walker M. G., Shaw J. W., Thomson G. J. L., Cumming J. G. R., M. L. Thomas. British Medical Journal 1987, 294, 1189.
2. Flores J. Flores. Farmacología Humana. 1997, 1, 108.

CROSSLINKED ELECTROSPINNED FIBERS AND PARTICLES OF PLASMA POLYANILINE

Rosario Ramírez^{1,2}, Guillermo J. Cruz¹, Ma. de los Ángeles Enríquez², Jaime Rosales², Fernando G. Flores², Maribel González-Torres^{1,3}, Lidia Ma. Gómez^{1,3}, Francisco González-Salgado^{1,4}, Juan Morales⁵, Ma. Guadalupe Olayo^{1*}

1. Departamento de Física, Instituto Nacional de Investigaciones Nucleares. Carretera México-Toluca s/n, La Marquesa, Ocoyoacac, Edo. Mex., CP 52750, México. *guadalupe.olayo@inin.gob.mx
2. Tecnológico de Estudios Superiores de Jocotitlán. Carretera Toluca-Atacomulco Km. 44.8, Ejido de San Juan y San Agustín, Jocotitlán, Edo. Mex., México, CP 50700.
3. Posgrado en Ciencia de Materiales, Universidad Autónoma del Estado de México Paseo Tollocan y Colón, Toluca, Edo. Mex., CP 52000, México.
4. Departamento de Posgrado, Instituto Tecnológico de Toluca, Av. Tecnológico s/n, Col. La Virgen, Metepec, Edo. Mex., CP 52140, México.
5. Departamento de Física, Universidad Autónoma Metropolitana Iztapalapa, Av. San Rafael Atlixco 186 Col. Vicentina Del. Iztapalapa, México D. F. CP. 09340, México.

Introduction

Plasma Polyaniline (PAN) is a complex networked polymer composed by alternated benzene rings and amines with conjugated bonding. The higher crosslinking induced by the plasma polymerization the lesser solubility. In spite of obtaining insoluble plasma PAN fibers directly from the synthesis on different substrates, soluble electrospun fibers and/or particles of this polymer have not been reported yet, maybe because electrospinning consists on applying a high voltage to a polymer solution. Therefore to form this kind of fibers of micro- and/or nano-metric diameter, soluble plasma PAN has to be obtained first to later electrospin the solution forming crosslinked fibers and particles.

Methodology

PAN was synthesized by plasma in a tubular vacuum reactor with RF glow resistive discharges. The soluble and insoluble fractions were separated with acetone and the soluble fraction was used to form crosslinked particles and fibers with micrometric size by electrospinning at 20 kV, 10 cm between injector and roll, roll speed of 174 rpm with 175 oscillations in the injector.

Results and discussion

Figure 1 shows a SEM micrograph of PAN synthesized at 20 W with crosslinked fibers and particles on a roughed surface. Different profiles were formed due to the combination of variables during the electrospinning: solution viscosity, potential difference, pulses and injector oscillations. The diameter of fibers is shown in **Figure 2**, the interval was between 0.04 and 3.22 μm with a mean of 0.83 μm . The length of fibers was between 2.24 and 22.3 μm with a mean of 8.47 μm . The approximated diameters of particles were between 1.07 and 16.0 μm with a mean of 5.76 μm . To obtain the distribution diameters and lengths, 125 fibers and particles were measured.

Conclusions

Soluble plasma PAN was synthesized to form electrospun fibers and particles in a crosslinked configuration that varies with

the experimental conditions in the electrospinning. The dimensions of fibers and particles are in the size interval of many human cells, so the networks obtained could be used as biomaterials because of their size and amines in the structure.

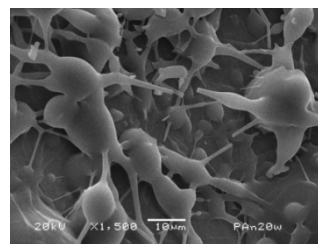


Figure 1. Crosslinked fibers and particles of PAN.

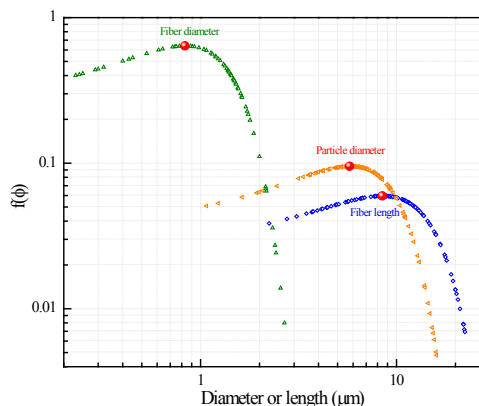


Figure 2. Diameters and lengths of PAN fiber and particles.

Acknowledgment: The authors acknowledge CONACYT for the partial support to this work with 154757 and FC-152 projects and to Jorge Perez for the SEM analysis.

References

1. Olayo M.G., Enríquez M.A., Cruz G.J., Morales J., Olayo R., Polymerization of halogenated anilines by plasma, J. Appl. Poly. Sci. 2006, 102, 4682-4689.

STRUCTURE OF PYRROLE-ALLYLAMINE PLASMA COPOLYMER FILMS

Ma. Guadalupe Olayo¹, E. Jocelyn Alvarado^{1,2}, Maribel González-Torres^{1,3}, Lidia Ma. Gómez^{1,3}, Francisco González-Salgado^{1,4}, Rosario Ramírez-Segundo^{1,5}, Fernando G. Flores-Nava^{1,5}, Guillermo J. Cruz^{1*}

1. Departamento de Física, Instituto Nacional de Investigaciones Nucleares, Carr. México-Toluca s/n, La Marquesa, Ocoyoacac, Edo. Mex., CP 52750, México. *guillermo.cruz@inin.gob.mx
2. Instituto Tecnológico de Morelia, Avenida Tecnológico #1500, Col. Lomas de Santiaguito. Morelia, Mich., CP 58120, México.
3. Posgrado en Ciencia de Materiales, Facultad de Química, Universidad Autónoma del Estado de México, Paseo Tollocan y Colón, Toluca, Edo. Mex., CP 52000, México.
4. Departamento de Posgrado, Instituto Tecnológico de Toluca, Av. Tecnológico s/n, Col. La Virgen, Metepec, Edo. Mex., CP 52140, México.
5. Tecnológico de Estudios Superiores de Jocotitlán. Carretera Toluca-Atlacomulco Km. 44.8, Ejido de San Juan y San Agustín, Jocotitlán, Edo. Mex., CP 50700, México.

Introduction

The synthesis of polymers by plasma has been studied as a technique to obtain biocompatible and biofunctional surfaces. This kind of synthesis is important because different monomers or chemicals can be combined to produce new materials with the main properties of the components. Additionally, ramifications and/or crosslinking can be handled for specific applications^{1,2}. Polypyrrole (PPy) and polyallylamine (PAI) are biocompatible materials because they have NH groups in their structure that can join with other groups in the living tissues. PPy has application in materials for implants, administration of drugs, etc; and combined with Polyethyleneglycol has been used in the reconnection of neuronal cells in the spinal cord with promising results^{1,3}. On the other hand, PAI has been used in biological applications to promote the adhesion and growth of cells, which increase the biocompatibility of different materials. In this work, pyrrole-allylamine copolymers doped with iodine were synthesized to join the properties of both and chemically studied to find the evolution of the main functional groups.

Experimental Part

Random copolymers of pyrrole (Py, Aldrich, 98%) and allylamine (Al, Aldrich, 98%) (PPy-PAI) doped with iodine (Aldrich, 99.5%) were synthesized in a tubular glass reactor with diameter and length of 9 and 26 cm, respectively. The monomers were placed in different containers, connected and introduced to the reactor mixing inside at room temperature. The plasma was produced with electric glow discharges at 13.56 MHz, 10⁻¹ mbar and power in the range of 40 to 100 W. The copolymers were obtained as thin films adhered to the inner surfaces of the reactor.

Results and Discussions

The IR absorption of PPy-PAI/I, Py and Al is shown in Figure 1. Multiple bonds as =C=, C≡C and C≡N that do not show in the monomers appear in the copolymers suggesting a high oxidation and dehydrogenation due to the conditions in the plasma. The most intense absorption in pyrrole at 721 cm⁻¹ appears also in the

copolymers suggesting that pyrroles have more participation than allylamines. In the same context, the most intense absorption of Allylamine at 910 cm⁻¹ is absent in the copolymers.

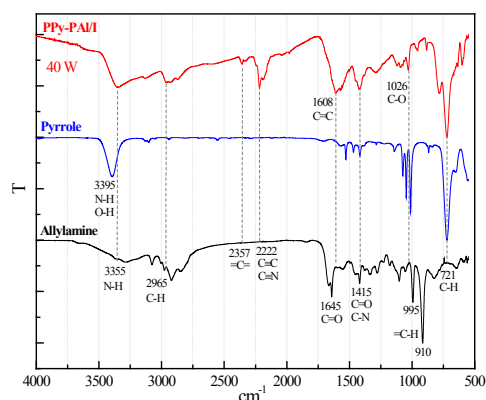


Figure 1. IR of PPy-PAI/I thin films and monomers.

Conclusions

Pyrrole and allylamine were randomly polymerized by plasma obtaining copolymers with the main chemical groups of both components. The results indicated that the copolymers have mainly the most intense groups of pyrrole.

Acknowledgment: To CONACyT for the partial financial support to this work with the projects 154757 and FC-152.

References

1. R. Olayo, C. Rios, H. Salgado-Ceballos, G.J. Cruz, J. Morales, M.G. Olayo, M. Alcaraz-Zubeldia, A.L. Alvarez, R. Mondragon, A. Morales, A. Diaz-Ruiz, J. Mater. Sci.: Materials in Medicine 2008, 19(2), 817.
2. G.J. Cruz, J. Morales, M. M. Castillo-Ortega, R. Olayo, Synth. Met. 1997, 88, 213.
3. E. Colin, M.G. Olayo, G.J. Cruz, L. Carapia, J. Morales, R. Olayo, Progress in Organic Coatings 2009, 64, 322.



KGM/CHI ASYMMETRIC MEMBRANES AS WOUND DRESSING

Giovana Genevro¹, Carla França¹, Mariana de Moraes^{1,2}, Marisa Beppu¹

1. University of Campinas, Rua Albert Einstein 500, 13083-852, Campinas, Brazil. beppu@feq.unicamp.br

2. Federal University of Sao Paulo, Rua Sao Nicolau, 210, 09913-030, Diadema, Brazil

Introduction

Asymmetrical membranes have interesting characteristics to be used as dressings, since they present a dense top surface to control the loss of water and the passage of microorganisms and a porous surface for contact with the wound bed in order to absorb and drain off excess exudate and maintain moisture.¹

Konjac glucomannan (KGM) is a neutral, water-soluble and high molecular weight polysaccharide, found in roots and tubers of the *Amorphophallus konjac* plant. It presents interesting characteristics for use as dressings such as elasticity, good capability to form gels and films and good mechanical properties.²

Chitosan (CHI) is a polysaccharide derived from chitin, which has a number of biologic properties such as hemostatic action, antimicrobial activity and biocompatibility.³

In this study, we developed KGM/CHI asymmetric membranes for use as wound dressings.

Experimental Part

Asymmetric membranes were obtained by drying 1% KGM (Konjac Foods, China) solution until 10% of its initial mass. So, 0.8% chitosan solution (pH~5) was added and dried until 25% of its initial mass. Drying was performed at 60 °C. Then, the samples were frozen in a conventional freezer for 24 h. The frozen membranes were put into a coagulation bath containing 1.25 mol/L NaOH and 75 vol% ethanol for at least 3 h. Then, the membranes were washed with distilled water to neutralize pH.

The morphology of the samples was analyzed by SEM. To determine the water vapor transmission (WVT) the samples were placed in a recipient with permeation area of 15.2 cm² containing anhydrous calcium chloride as desiccant and this recipient was then placed in a desiccator containing saturated aqueous NaCl solution, maintaining the ambient at 75% of relative humidity. The WVT through the films was determined gravimetrically by weighing the recipient every 12 h, for a period of 5 days. The rate of WVT was calculated as $WVT = (G/t)/A$, where G/t is the mass variation rate in g·day⁻¹; A is the test area, in m².

Results and Discussions

The KGM/CHI asymmetric membrane is resistant to handling and presents an interesting aspect to the proposed application. At SEM images (Fig. 1) it was observed a dense and a porous

surface, proving that an asymmetric membrane structure was achieved.

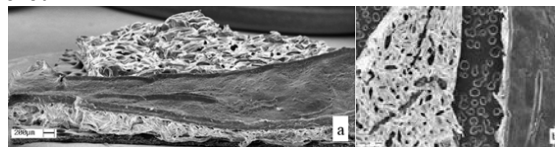


Figure 1. SEM images of a) fracture and b) porous and dense surfaces of KGM/CHI membranes

The WVT across the surface of the membrane determines the wet environment of the wound, that is critical to the healing process. Excessive WVT results in a rapid loss of water, which can result in dehydration of the wound, and also adhesion of the dressing to the wound bed, which can cause discomfort and pain. On the other hand, a low value of WVT can cause retention of exudates, excess moisture, which leads to maceration of healthy tissue surrounding the wound.^{4,5}

The WVT of KGM/CHI asymmetric membranes observed in this study is 261.8 ± 85.9 g/m².day, which is in agreement with the range of values for commercial dressings (76-9,360 g/m².day) found in the literature.⁶ Normal human skin has permeability of ~204 g/m².day, the skin with first degree burns ~279 g/m².day, and when there is granulation tissue formation is about 5,138 g/m².day.⁷ So, KGM/CHI asymmetric membranes present WVT suitable for wounds with low exudate production.

Conclusions

KGM/CHI asymmetric membranes were produced with well defined dense and porous structures. The membranes can be used as dressing for low exudative wounds. The developed material has a high potential of application in tissue engineering, as wound dressing. Further experiments need to be realized.

Acknowledgment: The authors thank #2013/18958-6, São Paulo Research Foundation (FAPESP) and CAPES for grant support.

References

1. Morgado, P. I.; Aguiar-Ricardo, A.; Correia, I. J. *Journal of Membrane Science* 2015, 490, 139.
2. Nishinari, K. *Novel Macromolecules in Food Systems* 2000, 41, 309.
3. De Paiva, R. G. et al. *Journal of Applied Polymer Science* 2000, 126, E17.
4. Chen, Y. et al. *Journal of Applied Polymer Science* 2011, 119, 1532.
5. Elsner, J. J.; Zilberman, M. *Journal of Tissue Viability* 2010, 19, 54.
6. Wu, P. et al. *Biomaterials* 1995, 16, 171.

CHEMICAL STRUCTURES OF BIOCOMPATIBLE PLASMA POLYALLYLAMINE

Guillermo J. Cruz¹, E. Jocelyn Alvarado^{1,3}, Lidia Ma. Gómez^{1,4}, Maribel González-Torres^{1,4}, Francisco González-Salgado^{1,5}, Rosario Ramírez-Segundo^{1,6}, Fernando G. Flores-Nava^{1,6}, Rafael Basurto², Ma. Guadalupe Olayo^{1*}

1. Departamento de Física, 2. Departamento de Química, Instituto Nacional de Investigaciones Nucleares, Carr. México-Toluca s/n, La Marquesa, Ocoyoacac, Edo. Mex., CP 52750, México. *guadalupe.olayo@inin.gob.mx
3. Instituto Tecnológico de Morelia, Avenida Tecnológico #1500, Col. Lomas de Santiaguito. Morelia, Mich., CP 58120, México.
4. Posgrado en Ciencia de Materiales, Facultad de Química, Universidad Autónoma del Estado de México, Paseo Tollocan y Colón, Toluca, Edo. Mex., CP 52000, México.
5. Departamento de Posgrado, Instituto Tecnológico de Toluca, Av. Tecnológico s/n, Col. La Virgen, Metepec, Edo. Mex., CP 52140, México.
6. Tecnológico de Estudios Superiores de Jocotitlán. Carretera Toluca-Atlacomulco Km. 44.8, Ejido de San Juan y San Agustín, Jocotitlán, Edo. Mex., CP 50700, México.

Introduction

Many biocompatible polymers have amines in their structure, the most common is Polyallylamine (PAI). Allylamine has double bonds in one side of the molecule and amines on the other side ($\text{CH}_2=\text{CH}-\text{CH}_2-\text{NH}_2$). If the polymerization mechanism is by free radicals, the monomers join transforming double into single bonds leaving untouched the $-\text{CH}_2-\text{NH}_2$ segments. If the mechanism is by dehydrogenation, the monomers join mainly on both sides leaving untouched the double bonds ($-\text{CH}=\text{CH}-\text{CH}_2-\text{NH}_2$). It has been said that in plasma, the polymerization is mainly promoted by dehydrogenation, preserving double bonds and even creating new ones and additional triple bonds. Considering these interrogatives, the objective of this work is the study of both mechanisms in plasma PAI identifying and quantifying the typical chemical states in both cases.

Experimental Part

Allylamine (Aldrich, 95%) was polymerized by plasma in a vacuum tubular glass reactor with resistive glow discharges at 80 W. The polymers were formed as thin films on the inner wall reactors. After the polymerization, the films were swelled and separated from the walls. Chemical analyses on the films were done with a K-Alpha Thermo Scientific XPS spectrometer. The energy distribution of C1s and N1s orbitals were fitted with gaussian curves and associated with the principal chemical states in both elements, relating the formation energy of chemical states with the maximum orbital energy of each curve, first identifying and quantifying the chemical states, and later grouping the percentages that belong to each, linear or double bond structures [1,2].

Results and Discussions

Allylamine has three Carbon chemical states with 33.3% each, $\text{CH}_2=\text{C}$, $\text{C}=\text{CH}-\text{C}$ and $\text{C}-\text{CH}_2-\text{N}$. C in bold identify the C atom in study. The results indicated that $\text{CH}_2=\text{C}$ disappeared in PAI indicating that this is the most reactive point during the polymerization. $\text{C}=\text{CH}-\text{C}$, reduced its participation from 33.3% to

approximately 22% in PAI. On its part, $\text{C}-\text{CH}_2-\text{N}$ could only be identified in combination with another chemical state, $\text{C}_3-\text{C}-\text{H}$, because of their similar formation energy. The participation of both was approximately 36%, maybe with 18% each, although they cannot be separated in this analysis, and can be identified only in the single bond PAI structure. Other new chemical states appeared in PAI that were not in the monomer, $\text{C}-\text{CH}_2-\text{C}$ (15%), the combination (15%) of $\text{C}=\text{CN}-\text{C}$ and $\text{C}=\text{CH}-\text{N}$, $\text{C}=\text{C}-\text{N}_2$ (8%) and triple bond groups as $\text{C}\equiv\text{C}-\text{C}$ and $\text{C}\equiv\text{C}-\text{N}$ (4%).

The sum of the three C states with only single bonds is 51%, which suggest that this is the predominant configuration in plasma PAI. The double bond chemical states sum 45%. The rest belongs to triple bond configurations (4%) that represents the fragmentation due to the high energy collision of particles in the plasma. Remember that these percentages belong to PAI synthesized at 80 W, at other power, the numbers most surely are different.

Conclusions

Free radical and dehydrogenation mechanisms may produce single and double bond chemical structures in plasma PAI, respectively. The percentages discussed here of the different chemical states found in PAI suggest that both structures and mechanism can be identified in the same polymer. The first mechanism has a little bit more participation with 51% vs 45% of the other. This means that the plasma polymerization occurs with both mechanisms at that level of synthesis power.

Acknowledgment: To CONACyT for the partial financial support to this work with the projects 154757 and FC-152.

References

1. M. González-Torres, M.G. Olayo, G.J. Cruz*, L.M. Gómez, V. Sánchez-Mendieta, F. González-Salgado, *Advances in Chemistry*, Vol 2014, ID: 965920, 1-8.
2. M.G. Olayo, R. Zúñiga, F. González-Salgado, L. M. Gómez, M. González-Torres, R. Basurto, G. J. Cruz, es, *Polym. Bull.*, Publicado en Línea, 2016, DOI 10.1007/s00289-016-1730-3.



Efecto de las técnicas para elaboración de membranas en las propiedades eléctricas de un polímero de conducción iónica para ingeniería de tejidos

Estefanía Correa Muñoz^{1,2}, María E. Moncada Acevedo², Víctor H. Zapata Sanchez¹

1. Universidad Nacional de Colombia, Calle 59 A N 63-20, 050034, Medellín, Colombia. ecorream@unal.edu.co

2. Instituto Tecnológico Metropolitano, Calle 73 No 76A - 354, 050034, Medellín, Colombia.

Introducción

Las propiedades eléctricas del hueso han sido ampliamente estudiadas a partir de lo cual se ha planteado que estímulos electromagnéticos generados dentro del mismo juegan un papel importante en el control de los procesos de formación y remodelación. Debido a esto la ingeniería de tejidos óseos ha involucrado el uso de polímeros conductores, los cuales pueden emular dichas propiedades. Una alternativa poco explorada en la ingeniería de tejidos son los polímeros conductores iónicos. Estos son comúnmente preparados mediante la evaporación lenta del solvente, sin embargo es necesaria la construcción de andamios como base para la regeneración. En este trabajo se pretende diferenciar los comportamientos eléctricos de membranas obtenidas mediante la evaporación lenta del solvente y la técnica de electrohilado.^{1,2}

Parte Experimental

Se empleó Policaprolactona (PCL) Mn= 80kDa y Nitrato de magnesio (Mg(NO₃)₂ · 6H₂O de Sigma Aldrich y como solvente común acetona 99%. Inicialmente fue añadido PCL a la acetona y se agitó a temperatura de 40°C para disolver. Luego la sal fue añadida a la solución a una relación de 10% mol Mg²⁺ /mol PCL. La solución se dejó agitando por 24 horas para garantizar la disolución de la sal en el polímero y formar el complejo. Para obtener la membrana mediante la evaporación lenta del solvente, se utilizaron cajas Petri con la solución para dicho proceso, la eliminación de solvente demoró un total de 3 días. En la técnica de electrohilado se preparó la misma solución considerando una concentración 10%w entre el polímero y la acetona. Además se usaron como parámetros en el proceso, una distancia de la jeringa al colector de 10 cm, un flujo de 6ml/hr y voltaje de 25kV. Las membranas obtenidas por las diferentes técnicas fueron caracterizadas por XRD, espectroscopia de impedancia compleja, TGA, DSC y SEM. Las membranas fueron sumergidas en agua desionizada para simular la humedad del hueso antes de realizar la caracterización eléctrica.

Resultados y discusiones

La Fig. 1 a), b), c) y d) muestran los XRD de las membranas obtenidas por ambos métodos. Con estos resultados se puede garantizar la formación del complejo al no presentarse picos diferentes a los del polímero puro, es decir, no presenta picos representativos de la sal de magnesio en ninguno de los métodos. Es de resaltar que los difractogramas de las membranas obtenidas por electrohilado muestran una fase más amorfa y la desaparición del pico ubicado en 19°. Esto puede explicarse debido a que las membranas por evaporación lenta permiten que las cadenas poliméricas puedan reorganizarse

durante el tiempo prolongado de la desaparición de solvente en comparación a la técnica de electrohilado lo cual es inmediato.

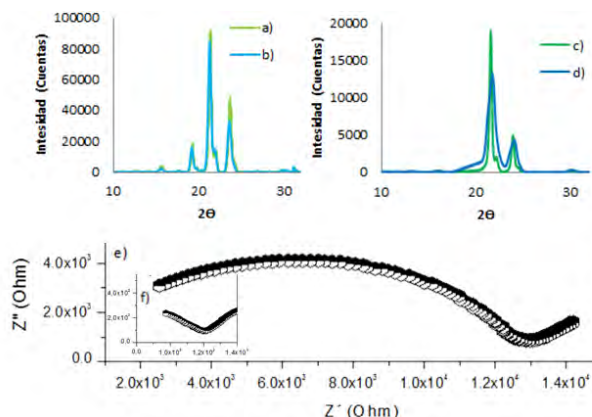


Figura 1. XRD: { a) PCL Puro y b) PCL + Mg²⁺ } por evaporación lenta del solvente; { c) PCL Puro y d) PCL + Mg²⁺ } por electrohilado; Z'' vs Z' Temperatura ambiente: e) Evaporación lenta f) Electrohilado.

Este cambio en la estructura del polímero genera beneficios para las propiedades eléctricas debido a la facilidad de los iones de moverse en una estructura más amorfa. En la Fig. 1 e) y f) se muestra la gráfica Z'' vs Z' de ambas membranas. Para e) el semicírculo corta en valores cercanos a 13000Ω mientras que en f) tiene el valor de 1200 Ω, lo que indica una menor resistencia de la movilidad de iones en el polímero electrohilado. Además de las diferencias en la estructura del polímero, se evidencia una mayor absorción de agua por parte de la membrana por electrohilado que permitirá mayor transporte iónico. Sin embargo, presentó mayor interacción con la interfaz lo cual puede deberse a la evaporación del agua contenida

Conclusiones

Se presenta una diferencia notoria en la obtención de las membranas de polímeros de conducción iónica por la técnica de electrohilado y la evaporación lenta del solvente. Esto se evidencia en los resultados obtenidos en el XRD y en las propiedades eléctricas que demuestran mejores resultados para las membranas obtenidas por electrohilado.

References

- Behari J. Biophysical bone behavior: Principles and applications 2009. John Wiley & SonS.
- Hardy J. G., Lee J. Y., Schmidt C. E. Current Opinion in Biotechnology 2013, 24, 847–85

COMPOSITE OF ZNO NANOPARTICLES AND FISH BONE HYDROXYAPATITE: SYNTHESIS AND CHARACTERIZATION

Víctor M. Ovando-Medina ¹, Miguel A. Corona-Rivera ¹, Karla D. Estrada-Martínez ¹, Hugo Martínez-Gutiérrez ²,
Lorena Farías-Cepeda ³, Nancy E. Dávila-Guzmán ⁴

1. *Coordinación Académica Región Altiplano - UASLP, Carr. A Cedarl KM 5+600, Ejido San José de las Trojes, 78700, Matehuala, SLP, Mexico. ovandomedina@yahoo.com.mx*
2. *Centro de Nanociencias y Micro y Nanotecnologías - IPN, Luis Enrique Erro S/N, 07738, Mexico City, Mexico.*
3. *Facultad de Ciencias Químicas, De Blvd. V. Carranza e Ing. José Cárdenas V. S/N, 25280, Saltillo, México.*
4. *Facultad de Ciencias Químicas, Universidad Autónoma de Nuevo León, Av. Universidad, Cd. Universitaria, 66451, San Nicolás de Los Garza, NL, México*

Introduction

Approximately 91 million tons of fish are caught annually and around 55% of these are used for human consumption, while the rest are discarded. Most of the fish used for human consumption are deboned and exported. The bones are usually discarded without any use giving an undesirable impact on the environment. These bones are a rich source of calcium phosphate, also known as hydroxyapatite (HAp).

On the other hand, oil esterification by alkaline or acid ways is limited by the free fatty acids content, which can deactivate the catalyst, giving low methyl ester yield. Therefore, new catalyst systems have been studied by the researchers; among the most recently studied catalyst are MgO, ZnO, ZnCl₂, etc. However, their catalytic activity in oil esterification is reported at temperatures in the range of 150 to 200 C.

In this work, ZnO nanoparticles were synthesized by precipitation using ZnCl₂ and sodium hydroxide as precursors, and in the presence of fish bone hydroxyapatite (HAp) in order to obtain composite of ZnO/HAp. The effect of using sodium dodecyl sulphate (SDS) on the ZnO morphology was studied.

Experimental Part

Hydroxyapatite (HAp) was obtained of fish bone waste and collected from a restaurant in Matehuala, SLP (Mexico). Fish bones were washed and dried at 60 °C by 24 h. Afterwards, bones were immersed in acetone through 24 h to extract oils and then were dried at 60 °C by 24 h. Samples were ball-milled until obtain a white dust (natural HAp). 10 g Natural HAp was dispersed in 30 g of distilled water in the presence of 0.05 g of SDS as stabilizing agent (when was used), then, 2.78 g of ZnCl₂ were added to reaction mixture under magnetic stirring. After 2 h, 30 g of NaOH solution at 4 mol/L was added drop by drop to star ZnO formation. After 2 h the reaction mixture was poured in a glass bottle, sealed and put at 80 °C by 5 h. After that, mixture was filtered and gently washed with distilled water, and dried at 60 °C until constant weight. Resulting materials were characterized by FTIR and Raman spectroscopy.

Results and Discussions

Figure 1 show the FTIR spectra of samples corresponding to the different prepared materials. It can be observed the main signals corresponding to HAp (calcium phosphate) between 1000 and 1120 cm⁻¹ ascribed to asymmetric stretching mode of vibration for PO₄ group. The band at 570 cm⁻¹ is due to P-O stretching vibration for the same PO₄ group. Signals of ZnO can be observed at 893 cm⁻¹ due to stretching mode of ZnO.

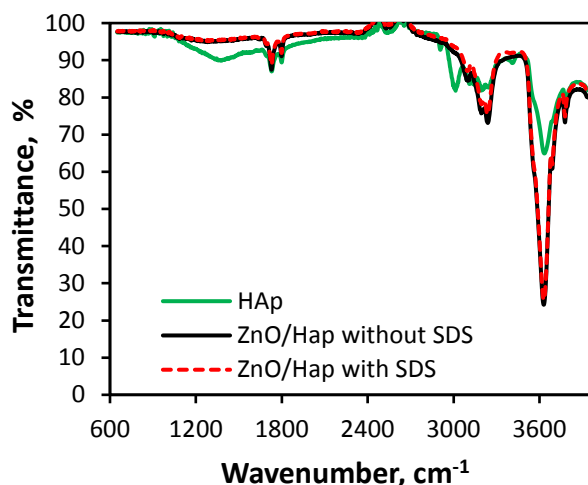


Figure 1. FTIR spectra of the different materials.

Raman spectra of materials showed the characteristics signals of ZnO corresponding to hexagonal structure.

Conclusions

Composites of ZnO/HAp were successful obtained and characterized. More results will be presented at the congress.

Acknowledgment: This work was supported by PRODEP SEP through grant: Red de Investigación y Desarrollo de Nanomateriales híbridos para aplicaciones Ambientales Avanzadas convenio: DSA/103.5/15/14160

References

1. Sahu H, Mohanty K. *RSC Adv*, 2016, 6, 8892-8901



EFFICIENT CONDENSATION OF DNA INTO ENVIRONMENT-RESPONSIVE POLYPLEXES PRODUCED FROM A NOVEL BLOCK CATIONIC COPOLYMER CARRYING TWO AMINE GROUPS

Lindomar Albuquerque¹, Eliézer Jäger², Petr Stepánek², Vanessa Schmidt³, Cristiano Giacomelli³ and Fernando Carlos Giacomelli¹

1. Centro de Ciências Naturais e Humanas, Universidade Federal do ABC, 09210-580, Santo André, Brazil. fernando.giacomelli@ufabc.edu.br
2. Institute of Macromolecular Chemistry, Academy of Sciences of the Czech Republic, 162 06, Prague, Czech Republic.
3. Departamento de Química, Universidade Federal de Santa Maria, 97105-900, Santa Maria, Brazil.

Introduction

The intracellular delivery of nucleic acids requires a vector system as they cannot diffuse across lipid membranes. Although polymeric transfecting agents have been extensively investigated, none of the proposed gene delivery vehicles fulfills all the requirements needed for an effective therapy namely ability to bind and compact DNA into polyplexes, stability in serum environment, endosome-disrupting capacity, efficient intracellular DNA release and low toxicity. The challenges are mainly attributed to the conflicting properties such as for instance stability vs. efficient DNA release and toxicity vs. efficient endosome-disrupting capacity.¹ Accordingly, investigations aiming at safe and efficient therapies are still essential to achieve clinical success of gene therapies.

Experimental Part

Taking into account the mentioned issues, herein it has been evaluated the DNA condensation ability of a novel block cationic copolymer carrying two amine groups named POEGMA₇₀-*b*-P(OEGMA₁₀-*co*-DEA₄₇-*co*-DPA₄₇) - Fig. 1. The condensation capability has been evaluated by agarose gel electrophoresis and isothermal titration calorimetry. The structure of the supramolecular aggregates was determined by scattering techniques (DLS, SLS, ELS and SAXS) and imaging (AFM). Conformational changes were probed *via* circular dichroism spectroscopy (CD) and UV-Vis.

Results and Discussions

The agarose gel electrophoresis data (Fig 1. - right down) suggests that the polymer POEGMA₇₀-*b*-P(OEGMA₁₀-*co*-DEA₄₇-*co*-DPA₄₇) properly condenses DNA. The blocking of illuminating intensity confirms that the block copolymer bind to and completely neutralize the negative charges of DNA. The supramolecular aggregates has desirable size for cellular uptake *via* endocytic pathways ($R \sim 100$ -200 nm) as confirmed *via* AFM imaging (Fig. 1 - left top). The structure of the polyplexes was detailed characterized by scattering techniques where it has been evidenced the high degree of hydration of the entities. The isothermal titration calorimetric data revealed that the binding is

endothermic and therefore the process is entropically driven. Finally, circular dichroism spectroscopy indicated that the conformation of DNA remained the same after complexation and that the polyplexes are highly stable in serum environment.²

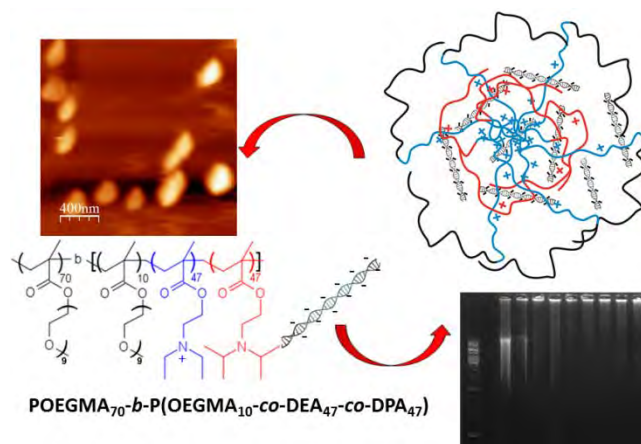


Figure 1. Clockwise: schematic representation of polymer/DNA polyplexes, agarose gel electrophoresis, block copolymer structure and AFM image of polyplexes produced at N/P = 2.0.

Conclusions

The novel synthesized block copolymer efficiently condenses DNA into nanoparticles with desired size for cellular uptake *via* endocytic pathways. They are highly stable in serum environment and biological assays are currently underway to attest the potential application of the novel material in the gene delivery field.

Acknowledgment: The investigations are being sponsored by FAPESP through the Grant 2014/22983-9.

References

1. Lächelt, U.; Wagner, E. Chem. Rev. 2015, 115, 11043.
2. Albuquerque, L. J. C.; Giacomelli, F. C. Langmuir 2016, 115, 11043.

pH AND THERMAL RESPONSIVE HYBRIDS PREPARED FROM ISOPHORONE DIISOCYANATE-BASED POLYURETHANE AND 2-(DIISOPROPYLAMINO) ETHYLMETHACRYLATE

Francisco M. Pardini¹, Oscar R. Pardini^{1,2}, Paula A. Faccia³, Javier I. Amalvy^{1,2,3}

1. Centro de Investigación y Desarrollo en Tecnología de Pinturas (CIDEPINT), 1900, La Plata, Argentina.
2. Instituto de Investigaciones Fisicoquímicas Teóricas y Aplicadas (INIFTA), Calle 64 y Diag. 113, 1900, La Plata, Argentina.
3. Centro de Investigación y Desarrollo en Ciencia y Tecnología de Materiales (CITEMA), Facultad Regional La Plata (Universidad Tecnológica Nacional) 60 y 124, 1900, La Plata, Argentina. jamalvy@inifta.unlp.edu.ar

Introduction

Stimuli-sensitive polymers are very attractive materials for application in different fields of science and technology.¹ These materials have the characteristic of changing its structure and physical properties in response to external stimuli such as pH, ionic strength, temperature, light, or to a specific chemical compound.² In this work acrylic-polyurethane hybrids containing different amounts of 2-(diisopropylamino)ethyl methacrylate (DPA) monomer (10, 30 and 50 wt. %) were prepared and characterized by thermal analysis and FTIR and UV-visible spectroscopies, while measuring water content and the dynamic swelling degree of water. The influence of DPA on swelling behavior, thermal properties and pH and temperature sensitivity was evaluated.

Experimental Part

The hybrid polymers were prepared as follows. First, a vinyl terminated polyurethane (PU) prepolymer was prepared following a previous method³ and then an aqueous dispersion of PU was obtained by adding the PU prepolymer to water. Pure homopolymer of DPA synthesis was performed as detailed in reference⁴. Hybrid polymers were prepared by polymerizing the vinyl-terminated PU with the appropriate amount of DPA monomer using ammonium persulfate as thermal initiator. FTIR and UV-visible spectra were measured using a FTIR Nicolet 380 and Genesys 10S spectrometers (ThermoFisher, USA) respectively. DSC and TGA-DTA were performed using a Q 200 (TA Instruments, USA) and a DTG-60 (Shimadzu Scientific Instrument) respectively. The water content (WC) of the films was determined by immersing the samples in buffers at the desired pH (ranging from 4 to 8) and a temperature of 30, 37 and 50 °C.

Results and Discussions

Hybrid polymers of PU and DPA show good film forming properties with high transparency. By incorporating DPA to PU the T_g values follow the Gordon-Taylor equation, indicating a random distribution of PDPA on the PU polymer ($k_{GT} = 0.3$). The water equilibrium swelling degree at 30 °C vs. pH, show in Figure 1, illustrates the pH dependent behavior properties of hybrids and Figure 2 the dependence with temperature.

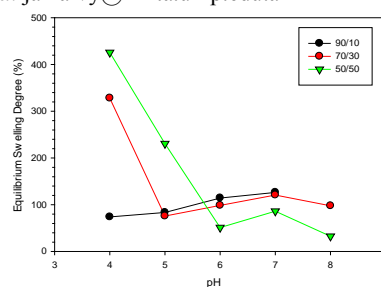


Figure 1. Equilibrium water swelling degrees vs pH, at 30 °C.

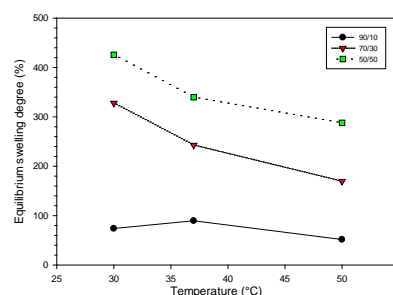


Figure 2. Equilibrium water swelling degrees vs T, at pH 4.

Conclusions

Hybrid polymers of PU and DPA, having good film forming properties were prepared and characterized. The incorporation of DPA monomer modifies the interactions between polyurethane chains as revealed by FTIR analysis, and causes the water uptake process to become pH and temperature-dependent.

Acknowledgment: CICPBA and ANPCyT (PICT 2014–1785).

References

1. Chen, J-K; Chang, C-J. *Materials*, 2014, 7, 805.
2. Schattling P; Jochum F.; Theato P. *Polym. Chem.*, 2014, 5, 25.
3. Pardini O.R. Amalvy J.I. *J. Appl. Polym. Sci.*, 2008, 107, 1207.
4. Amalvy, J. I.; Wanless, E. J.; Li, Y.; Michailidou, V.; Armes, S. P.; Duccini, Y. *Langmuir* 2004; 20, 8992.



SCALING-UP OF PDEAEM(CORE)–PEGMA (SHELL) NANOGEL SYNTHESIS

Iván Zapata-González¹, Angel Licea-Claverie¹, Edgar Medina-Monroy¹

1. CONACYT Research Fellow, Centro de Graduados e Investigación en Química, Instituto Tecnológico de Tijuana, A.P. 1166, 22000 Tijuana, B.C., México, idejzapatago@conacyt.mx, ivan.zapata@tectijuana.edu.mx

Introduction

Recently, the great develop of the polymeric nanogels as carrier systems, has strongly call the attention to cancer treatment application. Between the most attractive characteristics of these materials one could mention: nanometric particle sizes, high stability in dispersions of aqueous media, biocompatibility, ability to control the swelling ratio, drug protection against biochemical attacks, flexibility in complex molecular architectures, dual functionality of their structures, ability to incorporate functional groups and fast response to diverse stimuli. Obviously, the nanoparticle size is a preponderant factor to use them as advance drug delivery systems, since the fenestrations present in “leaky” tumor vasculatures have size from 20 to 200 nm,¹ it limits the applicability of the nanogels. As well known, the aim of this studies is to reach clinical treatment, but during *in-vivo* analysis (Phase II) the most of the works are stopped, being the amount of synthetic material an important aspect to consider. In this work we present the scaling-up of core/shell nanogel polymerization, using *N,N*-diethylaminoethyl methacrylate (DEAEM) and poly(ethylene glycol) methacrylate (PEGMA).

Experimental Part

Synthesis procedure

PDEAEM-PEGMA nanogels were prepared by Surfactant Free Emulsion Polymerization² method in a 1L jacketed glass chemical reactor, connected with a nitrogen inlet and reaction temperature at 82°C and 500 RPM. Ratios of PEGMA, EGDMA, and APS with respect to DEAEM in the feed were 42 wt %, 4 mol %, and 4 mol %, respectively. Samples was taken to 5, 10, 15, 30 and 60 min during the polymerization.

The resulting dispersions were purified via dialysis against deionized water during 5 days, using dialysis membrane, (Spectra/Por®, MWCO = 12,000–14,000), by changing water every day to remove any unreacted monomer and other impurities. Finally, purified nanohydrogels were recovered by freeze drying. The samples were frozen at -4°C in a conventional freezer for 12 h, precooled to -50°C, drying was performed at a pressure of 0.05 mbar for 2 days.

Characterization

Dynamic light scattering (DLS) was used to obtain the size distributions of the nanohydrogels by using a Zetasizer Nano ZS equipped with a red laser (630 nm). The angle of measurement was 90°. Samples were analyzed in DLS without any purification.

Results and Discussions

The hydrodynamic diameters obtained by the polymerization using a 1L reactor (112 nm at 60 min) considerably decrease in comparison with that produced by 50 mL Schlenk flask (160 nm at 60 min), Figure 1. The result is due to the high shear stress produced by the mechanical stirring.

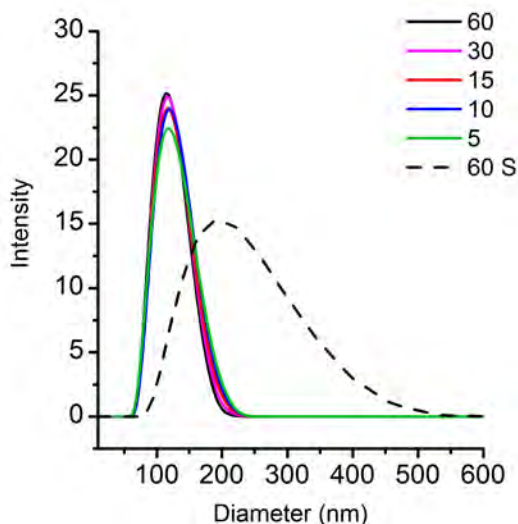


Figure 1. Comparison of size distribution by intensity of nanogels based on PDEAEM-PEGMA, obtained by 1L reactor (continuous lines) and 50 mL Schlenk flask (dash line).

Conclusions

The use of a 1L reactor to synthesize PDEAEM-PEGMA nanogels was successfully carried out, resulting an important decrease of the nanoparticle size.

Acknowledgment: IZG gratefully acknowledges the support of CONACYT, (Cátedras para Jóvenes Investigadores) and Conacyt CB-2012-01-178709.

References

- 1 Matsumura, Maeda, Cancer Res. 1986, 46, 6387.
- 2 M. González-Ayón, et al. J. Polym. Sci. A Polym. Chem. 2015, 53, 2662.



THERMORESPONSIVE SYSTEMS FOR DRUG DELIVERY BASED ON XANTHAN AND GELLAN DERIVATIVES

Jacques DESBRIERES¹, Mihaela HAMCERENCU^{1,2,3}, Marcel POPA², Gerard RIESS³

1. Université de Pau et des Pays de l'Adour, IPREM, Helioparc Pau Pyrenees, 2 Avenue P. Angot, 64053 PAU cedex9, France, jacques.desbrieres@univ-pau.fr
2. Technical university « Gheorghe Asachi », 71A, Bd D. Mangeron, 700050 Iasi, Romania
3. Université de Haute Alsace, ENSCMu, 3 Rue A. Werner, 68093 Mulhouse, France

Introduction

Within the biomedical domain, hydrogels and microparticles may allow the sustained and controlled release of drugs. In this context polysaccharide based materials are more and more used thanks to their specific properties – the biocompatibility, biodegradability and non-toxicity of their biodegradation by-products.

Experimental Part

Gellan and xanthan unsaturated esters were prepared by addition of free-radical polymerizable groups (acrylic acid, acryloyl chloride or maleic anhydride).^{1,2} Grafting-crosslinking free-radical reaction with N-isopropylacrylamide (NIPAm) allows obtaining hydrogels when N,N' methylene-bis-acrylamide (BIS) or cyclodextrin triacrylate (A-CD) are used as crosslinking agents.³

Results and Discussions

The chemical modification of xanthan and gellan is carried out under homogeneous (water) or heterogeneous (DMF) conditions. The degree of substitution could be controlled by varying the chemical nature of functionalization agent, reaction time and temperature. Maleic anhydride presents a higher reactivity as compared to acrylic acid and acryloyl chloride. By copolymerization of maleate polysaccharides with NIPAm, water-swollen hydrogels with interpenetrating polymer networks (IPN) are obtained. These hydrogels are temperature and pH-responsive. The role of the different components on LCST, morphology and swelling was investigated. It turned out that A-CD, as compared to BIS crosslinking, leads to hydrogels with increased LCST. Swelling is of major importance related with loading and release of drugs. Swelling kinetics is typical of limited swelling network. It appeared that the predominant co-continuous phase, NIPAm or polysaccharide, of the polymer network, determines the swelling characteristics of the hydrogel as a function of pH and electrolytes. Moreover A-CD crosslinked hydrogels are less sensitive to electrolytes than those obtained with BIS.

Inclusion, and release, of hydrophilic (chloramphenicol) or hydrophobic (progesterone) drugs are controlled by diffusion phenomena depending on morphology of the hydrogel and its crosslinking density (in relation with swelling properties). Release

kinetics curves demonstrate a quick initial release of active matter ("burst effect"). Hydrogels crosslinked with cyclodextrin acrylate are able to include either water- or lipo-soluble drugs, due to the nature of the crosslinking agent and its specific complexing properties. Hydrogels based on gellan esters were considered for ophthalmic applications. They can collapse and release adrenaline, the used drug, instantly when placed in contact with the human eye, at 37°C in relation with their temperature-sensitive properties (Figure 1).

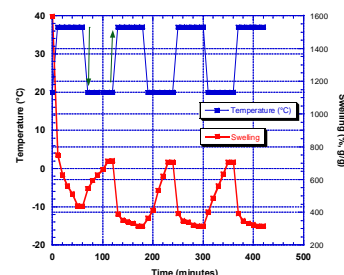


Figure 1. Influence of temperature on swelling of hydrogels based on gellan ester.

Biocompatibility, biodegradability and toxicity properties were evaluated and these hydrogels can be considered as non-toxic.

Conclusions

Hydrogels based on polysaccharide derivatives were elaborated without cytotoxic crosslinking agents and they are able to include (and then release) water- or lipo-soluble drugs according to their components. They present interesting biologic activity and they can be considered as candidates for biomedical applications.

References

1. Hamcerencu, M.; Desbrieres, J.; Popa, M.; Khoukh, A.; Riess, G., *Polymer*, 2007, 48, 1921.
2. Hamcerencu, M.; Desbrieres, J.; Khoukh, A.; Popa, M.; Riess, G., *Carb. Polym.*, 2008, 71, 92.
3. Hamcerencu, M.; Desbrieres, J.; Popa, M.; Riess, G., *Carb. Polym.*, 2012, 438.



POLYACRYLAMIDE-BASED RESPONSIVE NANOCOMPOSITE HYDROGELS ADDED BY MAGNETITE NANOPARTICLES AND MONTMORILLONITE CLAY

Adriel Bortolin^{1,3}, Fauze A. Aouada², Luiz H. C. Mattoso¹, C. Ribeiro¹

1. LNNA-Embrapa, CNPDIA, São Carlos, SP, Brazil adrielbortolin@gmail.com
2. DQ, State University of São Paulo, Ilha Solteira, SP, Brazil
3. DQ, Federal University of Sao Carlos, São Carlos, SP, Brazil

Introduction

Hydrophilic nanocomposites have been widely studied for the controlled release of different molecules, but the practical applicability of this process is limited by the diffusion behavior of the target molecule. [1] Thus, the development of hydrogels that are responsive to external stimuli (e.g. magnetic field and lighting intensity) is of particular interest in order to trigger and stop the release process in a remote fashion. The major challenge is to convert nanoparticle properties into stimulus to the hydrogel structure. For this, it is necessary that nanoparticles are chemically bound to the polymer structure, wherein the surface of the nanoparticle is covalently bonded to the polymer so that to behave like a rigid polymer chain group. [2] Thus, this work presents a method through which it was possible to synthesize nanocomposite hydrogels based on functionalized magnetic nanoparticles (Np's) chemically bonded to polymer chains.

Experimental Part

Hydrogels comprising polyacrylamide were obtained by chemical polymerization of acrylamide monomers in aqueous solution containing functionalized nanoparticles of magnetite and other modifiers such as mineral clay (calcium montmorillonite) and polysaccharide (carboxymethylcellulose). These materials were initially characterized by hydrophilic (Swelling degree), morphological and structural properties by FTIR, XRD and SEM.

Results and Discussions

It was possible to observe the incorporation of magnetic nanoparticles as well as the effects of each nanocomposite constituent in the swelling degree, with the presence of magnetic nanoparticles and clay mineral decreasing this property. Such reduction was minimized by the presence of the carboxymethylcellulose and when the nanocomposite was submitted a hydrolysis treatment. In table 1 is possible to observe when the nanocomposite was submitted a hydrolysis process (hydrogel (3:1) Hd.) there is no significant reduction of the swelling degree between the samples and this property increases about 100 times with this treatment. The FTIR spectra showed high evidence of chemical interactions among constituents through the displacement of characteristic peaks of both nanoparticle and mineral clay, as well as the polymer chain groups. These results

are further corroborated by XRD diffractograms. Morphological difference was also evaluated by scanning electron microscopy (SEM) and energy-dispersive X-ray spectroscopy (EDS). The EDS is showed in Figure 1 indicated an excellent dispersion of both magnetic nanoparticles and the mineral clay within nanocomposite.

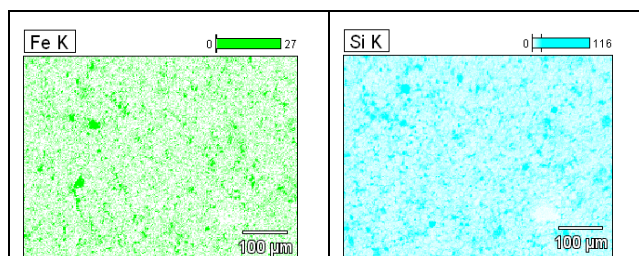


Figure 1: Energy-dispersive X-ray spectroscopy (EDS) map for nanocomposite with 2.0 % of NP's.

Also, it was possible to observe the magnetic activity in all nanocomposites synthesized with nanoparticles.

Table 1. Swelling degree at equilibrium for nanocomposites in function of amount magnetic nanoparticles.

Hydrogel	0.0% of Np's	0.5% of Np's	2.0% of Np's
(3:1)	62.3 ± 1.0	34.1 ± 0.5	31.7 ± 0.3
(3:1) Hd.	3383 ± 172	2906 ± 156	3300 ± 392

Conclusions

It was possible to synthesize a new magnetic hydrogel incorporating functionalized magnetite nanoparticles and the initial results denotes an excellent evidence for the continuation of this work.

Acknowledgment: FAPESP/CMDMC, CNPq/INCTMN, MCT/FINEP and EMBRAPA.

References

1. Joseph C. Grim, Ian A. Marozas, Kristi S. Anseth. Journal of Controlled Release 2015: 219, 95-106.
2. Hui Zhao, Jun Gao, Ruina Liu, Sanping Zhao. Carbohydrate Research. 2016: 428, 79-86.

MAGNETIC FILMS BASED ON BIO-POLYMERS AND NANOMAGNETITE

 Gianina A. Kloster¹, Diego Muraca², Mirna A. Mosiewicki¹, Norma E. Marcovich¹

1. Institute of Material Science and Technology (INTEMA)- National University of Mar del Plata, Juan B. Justo 4302, 7600 Mar del Plata, Argentina
2. Institute of Physics Gleb Wataghin, University Estadual de Campinas, CEP 13083-859 Campinas-SP Brazil

Introduction

The synthesis of monodisperse nanostructures of iron oxide is currently of tremendous interest since they are extensively used in magnetic materials as photocatalyst, sensors and medical applications such as hyperthermia, targeted drug delivery, magnetic resonance imaging, etc.¹ However, magnetic iron oxide nanoparticles have hydrophobic surfaces with large surface area to volume ratio and thus, the coupling of the hydrophobic interactions with magnetic ones results in particle aggregation, leading to a decrease in the magnetic properties of the agglomerated nanoparticles respect to those of the disaggregated ones. In this sense, synthesis methods that embed nanoparticles into polymers, glass or SiO₂ matrices have the added benefits of minimizing nanoparticle aggregation and forming uniform particle dispersion with a narrow particle size distribution.² In addition, if the polymer matrix is a biopolymer, several advantages are incorporated to the final material: biodegradability, biocompatibility, use of renewable resources with the consequent decrease in the environmental impact, among others.

In this work, the preparation and characterization of nanocomposite films based on chitosan and alginate biopolymers, and magnetite nanoparticles (MNP) are presented and discussed.

Experimental Part

Chitosan nanocomposite films were prepared by casting of iron salts /biopolymer/glycerol solutions (*in situ* precipitation of iron oxides). Chitosan solution (2% wt) was obtained in acetic acid (1% v/v) while alginate solution (2% wt) was prepared in 0.30 mol/L NaOH. The iron salts solution (0.2 M) was prepared in 1% v/v acetic acid at Fe²⁺:Fe³⁺=1:2 molar ratio. The solutions were mixed at the necessary proportions to obtain nanoparticle contents of 2 to 10 wt.%. Glycerol (plasticizer) was added in some samples. The suspensions were poured into Teflon Petri dishes and dried in a convective oven at 35°C for 24 h. The precipitation of nanomagnetite occurs spontaneously during mixing the solutions for alginate films (basic media) but had to be induced by immersing dried chitosan films in a NaOH solution during 30 minutes. The magnetic properties of the composites were determined by using a commercial SQUID magnetometer (Quantum Design, MPMS XL). Isothermal magnetization curves and Zero field cooling/field cooling (ZFC/FC) measurements were performed to determine the static magnetic properties of the films.

Results and Discussions

Magnetic characterization of films based on both biopolymers

revealed that they exhibit typical super-paramagnetic behavior. ZFC-FC curves for selected samples are shown in Figure 1.

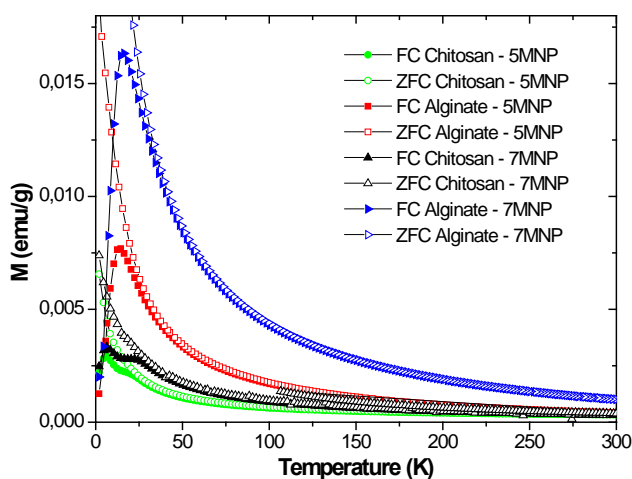


Figure 1. ZFC-FC curves for plasticized samples (30%wt. glycerol).

In general low concentrated or alginate based samples present a low blocking temperature (T_B , maximum in the ZFC curve) which is related to a small particle / agglomerate size. However, plasticized chitosan films with relatively high NMP content present two different T_B appearing at low and high temperatures, indicating a bimodal particle size distribution. This last effect was explained considering the two-phase structure of plasticized chitosan films (glycerol-rich and biopolymer-rich phases) and it is an interesting characteristic that could be used in technological applications where two work regimes, associated to the two magnetic nanoparticles sizes, are required.³ The size of the particles / agglomerated precipitated into the films was corroborated by TEM and SAXS measurements and a fractal association was proposed for the particles precipitated into plasticized films.

Acknowledgments: The authors gratefully acknowledge to CONICET, ANPCyT, UNMdP (Argentina) and FAPESP, CNPq (Brazil).

References

1. Sharifi, I., Shokrollahi, H., & Amiri, S. J Magn Magn Mater 2012, 324, 903–915.
2. Naik, R., Senaratne, U., Powell, N., Buc, E. C., M. Tsoi, M.G. 2005. Journal of Applied Physics 97, 10J313.
3. Kloster, G.A., Muraca, D., Meiorin, C., Pirota, K.R., Marcovich, N. E., Mosiewicki, M.A. 2015. European Polymer Journal, 72, 202-211, 2015.



FLAME RETARDANCY AND THERMAL STABILITY BEHAVIOR OF LDPE / EVA / CLAY / METAL HYDROXIDES NANOCOMPOSITES

Eduardo Ramírez ¹, Saúl Sánchez ¹, Mario Valera ²

1. Centro de Investigación en Química Aplicada, Blvd Enrique Reyna 140, Saltillo, México, 25294, eduardo.ramirez@ciga.edu.mx
2. Instituto de Química Aplicada, Universidad del Papaloapan, Circuito Central 200, Tuxtpec, Oaxaca, México, 68301

Introduction

In the last years there has been great interest in the industry for the incorporation of halogen-free flame retardants (FRs) regarding the healthy and environmental hazards associated with the use of their halogenated counterparts. In this work we analyzed the synergistic effect of organo-modified montmorillonite (Nanomer I28E and Cloisite 20A) and metal hydroxides (Mg(OH)₂ and ATH) as flame retardants in LDPE/EVA nanocomposites compatibilized with amino alcohol grafted polyethylene (PEgDMAE).

Experimental Part

Morphological characterization was carried out by means of X-ray diffraction (XRD) and Scanning Transmission Electron Microscopy (STEM). Flame-retardant properties were evaluated by the UL-94 Horizontal Burning and Cone Calorimeter Tests and Limiting Oxygen Index (LOI). Thermal stability behavior was analyzed with a Fourier Transform Infrared coupled with the Thermogravimetric Analyzer (TG-FTIR). The XRD analysis showed a displacement of the d001 plane characteristic peak of clay to lower angles, which indicates an intercalated-exfoliated morphology. From STEM images it was observed a good dispersion of flame retardants throughout the polymer matrix which was reflected in flame-retardant properties. TG-FTIR showed a better thermal stability of nanocomposites and the gases evolved during combustion showed an important reduction. Based on thermal stability and thermal degradation results, the flame-retardant mechanism of nanocomposites was proposed.

Results and Discussions

In order to understand the effects of fillers on the main produced gases during combustion, the absorbance versus time of the main pyrolysis products (hydrocarbons, acetic acid and CO₂) are plotted in Fig.1. It can be observed that the produced gases are reduced by the addition of MH and clay to the polymer matrix, especially for hydrocarbons and acetic acid. In the case of hydrocarbons, the absorbance decreased as the increased the content of MH from 20 to 30 wt%. For acetic acid, a similar reduction can be observed; resulting in delaying the composition of the EVA component of the blend. For CO₂, MH does not greatly affect its evolution. It can be concluded that during the decomposition of MH in the blend, the water released can dilute the gases produced during pyrolysis. Peak heat release rate (Peak HRR) is showed in Fig.2. This Indicate that samples with clay do not protect from self-propagation of the flame. In contrast nanocomposite samples with PEgDMAE as compatibilizer show a remarkable reduced peak HRR vale.

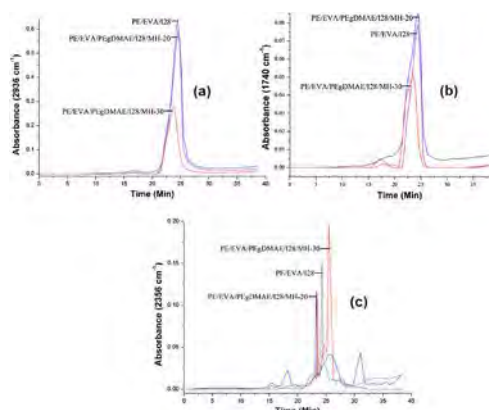


Figure 1. TG-FTIR spectra of pyrolysis products. (a) Hydrocarbons, (b) Acetic acid and (c) CO₂.

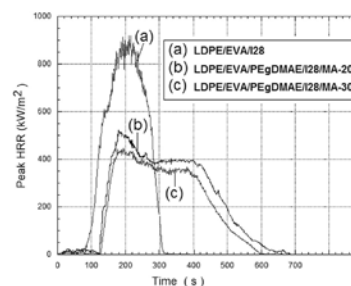


Figure 2. Heat release rate (HRR) for nanocomposites.

Conclusions

It was found that the better flame-retardant mechanism is due to the synergistic effect of Mg(OH)₂ and clay, and occurs primarily in the condensed phase. The clay by the generation of Brønsted acidic sites during early decomposition of the surfactant, promotes the formation of a carbonaceous char and the increment in viscosity which prevents dripping. The metal hydroxide dilutes the evolved gases produced during combustion. It can be concluded that the better flame-retardant mechanism is due to the synergistic effect of clay and metal hydroxides and their better dispersion throughout the matrix. The PEgDMAE promotes the interaction.

Acknowledgment: Authors thank J. Zamora, M. Lozano, B. Huerta, J. Rodriguez, J.L. Rivera, A. Espinoza,

References

1. E. Ramirez-Vargas, et al, J. Appl. Polym. Sci. 123 (2012) 1125-1136.
2. Song N., Eng Chem Res. 2014, 53, 19951.

CLAY DISTRIBUTION BETWEEN PHASES IN HETEROGENEOUS BLENDS POLYSTYRENE/POLYVINYL CHLORIDE

Helen Inciarte¹, Angel Ysea¹, Haydée Oliva¹, David Echeverri², Luis Rios²

1. Laboratorio de Polímeros y Reacciones, Universidad del Zulia, 4011, Maracaibo, Venezuela. holiva@fing-luz.edu.ve
2. Grupo Procesos Químicos Industriales, Universidad de Antioquia, 050010, Medellín, Colombia.

Introduction

An average size reduction of the dispersed domains in a binary immiscible polyblends has been observed in the presence of clay nanoparticles. Depending on the location of the filler, different stabilization mechanisms have been proposed.¹ In this work, the commercial modified clay Cloisite® 10A, (C10A) was used to investigate the behavior of blends composed by two incompatibles thermoplastic homopolymers: polystyrene (PS) and polyvinyl chloride (PVC). A simple methodology was developed in order to determine the stability of these polyblends and the distribution of each component between the phases.

Experimental Part

Polyblends with different compositions (Table 1) were prepared by solution blending at room temperature. First, 0.6 g of C10A (montmorillonite modified with dimethyl benzil hydrogenated tallow quaternary ammonium) were pre-dispersed in 100 mL of THF. Then, 15 g of total polymer (PVC+PS) were sequentially added to the flask, according to the weight fractions shown in Table 1. Both processes were carried out under continuous agitation at 250 rpm and 500 rpm, respectively. Equivalent blends but without clay were prepared for comparative purpose (Blends 1-3). Blends stability was evaluated by monitoring their tendency to demixing. Each phase was isolated 20, 30 and 40 days after having prepared the blends. Its volume was recorded. Composition of the separated phases was determined by a combination of gravimetric and FTIR techniques. Morphologies and elemental compositions of the composites were investigated via SEM and EDX. Moreover, the C10A dispersion and thermal decomposition for blends were analyzed through XRD and TGA, respectively.

Results and Discussions

Except for the Blend 6, all blends in Table 1 demixed in two phases: an upper PS-rich phase and a lower PVC-rich phase. The most important migration of components between phases occurred during the first 20 days. In Table 1 only the resulting component distribution (R_i) after 40 days are shown.

Upper phases contained PS and THF, whereas PVC, PS, THF and C10A were found in the lower phases. In spite of the structural similarity between modifier of clay and PS, results showed the preference of C10A for the PVC-rich phases (Table 1). In Table 2, the Cl signal confirms the presence of PVC in the matrix or drops, whereas the signals for the elements Al and Si proofed the presence of clay only in PVC-rich phase. Both, the demixing test

and the SEM-EDX analysis indicated that C10A was effective as compatibilizer only when it was located in the continuous PVC phase. Nanoparticles stabilize the system by steric hindrance when it is located in the matrix. Additionally, the resistance to demixing of Blend 6 can be attributed to a kinetic factor, because this blend had the highest viscosity.

Table 1. Partition for each component in polyblends.

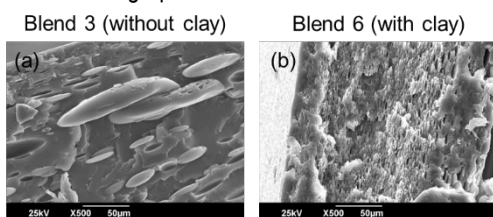
N°	Blends			Upper Phase			Lower Phase		
	WPVC	WPS	%C10A	RPVC	RPS	RC10A	RPVC	RPS	RC10A
1	0.2	0.8	0	0	96	-	100	4	-
2	0.5	0.5	0	0	95	-	100	5	-
3	0.8	0.2	0	0	81	-	100	19	-
4	0.2	0.8	4	0	99	0	100	1	100
5	0.5	0.5	4	0	56	0	100	44	100
6	0.8	0.2	4	No demixing					

In Figure 1 a significant reduction of the dispersed domains in the presence of C10A can be observed.

Table 2. EDX analysis for Blend 6.

Analysis Points	W _{Element} (%)				
	C	Cl	O	Al	Si
Matrix	-	73	23	1	3
Droplets	83	1	16	-	-

Figure 1. SEM micrograph for blends PVC80/PS20.



Conclusions

A morphology refinement in PVC/PS blends was possible in the presence of exfoliated C10A when PVC was the continuous phase. A relationship between results of demixing test and stability of the dispersed domains was found for this system.

Acknowledgment: CONDES-LUZ (Project CC-0055-16)

References

1. Ray, S.; Fouliot, S.; Bousmina, M.; Utraki, L. 2004. *Polymer*. 45, 8403.

IN-SITU SYNTHESIS AND CHARACTERIZATION OF P3HT-FeO COMPOSITES.

Marcos Fuentes Perez¹, María E. Nicho Diaz¹, Mérida Sotelo Lerma², Patricia E. Altuzar Coello³, Jesús Castellón Uribe¹, Giovanni S. Jiménez Bahena⁴

1. Centro de Investigación en Ingeniería y Ciencias Aplicadas de la Universidad Autónoma del Estado de Morelos, Av. Universidad 1001, Col. Chamilpa, C.P. 62209, Cuernavaca, Morelos, México. E-mail: mar120@live.com.mx; menicho@uaem.mx.
2. Departamento de Ciencias Químico-Biológicas de la Universidad de Sonora, Sonora 83000, México.
3. Instituto de Energías Renovables, Universidad Nacional Autónoma de México, Temixco, Morelos 62580, México, México.
4. Universidad Tecnológica Emiliano Zapata del Estado de Morelos, Av. Universidad Tecnológica No. 1, C.P. 62760, México.

Introduction

P3HT is a great candidate for applications in photovoltaic devices due his to high absorption coefficient in the visible region.¹ However, once that an exciton is photogenerated in P3HT, it is recombined quickly without producing free charges.² Two semiconductors are needed for that a solar cell works, one p-type (electron donor: polymer) and other n-type (electron acceptor: inorganic).² To achieve good efficiency in the solar cell, it is necessary to maximize the interfacial area between the two components, forming a heterojunction distributed. This can be achieved by incorporating both components during the polymerization reaction, which could allow better distribution of both components in the volume for charge transfer benefit.³ Thus in this work, the in-situ synthesis of P3HT was proposed by oxidative method in the presence of nanoparticles FeO. Currently, several hybrid solar cells have been proposed, however the inorganic materials are very harmful to the environment. Therefore in this work it was proposed to use the FeO, which is friendly to the environmentally. Additionally to our knowledge, the physicochemical, optical and electrical properties that have a P3HT-FeO nanocomposite are not known yet.

Experimental Part

P3HT-FeO composites were synthesized by in-situ oxidative chemical synthesis of 3HT (Sugimoto method) in the presence of FeO particles, FeCl₃ was used as oxidant/catalyst. The reaction was carried out at 0 ° C, under inert atmosphere and for a time of 24 hours. The composites were synthesized with different concentrations of FeO (3, 5 and 8% by weight), the products were washed with two different techniques for comparison (centrifugation and Soxhlet system). Prior to the polymerization reaction, the nanoparticles were dispersed by sonication in CHCl₃. Thin films of the P3HT/FeO composites were prepared by the spin-coating technique. The composites were characterized by UV-vis, XRD, SEM, Photoconductivity, FTIR, Photoluminescence and TGA.

Results and Discussions

The presence of FeO in the P3HT/FeO composites was determined by Fourier Transform Infrared Spectroscopy (FTIR). All composites showed lower absorbance than P3HT, which

indicated the incorporation of FeO within the P3HT: The P3HT/FeO composites showed photoluminescence. By X-ray (XRD), the crystalline phases of the products were identified and it was determined that with the presence of FeO in the synthesis of P3HT, the products showed higher crystallinity. Additionally, the composites were characterized by Thermogravimetry (TGA) to determine its thermal stability and its decomposition temperature; and by Scanning Electron Microscopy (SEM) to determine the surface morphology, particle size and distribution of FeO within the polymer matrix. Furthermore EDX analysis was performed to determine the incorporation of FeO in the P3HT.

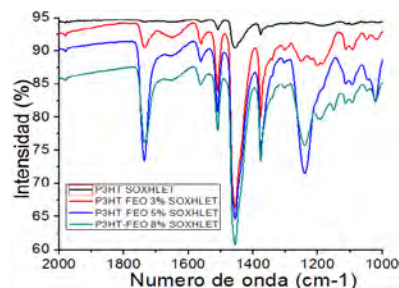


Figure 1. FTIR spectra of P3HT-FeO nanocomposites washed by soxhlet system.

Conclusions

Incorporating of FeO nanoparticles in P3HT modified the optical, electrical and physical properties of the nanocomposites. The washing method determined the incorporation of FeO in P3HT and purity of the nanocomposite. The obtained composite are promising materials for optic and electronic applications.

Acknowledgment: The authors acknowledge to the "FONDO SECTORIAL CONACYT –SENER –SUSTENTABILIDAD ENERGÉTICA" through the CEMIE-Sol/27 (project no. 207450).

References

1. Campoy Q.M. Células solares basadas en plásticos semiconductores. Barcelona. 2014. Pp.8.
2. B. Gburek, V. Wagner, Org. Electron. 11 (2010) 814-819.
3. Zhao, H.H. Presentación: Celdas solares hibridas a base de poli3-hexiltiofeno (P3HT)/CdS. CIE, UNAM. 2013. Pp.42.



FOTO-DEGRADACIÓN DE NANOCOMPUESTOS DE POLIPROPILENO Y MONTMORILLONITA

Julie Merchan-Sandoval¹, Roberto Chávez¹, Lidia Quinzani¹, Marcelo Failla^{1,2}

1. Planta Piloto de Ingeniería Química (PLAPIQUI), UNS-CONICET, Bahía Blanca, Argentina. jmerchan@plapiqui.edu.ar
2. Departamento de Ingeniería, Universidad Nacional del Sur (UNS), Bahía Blanca, Argentina

Introducción

En este trabajo se sintetizaron nanocompuestos de polipropileno (PP) y una montmorillonita organofílica (o-MMT) mediante funcionalización in-situ con anhídrido maleico (AM). Esta metodología permite la generación del compatibilizante simultáneamente con la dispersión y delaminación de la arcilla.^{1,2} Se analizó el efecto de la composición de los compuestos en su microestructura y en las propiedades mecánicas y térmicas luego de un tratamiento de envejecimiento acelerado en una cámara de UV siguiendo las pautas propuestas por la norma ASTM G154. Los resultados presentados corresponden a una concentración fija de agente funcionalizante e iniciador y distintas concentraciones de arcilla.

Experimental

Se utilizó PP isotáctico de *Petroquímica Cuyo S.A.I.C.* ($M_w = 330$ kg/mol), o-MMT *Nanomer 1.44P* de *Nanacor*, AM de *Merck* como agente funcionalizante y 2,5-dimetil 2,5-diterbutil peroxi-hexano (DBPH) de *Akzo Nobel* como iniciador de la reacción de funcionalización. Las concentraciones empleadas son: 1%p/p de AM, 0.075%p/p de DBPH y 0, 2, 5 y 10%p/p de o-MMT. Los materiales se prepararon en una mezcladora de laboratorio *Brabender Plastograph* a 180°C bajo atmósfera de N_2 . En el procedimiento de mezclado primero se fundió PP durante 2 min, luego se añadió DBPH y AM y se procesó 20 min, y posteriormente se añadió arcilla y se procesó 20 min más. Los materiales fueron entonces moldeados en una prensa calefaccionada a 180 °C para su futura caracterización. Para ello se utilizó: difracción de rayos X (DRX, *Philips PW1710*), microscopía electrónica de barrido (SEM, *LEO EVO-40 XVP*), calorimetría diferencial de barrido (DSC, *Pyris 1 Perkin-Elmer*) y medición de resistencia mecánica bajo tracción (máquina universal de ensayos *Instron*). El tratamiento UV se realizó en ciclos de 12 h (8 h de radiación UVA a 60°C y 4h de condensación sin radiación a 50°C) en un equipo *QUV* accelerated weathering tester de *Q-LAB*. Se extrajeron muestras cada 6 h.

Resultados y Discusión

De acuerdo a los resultados de DRX y SEM, los tres compuestos presentan una distribución homogénea de arcilla intercalada (con un aumento del espaciado basal de ~1.4 nm) y altamente exfoliada. En este sentido, el método de preparación por mezclado y funcionalización in-situ resulta altamente efectivo en la generación de nanocompuestos de PP.

La Fig. 1 (izq.) presenta los resultados del ensayo mecánico del PP, el PP funcionalizado (con DBPH y AM), y los tres compuestos. El PP presenta un comportamiento dúctil con una deforma-

ción máxima de 250%. Su modificación da lugar a un material con comportamiento en transición dúctil-frágil con esfuerzo de fluencia superior al del PP y deformación máxima de ~5%. El agregado de arcilla produce materiales frágiles con esfuerzo de rotura y deformación máxima que disminuyen con la concentración de arcilla.

El tratamiento UV da lugar a materiales con menor deformación máxima. En los compuestos se observa, además, una marcada disminución de la capacidad de soportar esfuerzo. La comparación del cambio relativo sufrido por los compuestos durante el añejamiento respecto al del PP funcionalizado (que constituiría la matriz de los compuestos) permite inferir que la arcilla actuaría acelerando el proceso de degradación del polímero.

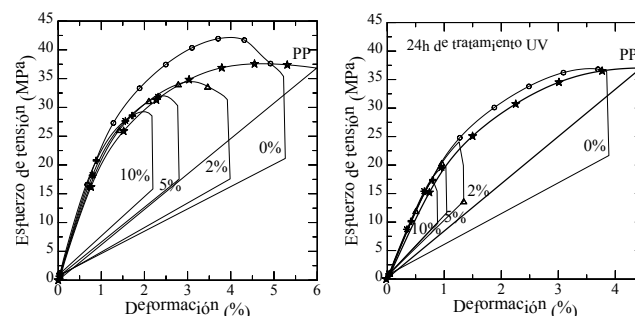


Figura 1. Diagrama esfuerzo- deformación de PP, PP funcionalizado (0%) y compuestos antes (izq.) y luego de 24 h de tratamiento UV (der.)

Es interesante señalar que no se detectaron diferencias en las temperaturas y entalpías de fusión de los materiales añejados respecto de los originales. Esto indica que la estructura cristalina no estaría participando en los cambios observados de la respuesta mecánica.

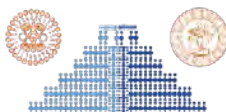
Conclusiones

El conjunto de los resultados muestra que es posible obtener nanocompuestos de PP y o-MMT en los que la nanocarga cumple un papel importante en el proceso de degradación del polímero. El sistema obtenido tiene potencial para ser usado como masterbatch en la preparación de nanocompuestos de PP.

Agradecimientos: Los autores agradecen al CONICET, la UNS y la ANPCyT por el apoyo económico brindado.

Referencias

1. Song, P; Tong, L; Fang, Z. *J Appl Polym Sci* 2008, 110, 616.
2. Zhang, Y; Lee, J; Rhee, J; Rhee, K. *Compos Sci Technol* 2004, 64(9), 1383.



SÍNTESIS Y CARACTERIZACIÓN DE NANOCOMPUESTOS DE POLIPROPILENO RAMIFICADO Y MONTMORILLONITA

Anibal Ferrofino¹, Facundo Ramos¹, Lidia Quinzani¹, Marcelo Failla^{1,2}

1. *Planta Piloto de Ingeniería Química (PLAPIQUI), UNS-CONICET, Bahía Blanca, Argentina*
2. *Departamento de Ingeniería, Universidad Nacional del Sur (UNS), Bahía Blanca, Argentina*
aferrofino@plapiqui.edu.ar

Introducción

La incorporación de ramificaciones largas en el polipropileno (PP) afecta su comportamiento mecánico y de flujo extensional¹. Por otro lado, la incorporación de nanocargas, tal como las arcillas, es otro método que tiene potencial para mejorar las propiedades del PP. Ambas metodologías conducen al aumento del rango de aplicaciones de esta poliolefina^{1,2}. El objetivo de este trabajo es sintetizar PP ramificado (PPr) y utilizarlo en la elaboración de nanocompuestos. El PPr fue obtenido por entrecruzamiento de un PP lineal comercial funcionalizado con anhídrido maleico (PPg) y los nanocompuestos se prepararon usando distintas concentraciones de una arcilla organofílica (o-MMT) y un copolímero de etileno vinilacetato (EVA) como compatibilizante.

Parte Experimental

Los polímeros utilizados son un PPg de *Chemtura* (Mw=120kg/mol, 1%p/p de grupos anhídrido), y un EVA de *Braskem* (MFI=150, 20%p/p de grupos vinilacetato). El entrecruzante utilizado es mililendiamina de *Aldrich*. La arcilla es una o-MMT (*Nanomer 1.44P* de *Nanocor*). El PPr se elabora mezclando el PPg con 0.2%p/p de amina a 180°C en una mezcladora de laboratorio *Brabender Plastograph* bajo atmósfera de nitrógeno. Los compuestos (cE#) se prepararon en la misma mezcladora de fundido usando 1 a 8%p/p de arcilla y una relación 3:1 de EVA/o-MMT. También se prepararon mezclas PPr/EVA (mE#) en relaciones equivalentes a las concentraciones de los compuestos. Las técnicas de caracterización usadas son: microscopía electrónica de barrido (SEM, *LEO EVO-40 XVP*), reología rotacional (*AR-G2 TA Instruments*) con medición de módulos dinámicos, calorimetría diferencial de barrido (DSC, *Pyris 1 Perkin Elmer*) y termogravimetría (TGA, *Discovery TA Instruments*).

Resultados y Discusión

El estudio por SEM permite inferir que el mezclado en fundido produce una adecuada dispersión y exfoliación de las partículas de arcilla en las matrices poliméricas y que el EVA y el PPr son polímeros inmiscibles. Los termogramas de cristalización de las mezclas confirman este resultado al presentar dos exotermas que se corresponden con los dos polímeros. El agregado de arcilla prácticamente no afecta el proceso de cristalización.

La Fig. 1 muestra el módulo elástico y la viscosidad dinámica de los compuestos y de una de las mezclas (mE8). Las mezclas presentan el comportamiento reológico típico de sistemas inmiscibles, con módulos dinámicos que aumentan marcadamente (sobre todo G') a bajas frecuencias respecto de ambos polímeros. La presencia de arcilla produce un aumento adicional de los módulos (ver datos de mE8 y cE8), sobre todo de G' a bajas frecuencias. El comportamiento reológico casi-sólido (G' mayor o semejante a G'')

de los compuestos con 5 y 8%p/p de o-MMT señala la existencia de un alto grado de interacciones partícula-partícula que indica un estado altamente exfoliado de la arcilla (con percolación).

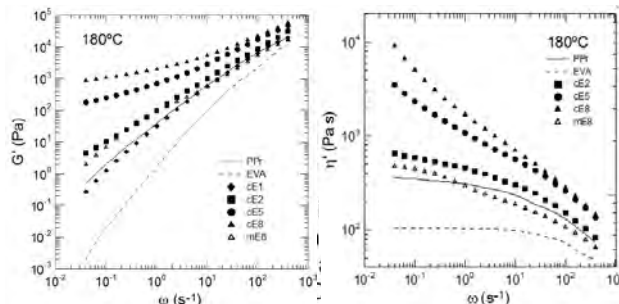


Figura 1. Módulo elástico y viscosidad dinámica a 180°C

La Fig. 2 presenta las curvas de degradación térmica de los materiales. Las mezclas (aquí ejemplificadas con mE5) presentan dos etapas de degradación, una que inicia a ~300°C correspondiente a la desacetilación del EVA, y otra a partir de ~400°C por la degradación de las cadenas poliméricas. Los compuestos también presentan dos etapas de degradación, aunque la primera se debe al efecto combinado de la degradación del componente orgánico de la arcilla y la desacetilación del EVA. Se observa, además, que la presencia de arcilla produce una aceleración de la degradación del PPr (que finaliza unos 30°C antes).

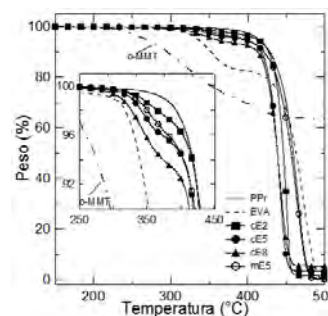


Figura 2. Termogramas obtenidos a 10°C/min en atmósfera de nitrógeno

Agradecimientos: Los autores agradecen el soporte financiero de CONICET, ANPCyT y UNS.

Referencias

1. Li, S.; Xiao, M.; Guan, Y.; Wei, D.; Xiao, H.; Zheng, A. *European Polymer Journal* 2012, 48, 362.
2. Zhang, Z.; Wan, D.; Xing, H.; Zhang, Z.; Tan, H.; Wang, L.; Zheng, J.; An, Y.; Tang, T. *Polymer* 2012, 53, 121.



ESR AND OTHERS TECHNIQUES IN THE CHARACTERIZATION OF RECYCLED POLYAMIDE WITH MAGNETITE (Fe_3O_4) NANOPARTICLES

Lucas Gabriel dos Santos¹, Mariana Fontana², Daniel Farinha Valezi¹, Jonathan Baum², Carmen Luísa Barbosa Guedes², Alexandre Urbano¹, Eduardo Di Mauro¹

1. Departamento de Física, CCE, Universidade Estadual de Londrina, Rodovia PR 445 Km 380, Campus Universitário, 86.057-970, Londrina, PR, Brazil dimauro@uel.br
2. Departamento de Química, CCE, Universidade Estadual de Londrina, Rodovia PR 445 Km 380, Campus Universitário, 86.057-970, Londrina, PR, Brazil

Introduction

Magnetic nanoparticles of diameters varying from 1 to 100 nm have many unique magnetic properties and are of great interest in some areas¹. Hybrid nanoparticles comprising polymers and magnetic nanoparticles can be classified in two types. In most of the cases a polymeric layer is coated on the magnetic nanoparticles surface or magnetic nanoparticles are embedded on a polymer network². Electron Spin Resonance (ESR) is based on the interaction of an external magnetic field with magnetic moments of unpaired electrons in a sample, which leads to the splitting of the electron energy levels and simultaneous resonant absorptions of a microwave field¹. The aim of this investigation is to analyze how the magnetite (Fe_3O_4) coated recycled polyamide using ESR and other techniques.

Experimental Part

The recycled polyamide (RP) was prepared according to the patent filed by State University of Londrina (n° BR 10 2013 032153 2). The preparation of Fe_3O_4 nanoparticles and recycled polyamide coated (RPC) was performed according to the methodology adapted proposed by Xie and Ma³. The ESR experiments were performed on a JEOL spectrometer (JES-PE-3X) operating at X-band (~9.5GHz). Bragg-Brentano geometry was employed for XRD measurement at 0.05 °/s. Crystallite size was estimated by Scherrer methodology employing 0.9 for form constant and Lorentz function for β fitting.

Results and Discussions

Fig. 1 shows the XRD patterns for the recycled polyamide (RP), magnetic nanoparticles (Fe_3O_4) and recycled polyamide coated with magnetic nanoparticles (RPC). The magnetic component was identified as cubic Fe_3O_4 and the value for crystallite size was 13.66 nm for Fe_3O_4 and 21.91 nm for RPC. By the fact that magnetite 2θ peak position do not vary is an indication that RP do not intercalate into the oxide structure. The ESR spectra (Fig. 2) show a broad signal for both Fe_3O_4 as RPC. The resonant field is equal and differing in line width peak-to-peak. The similarity between the signals suggest that the presence of the same magnetic species in both Fe_3O_4 and RPC samples, indicating a possible coating of Fe_3O_4 in the RP. Electron microscopy and magnetization measures are planned in this research with the

purpose of provide more information about magnetization dynamics.

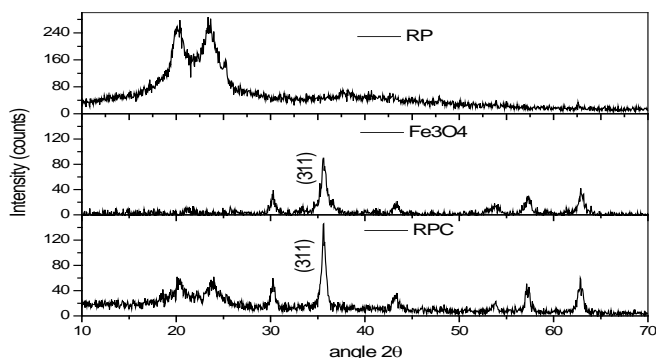


Figure 1. XRD diffractogram of RC, Fe_3O_4 and RPC.

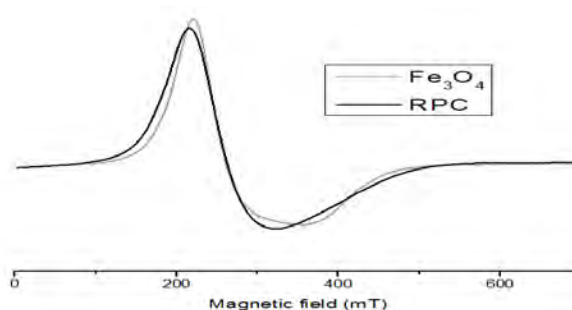


Figure 2. ESR spectra of Fe_3O_4 and RPC.

Conclusions

The XRD indicates that RP do not intercalate into the oxide structure and ESR measurements showed a possible coating of Fe_3O_4 in the RP.

Acknowledgment: Capes and CNPq.

References

1. Dobosz, B.; Krzyminiowski, R.; Schroeder, G.; Kurczewska, J. Journal of Phy. and Chem. of Solids 2014, 75, 594.
2. Reyes-Gallardo, E. M.; Lucena, R.; Cárdenas, S.; Valcárcel, M. Journal of Chromatography A 2014, 1345, 43.
3. Xie, W.; Ma, N. Energy & Fuels 2009, 23, 1347.

STUDY OF COMPOSITES CURED BY MICROWAVES IRRADIATION USING DMA

Daniel Kersting ¹, Hélio Wiebeck ², Fábio Esper ³

1. Escola Politécnica da USP, Av. Prof. Mello Moraes 2463, 05508-030, São Paulo, Brasil daniel.kersting@usp.br
2. Escola Politécnica da USP, Av. Prof. Mello Moraes 2463, 05508-030, São Paulo, Brasil
3. Centro Universitário Radial de São Paulo, Av. Jabaquara 1870, 04046-300, São Paulo, Brasil.

Introduction

The use of microwaves for polymerizations comes from 1950's, and since of that, its was little used. The heating by microwave irradiation is independent of thermal conductivity of irradiated material, and offers a interesting solution to operate with materials without a good thermal conductivity. The epoxy resins are a typical resin used for produce composites, and usually presents a poor thermal conductivity. The use of microwaves offers a fast heating (almost instantaneous), and controllable, perfect conditions for an application in composites made with epoxy resins. In this work it was studied how efficient the curing by microwaves can be, verifying different rates of heating (power levels of microwave oven) and the mechanical properties observed thought DMA tests. The thermal curing its was also executed in this work, for a comparison with results obtained ¹⁻².

Experimental Part

The composite samples were prepared with a fiberglass and epoxy resin by manual lamination in form of plates with 75X75X1,5mm, with a mass close to 11g . The resin (DGEBA), the hardener (MTHPA), and the accelerator (BDMA) used were provided by Araltec, a Huntsman distributor. The proportion for preparation of composites was 100:85:0,5 (in weight). The fiberglass used was a glass fiber E type, with density of 110g/m², produced by Owens Corning. The curing process by microwave irradiation was made with a domestic oven , Continental brand, MOCT022SD2A!BR model, adapted specially to operate with composites. The thermal curing it was executed with a kiln, Quimis brand, Q317B model. The DMA analysis was provided by a DMA equipment, TA Instruments brand, DMA Q800 model. The tests in DMA used a samples with 50x13x1,5mm, submitted a 10C/min, and a 1Hz.

Results and Discussions

Increasing the power levels, for a determinated irradiation time, increases the storage modulus e moves the loss modulus to the right, in a diagram storage modulus versus temperature. Using higher power levels can be also observed more collisions between the molecules, became the polymerization reaction more effective. An increase of T_g when the power levels are higher is a one of principal consequences observed. For evaluations with Tan(delta)

versus temperature its possible provide more informations about the curing process.

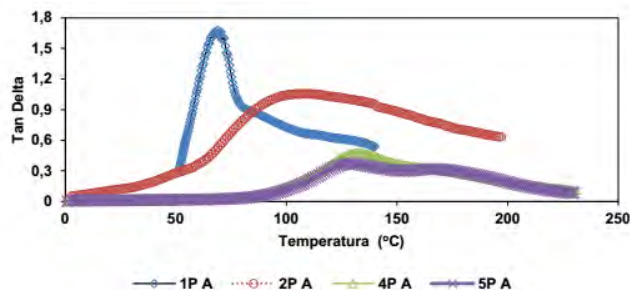


Figure 1– Tan(delta) versus temperature: different power levels (10 to 50) to 15 min. irradiation.

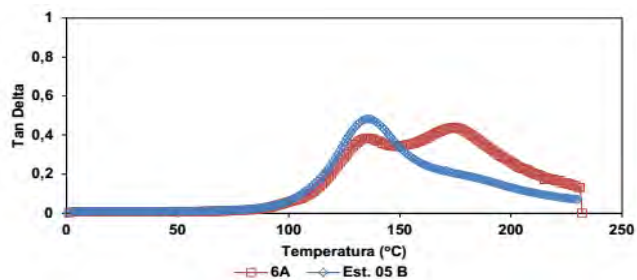


Figure 2 - Sample cured by microwave irradiation (6A) with sample produced by thermal curing (Est 05B).

Conclusions

The results obtained indicates that higher power levels improve a better heat dispersion, resulting in a superior mechanical properties if compared with the themal process applied in this work.

Acknowledgment: USP, UFABC, e CTMSP

References

1. Sadicoff, B.L.; Amorim, M.C.V.; Mattos, M.C.S. Química Nova, vol. 23, nº 4, 557-559, 2000;
2. Tanrattanakul, V.. Jo. of Applied Pol. Sci., Vol. 97, 1442–1461, 2005;
3. Yusoo, R.. Jo. of Eng. Sci. and Tech., Vol. 2, n 2, 151-163, 2007.



A ZOOM INTO THE STRUCTURE OF PYRROLE AND TITANIUM OXIDE HYBRID COMPOUNDS

F. González-Salgado^{1,3}, M.G. Olayo¹, G. García-Rosales³, M. González-Torres^{1,4}, L.M. Gómez^{1,4}, R. Basurto², E. Colín⁵, J. C. Palacios⁵, G.J. Cruz^{1*}

1. Departamento de Física, 2. Departamento de Química, Instituto Nacional de Investigaciones Nucleares, Carr. México-Toluca Km 36.5, Ocoyoacac, Edo. Mex., CP 52750, México. *guillermo.cruz@inin.gob.mx
3. Departamento de Posgrado, Instituto Tecnológico de Toluca, Av. Tecnológico s/n, Col. La Virgen, Metepec, Edo. Mex., CP 52140, México.
4. Posgrado en Ciencia de Materiales, Universidad Autónoma del estado de México Paseo Tollocan y Colón, Toluca, Edo. Mex., CP 52000, México.
5. Facultad de Ingeniería, Universidad Autónoma del Estado de México Cerro de Coatepec, s/n Ciudad Universitaria, Toluca, Edo. Mex., CP 50130, México.

Introduction

Pyrrrole (Py) and titanium oxide (TiOx) have been chemically joined by plasma in hybrid structures to be applied in the absorption of electromagnetic energy. The resulting complex structures have segments with pyrroles, -CH₂- and TiO with different atomic x=Ti/O ratios. XPS chemical analyses have been used to understand the structure of such not conventional organometallic polymers [1], however as the chemical reactions are complex involving organic and inorganic intermediate compounds, it is necessary to analyze those structures from perspectives, as hydrogenation, carbonization, nitridation, oxidation and titanization. This work presents analyses of the organic fraction of TiOx-Py hybrid structures from those perspectives.

Experimental Part

The chemical structure of TiOx-Py was analyzed by X-Ray Photoelectron Spectroscopy (XPS). The elements studied were O, Ti, C and N. The energetic distribution of O1s, Ti2p, C1s and N1s orbitals were adjusted with internal Gaussian curves whose area percentage was associated with at least one probable chemical state. C-C, C=C and C≡C bonds in those states were quantified and plotted as a function of the characteristic variables of the synthesis, time of reaction or power of synthesis. The sum of these percentages was named Carbonization. In a similar way, Hydrogenation was defined as the sum of C-H percentages, Nitridation as the sum of C-N, C=N and C≡N percentages and Oxidation considering O-C and C=O bonds. As Carbon atoms form the backbone of most polymers they were considered the axis of the organic analysis.

Results and Discussions

The percentages of C (carbonization), H (hydrogenation), and N (nitridation) in TiOx-Py are plotted in Figure 1 as a function of the time of synthesis. In t=0 the percentages belonging to the promoters pyrrole and Titanium Tetrapropoxide (TTP) before the synthesis are plotted. With the chemical reactions, C increases from 41% to 80%, H reduces from 50% to 10%, N increases from 3% to 6% and oxidation slightly reduces from 6% to 5% with the time of synthesis. Carbonization and dehydrogenation may be

related with crosslinking among the chemical groups due to the constant collisions in the plasma. In a similar pattern Nitridation increases with the chemical reactions. Oxidation is almost constant in TTP and in TiOx-Py.

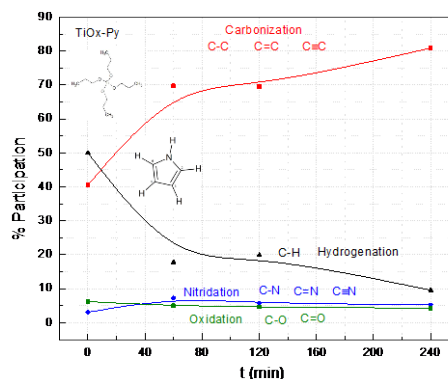


Figure 1. Evolution of C (carbonization), H (hydrogenation) and N (nitridation), and O (oxidation) in TiOx-Py as a function of the time of synthesis.

Conclusions

Chemical analysis of the organic fractions of plasma TiOx-Py hybrid compounds considering Carbonization, Hydrogenation, Nitridation and Oxidation were studied by XPS. Carbonization increased with the synthesis time and hydrogenation reduced. It has been stated before that the plasma promotes dehydrogenation and the formation of multiple bonds during the chemical reactions, but they have not been measured. In this work these variables were quantified as a function of the time of synthesis. The procedure can also be applied to conventional polymers.

Acknowledgments: To CONACyT for the support provided through projects 130190 and 154757 and for the doctoral scholarships of F. Gonzalez, M. Gonzalez and L.M. Gomez.

References

- 1 Davis Z. D., Tatarchuk B. J. *Applied Surface Science* 2015, 353, 679–685.



FLEXURAL BEHAVIOR OF TIMBER STRUCTURES REINFORCED BY POLYMERIC COMPOSITE

Andressa Cecília Milanese ¹, Maria Odila Hilário Cioffi ²

1. IFSP – Instituto Federal de Educação, Ciência e Tecnologia de São Paulo - Campus Itapetininga, Avenida João Olímpio de Oliveira 1561, 18202-000, Itapetininga, Brazil. andressa.cm@hotmail.com
2. UNESP – Univ Estadual Paulista, Fac de Eng de Guaratinguetá, Av Dr Ariberto Pereira da Cunha 333, 12516-410, Guaratinguetá, Brazil.

Introduction

Wood was the most material used as structure and usually can be found in historical buildings. This natural material constantly suffers offensive damages by physical, chemical and biological agents that can implicate its durability. Many times, timber structures are restored and reinforced with materials that present high density, low resistance to high temperatures, in fire cases, and susceptibility to bad weather. ¹ Nowadays, the rehabilitation of timber structures can be realizable through “traditional methods” – original structure is substitutes for a new piece with dimensions and properties analogous to the original wood, “mechanical” – structural repair is realized with metal connectors or by “adhesives” – polymeric adhesives were combined with metallic parts to structure recuperation. ² Therefore, this research presents the mechanical behavior of wood reinforced with polymeric composites composed by natural fibers. The objective of the use of sisal/epoxy composite as reinforcement is to become stronger the joints of damaged timber structures and to propose an increase in flexural strength.

Experimental Part

Matrix: The bi-component epoxy resin used is a low viscosity system that cures at room temperature. After mixing, the components present a pot life of 110 min at 25°C and a density of 1.22 g/cm³ after the cure.

Fiber: Woven sisal fabric used as reinforcement was obtained from the Northeast region of Brazil and received in form of plain weave. The fabric presents 2.4 millimeters of thickness and a mesh of 947 g/m². The fabrics were washed in boiling water and thermally treated in the oven at 60°C for 72 hours before molding.

Composite: Sisal/epoxy composites were prepared with 37% of reinforcement and processed by resin transfer molding (RTM) at room temperature. Laminate thickness is the equivalent of 4.4 mm and composed by two fabric layers. Composite was used into the joint between two pieces of wood.

Wood: The *Aspidosperma polyneuron* (Peroba-rosa) is a tree native from Brazil, Colombia, Peru, Argentina and Paraguay. According to Carvalho ³ it is an angiosperm of the dicotyledonous classes and Apocynaceae family.

Wood/composite system: The composite was cut with 50 mm width X 380 mm length and inserted as reinforcement into the junction of two pieces of wood (joint) and the lacuna was filled with epoxy resin.

Flexural test: Three-point bending tests of wood samples with a center joint (Fig. 1a) and wood/composite system (Fig. 1b) were

performed according to the ABNT NBR 7190 standard ⁴ using a universal machine, Shimadzu, model AG-X at a load-cell of 50 KN. The specimens were made with 50 mm width x 50 mm thickness x 115 mm length. A minimum of six specimens per test condition was tested and the load was applied in two cycles of charge and discharge before the final loading which proved the rupture. The tests used a crosshead speed of 10 MPa/min and a support span of 105 mm.



Figure 1. Wood specimens: a) Sample with a joint glued at the center, b) Sample with a joint at the center and reinforced by sisal/epoxy composite

Results

Table 1. Flexural data

Properties	Material	Wood with a center joint	
		without reinforcement	reinforced by composite
Flexural strength (MPa), MC = 9.93%		6.01	8.88
Flexural strength (MPa) ± SD, MC = 12%		5.64 ± 2.19	8.33 ± 1.87
Elastic Modulus (GPa), MC = 9.93%		7.50	4.68
Elastic Modulus (GPa) ± SD, MC = 12%		7.34 ± 1.27	4.58 ± 3.81

SD – Standard deviation; MC – Moisture content

Conclusions

Experimental results show that the use of composite as reinforcement, into the joint, increases in 47% the flexural strength of timber structures.

Acknowledgment: CAPES/PNPD

References

1. Cruz, I. P.; Mendonça, M. M. *Tecnologia y Construccion* 2002, 18, 37.
2. Fiorelli, J. Exploitation of carbon fiber and glass fiber to reinforcements of timber beams. Dissertation. São Carlos: University of São Paulo, 2002.
3. Carvalho, P. E. R. Circular Técnica: Embrapa Florestas 2004, 96, 1. Available: <<http://ainfo.cnptia.embrapa.br/digital/bitstream/CNPF-2009-09/41467/1/circ-tec96.pdf>>. Accessible: june 7th 2016.
4. ABNT NBR 7190: Projeto de estruturas de madeira. Associação Brasileira de Normas Técnicas 1997.

PRODUCCION DE LATEX ACRILICO / MELAMINICO CON ALTO CONTENIDO DE SOLIDOS PARA SU APLICACIÓN COMO PELICULA CURABLE A ALTA TEMPERATURA

Carlos Córdoba ¹, Luis Gugliotta ¹, Roque Minari ¹

1. INTEC (UNL-CONICET), Güemes 3450, (3000), Santa Fe, Argentina. rjminari@santafe-conicet.gov.ar

Introducción

La polimerización en miniemulsión (ME) directa representa una alternativa para la síntesis de látex híbridos, ya que permite la incorporación de componentes hidrofóbicos en las partículas de polímero, evitando su difusión a través de la fase acuosa.¹ Así, es posible la incorporación directa de una resina melamina-formaldehído (MF) en nanopartículas de polímeros acrílicos, con el propósito de sintetizar materiales poliméricos híbridos acrílico-melamínicos, de altos contenidos de sólidos, para su potencial aplicación en esmaltes horneables acuosos.

En el presente trabajo, se investigó la polimerización en ME, con alto contenido en sólidos, de una formulación monomérica acrílica en presencia de una resina MF isobutilada comercial.

Trabajo Experimental

Se utilizaron: persulfato de potasio como iniciador; octadecil acrilato (OA) como coestabilizante; Dowfax 2EP como emulsificante; hidroxietil metacrilato (HEMA), estireno (St), acrilato de butilo (BA), metacrilato de metilo (MMA), agua desmineralizada y la resina MF isobutilada provista por INDUR, INDUMEL MF1660.

Las MEs están compuestas por: 50% de sólidos; 2% wbp (peso en base a fase orgánica) de emulsificante; 0.2% wbw (peso en base agua) de buffer NaHCO₃; y 4% wbm (peso en base al monómero total) de OA. Las formulaciones incluyen BA/MMA/St/HEMA en relación 41.5/40.5/11.2/6.8; y 10, 15 y 25% wbm de MF en MF₁₀, MF₁₅ y MF₂₅, respectivamente. Las fases orgánica y acuosa se homogenizaron mediante ultrasonido (Sonic VC 750). Las polimerizaciones se llevaron a cabo en un reactor encamisado de vidrio (0.2 L) con agitación mecánica; a 70 °C durante 3 h. Se determinó: la conversión por gravimetría; y los diámetros medios de gotas y de partículas por DLS a 90° (Brookhaven BI-9000 AT). También, se calculó el número de gotas (N_d) y partículas (N_p), y su relación (N_p/N_d).

Las películas de polímero se prepararon en moldes de silicona, secando los látex a 22 °C y 55% humedad relativa (HR). El contenido de gel (fracción insoluble) de los films, se determinó mediante extracción soxhlet, con tetrahydrofurano, antes y después del curado a 150 °C durante 1 h. Los ensayos de tracción se realizaron con un equipo Instron 334, según norma ASTM D638. Con él, se realizaron los ensayos de dureza, utilizando un indentador cilíndrico de punta plana, de 2 mm de diámetro. El valor de dureza se midió como la fuerza máxima en compresión cuando la película es penetrada 1 mm.

Resultados y Discusión

Se observó un $N_p/N_d \approx 1$ en todos los casos, lo que indica que el mecanismo de nucleación fue predominantemente en miniemulsión. El HEMA presenta funcionalidad carboxilica, disponible para la reacción de curado con los grupos iso-butoxi de la MF. Esta reacción se ve favorecida a pH bajos. La hidrólisis del HEMA en ácido metacrílico y etilenglicol, es muy rápida en soluciones alcalinas, incluso a temperatura ambiente; y conjuntamente con la descomposición homolítica del iniciador, contribuyen a la disminución del pH de los látex a valores 5-6, promoviendo la formación de gel (> 70%). Posterior al tratamiento térmico, se logran geles cercanos al 100%, provocando un aumento significativo en la dureza y en la resistencia tensil; y una disminución de la deformación (Tabla 1). De la Figura 1, se observa el efecto del curado en las películas con diferentes contenidos de MF.

Tabla 1. Propiedades antes y después del tratamiento térmico.

Film	N_p/N_d	TS ⁱ	Def ⁱⁱ	Dur ⁱⁱⁱ	Gel ^{iv}	TS ⁱ	Def ⁱⁱ	Dur ⁱⁱⁱ	Gel ^{iv}
		Antes de curar (MF)				Después del curado (MF _c)			
MF ₁₀	0.9	13.0±1.2	4.1±0.8	1.4±0.1	89	15.6±0.7	2.5±0.1	1.6±0.1	102
MF ₁₅	1.0	11.0±0.4	3.7±0.4	1.1±0.0	76	15.1±0.2	1.2±0.1	1.2±0.1	100
MF ₂₅	1.1	11.9±0.6	4.3±0.2	0.7±0.0	71	13.3±1.3	0.8±0.0	1.2±0.0	96

ⁱTS: Resistencia tensil [MPa], ⁱⁱDef: Deformación [$\times 10^2$ %], ⁱⁱⁱDur: Dureza [$\times 10^2$ N], ^{iv}Gel [%]

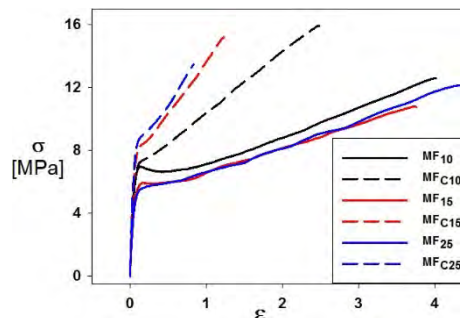


Figure 1. Resultados de los ensayos mecánicos de tracción.

Conclusiones

Se observó que la polimerización en ME es un proceso apropiado para la síntesis de nanopartículas híbridas acrílico/melamínicas con propiedades controladas, para una posible aplicación en recubrimientos horneables.

Agradecimientos: A CONICET, ANPCyT, y Universidad Nacional del Litoral por su ayuda económica.

Referencia

1. Asua, J. M. Prog. Polym. Sci. 2002, 27, 1283–1346.



DEGRADATION OF PLA-NATURAL FIBER COMPOSITES UNDER CONTROLLED COMPOSTING CONDITIONS AND ITS EFFECT ON TENSILE PROPERTIES

Erick Omar Cisneros-López¹, Aida Alejandra Pérez-Fonseca¹, Yolanda González-García², Carlos Federico Jasso-Gastinel¹, Daniel Edén Ramírez-Arreola³, Jorge Ramón Robledo-Ortiz²

1. Departamento de Ingeniería Química, Universidad de Guadalajara, Blvd. Gral. Marcelino García Barragán No. 1451, 44430, Guadalajara, Jalisco, México.
2. Departamento de Madera, Celulosa y Papel, Universidad de Guadalajara, Carretera Guadalajara-Nogales km 15.5, Las Agujas, 45510, Zapopan, Jalisco, México. jorge.robledo@ucei.udg.mx
3. Departamento de Ingenierías, Universidad de Guadalajara, Av. Independencia Nacional No. 151, 48900, Autlán de Navarro, Jalisco, México

Introduction

The use of cellulosic fibers to reinforce polymers has received much attention in recent years because of their ecological character, low cost and high specific properties.¹ Nevertheless, petroleum-based polymers have the disadvantage of not being biodegradable, for this reason, the demand for biodegradable polymers such as polylactic acid (PLA) has recently increased.² PLA has become one of the most used biopolyesters for the food packaging industry due to its easy processability, superior properties and reasonable rate of disintegration in compost.¹ In this work, PLA biocomposites were produced by a combination of extrusion and injection molding with three different cellulosic fiber reinforcements (agave, coir, and pine). The composites degradation under a compost and its effect on tensile properties and weight loss were studied.

Experimental Part

The matrix used was PLA 3251D (NatureWorks LLC). Agroindustrial residues of natural fibers were obtained in Mexico to be used as reinforcement: agave fibers (*Agave tequilana* Weber var. Azul), coir fiber (*Cocos nucifera*) and pine sawdust (*Pinus* spp.). The fibers were milled and sieved to keep particles between 50 and 70 mesh. Composites were produced with 20 wt % of fibers in a twin-screw extruder Leistritz Micro 27 GL/GG 32D. After extrusion the composites were pelletized and oven-dried in order to be processed by injection molding on a NISSEI PS 60E9ASE with a temperature profile of 165/185/190/185 °C. The samples molded were type IV dog-bone specimens (ASTM D638). The degradation under composting conditions of PLA and composites was carried out according to ISO 20200 standard during 3 weeks. Tensile properties were measured on an INSTRON model 3345 universal testing machine.

Results and Discussions

Figure 1 shows the tensile properties and weight loss of composites and PLA. The fibers presence delays the degradation; however, since the fibers promote the direct and rapid ingress of water and microorganisms into the composite², positive degradation results for weight loss (specially coir) and strength (in all composites) can be observed since the second week

composting; pine samples lost physical integrity after three weeks. Figure 2 presents typical images of the materials before and after composting showing the darkening effect caused by oxidation with composting time.

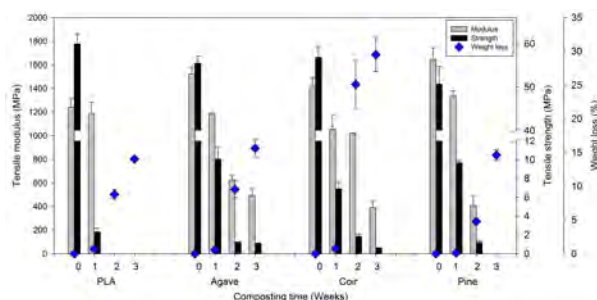


Figure 1. Tensile properties and weight loss of PLA and composites under controlled composting conditions.



Figure 2. Effect of composting on the aspect of (a) neat PLA and the composites: (b) PLA–agave, (c) PLA–coir, and (d) PLA–pine.

Conclusions

The fibers promote an increase in modulus, with a decrease in material cost. Coir fibers promoted the highest weight loss showing the preference of microorganisms. The degradation was reached with all cellulosic fibers.

Acknowledgment: CONACyT; ucei.udg.mx

References

1. Arrieta, M.P.; Fortunati, E.; Dominici, F.; Rayón, E.; López, J.; Kenny, J.M. *Polym. Degrad. Stab.* 2014, 107, 139.
2. Iovino, R.; Zullo, R.; Rao, M.A.; Cassar, L.; Gianfreda, L. *Polym. Degrad. Stab.* 2008, 93, 147.
3. Ochi, S. *Mechanics of Materials.* 2008, 40, 44.

EFFECT OF AGAVE FIBER SURFACE TREATMENT ON THE TENSILE PROPERTIES OF POLYETHYLENE COMPOSITES PRODUCED BY COMPRESSION MOLDING

Erick Omar Cisneros-López¹, Martí Estaban Gonzalez-López³, Aida Alejandra Pérez-Fonseca¹, Rubén González-Núñez¹, Denis Rodrigue², Jorge Ramón Robledo-Ortiz³

1. Departamento de Ingeniería Química, Universidad de Guadalajara, Blvd. Gral. Marcelino García Barragán No. 1451, 44430, Guadalajara, México.
2. Department of Chemical Engineering and CERMA, Université Laval, Quebec City, G1V 0A6, Quebec, Canada.
3. Departamento de Madera, Celulosa y Papel, Universidad de Guadalajara, Carretera Guadalajara-Nogales km 15.5, Las Agujas, 45510, Zapopan, México. jorge.robledo@ucei.udg.mx

Introduction

For several years now, natural fiber composites (NFC) have gained high interest.¹ However, NFC have some drawbacks, the most important one being low compatibility between natural fibers and most polymers (especially polyolefins).² To solve this problem, several methods like chemical, physical and thermal treatments have been proposed to improve adhesion between both phases.³ In this work, the effect of natural fiber surface treatment with maleated polyethylene (MAPE) is presented to improve the mechanical properties of natural fiber composites (NFC). In particular, a simple dry-blending technique was used to disperse natural fibers (agave) in a polymer matrix (linear low density polyethylene) and composite samples were produced via compression molding.

Experimental Part

The polymer matrix was linear low density polyethylene (LLDPE). Agave fibers (*Agave tequilana* Weber var. Azul) were obtained from residues of a local tequila company. Sodium hydroxide, MAPE and 1,2,4- trichlorobenzene (TCB) were used. For surface treatment, the agave fibers were placed for 15 min in 2% NaOH at 25°C. After washing with water and drying, MAPE treatment was performed in 1% wt. MAPE in TCB at 90°C during 30 min under high intensity mixing. After recuperation by filtration, the treated fibers were dried. Fiber contents between 0 and 40% wt. were prepared by Dry-blending for 2 min at 18000 rpm. Finally, the blends were compression molded in a Carver laboratory press during 6 min at 200°C and 3,000 kg. Micrographs of cryogenically fractured samples were taken using a scanning electron microscope HITACHI TM-1000. Tensile properties were measured on an Instron model 5565 universal testing machine using Type V samples according to ASTM D638.

Results and Discussions

Micrographs in Fig. 1 clearly show changes at the fiber-matrix interface of untreated composites (UFC) and treated ones (TFC). Some gaps between untreated fibers and LLDPE can be seen, which is not the case for treated fibers. According to literature, MAPE is deposited (mechanical anchoring) as well as chemically grafted (chemical anchoring) on fiber surface.³

The tensile strength (Fig. 2) of TFC increased with fiber content: the 40% TFC presented an increase of 120% over UFC and LLDPE. Once again, these results indicate that good fiber-matrix interaction was achieved.³

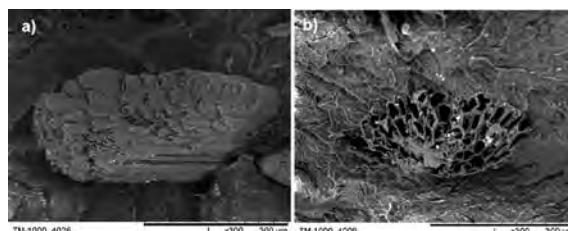


Figure 1. LLDPE-agave fiber interface for: (a) UFC and (b) TFC.

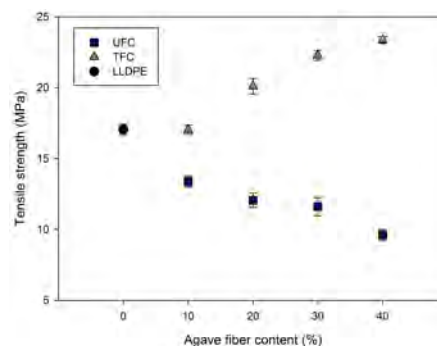


Figure 2. Tensile strength for LLDPE, UFC and TFC.

Conclusions

From the results obtained, it is clear that the simple dry-blending technique combined with a solution surface treatment of the fibers is a simple and efficient way to develop composite materials with enhanced properties.

Acknowledgment: CONACyT; ucei.udg.mx

References

1. Ashori, A. *Bioresource. Technol.* 2008, 99, 4661.
2. Bledzki, A.K.; Gassan, J. *Prog. Polym. Sci.* 1999, 24, 221.
3. Cisneros-López, E.O.; Anzaldo, J.; Fuentes-Talavera, F.J.; González-Núñez, R.; Robledo-Ortiz, J.R.; Rodrigue, D. *Polym. Compos.* 2015.

INFLUENCE OF NANOCCLAYS ON THE THERMAL AND MECHANICAL PROPERTIES OF POLYLACTIC ACID

Alan Salvador Martín del Campo-Flores¹, Jorge Ramón Robledo-Ortiz², Rubén González-Nuñez¹, Martín Arellano-Martínez¹, Aida Alejandra Pérez-Fonseca¹

1. Departamento de Ingeniería Química, Universidad de Guadalajara, Blvd. Gral. Marcelino García Barragán # 1451, 44430, Guadalajara, Jalisco, México aaperezfonseca@gmail.com
2. Departamento de Madera, Celulosa y Papel, Universidad de Guadalajara, Carretera Guadalajara-Nogales km 15.5, 45510, Las Agujas, Zapopan, Jalisco, México.

Introduction

Polylactid acid (PLA) is a versatile thermoplastic biopolymer produced from lactic acid monomer coming mainly from the fermentation of corn, potato, sugar bee, and sugar cane.¹ Currently it is the most used biopolymer owing to its high mechanical strength and easy processability.² In the other hand PLA has some disadvantages such as brittleness, sensitivity to high temperature and humidity, low impact strength and high cost. However, it has been reported that these properties can be improved by adding low amounts of nanoclays.³ Nano-reinforcements are mainly used in polymer nanocomposites to enhance properties of neat polymer, including their mechanical strength and thermal stability.⁴ In this study, the effect of three different nanoclays over the mechanical and thermal properties of PLA was evaluated.

Experimental Part

PLA 3251D from Nature Works LLC was used as polymeric matrix. The nanoclays used were 1.44P and 1.34MN from Sigma Aldrich and 15A from Cloisite. Pellets of PLA-clay nanocomposites were prepared in a twin-screw extruder with a clay content of 1, 3 and 5 wt% in order to evaluate the effect of clay amount as well as nanoclay type. Afterwards the nanocomposites pellets were processed by injection molding to obtained samples for the evaluation of their mechanical properties (flexural, tensile and impact) as well as thermal properties by DSC and TGA.

Results and Discussions

The results obtained from the mechanical tests showed that PLA flexural strength (Fig. 1) increased around 11 and 23 % by the addition of nanoclay 1.44P and 1.34MN respectively. The flexural modulus was increased by nanoclays content in a similar way for the three nanoclays used. The maximum values achieved were with 5% of 1.44P and 1.34MN content. It was observed that tensile modulus increases 20% with 5% of nanoclay for all the nanoclays used while tensile strength increased less than 10%. In the case of impact strength, it remained similar with nanoclay addition. It has been reported that nanoclays influence the thermal stability of PLA⁴, nevertheless in this study it was observed from TGA results that the nanoclays used did not affect PLA thermal stability. By DSC experiments, the values obtained of T_g , T_m and ΔH were also very similar for neat PLA and the nanocomposites.

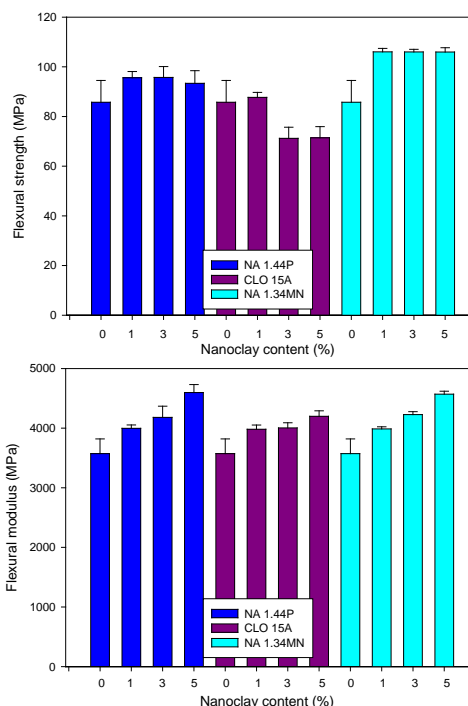


Figure 1. Flexural properties of PLA-nanoclays composites

Conclusions

In this study it was observed that nanoclay addition improved some mechanical properties, i.e. flexural and tensile; on the opposite, the nanoclays did not modify the thermal behavior of composites.

Acknowledgment: CONACyT (262892)

References

1. Porras, A.; Maranon, A. *Compos. Part. B* 2012, 43, 2782.
2. Arrieta, M.P.; López, J.; Rayón, E.; Jiménez, A. *Polym. Degrad. Stabil.* 2014, 108, 307.
3. Araujo, A.; Botelho, G.; Oliveira, M.; Machado, A.V. *Appl. Clay Sci.* 2014, 88, 144.
4. Cele, H.M.; Ojijo, V.; Chen H.; Kumar, S.; Land, K.; Joubert, T.; Villiers, M.F.R.; Ray, S.S. *Polym. Test.* 2014, 36, 24.



SYNTHESIS AND CHARACTERIZATION OF PVDF/PMMA COMPOSITES

J.R. Leppé¹, M.E. Nicho¹, F.Z. Sierra¹, F.F. Hernández¹, M. Fuentes¹, G. Alvarado-Tenorio¹---

1. Centro de Investigación en Ingeniería y Ciencias Aplicadas de la Universidad Autónoma del Estado de Morelos, Av. Universidad 1001, Col. Chamilpa, C.P. 62209, Cuernavaca, Morelos, México. E-mail: ingleppe@gmail.com; jose.leppener@uaem.edu.mx; menicho@uaem.mx; fse@uaem.mx;

Introduction

One method often used to improve properties of a specific polymer is to prepare composites. In recent times it has increased the interest in polymeric composites to be used in a variety of devices^{1,2}. The aim of this work is developing alternative polymers with enhanced mechanical and piezoelectric properties applied for electricity generation in automobiles³. Two of the most studied polymers for this purpose are polyvinylidene fluoride (PVDF) and polymethyl methacrylate (PMMA). The properties and morphology of these will depend, among other things, of the solvent or solvents used^{1,2,4,5}. Both polymers have two common solvent, tetrahydrofuran (THF) and Metilpirrolideno (NMP). PVDF is a good piezoelectric, we combined it with PMMA, pretending to maintain or improve the electrical and mechanical properties, as well as reducing costs.

The research is focused on the preparation and characterization of polymeric composites based on PVDF and PMMA. The composites were prepared by varying the concentration of the polymers, using as solvent a 50:50 mixture of THF and NMP. This in order to determine the influence of the polymers concentration on the properties of the composites.

Experimental Part

The PVDF/PMMA composites were prepared by sweeping the polymers concentration of 100 to 0 wt%. To dissolve the polymers, THF and NMP were used in a 50/50 vol% ratio, the solution concentration was 75 mg/ml. All composites were performed at room temperature.

The products were characterized by UV-Vis, FTIR, SEM-EDS, optical microscopy, DHM, TGA and electrical and mechanical characterization.

Results and Discussions

By UV-Vis was determined that the values of the band gap increased when the PMMA concentration was higher. The FTIR spectra of the different blends did not indicate the formation of any new chemical reaction product between PVDF and PMMA. The graphs looked like a superposition of the FTIR spectra of PMMA and PVDF. The morphology was changed with the polymers concentration, Fig. 1 shows that with the increase of PMMA, the granular structure of PVDF decreased. To higher PMMA concentration the dispersed grains were covered by PMMA. Future activities in this investigation will focus on testing additional electrical properties of the materials developed.

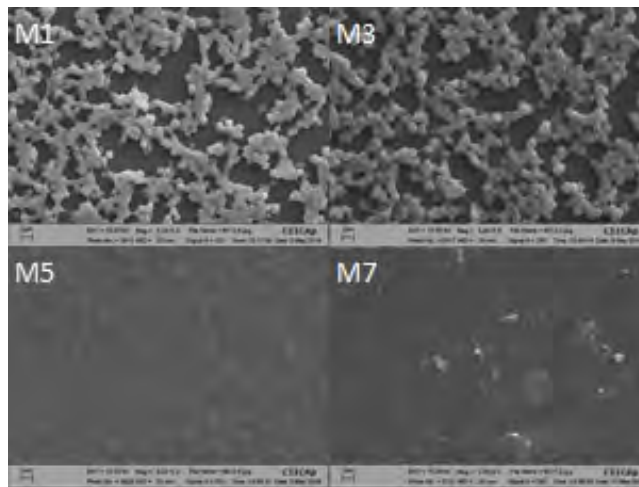


Figure 1. SEM of PVDF/PMMA samples.

Conclusions

The effect of polymers concentration on the morphology of thin films was studied for blends of PVDF/PMMA. It was observed that the surface morphology depends on the concentration of polymers in the blend. The physical mixture between PVDF and PMMA was corroborated by FT-IR, TGA and SEM studies.

In the UV-Vis spectra we noted that the higher the amount of PMMA, the lower the conductivity of the sample. The stability of the composites and the electrical and mechanical properties depends on the concentration of the polymers in the blend.

Acknowledgment: To "FONDO SECTORIAL CONACYT-SENER-SUSTENTABILIDAD ENERGÉTICA" through the CEMIE-Sol/27 (project no. 207450).

References

1. B. Scrosati, Applications of Electroactive Polymers, Chapman and Hall, London, 1993.
2. F.M. Gray, Polymer Electrolytes. The Royal Society of Chemistry, England 1997
3. J. Y. Song, Y.Y. Wang, C.C. Wan, J. Power Sources 77 (1999) 183-197.
4. C.A. Varela, F.Z. Sierra, Cyclic strain rate in tyres as power source to augment automobile autonomy, Int. J Vehicle Design, 65, No. 2, pp. 270-285, 2014.
5. A. Manuel Stephan, European Polymer Journal 42 (2006) 21-42.

ARTIFICIAL WEATHERING OF POLYETHYLENE NANOCOMPOSITES WITH CARBON NANOPARTICLES FOR OUTDOOR APPLICATION IN SOLAR WATER HEATERS

J. Martínez-Colunga¹, J. Valdéz-Garza¹, J. Mata-Padilla¹, V. Cruz-Delgado¹, C. Ávila-Orta¹

1. Centro de Investigación en Química Aplicada, Blvd. Enrique Reyna Hermosillo 140, 25294, Col. San José de los Cerritos, Saltillo, Coahuila, México. guillermo.martinez@ciqua.edu.mx

Polymeric materials are proved to be suitable materials for the fabrication of solar water heaters, where they are exposed to direct sunlight where the absorbed heat is transferred to the water.^{1,2} Thus, it is very important to protect the polymeric material against the photodegradation induced by UV light in outdoor conditions. Several UV light stabilizers from the family of benzophenones have been proved successfully in the past, however one of their disadvantages is the tendency to migrate reducing the protection over the time.^{3,4} The addition of carbon nanoparticles has been proved successful to reduce dramatically the photodegradation of several polymers besides they are non-migrating additives, with the advantage of increasing thermal stability, mechanical strength, thermal and electrical conductivity.⁵

Experimental Part

Three types of carbon nanoparticles with different morphologies (i.e. carbon nanotubes CNT, graphene nanoplatelets GNP and carbon black CB) were mixed with a polyethylene resin in different concentrations of 1, 2.5 and 5 wt % of each nanoparticle. Type V specimens for tensile test, according to the ASTM D638 standard were obtained from compression molding plaques and placed in an artificial weathering chamber QUV and irradiated with a wavelength of 340 nm with cycles of 16 h irradiation and 8 h condensation (accord ASTM G154 standard) during 0, 250, 500, 750 and 1000 h exposure. The tensile test were performed in a universal testing machine (Instron model 1000), with 10 kN load force at a 50 mm/min rate, 5 specimens were tested for each exposure time.

Results and Discussions

Fig. 1A compares the tensile strength versus the exposure time for nanocomposites with 1 wt % of three types of carbon nanoparticles. The addition of different carbon nanoparticles, increases the tensile strength up to 60% for the 3 types of nanoparticles at 500 h respect of the polyethylene resin. At higher times such as 1000 h the retention of tensile strength increases up to 250% with respect of the polyethylene resin. A similar tendency is observed for composites with 2.5 and 5% wt/wt in which carbon black show the best response. Fig. 1B compares the elongation at break vs. the exposure time for nanocomposites with 1 wt % of three types of carbon nanoparticles. With the addition of 1 wt % it is possible to observe elongations higher than

700% and only a slight reduction after the total time of exposure, demonstrating the ability of carbon nanoparticles to prevent the degradation by UV light on the polyethylene resin.

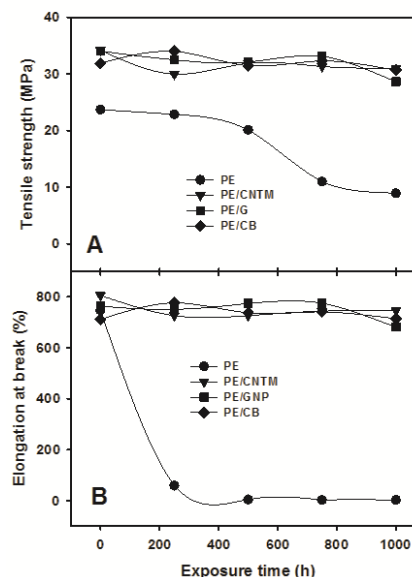


Figure 1. Tensile strength (A) and elongation at break (B) for nanocomposites with 1 wt % of different nanoparticles

Conclusions

This study suggests that a small content of carbon nanoparticles are effective to reduce the degradation of polyethylene by UV light and promotes the retention of mechanical properties.

Acknowledgment: We thank the support from Fondo SENER/CONACYT under CEMIE-Sol program Project 207450/12.

References

1. Whillier, A.; Saluja, G. *Sol. Energy* 1965, 9, 21.
2. Raman, R.; Mantell, S.; Davidson, J.; Jorgensen, G. *J. Sol. Energy Eng.* 2000, 122, 92.
3. Yang, R.; Li, Y.; Yu, J. *Polym. Degrad. Stab.* 2005, 88, 168.
4. Botta, L.; Dintcheva, N.; La Mantia, F. *Polym. Degrad. Stab.* 2009, 94, 712.
5. Andradý, A.; Hamid, H.; Torikai, A. *Photochem. Photobiol. Sci.* 2011, 10, 292.
6. Ávila-Orta, C.; Quiñones-Jurado, Z.; et al. *Materials* 2015, 8, 7900.



INFLUENCE OF CLAYS AND ORGANIC FILLERS ON THE VULCANIZATION CHARACTERISTICS AND MECHANICAL PROPERTIES IN NATURAL RUBBER-ORGANOCLAY NANOCOMPOSITES

Marcos G. Fernandes^{1,2,3}, Christiano G. B. Andrade^{1,3}, Fabio J. Esper¹, Francisco R. V. Diaz¹, Hélio Wiebeck¹

1. USP-University of São Paulo, Av. Prof. Luciano Gualberto, Trav.3 n° 380, 05508-900, São Paulo, Brazil. mgf@usp.br

2. IFSP-Federal Institute of São Paulo, Rua Pedro Vicente, 625, 01109-010, São Paulo, Brazil.

3. FMU-United Metropolitan Colleges, Av. Brigadeiro Luís Antônio, 1089, 01317-001, São Paulo, Brazil.

Introduction

The incorporation of organic fillers and organoclay into elastomers matrices leads to a significant improvement in the physical, mechanical properties of crosslinked elastomeric nanocomposites. This reinforcing effect is primarily due to hydrodynamic interactions between the rubber and filler surfaces. The ability of the layered silicate to disperse into polymer matrices at nanoscale level has attracted considerable attention from polymer researchers. However, there are hardly any reports on the preparation and dispersion of nanolayered silicates into natural rubber, in particular by means of a conventional rubber compounding process.^{1,2} As a consequence, the main goal of this investigation is the preparation and characterizing of NR vulcanized compounds reinforced with organophilic nanolayered silicate. It could be of a great interest to use white fillers as substitutes for carbon black in rubber compounding.

Experimental Part

The materials used for the preparation of the compounds are natural rubber (NR), Na⁺-activated montmorillonite, organophilized with HDTMA-Cl salt (CHO10) and piaçava fiber (PIA1). Rubber compounds were prepared in an open two-roll mill at room temperature. The rotors operated at a speed ratio of 1:1.25. The vulcanization ingredients were added to the elastomer previously to the incorporation of the filler and, finally, Sulphur was added. The curing behavior was determined, at 170°C with an oscillating disc rheometer. The material was vulcanized in an electrically heated press. Specimens were mechanically cut out from the cured plaques.

Results and Discussions

The curing characteristics, expressed in terms of the induction time, optimum cure time and torque value, are reported by curemeter curves at 170°C in Fig. 1. The tensile strength and elongation at break are reported in Fig. 2. From the obtained results, it can be deduced that the incorporation of small amounts of organosilicate (10 phr) gives rise to a strong reinforcing effect of these inorganic fillers.

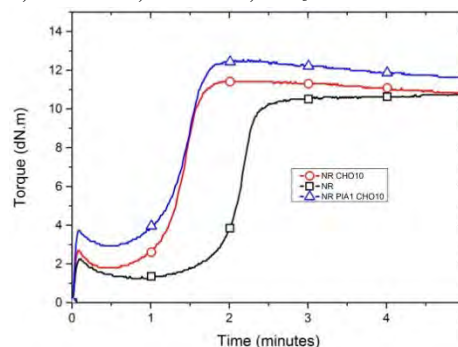


Figure 1. Influence of the organoclay and filler on the NR rheometer curves at 170°C.

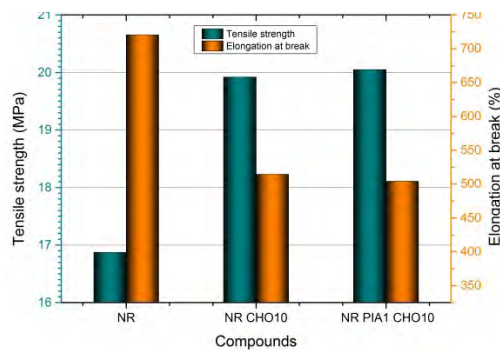


Figure 2. The nanoclay addition does affect significantly the tensile strength of the standard rubber compound.

Conclusions

A noticeable increase in the torque value, measured as the difference between the maximum and the minimum torque, was obtained in the presence of the organoclay, which suggest that a higher degree of crosslinking is obtained, which is reflected in a considerable increase in the mechanical properties of the elastomer.

Acknowledgment: IFSP, CNPq

References

- Galimberti, M. (Ed) (2011) Rubber-Clay Nanocomposites: Science, Technology, and Application, First Edition, John Wiley & Sons, Inc.
- Thomas, S., & Stephen, R. (Eds) (2010). Rubber Nanocomposites-Preparation, properties, and applications. Singapore: John Wiley & Sons (Asia)
-

INCREASED OF ANTIOXIDANT ACTIVITY OF ERIOCITRIN, A CITRIC FLAVONOID, IMMOBILIZED ONTO POLYURETHANE-HEMA/HTDMA-MMT OBTAINED BY PHOTOPOLYMERIZATION

Noelia Bertorello¹, Hugo Destéfani¹, Javier Amalvy^{2,3*}

1. INIQUI. (CCT CONICET Salta – UNSa), Avenida Bolivia 5150 (4400) Salta, Argentina.
2. INIFTA. (CCT CONICET La Plata – UNLP), Diag. 113 y 64 (1900) La Plata, Argentina.
3. CITEMA, UTN-FRLP, Av. 60 y 124, Berisso, Argentina.

*jamalvy@inifta.unlp.edu.ar

Introduction

Synthesis of nanoclay/polyurethane system with different contents of nanoclay (0.5, 1 and 2% w/w) was carried out using a montmorillonite organomodified with hexadecyltrimethylammonium bromide (MMT-HDTMA). The polyurethane (PU) with terminal vinyl groups, based on polypropylene glycol, 2-hydroxyethyl methacrylate (HEMA) and isophorone diisocyanate was synthesized by in-situ polymerization process¹.

In order to study the sorption properties of the polymer, the PU-based composites films were put in contact with a concentrated solution of eriocitrin, an antioxidant citric flavonoid, testing the adsorption in function of time. The resulting materials were characterized by FT-Raman and MDSC. The maximum adsorption was reached at 96 hs for PU with 1% MMT-HDTMA (62.96 mg eriocitrin/g PU-HEMA/MMT-HDTMA)².

There are many methods of measuring antioxidant activity, being the DPPH Method³ one of the most widely used to quantify the activity of capture of free radical because of its simplicity. DPPH Method was used to determine the antioxidant property of eriocitrin immobilized in PU films. The DPPH method uses 1,1-diphenyl-2-picrylhydrazil radical which is used as a quantification factor. The addition of the antioxidant caused a decrease in signal due to the decreasing concentration of the radical.

Experimental Part

Antioxidant activity of PU, PU/MMT-HDTMA 1%, eriocitrin, and PU/MMT-HDTMA 1% in contact with eriocitrin were determined using the DPPH radical which consisted in mixing 0.1 mL of liquid sample or a given mass of solid sample with 1.9 ml of DPPH 60 μM in methanol. The absorbance at 518 nm was measured as a function of the time taken for the reaction until reach the steady state (5 hours). The results of the assays are presented as percentages of remaining DPPH, calculated as follows:

$$\%DPPH = \frac{[DPPH]_t}{[DPPH]_0} * 100\%$$

where $[DPPH]_t$ is the concentration of DPPH at steady state and $[DPPH]_0$ is the initial concentration of DPPH. According to Brand and Williams³ the antiradical activity is defined as the amount of antioxidant required to reduce the concentration of DPPH by 50% (EC_{50}) and Anti-Radical Power (ARP) is defined as $1 / EC_{50}$.

Results and Discussions

In Figure 1 the profiles obtained for % DPPH remaining vs. molar ratio of sample/DPPH according to this method are presented.

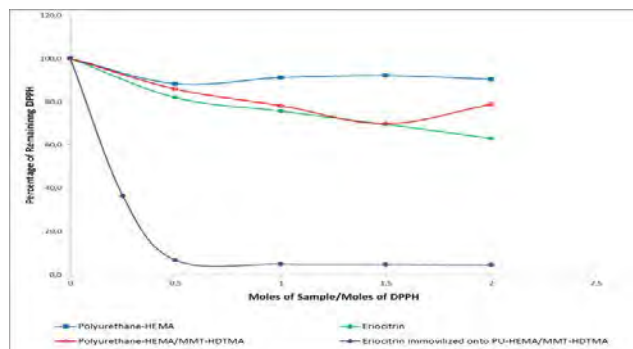


Figure 1. % DPPH remaining in the steady state (5 hours) versus (moles of sample/moles of DPPH), for eriocitrin, PU-HEMA, PU-HEMA/MMT-HDTMA and eriocitrin immobilized onto PU-HEMA/MMT-HDTMA.

Figure 1 shows that the antioxidant power of eriocitrin is increased when it is adsorbed on the solid in relation to eriocitrin in solution. PU-HEMA does not present antiradical activity, thus not affecting in determination of the antiradical capacity of the flavonoid. In the PU-HEMA/MMT-HDTMA a slight decrease in DPPH concentration is observed. It can be attributed to adsorption of radical cation in the MMT-HDTMA. Eriocitrin immobilized onto PU-HEMA/MMT-HDTMA exhibits a curve with a pronounced decline, indicating their high antiradical power. Comparing the values of the ARP of eriocitrin immobilized onto PU-HEMA/MMT-HDTMA (5.3) with ARP values of compounds like butyl hydroxy toluene (4.2) and butyl hydroxy anisole (4.2), the Polyurethane/eriocitrin films seem to compounds currently used as protectors of food oxidation.

Conclusions

Eriocitrin adsorbed into the PU-HEMA/MMT-HDTMA films exhibits higher antiradical activity than the free flavonoid in solution. It could be useful to pharmacological and food applications, for example, like food oxidation retardants films.

Acknowledgment: CIC, ANPCyT (PICT 2014 – 1785), UNSa and CONICET.

References

1. Bertorello, N.; Peruzzo, P.; Cordero, A.; Destéfani, H.; Amalvy, J. II Workshop de Nanoarcillas y sus aplicaciones. November 2014, Mar del Plata, Buenos Aires, Argentina.
2. Bertorello, N.; Peruzzo, P.; Destéfani, H.; Amalvy, J. XI Simposio Argentino de Polímeros. October 2015, Santa Fé, Argentina.
3. Brand-Williams, W.; Cuvelier, M. E.; Berset, C. *LWT-Food, Science and Technology* 1995; 28, 25.

MICROSTRUCTURAL, THERMAL AND MECHANICAL PROPERTIES OF GRAFTED POLYPROPYLENE COMPOSITES WITH ACETYLATED WHEAT STRAW FIBERS

Vladimir Fernández ¹, Santiago Duarte ², Ramón Sánchez ¹, Jacobo Aguilar ¹, Francisco Moscoso ³ and Gonzalo Canché ²

1. Departamento de Ciencias Tecnológicas, Universidad de Guadalajara, Av. Universidad No. 1115, 47810, Ocotlán, Jalisco, México. vladkrm@hotmail.com
2. Centro de Investigación Científica de Yucatán (CICY), Calle 43 No. 130, col. Chuburná de Hidalgo, 97200, Mérida, Yucatán, México
3. Departamento de Química, Universidad de Guadalajara, Bv. Marcelino García Barragán No. 1421, 44430, Guadalajara, Jalisco, México.

Introduction

The utilization of lignocellulosic fibers as reinforcement fillers in thermoplastics polymers and elastomers composites have been attracting attention recently because the natural fibers provide to the composites which better properties such as low density, biodegradability in comparison with other fillers as talc, glass fiber, etc. The lignocellulosic fiber have a sustainable value, because they could be obtained from agricultural residues such as stalks of cereal crops, rice husks, coconut fibers (coir), bagasse. ¹ The wheat straw fiber is a natural fiber, available, renewable, nontoxic, low density, and his low cost is of industrial and economic interest. These residues, as whole fiber or as cellulose fiber, have been used to obtain composite either with polyolefin or other polymers as matrix. ²

Experimental Part

The straw wheat fibers were harvested in the region of Ocotlán Jalisco. Isotactic polypropylene (PP) type PP-30 from PEMEX was used as matrix polymer. The fiber acetylation process was performed according to a process reported elsewhere. ³ PP matrix was grafted with 5 wt.% of anhydride maleic (MA) (Polybond 3200) as a coupling agent. The PP and PP-g-MA composites were obtained using a mixing chamber Brabender at 180 °C and 20 rpm. The content of fibers was of 10, 20, 30 wt.%. Specimens for testing were molded by thermo-compression and were cut according to the ASTM-D638 norm. Mechanical properties were performed in a universal testing machine INSTRON 5500 R. The thermal properties and microstructural characteristics were obtained with a DSC 6 differential scanning calorimeter Perkin Elmer and a JEOL-JSM-5900LV Scanning electron microscope, respectively.

Results and Discussions

Young's modulus of PP-g-MA composites were higher than the pure PP matrix, and increased with the non-acetylated fibers. This result suggests that the fibers act as a nucleation agent, favoring their strengthening. However, when the fibers were acetylated for both, PP and PP-g-MA composites, the Young's modulus was

lower than those materials prepared with the non-acetylated fibers. The increase of Young's modulus of grafted composites is related to the improvements of compatibility of the fiber and the matrix, because the PP-g-MA can form covalent linkages and hydrogen bonds between the anhydride maleic and the hydroxyl group of the fiber. On the other hand, the DSC measurements showed an increase of the crystallinity with the fiber content; whereas the SEM micrograph showed a good fiber dispersion for the PP-g-MA composites with non-acetylated fibers.

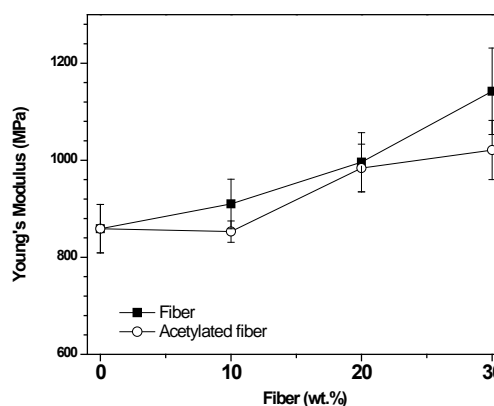


Figure 1. Young's modulus of composites with fibers and PP-g-MA.

Conclusions

In general, the PP-g-MA composites with non-acetylated fibers showed better mechanical properties than those prepared with acetylated fibers, due to the repulsion between the anhydride maleic and the acetate groups of the acetylated fibers.

References

1. Qiu W, Endo T, Hirotsu T. *J Appl Polym Sci* 2004; 94: 1326–35.
2. F.J. Moscoso, L. Martínez, G. Canché, D. Rodrigue, R. González-Núñez, *J. Appl Polym Sci* 2013; 127: (1) 599–606,
3. E. Obataya, K. Minato, *Wood Sci. Technol.* 2008 42, 567.



SEMICONTINUOUS EMULSION POLYMERIZATION OF n-BUTYL ACRYLATE IN PRESENCE OF GRAPHENE OXIDE

Victoria Padilla¹, Raquel Ledezma², Esther Treviño³

1. Centro de Investigación en Química Aplicada, Blvd. Enrique Reyna 140, 25294, Saltillo, Coah., México esther.trevino@gmail.com

Introduction

In the last 5 years have been reported several studies about the polymerization of Pickering emulsions stabilized with graphene oxide (GO). The most studied monomers are styrene¹⁻⁴ and methyl methacrylate.⁵⁻⁷ The concentration of GO (regards the monomer) varied from 0.1 to 5 wt. %. Sometimes, was used an anionic surfactant.^{4,6} In most cases stable hybrid latexes were successfully prepared. However, the solids content was very low (under 10 wt. %). In this paper, are presented the results obtained in the emulsion polymerization of n-Butyl Acrylate (n-BA) in presence of GO. The monomer was fed in a semicontinuous way in order to increase the solids content of the final latex.

Experimental Part

The GO was prepared by oxidation of graphite powder using the well-known modified Hummers method and characterized by TEM, SEM, AFM, EDX, IR, RAMAN and contact angle measurements. Latexes were prepared by dropping the n-BA onto an aqueous solution of GO and sodium dodecyl benzene sulfonate (SDBS). Polymerizations were carried out at 70°C using potassium persulfate (KPS) as initiator. The monomer as well as the initiator aqueous solution were fed in a semicontinuous way. The recipe was calculated for a 20 wt. % of solids content. The effect of GO concentration (0, 0.05 and 0.1 wt. % based on the total amount of polymer) was evaluated on the colloidal stability of the latex during polymerization. Conversion and coagulum were determined gravimetrically. Particle size was measured by DLS.

Results and Discussions

The evolution of particle size was monitored by taking samples during the polymerization (see Figure 1). Two different SDBS was studied looking for a better colloidal stability. The GO had no effect on the particle diameter regardless the SDBS concentration. This behavior may be because the synthesized GO had a high oxidation degree and, therefore, high hydrophilicity. This situation made the GO remain solubilized in water and did not compete with the surfactant to be located on the surface of the particles. The inverse effect of SDBS on the particle diameter is related with the capacity to cover a higher interfacial area. In all cases, conversion of n-BA was close to 100 %, however an important part of polymer was recovered from the stirrer and walls of the reactor. In Figure 2 is shown the effect of GO on the coagulum formation. Nevertheless, the latexes had a solids content around 15 wt. %.

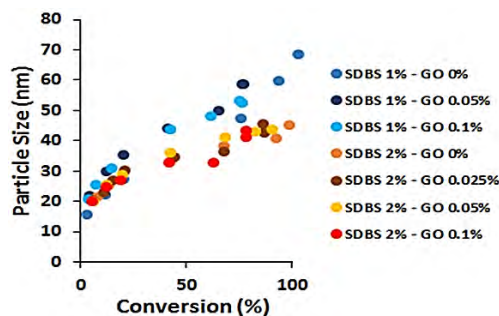


Figure 1. Effect of GO concentration on the particle size growth with conversion throughout the n-BA polymerizations.

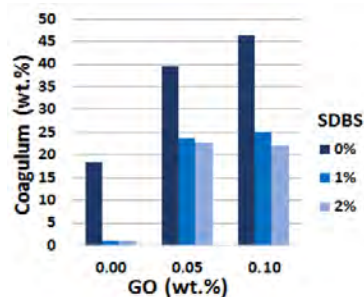


Figure 2. Effect of GO concentration on the coagulum content at the end of the n-BA polymerizations.

Conclusions

The GO did not show the expected amphiphilic character, so it was necessary the addition of SDBS to enhance the colloidal stability of the latexes. Despite of this problem, it was possible to prepare latexes with 15 wt. % of solids content that produced lightly grayish colored but translucent and homogeneous films.

Acknowledgment: The authors acknowledge the financial support of CONACyT through grant 181893.

References

Arial Narrow 9

- Xie, *et al.*, *Colloid Polym. Sci.* 2013, 291, 1631.
- Che *et al.*, *J. Polym. Sci. Part A Polym. Chem.* 2013, 51, 5153.
- Yin, *et al.*, *J. Colloid Interface Sci.* 2013, 394, 192.
- Etmimi *et al.*, *Polymer* 2013, 54, 6078.
- Gudarzi, *et al.*, *Soft Matter*. 2011, 7, 3432.
- Kuila, *et al.*, *Compos. Part A Appl. Sci. Manuf.* 2011, 42, 1856.
- Man, *et al.*, *J. Polym. Sci. Part A Polym. Chem.*, 2013, 51, 47.



SYNTHESIS AND DYNAMICAL MECHANICAL CHARACTERIZATION OF POLYURETHANE MATRIX COMPOSITES REINFORCED WITH KERATIN MATERIALS

Vicente Amaya Amaya¹, Ana Laura Martínez Hernández¹, Miguel de Icaza Herrera², Carlos Velasco Santos¹

1. División de Estudios de Posgrado e Investigación, Instituto Tecnológico de Querétaro, Avenida Tecnológico s/n, Esquina Gral. Mariano Escobedo, Colonia Centro Histórico, 76000, Santiago de Querétaro, México. almh72@gmail.com.
2. Centro de Física Aplicada y Tecnología Avanzada, UNAM, Boulevard Juriquilla No. 3001, 76230, Juriquilla, Santiago de Querétaro, México.

Introduction

In recent years a global trend toward environmental friendly materials has been growing. Thus it is needed to investigate new sources of raw materials with high performance, amply availability, and less aggressive manufacturing process. In this sense, nature can provide excellent opportunities to a proper exploit of new materials. In this research keratin materials obtained from poultry wastes were applied as reinforcement of polyurethane matrix. This fiber was previously characterized and used in other kind of synthetic and natural matrices¹. There exists a natural compatibility between keratin and polyurethane due to chemical groups related to amides in protein and urethane linkages. However in order to increase the possibilities to form a strong interface a traditional chemical treatment with NaOH was applied to keratin fibers. In this work, the thermomechanical properties achieved by these new materials are reported. The results showed that keratin can be considered as an interesting alternative due to it is a renewable and harmless reinforcement material.

Experimental Part

Two different keratin materials – barbs feather fiber and rachis feather fiber were included as reinforcement in a polyurethane matrix (PU). Keratin fibers were modified through an alkaline treatment with NaOH 0.1 N, at 50°C for 5 h. PU composites were obtained via condensation of commercial toluene diisocyanate (TDI) and poly (propilenglycol) (PPG). Different concentrations of reinforcements (10 and 20% w/w) were dispersed in PPG, after in situ polymerization was realized with TDI by poly(tetrafluoroethylene) moulding. The Dynamic Mechanical Analysis (DMA) was performed using a DMA Q800 (TA Instruments, USA) in three point bending mode between room temperature and 180°C at 5 °C min⁻¹.

Results and Discussions

Dynamic Mechanical Analysis was used to observe the viscoelastic response of polyurethane composites and the influence of keratin reinforcement in the performance of these composites. Fig. 1 compares the storage modulus versus temperature of pure polyurethane and PU-keratin composites. It is observed an evident increase in all composites with regard to pure matrix. The alkaline modification produced an increase in storage

modulus in both systems reinforced with keratin that can be attributed to the improvement in the mechanical interface. The most important increasing of Storage modulus was achieved with 20 % w/w of alkaline modified rachis (856% with respect to pure PU).

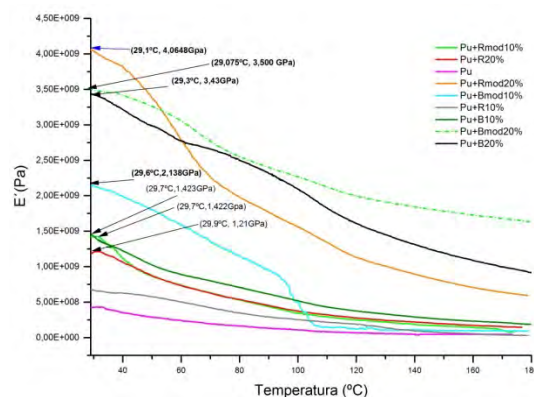


Figure 1. Storage modulus vs temperature of polyurethane composites.

Conclusions

Keratin materials were properly distributed in polyurethane matrix. Natural roughness and hydrophobic behavior of keratin (previously reported)¹ are useful characteristics to achieve a strong interface between natural reinforcement and synthetic matrix. This was reflected in the better performance shown by composites, especially when modified keratin was included. Composites with modified fiber show higher storage modulus. Polyurethane-Keratin system has good thermal stability as clearly observed in DMA performance at higher temperatures.

Acknowledgments: Vicente Amaya Amaya thanks to Consejo Nacional de Ciencia y Tecnología for the financial support through his master degree scholarship.

References

1. Martínez-Hernández AL, Velasco-Santos C, De Icaza M, Castaño VM, Microstructural characterisation of keratin fibres from chicken feathers. Int. J. Environ. Poll. 2005; 23: 162-178.



KERATIN, RENEWABLE MATERIAL IN POLYMER COMPOSITES: NATURAL AND SYNTHETIC MATRICES

Martínez-Hernández A.L.^{1,*}, Flores-Hernández C.G.¹, Jiménez-Cervantes-A. E.¹, Saucedo-Rivalcoba V.¹, Rivera-Armenta J.L.², Velasco-Santos C.¹.

¹División de Estudios de Posgrado e Investigación, Instituto Tecnológico de Querétaro, Av. Tecnológico s/n, 76000, Querétaro, México. *Corresponding author email:almh72@gmail.com; ² Instituto Tecnológico de Ciudad Madero, División de Estudios de Posgrado e Investigación, J. Rosas y J. Urueta, s/n, col. Los Mangos, Ciudad Madero, Tamaulipas, México. ³ Departamento de Posgrado e Investigación, Instituto Tecnológico Superior de Tierra Blanca, Av. Veracruz s/n, Tierra Blanca, Veracruz, México.

Introduction

Keratin is a structural fibrous protein, considered as the main constituent of wool, hair, horns, feathers and other outer coverings of mammals, reptiles and birds. This protein represents an inexhaustible source of non-contaminant materials for possible diverse applications. In the last decade the use of keratin in different forms to elaborate polymer composites has opened a novel and outstanding research field. Several researches have been developed using keratin materials from diverse sources as reinforcements. These have been in the form of fibers, particles, nanoparticles or powder among others. In this work are presented some polymer composites developed in our research group, with keratin materials obtained from chicken feathers in synthetic and natural matrices, the results show the advances obtained in thermomechanical properties and the possibility to incorporate this reinforcement in different polymer matrices.

Experimental Part

Synthesis and Processing

The composites presented were synthesized or processed by different techniques such as: Poly (methyl methacrylate) (PMMA) (in situ polymerization)¹, Polyurethane (PU) (in situ)², Polypropylene (extrusion)³, Polylactic acid (PLA) (3D Printing), Chitosan-Starch (Ch-S)⁴ casting. The keratin was included as reinforcement in different forms as powder, fiber and chopped, obtained from quill and barbs of the feathers.

Characterization

The characterization is focused only to thermomechanical properties of the composites, dynamical mechanical analysis (DMA) was carried out in different ranges of temperatures, depending on the polymer matrices used, all experiments were achieved with 1 Hz, and in tension and 3 point bending modes depending on polymer matrices.

Results and Discussions

Figure 1 and 2 show the results obtained by DMA for the materials obtained by casting with chitosan-starch matrix reinforced with keratin fibers and keratin quill respectively. The complete work

covers the analysis of thermomechanical properties of different polymer matrices reinforced with natural keratin materials matrices.

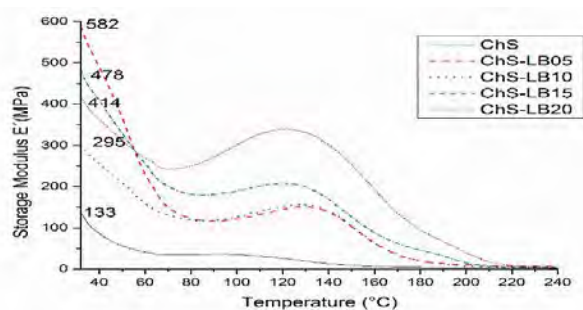


Figure 1. Storage modulus (E') for composites (ChS-LB (large biofiber)), with 5–20 wt % of keratin biofiber included.

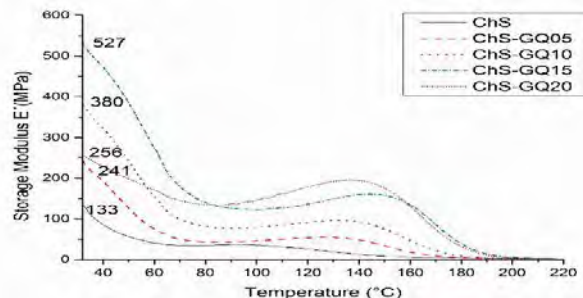


Figure 2. Storage modulus (E') for composites (ChS-GQ), with 5–20 wt% of keratin ground quill included.

Conclusions

The form and structure of keratin material as reinforcement play an important role in the interactions and properties of polymer composites developed with keratin. Feathers are important source of keratin as different reinforcements in synthetic and natural matrices.

References

- Martínez-Hernández A.L. et al., *Composites Part B* 2007, 38, 405.
- Saucedo-Rivalcoba V. et al. *Applied Phys. A.*, 2011, 104, 219
- Jiménez-Cervantes-A. E. *Comp. Materials.* 2015, 49, 275.
- Flores-Hernández et al., *P. Polymers* 2014, 6, 686



DEVELOPMENT OF COMPOSITES BASED ON GREEN POLYMERS: POLYLACTIC ACID MATRIX REINFORCED WITH KERATIN, BY THREE DIMENSION PRINTING.

Ana L. Hernández-Zea¹, Ana L. Martínez-Hernández^{1*}, Cynthia G. Flores-Hernández¹, Armando Almendarez-Camarillo², Carlos Velasco-Santos¹

1. *División de Estudios de Posgrado e Investigación, Instituto Tecnológico de Querétaro, Av. Tecnológico s/n esq. Mariano Escobedo, CP. 76000, Col. Centro, Querétaro, Qro. México.* almh72@gmail.com*
2. *Departamento de Ingeniería Química, Instituto Tecnológico de Celaya, Av. Tecnológico S/n CP. 38010, Celaya, Guanajuato, México.*

Introduction

Actually, substitution of synthetic polymers is one of the most remarkable challenges in materials field, but in spite of all realized efforts this is not an easy target. From this point of view, different studies with natural polymers as matrix or reinforcements has been developed, however combination of both components involving non-synthetic sources has been little explored. This is mainly because of natural polymers have not enough thermal performance to be processed by common techniques, such as: extrusion or injection processes. Emergent methods like electrospinning or three dimension (3D) printing seem to be an important alternative to solve the thermal inconvenience. Thus, this research has been focused to generate answers to these tasks. The synthesis of new composites with two promising non-synthetic polymers: polylactic acid (PLA) as matrix reinforced by keratin fibers and using 3D printing.

Recent studies show that keratin obtained from chicken feathers can be used as reinforcement of chitosan-starch matrix¹, this is a combination of natural polymers that show thermomechanical properties improved by addition of keratin biofibers. Taking into account the results of that previous research, the aim of this work is to develop and characterize the thermal, mechanical and degradation properties from an eco-composite material synthesized by 3D printing based on PLA reinforced with keratin.

Experimental Part

The eco-composite was obtained from PLA matrix and keratin reinforcement (fibers and ground rachis obtained from chicken feather) at 0.5, 0.75 and 1 % concentrations. The synthesis process involved an extrusion of filament that combined PLA and keratin; this was realized at 172 °C. After, the 3D printing was adjusted at 210°C. 3D printing samples were exposed to UV radiation at 254 nm during 30 hours. Afterwards, the samples were exposed to pH 7 aqueous solutions during 20 days for hydrophilic degradation. The dynamic mechanical analysis (DMA) was performed for all samples with a heating rate of 5 °C from room temperature to 100 °C.

Results and Discussions

PLA 3D printing produces a low density material; this characteristic can be configured by the specific parameters needed by the printing software. Figure 1 shows a SEM micrograph of PLA gaps between the layers produced by the equipment. These unfilled spaces reduce density of composites, which can be useful in light weight applications such as: aeronautic or automobile industries.

DMA results show that keratin fiber and quill modify thermomechanical performance of eco-composites, since storage modulus and Tg were increased with keratin reinforcement.

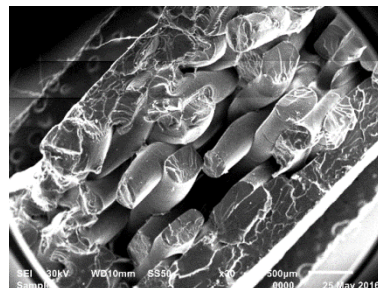


Figure 1. SEM 3D printing matrix PLA.

Conclusions

PLA reinforced with keratin fibers or ground quill is an excellent alternative to novel 3D printing process. Thermomechanical performance was improved with keratin addition.

Acknowledgments: Authors are grateful to Dr. Marina Vega Gonzalez from Centro de Geociencia UNAM for her assistance in analysis by SEM. Ana L. Hernandez-Zea thanks to Consejo Nacional de Ciencia y Tecnología for the financial support through his master degree scholarship. Cynthia G. Flores-Hernandez is also grateful for her postdoctoral support by PRODEP. This research was supported by Tecnológico Nacional de México through the project 5602.15P.

References

1. Flores-Hernández, C.G.; Colín-Cruz, A.; Velasco-Santos, C.; Castaño M., V.; Rivera-Armenta J.L.; Martínez-Hernández A.L.; *Polymer* 2014, 6, 686-705.

THERMAL, MECHANICAL AND MORPHOLOGICAL CHARACTERIZATION OF POLYETHYLENE/CARBON FIBER COMPOSITES PREPARED BY THERMOCOMPRESSSION

Zenen Zepeda Rodríguez¹, Rubén González Núñez¹ Gustavo Castellanos López¹, Milton Vázquez Lepe²

¹Departamento de Ingeniería Química, ²Departamento de Ingeniería de Proyectos, Universidad de Guadalajara, Blvd. M. G. Barragán 1451, 44430, Guadalajara, Jalisco, México. milton.vazquez@cucei.udg.mx

Introduction

Carbon fibers (CF) have been used for a wide of applications including reinforcement in composites due to the high elongation resistance. The aim of this study is the modification and interaction of CFs measuring thermal and mechanical properties and morphology of CF/linear medium density polyethylene (LMDPE) composites using maleic anhydride-grafted-polyethylene (MAPE) as compatibilizer.

Experimental Part

The CF was incorporated with and without previous treatment at 0%, 5%, 10% and 15% wt. in LMDPE. The composites were prepared by thermo-compression using a hydraulic press at 160°C and 200 bars during compression for 10 minutes. After 24 hour of cooling, specimens were obtained for mechanical (Impact, flexure and tension) and thermal analysis (TGA and DSC). The functionalization of the CF and compatibilization with MAPE was analyzed by FT-ATR, while the morphology of the composites was obtained by SEM.

The carbon fiber functionalized with –OH and –COOH (CFF) groups was obtained by the immersion of the CF in a 3:1 HNO₃ and H₂SO₄ solution at 60°C during 30 minutes using magnetic stirring¹, whereas the functionalized and treated with MAPE was obtained by the addition of the CFF into a solution of 3% MAPE/Xylene at room temperature and constant stirring for 2 hours.

Results and discussion

From Figure 1 we observe a linear decay trend of the impact resistance and the fiber content without treatment in the polymeric matrix, and a lower stiffness, which results in a brittle material. In the tensile Young modulus, we see a linear increase with the amount of fiber remarking that 15% wt. CF composites has outstanding tensile modulus (330%), this behavior is due to the matrix reinforcement. The presence and orientation of longer fibers as the good dispersion, and fiber-polymer matrix adhesion was corroborated by SEM² (Figure 2). The flexure modulus had an increment (30%) due to the addition of fiber, in contrast with the impact resistance, suggests that decrease the toughness of the polymeric matrix. The composites with greater flexion module and impact resistance is which contains 10% wt. of CF suggesting with a greater quantity, can occur an agglomeration leading to a

bad interfacial bonding between the untreated filler and the matrix.³ We expect that the proposed treatment of the CF will improve the bonding interaction that results in better mechanical and thermal properties.

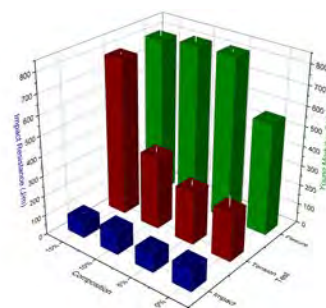


Figure 1. Mechanical properties of LMDPE/CF composites.

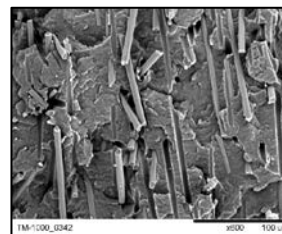


Figure 2. Micrograph of 10% wt. CF in LMDPE without MAPE.

Conclusions

The addition of CF induced modifications in the mechanical properties, and morphology of LMDPE. Such modification is given by the length and dispersion of the fibers in the polymeric matrix, all this, corroborated by SEM and thermal analysis.

Acknowledgements: To the National Council of Science and Technology (CONACYT).

References

- Zhang G, Sun S, Yang D, Dodelet J-P, Sacher E. Carbon 46(2) 196-205 (2008).
- Savas LA, Tayfun U, Dogan M. Composites Part B Eng. 99, 188-195 (2016).
- Chunzheng P. Surface Interface Analysis. 47(3), 357-361 (2015).

MULTIFUNCTIONAL BIONANOCOMPOSITES WITH SHAPE MEMORY EFFECT

 Laura Peponi¹, Valentina Sessini^{1,2}, Marina P. Arrieta¹, Daniel López¹

1. Instituto de Ciencia y Tecnología de Polímeros, ICTP-CSIC, calle Juan de la Cierva 3, 28006 Madrid, Spain
lpeponi@ictp.csic.es
2. Dipartimento di Ingegneria Civile e Ambientale, University of Perugia, Strada di Pentima 4, 05100 Terni, Italy

Introduction

Shape-memory polymers (SMP) are a class of smart materials able to change reversibly their shape in response to external stimuli such as temperature, pH, electrical or magnetic fields, among others¹. Among the SMP, those based on biocompatible and/or biodegradable polymers play an important role in applications in the biomedical sector due to their biocompatibility, biodegradability, and appropriate mechanical properties in addition to their multifunctionality. In order to offer shape-memory behaviour, polymers have to present permanent domains formed by chemically or physically cross-linked structures, and switching domains able to respond to the external stimulus. In this work, we propose to design different shape memory systems, based on polyester-urethanes and blends of PLA and PCL, as well as their bionanocomposites reinforced with synthesized cellulose nanocrystals. Also nanocomposites based on EVA-TPS blends reinforced with bentonite.

Experimental Part

Polyester-urethanes, PU; based on block copolymer of PLLA and PCL, have been successfully obtained as well as blends of PLA and PCL. At the same time blends of EVA and TPS have been processed. Finally, nanocomposites have been obtained by adding cellulose nanocrystals and bentonite to the polymeric matrix. Cellulose nanocrystals have been synthesized by acid hydrolysis and functionalized with PLLA chains in order to incorporate in the PU matrix. To study the crystalline structure of each material, differential scanning calorimetry (DSC) was performed in a Mettler Toledo 822e instrument. Mechanical properties and shape-memory characterization were carried out using an Instron, Universal Testing Machine.

Results and Discussions

Firstly, a correlation between the molecular weight of the blocks and their amorphous/crystalline structures has been verified¹. Moreover, the influence of the presence of each block in their crystalline nature has also been studied in order to obtain PU with both crystalline blocks. At the same time their mechanical response has been obtained. Regarding the shape-memory behaviour, we use the PCL as “switch phase” while PLLA provides the “fixity phase” and the TmPCL is the switching temperature (See diagram in Figure 1).

During the thermo-mechanical programming test, the test specimen, clamped into the tensile tester, was heated at a

maximum temperature of 40 °C and kept for 10 minutes in order to allow relaxation of the polymer chains.

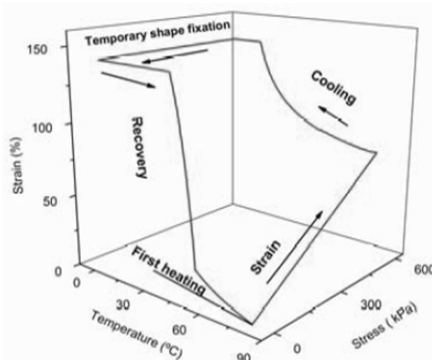


Figure 1. Classical thermo-mechanical cycle to study the shape memory behaviour.

Then, the specimen was stretched to a certain elongation by applying a constant deformation stress. The designed polyurethane shows shape memory behavior at a temperature of about 40 °C, useful to be used for future application in the biomedical sector. At the same time the reinforced PU show shape-memory properties as well as the PLA/PCL blends, even if at different temperature. Finally, EVA/TPS blends showed shape memory behaviour in both temperature and humidity.

Conclusions

The designed polyurethane shows shape memory behavior at about 40 °C, useful to be used for future applications in the biomedical sector. Furthermore, in order to obtain biodegradable nanocomposites, cellulose nanocrystals have been synthesized, functionalized and incorporated into the PU matrix; affecting the final properties of the bio-nanocomposites in terms of crystallinity, mechanical properties and consequently, their shape memory properties.

Acknowledgment: We are indebted to the MINECO for the MAT2013-48059-C2-1-R. L.P. acknowledges MINECO for the “Ramon y Cajal” (RYC-2014-15595) contract.

References

1. Peponi, L, Navarro-Baena, I, Báez, JE, Kenny, JM, Marcos-Fernández, A. *Polymer* 2012; 53(21), 4561.
2. Peponi, L, Navarro-Baena, Kenny, JM. *Cellulose*, 2014, 21(6), 4231.

SÍNTESIS Y CARACTERIZACIÓN DE POLIURETANOS ALIFÁTICOS FOTO-ENTRECRUZABLES BASADOS EN POLICAPROLACTONA

Ángel Marcos-Fernández¹, Rubén Seoane Rivero², Koldo Gondra², Pilar Bilbao²

1. Instituto de Ciencia y Tecnología de Polímeros (CSIC), Juan de la Cierva 3, 28006 Madrid, España, amarcos@ictp.csic.es
2. GAIKER-IK4 Centro Tecnológico, Parque Tecnológico Edificio 202, 48170 Zamudio, España

Introducción

Recientemente se han dedicado muchos esfuerzos al desarrollo de polímeros autorreparables, que son capaces de reparar de forma autónoma un daño sufrido.¹ Existen muchos estudios en los que se ha empleado luz como desencadenante de la autorreparación. La ventaja más importante de emplear luz es que los procesos pueden pararse o continuarse con solo encender o apagar la luz. Las moléculas de cumarina pueden foto-dimerizar cuando se irradian a longitud de onda >300 nm para dar lugar a un ciclobutano, y este ciclobutano puede romperse para restituir las moléculas originales de cumarina cuando se irradia a 254 nm.² En este trabajo se presentan los resultados obtenidos para unos poliuretanos lineales segmentados basados en policaprolactona en los que los grupos cumarina se sitúan en los segmentos blandos, en los segmentos duros o en ambos.

Parte Experimental

Se sintetizó un diol derivado de cumarina y se empleó para preparar una policaprolactona diol.³ A partir de estos dos compuestos, el diisocianato de isoforona, policaprolactona diol de 527 g·mol⁻¹ y butanodiol, se prepararon poliuretanos con un 10% en peso de cumarina en el segmento blando, en el segmento duro y distribuido entre ambos. Se estudió la reversibilidad de la foto-reacción de la cumarina por UV y Raman y las propiedades físicas de los poliuretanos foto-dimerizados (propiedades térmicas y mecánicas).

Resultados y Discusión

Se logró preparar una policaprolactona diol con cumarina y poliuretanos con cumarina dentro del segmento blando. Este tipo de materiales es la primera vez que se describen. Los poliuretanos mostraron una morfología con una sola fase homogénea y una sola T_g. Los materiales pudieron foto-dimerizarse y foto-escindirse varios ciclos con cierta pérdida de eficacia. Las propiedades mecánicas de los poliuretanos sin irradiar dependieron principalmente del contenido de segmento duro. Todos los materiales mejoraron sustancialmente sus propiedades mecánicas tras el entrecruzamiento producido por la irradiación, siendo especialmente llamativo el caso del poliuretano con la cumarina dentro del segmento blando, que pasó de ser un material blando sin apenas propiedades mecánicas (< 1 MPa) a un material elastomérico blando muy tenaz (> 45 MPa) como se ve en la Figura 1.

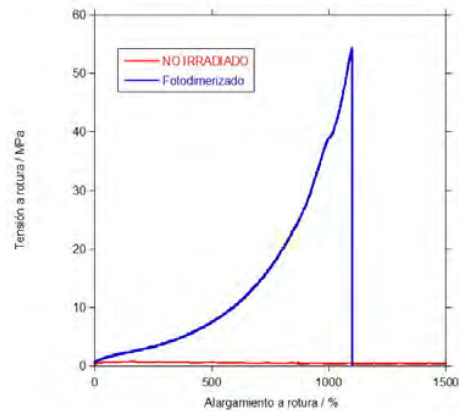


Figura 1. Curvas tensión-deformación para el poliuretano con la cumarina en el segmento blando antes y después de fotodimerizar

Conclusiones

Los poliuretanos preparados mostraron fotorreversibilidad con una pérdida de eficacia en la fotodimerización y en la fotoescisión con el aumento del número de ciclos. El entrecruzamiento producido por la dimerización mejoró enormemente las propiedades mecánicas de los poliuretanos, obteniéndose materiales elastoméricos muy tenaces.

Agradecimientos: Los autores agradecen al Ministerio de Economía y competitividad por el apoyo económico de este trabajo dentro del Plan Nacional de I+D+i, proyectos MAT2013-48059-C2 y MAT2014-52644-R, y proyecto INNFACTO IPT-2012-0324-420000. El trabajo ha recibido también el apoyo de la Comunidad de Madrid, proyecto S2013/MIT-2862, y de la Fundación Centros Tecnológicos-Iñaki Goenaga.

Referencias

1. W. Binder, "Self-Healing Polymers: From Principles to Applications" (Wiley-VCH Verlag, 2013).
2. S.R. Trenor, A.R. Shultz, B.J. Love, T.E. Long, *Chem. Rev.*, **2004**, 104, 3059-3077.
3. R. Seoane Rivero, P. Bilbao Solaguren, K. Gondra Zubieta, A. González-Jiménez, J.L. Valentín, A. Marcos-Fernández, *Eur. Polym. J.*, **2016**, 76, 245-253.



KINETIC STUDY AND MATHEMATICAL MODELING IN ATRP

Iván Zapata-González¹, Enrique Saldívar-Guerra², Robin A. Hutchinson³

1. CONACYT Research Fellow, Centro de Graduados e Investigación en Química, Instituto Tecnológico de Tijuana, A.P. 1166, 22000 Tijuana, B.C., México, idejzapatago@conacyt.mx, ivan.zapata@tectijuana.edu.mx
2. Centro de Investigación en Química Aplicada (CIQA) Blvd. Enrique Reyna 140, Saltillo, Coahuila, 25253, México
3. Department of Chemical Engineering, Queen's University, Kingston, ON K7L 3N6, Canada

Introduction

As well known, Atom Transfer Radical Polymerization is one of the most important techniques involving molecular control. In the beginning, a high amount of transition metal was required in the ATRP techniques, such as normal and SR&NI, in order to keep a high dormant concentration and to decrease the persistent radical effect. Recently, the evolution of new techniques, such as Initiators for Continuous Activation Regeneration (ICAR) and Activators Regenerated by Electron Transfer (ARGET), leads to use only ppm of transition metal, and therefore the polymers obtained can be used as medical devices and food products.

Due to the complexity of these systems the estimation of kinetic rate constants via experimental procedure is so difficult, being the modeling a better way to face this problem and to understand the kinetic behavior. Recently, Reduced Stiffness by Quasy State Approximation methodology has been used to modeling the kinetic in NMP, RAFT and traditional radical polymerization.¹ Results show new mechanistic insights do not reported before using another methodologies or commercial software.²

In this work we use RSQSSA methodology in ATRP techniques (normal, ICAR and ARGET) in order to understand the kinetic and predict the better operation conditions.

Experimental Part

The mass balance equations and moment equations are derived, resulting in an ODE system, assuming the QSSA as valid the system is converted to algebraic-differential system.

As explicit expressions for first radicals (R^*) and total living polymer (μ) will be needed, these are obtained by making the time derivatives equal to zero for the Normal and ICAR ATRP version. After some algebraic manipulations, explicit equations for the concentration of R^* and μ can be obtained the general form:

$$[R^*] = \frac{-b_1 + \{b_1^2 - 4a_1c_1\}^{\frac{1}{2}}}{2a_1} \quad \mu_0 = \frac{-b_2 + \{b_2^2 - 4a_2c_2\}^{\frac{1}{2}}}{2a_2}$$

The parameters a_i , b_i and c_i are shown in Zapata et al.³

Results and Discussions

The dynamic information lost using the RSQSSA is negligible and the QSSA holds true for the techniques practically in the full range of conversion. Additionally, ICAR polymerization is a perfect candidate to semibatch operations, in which initiator is fed on demand. ARGET-ATRP polymerization is strongly affected by a slow initiation of the alkyl halide, giving rise to a tail of low molecular weight emerged in the MWD due to the delayed formation of the living chains, Figure 1.

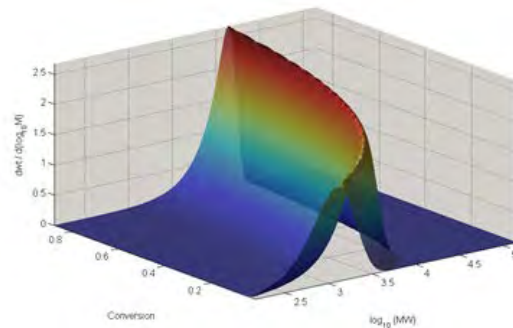


Figure 1. Simulation of the MWD in ARGET-ATRP technique for the polymerization of butyl methyl acrylate (BMA) using $\text{Sn}(\text{EH})_2$ as reducing agent, ethyl 2-bromoisobutyrate (EBiB) as ATRP initiator, and $\text{CuBr}_2/\text{TPMA}$ (TPMA: tris[(2-pyridyl)methyl]amine) as deactivator.

Conclusions

Acknowledgment: IZG gratefully acknowledges the support of CONACYT, (Cátedras para Jóvenes Investigadores).

References

1. Saldívar-Guerra, et al. *Macromol. Theory Simul.* 2010, 19, 151.
2. Zapata-González, et al. *Macromol. Theory Simul.* 2011, 20, 370.
3. Zapata-González, et al. *Aiche Journal*, 2016.



FREE-RADICAL POLYMERIZATION IN A MULTIZONE AUTOCLAVE REACTOR

Ramiro Infante Martínez¹, Enrique Saldívar Guerra¹, Luis Villarreal Cárdenas¹

1. Centro de Investigación en Química Aplicada, Blvd. Enrique Reyna 140 CP 25294, Saltillo, Coahuila México
ramiro.infante@ciqa.edu.mx

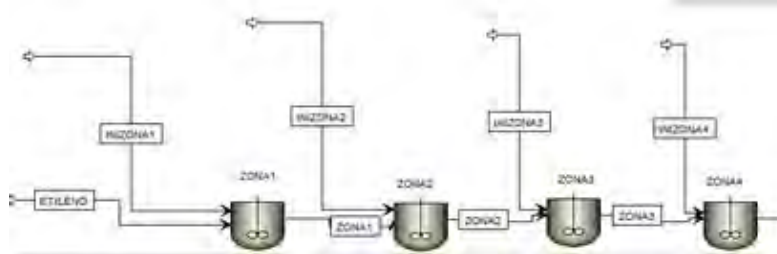


Figure 1. The multizone reactor modeled as a series of CSTR (Continuous Stirred Tank Reactors)

Introduction

This work describes the development of a model for the ethylene polymerization by conventional free radical mechanism⁽¹⁾. The reactor is of the stirred tank type in continuous operation. It has several zones connected in series and operating at different temperature. The implementation of the model is made in three simulation platforms, two of them with commercial software specialized in polymerization processes⁽²⁾ (ASPEN and POLYRED) and another using spreadsheet (EXCEL). The scheme for the process as is entered in the ASPEN environment is depicted in figure 1 for a 4 zone reactor.

Experimental-Theoretical Part

The kinetic mechanism included the conventional steps for the free-radical polymerization. This mechanism was applied to mass and energy balances for a complete mixed reactor composed of several zones as illustrated in fig. 1. The balances were applied in dynamic mode in order to study the dynamic behavior of the reactor. We report the development of a simplified model suitable for its solution in a sequential way³

Results and Discussions

Data on operation of two commercial plants were used for adjustment of parameters of the model. We execute several simulation exercises that demonstrate the utility of these tools. For one part, the model can be used for the design of new products by testing different profiles of temperature as well as different pressures. For another part, the model can also be used to: (i) training of operators; (ii) test of change of product strategies; (iii) new control strategies tests. It is noted the greatest ease of use that you have with the model done in spreadsheet, since modifying only a few cells get immediate results in tabular form and with graphs of the main process variables: temperatures of the different areas, molecular weight of each zone as well as the molecular weight of the final product. In figure 2 we show the molecular weight distribution obtained.

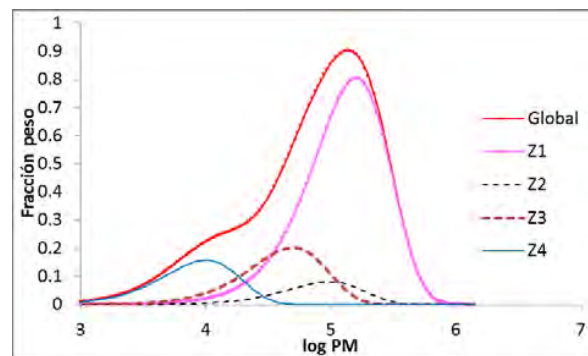


Figure 2. Instantaneous Molecular Weight Distribution produced in each zone of the reactor as well as the accumulated at the outlet

Conclusions

The strategy of modeling the ethylene polymerization through software tools readily available shows that it can be obtained robust models with applicability to plant engineering, control engineering, optimization process and personal training

References

1. W.-M. Chan, P. E. Gloor, A. E. Hamielec, Modelling and simulation of high pressure industrial autoclave polyethylene reactor, *AIChE J.* 1993, 39, 111. aster, J.; Fink, H. P.; Pinnow, M. *Composites* 2006, 37, Part A, 1796.
2. P. D. Iedema, M. Wulkow, H. C. J. Hoefsloot, Modeling Molecular Weight and Degree of Branching Distribution of Low-Density Polyethylene, *Macromolecules* 2000, 33, 7173
3. Saldívar-Guerra E., A Ordaz-Quintero, R. Infante-Martínez, J. Herrera-Ordóñez, L. Villarreal Cárdenas, D. Ramírez-Wong, E. Rivera-Rodríguez, R. Flores-Flores, L. Miramontes-Vidal, Some Factors Affecting the Molecular Weight Distribution (MWD) in Low Density Polyethylene Multizone Autoclave Polymerization Reactors, *Macromolecular Reaction Engineering*, 2015, DOI: 10.1002/mren.201500030



DETERMINATION OF MOLECULAR WEIGHT DISTRIBUTIONS OF DIFFERENT TYPES OF POLYETHYLENE FROM A SIMPLE REPTATION MODEL

Miguel A. Fernández Estrada, Javier Gudiño Rivera, Rubén Saldívar Guerrero, Rubén H. López Bañuelos

Centro de Investigación en Química Aplicada, Blvd. Enrique Reyna Herosillo No. 140, Colonia San José de los Cerritos, Saltillo, Coah.

C.P. 25294, javier.gudino@ciqa.edu.mx

Introduction

The physical and mechanical properties of a polymer, also its processability, depend on their average molecular weight and molecular weight distributions (MWD). Due to the relationship between viscoelastic properties to molecular motions, some mathematical models has been developed to obtain the MWD of polymers by deconvolution of dynamic rheological measurements, from the terminal and plateau zones¹. In this work we present the results of the application of a simple reptation model to the calculation of Mn, Mw, and MWD of five different grades of polydisperse polyethylenes (PE), and their comparison with results obtained experimentally by GPC.

Experimental Part

Five PE samples with different polydispersity indexes (PDI) were analyzed. Mw and Mn were measured in a Gel Permeation chromatographer using 1, 2 4-Trichlorobenzene as solvent. The dynamic storage and loss moduli of the samples were measured on an oscillatory rheometer at frequencies from 0.1 to 628 rad/s. All the measurements were performed into the linear viscoelastic region with a strain of 10%, and reduced to a single master curve at 190 °C.

Calculations

The plateau modulus (G_N^0) was calculated by the integration of the loss modulus in the terminal zone. To convert the weight-fraction differential function ($D(\tau)$) to a scale of molecular weight (M) we use the next equation².

$$\tau = \lambda M^\beta \quad (1)$$

Where τ is the relaxation time, λ and β are constants, and thus a normalized MWD is obtained. Mw was calculated with the next function³.

$$\eta_0 = 5.8 * 10^{-14} M_W^{3.41} \quad (2)$$

Results and Discussions

Fig. 1 shows the comparison of the calculated and experimental MWD of low and linear low density polyethylenes, and Table 1 summarizes the Mw and Mn of each sample. Due to the high PDI of the samples our model has a better prediction of Mw than Mn.

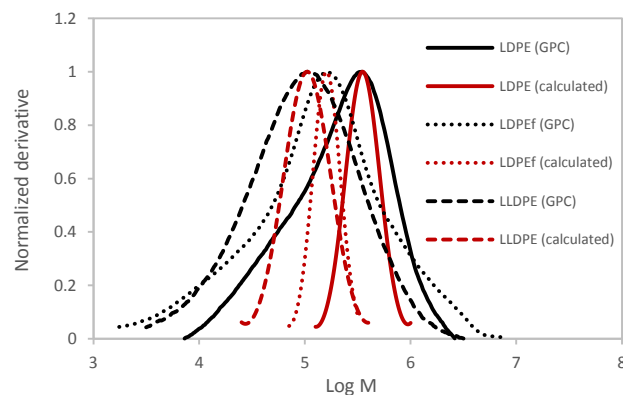


Figure 1. Calculated and experimental MWD of LDPE and LLDPE.

Table 1. Comparison of experimental and theoretical Mn and Mw.

SAMPLE	GPC DATA			CALCULATED FROM RHEOLOGICAL DATA		
	Mn	Mw	PDI	Mn	Mw	PDI
LDPE	40 177	127 362	3.17	45 990	144 338	3.13
LDPE-f	38 519	334 350	8.68	48 666	341 408	7.01
LLDPE	33 420	94 380	2.82	47 064	100 982	2.14
HDPE-f	31 516	200 408	6.35	59 039	196 716	3.33
HDPE	12 555	72 824	5.80	46 610	77 702	1.66

Conclusions

Comparing the experimental results obtained by GPC for five samples of PE with the theoretical results showed that the model has better prediction for low and linear low density than high density PE because these polymers have broader MWD.

Acknowledgment: To Dr. César A. García Franco for his valuable comments about this research.

References

1. S. Wu, *Macromolecules*, 1985, 18, 2023.
2. S. Wu, *Polym. Eng. Sci.*, 1985, 25, 2, 122.
3. R.G. Larson, *Macromolecules*, 2001, 34, 4556.



Enzymatic hydrolysis of the galactomannan from *Delonix regia* seed effect on solubility and viscosity

Wilbert Rodríguez Canto¹, Manuel Aguilar Vega¹, Luis Chel Guerrero²

1. Centro de investigación Científica de Yucatán A.C., calle 43 No 130, col. Chuburná de Hidalgo, C.P. 97200, Mérida, México. wilbert.rodriguez@cicy.mx
2. Facultad de Ingeniería Química, Universidad Autónoma de Yucatán, Periférico Norte Kilómetro 33.5, Tablaje Catastral 13615, Col. Chuburná de Hidalgo Inn, C.P. 97203. Mérida., México.

Introduction

Galactomannans are natural polymers constituted for β -1,4-D-mannopyranosyl backbone with D-galactosyl residue α linked to mannose C-6 sites.¹ It is commonly found in the endosperm of legume seeds, the most important galactomannans from the industrial point of view are guar, locust and tara gum. Galactomannans are widely used due to their rheological properties as thickening and stabilizing agents. They also form gels when they interact with other polysaccharides. These properties depend on their molecular weight, mannose:galactose ratio and distribution of galactose along the mannose backbone. *Delonix regia* seed has a galactomannan (DRG) with a molecular weight of 2.6×10^5 Da.², it forms dispersions with high viscosity that could have applications on the food, pharmaceutical and others industries³. It has a disadvantage as compared to guar galactomannan, since it solubilizes at higher temperature due to the distribution of mannose:galactose ratio (4:1) in the backbone which is different from the one presented by guar (2:1). Thus the use of a specific cleavage enzyme, a β -mannanase enzyme it is possible to cleave the linkage between unsubstituted mannoses and decrease the packing between chains. The enzymatic cleave is expected to improve the solubility of DRG.

Experimental Part

500 g *Delonix regia* seeds were stirred in 3.5 L of water for 6 h at 80°C. The endosperm was manually extracted from the hydrated seeds and it was crushed with a blender in a 1:2 volume ratio hydrated endosperm:water. The resulting paste was stirred for 30 min at 60°C, mesh filtrated (1 mm) and centrifuged at 4500 g; then, it was precipitated with 1:1 ethanol (96%) and dried at 60°C for 12 h. The dried material was reduced to powder in a blender with a mesh #20. DRG in water, 1% (w/v), was hydrolyzed with an endo β -mannanase in a sodium phosphate 0.1 M buffer solution with pH 7, at 1, 4.5 and 10 nkat/g of enzyme concentration, and a hydrolysis times of 30, 60 and 90 minutes, to stop the hydrolysis it was heated at 90°C for 20 min and precipitated in ethanol (1.5:1 volume) and the precipitated was dried in a convection oven. Shear viscosity flow curves were measured in 3% (w/v), DRG and hydrolysates in water, with a TA 2000 rheometer using a 4mm ϕ and 2° cone and plate geometry, at shear rates from 0.1 to 1000 1/s. Galactose:Mannose ratio was determined with a Zorbax carbohydrate HPLC column with water:acetonitrile 25:75 ratio as the mobile phase, using a RI detector and mannose and galactose standards. For solubility determination, 0.5% (w/v) DRG

in water was stirred for 2 h at 25 and 60°C, and the soluble and insoluble phases were separated by centrifugation at 40,000 g for 10 min. The dry residues were weighted. Hydrolysates were characterized by TGA, DSC and DRX.

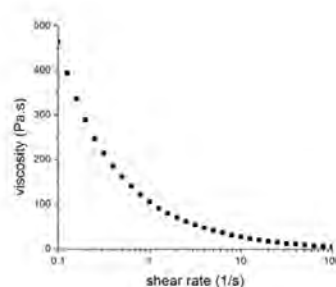


Figure 1. Shear thinning flow curve of *Delonix regia* galactomannan at 3% (w/v).

Results and Discussions

DRG Extraction yield was $11.5\% \pm 0.66$ with respect to seed weight. Shear thinning behavior as observed in Fig. 1 for 3% (w/v) concentration DRG is obtained for a mannose:galactose composition (1:3.8). Hydrolysates, mannose:galactose ratio, solubility and characterization are in progress. Hydrolysis should increase solubility at 25°C maintaining shear thinning behavior. Hydrolysis is also expected to decrease mannose:galactose ratio by decreasing mannose concentration.

Conclusions

Enzymatic hydrolysis of *Delonix regia* galactomannan, DRG, increase its solubility by changing the mannose:galactose ratio. As a result, shear viscosity decreases due to a decrease in molecular weight, but it is expected to allow the control of their thickening properties.

Acknowledgment: CONACYT by scholarship with CVU #483674

References

1. Mikkonen, K. S., Rita, H., Helén, H., Talja, R. A., Hyvönen, L., & Tenkanen, M. *Biomacromolecules* 2007, 8, 3198.
2. Tamaki, Y., Teruya, T., & Tako, M. *Biosci. Biotechnol. Biochem.* 2010, 74, 1110.
3. Srivastava, M., & Kapoor, V. P. *Chemistry and Biodiversity.* 2005, 2, 295



SYNTHESIS OF POLY(BUTHYL METHACRYLATE) NANOPARTICLES IN NANOEMULSIONS PREPARED BY PHASE INVERSION TEMPERATURE TECHNIQUE

Arturo Gómez¹, A Flores¹., Lourdes A. Pérez Carrillo¹, Martín Rabelero¹, Rosaura Hernández², Abraham G. Alvarado².

1. Departamento de Ingeniería Química, Universidad de Guadalajara, CUCEI, Blvd. Marcelino García Barragán 1451 col. Olímpica, 44430, Guadalajara, Jal. México.
2. Departamento de Ingeniería Mecánica Eléctrica, Universidad de Guadalajara, CUCEI, Blvd. Marcelino García Barragán 1451 col. Olímpica, 44430, Guadalajara, Jal. México. mrabelero@hotmail.com

Introduction

Nanoemulsions, also called miniemulsions and ultrafine emulsions, are kinetically stable emulsions formed by emulsified droplets much smaller than those in an emulsion¹. Subjecting an emulsion to high-shear fields is the common technique to produce nanoemulsions¹. However, recently, low energy methods have been developed, one is the so called *phase-inversion method*² and the other is based in changes in composition at constant temperature during the emulsification process¹. Polymerization in O/W nanoemulsions also allows the synthesis of nanoparticles dispersed in an aqueous medium with fast reaction rates^{3,4}. When the formulation is adequate, nanoemulsions droplets act as templates of the produced polymer particles, that is, about the same droplet size is preserved. This situation is met when the diffusion of monomer during the reaction is reduced, which is usually accomplished by the addition of a hydrotope or costabilizer⁴. In this work, the phase diagram for water/butyl methacrylate/Brij 56 using squalane as cosurfactant was prepared and polymerization kinetics, evolution of particle diameter along the reaction, molecular weight and glass transition temperature was studied as a function of initiator concentration.

Experimental Part

Nanoemulsions were prepared by rapidly quenching one-phase microemulsions obtained at higher temperatures. Nanoemulsion stability at 25 °C was followed by measuring particle size as a function of time in a Malvern Zetasizer Nano-Z90. Polymerizations were carried out in a 200-mL two-mouth glass reactor. The selected compositions were prepared in the reactor, which was immersed in a water bath at which the one-phase microemulsion forms. Once the microemulsion formed, the reactor was extracted from the high-temperature water bath and immersed into another one a 20 °C with rapid agitation and with N₂ bubbling to eliminate the dissolved oxygen. Separately, aqueous solutions of each of the par-redox initiators were made and added to the reactor once the nanoemulsion developed.

Results and Discussions

Figure 3 depicts conversion as a function of time for the nanoemulsions containing 1% of initiator concentration. Reactions are carried out very fast (near 100% conversion in 3 minutes) and, polymerization rate depicts only two rate intervals with a maximum at about 65 seconds. Notice that, contrary to

batch emulsion polymerization that depicts three intervals, here only two are observed, similar to microemulsion polymerization⁵. Also, stable latex was obtained with particle size of 38 nm.

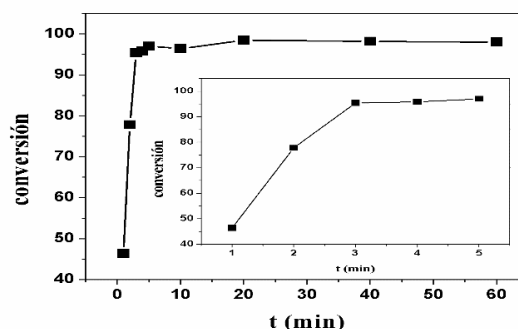


Figure 1. Conversion versus time for nanoemulsion polymerization of 12% brij 56, using an $o/(w + o)$ weight ratio of 0.2, being o the mixture of BuMa and Sq. and BuMa/SQ = 95/5 by weight.

Conclusions

The reactions were fast, reaching conversions of 90% within 3 minutes after the start of polymerization, for all the employed initiator concentrations. The latex particles obtained had size in the order of 35 to 40 nm (depending of initiator concentration) and particle size decreased as initiator concentration increased. Molar masses and polydispersity of the polymers obtained decreased as initiator concentration increased. The high values obtained indicate that chain transfer to monomer is the main termination mechanism

References

1. Solans C., Izquierdo P., Nolla J., Azemar N., Garcia-Celma M. J. (2005) *Curr. Opin. Colloid In.*, 10 (3-4): 102-110.
2. Kunieda, H., Shinoda, K. (1985) *J. Colloid Interface Sci.*, 107 (1): 107-121.
3. Sudol, E.D., El-Aasser, M.S., in *Emulsion Polymerization and Emulsion Polymers*, P.A. Lovel, P.A.; M.S. El-Aasser (editors), Wiley, New York (1997), Chap. 20, 699-741
4. Chern, C.-S., *Principles and Applications of Emulsion Polymerization*, Wiley, Hoboken (2008).
5. Puig, J.E., in *The Polymeric Materials Encyclopedia. Synthesis, Properties and Applications*, Vol. 6, J.C. Salamone (Ed.), CRC Press, Boca Ratón (1996), pp.4333-4341.



ASSOCIATION OF CHEMICAL MODIFICATIONS IN XANTHAN PRUNI

Paula Michele Abentroht Klaic^{1,3}, Yasser da Siveira Krüger², Claire Tondo Vendruscolo³, Ligia Furlan³, Patrícia Diaz Oliveira³, Angelita da Silveira Moreira³---

1. Instituto Federal de Educação Ciência e Tecnologia do Rio Grande do Sul, Campus Farroupilha, rua São Vicente, 785, CEP 95180-000, Farroupilha, RS, Brazil. paula.klaic@iffarroupilha.edu.
2. Instituto Federal de Educação Ciência e Tecnologia, Campus Pelotas, Praça Vinte de Setembro, 455, CEP 96.015-360, Pelotas, RS, Brazil
3. Universidade federal de Pelotas, Campus Universitário, Caixa Postal 354, CEP 96010-900 Pelotas, RS, Brazil

Introduction

Chemical modifications of a natural polysaccharide are an alternative for production of polymers with improved and new properties and applications. Several chemical modifications have been applied to xanthan, a biopolymer with great industrial use, mainly in food¹ and oil extraction², aiming to enhance rheological and thermal characteristics. Deacetylation and ion Exchange are preconized mainly to increase viscosity, whereas crosslinking to arise viscosity, viscoelasticity and thermal properties. Commercial xanthans are produced by *Xanthomonas campestris* pv *campestris*, but other species as *X. arboricola* pv *pruni* can produce efficiently xanthan with equivalent or better quality⁴. This work aimed to evaluate the combination of chemicals modification in the non-commercial polymer xanthan pruni.

Experimental Part

We use pruni xanthan produced by strain 106 de *X. arboricola* pv *pruni* at pH 7, as described previously³, named to as Xp 106 pH7, with acetyl content classified as higher ($4,09\% \pm 0,04$); various reagents, all of analytical grade; amberlite strong cation exchanges strongly acidic IR 120 H⁺ (Sigma-Aldrich®). All modifications were made in previously selected conditions. The deacetylation of natural pruni xanthan was in homogeneous basic medium, using 0,5% (w/v) polymer solution added with 0,01 mol L⁻¹ of NaOH, at 45°C for 3h. After that, recovery of xanthan was made by precipitation in 96% ethanol, dried at 55 °C and grinding², naming it as Xp 106 pH7 DESA. The cross-linking was made in natural and deacetylated xanthan, in 0,5% (w/v) solution with 1% (v:v) glutaraldehyde, for 2h at 45°C. After recovery, xanthans were named as Xp 106 pH7 RET and Xp 106 pH7 DESA RET. Lastly, natural, deacetylated and deacetylated crosslinked xanthans were subjected to ion exchange. Samples were hydrates (1:99 (w/v)) and agitated for 2h at room temperature and subjected to ion exchange. In free salt solution were added 5% of Na⁺, in relation to content of xanthan, by adding of NaCl⁵, and the polymer recovered as previously. These xanthan received next to its name termination TI 5% Na. Xanthan solutions 1% (w/v) viscosity were measured in rheometer (model RS 150, Haake), in the controlled rate mode, at 25°C, using cone-and-plate geometry (C35/1°; 0.052mm gap), during 400 s, with 100 acquisition points.

Results and Discussions

With the exception of the cross-linking of natural xanthan, the other changes, alone or combined, increased the viscosity of xanthan pruni. Ion exchange was more effective when performed after deacetylation. The best results, however, were obtained with the combination of deacetylation and cross-linking, which increased by more than 10 times the viscosity.

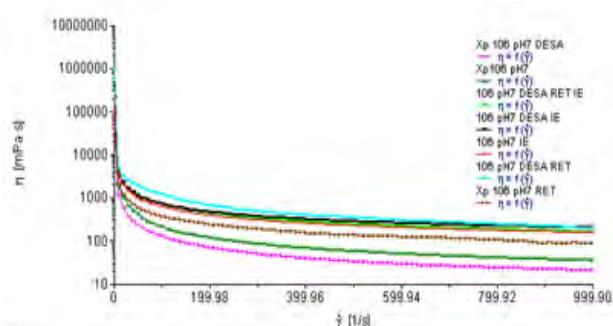


Figure 1. Viscosity curves (mPa.s) versus shear stress (0.01-1000s⁻¹) at 25°C of aqueous solutions (1% w/v) of natural xanthan pruni and chemically modified.

Conclusions

Deacetylation as single chemical modification on xanthan pruni is not recommended; crosslinking without previous deacetylation is not efficient to viscosity increasing; the combination between deacetylation and crosslinking in xanthan pruni result in a very viscous material; the ion exchange is recommended only to natural xanthan pruni.

Acknowledgment: The authors are grateful to CNPq for financial support.

References

1. Born, K.; Langendorff, V.; Boulenger, P. (2002). Xanthan. In A. Steinbüchel; E. J. Vandamme; S. de Baets (Eds.), *Biopolymers* (Vol. 5, pp. 259e291). Weinheim: Wiley-VCH.
2. Navarrete; Seheult; Coffey, 2000
3. Universidade Federal de Pelotas. WO/2006/047845, 2005.
4. Moreira, A. da S.; Vendruscolo, J. L. S.; GilTunes, C.; Vendruscolo, C. T. *Food Hydrocolloids* 2001, 15, 469.
5. Klaic, P. M. A.; Vendruscolo, C. T.; Furlan, L.; Moreira, A. da S. *Food Hydrocolloids* 2016, 56, 118-126.



CONTROLLED ACRYLIC ACID POLYMERIZATION BY COMBINING REDOX INITIATION AND CHAIN TRANSFER

Gerardo Cáceres Montenegro^{1,2}, Carolina G. Gutierrez², Roque J. Minari^{2,3}, Jorge R. Vega^{2,4}, Luis M. Gugliotta^{2,3}

1. Departamento de Química Orgánica, Universidad de Panamá, Ciudad Universitaria, Vía Simón Bolívar, Panamá.
2. INTEC (CONICET – Universidad Nacional del Litoral) Güemes 3450 (3000), Santa Fe, Argentina, lgug@intec.unl.edu.ar
3. Facultad de Ingeniería Química (Universidad Nacional del Litoral), Santiago del Estero 2829 (3000), Santa Fe, Argentina.
4. Facultad Regional Santa Fe (Universidad Tecnológica Nacional), Lavaisse 610 (3000) Santa Fe, Argentina.

Introduction

Polyacrylic acid (PAA) of low molar mass (MM) ($\approx 10^4$ g.mol⁻¹)¹ is mainly obtained by polymerization of acrylic acid (AA) in aqueous solution using thermal initiators and a chain transfer agent (CTA)². In this work, a "semibatch" AA polymerization at 45 °C is investigated to produce low MM PAA, by using redox initiators with an excess of reducing agent (RA), which also acts as CTA. Experiments were carried out at constant feed rates of AA, oxidizing agent and RA. A mathematical model was developed to estimate main reaction variables, with the following assumptions: homolytic decomposition of oxidizing agent, generation of secondary radical (SPR) carbon centered, intramolecular H transfer (backbiting), intermolecular transfer to the polymer giving tertiary radicals (MCR), propagation of MCR with AA, and termination of SPR and MCR by bimolecular combination. Termination by disproportionation was neglected.

Experimental Work

Polymerizations were carried out in a 1 L glass-reactor equipped with a stirrer, an automatic feeding system, a N₂ inlet, and a digital thermometer. Redox couples were potassium persulfate (KPS) with sodium metabisulfite (KPS/NaMBS) and KPS with sodium hypophosphite (KPS/NaHP). Feed-rates of aqueous solutions of AA, KPS, NaMBS or NaHP were controlled through a closed-loop system. All recipes were around 400 g, with 20% of AA, 1.225% of KPS and different amounts of NaMBS or NaHP (Table 1). Feeding times (FT) were 60, 120, or 210 min., and all reactions were stopped 30 min later. Samples were withdrawn every 30 min to measure fractional and total monomer conversions (x_f and x) by gravimetry, molar mass distribution (MMD) and number- and weight-averages (M_n and M_w) by size exclusion chromatography (SEC), and branching degree (BD) by ¹³C NMR.

Results and Discussions

By increasing the NaMBS concentrations ([NaMBS]), lower M_n and M_w were obtained (Table 1 and Fig. 1); however, such effect was more noticeable at low CTA concentrations (ES1 and ES2). MM evolutions suggest that the CTA rate constant is lower than the propagation rate constant (Fig. 1 g,h). In most reactions, the AA was polymerized to almost complete conversion. Besides, the way of addition of the RA seems to play an important role on MMD (compare ES4 and ES5), where M_w monotonically increase during polymerization when NaMBS was loaded in batch, compared with the almost constant control of the MMD achieved

with the RA feeding. By reducing the feeding time, both the MMs and M_w/M_n increased (EP1 – EP3). The BD decreased for increasing amounts of NaHP or NaMBS.

Table 1. Semibatch production of PAA. Amount of RA, feeding time (FT) and characteristics of PAA obtained with KPS/NaMBS (ES#) and KPS/NaHP (EP#) systems

Code	RA (g)	FT (min.)	x_f (%)	M_n (g/mol)	M_w (g/mol)	M_w/M_n	BD (%)
ES1	1.7	120	100.0	21000	63000	3.0	0.65
ES2	3.4	120	100.0	5200	10000	1.9	0.03
ES3	6.8	120	99.0	3200	7900	2.5	0.02
ES4	13.0	120	94.6	2100	3400	1.6	0.00
ES5 ^a	13.0	120	100.0	2400	6700	2.8	0.00
EP1	14.5	120	100.0	2100	4200	2.0	0.00
EP2	14.5	60	96.9	2200	4600	2.1	0.00
EP3	14.5	210	100.0	5400	15000	2.8	0.01

^a AA and KPS were fed during 120 min, while NaMBS was initially loaded.

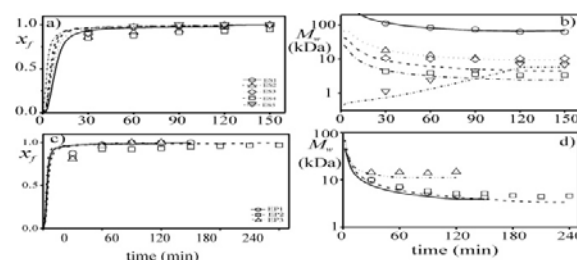


Figure 1. Evolutions of fractional monomer conversion and weight-average MM when employing NaMBS (a-b) and NaHP (c-d). (Simulations in curves and experimental values in symbols.)

Conclusions

The "semibatch" polymerization of AA at 45° C with KPS/NaMBS and KPS/NaHP can produce PAA of low MM ($M_n \approx 2000$ g.mol⁻¹), and relatively narrow MMD ($M_w/M_n \approx 2$), high final conversions ($\geq 94\%$), and low BD ($\ll 1\%$). The mathematical model adequately predicts the main measured variables. The ¹³C NMR analysis confirmed the assumptions adopted in this work.

Acknowledgment: To CONICET, ANPCyT, SENACYT, UNL and UTN for their financial support.

References

1. Barth, J.; Buback, M.; Meiser, W. *Macromol.* 2012, 45, 1339-1345.
2. Scott, R.; Peppas, N.A. *AIChE J.* 1997, 43, 135–144.



ROBUST STATE ESTIMATION OF POLYMERIZATION PROCESSES

Jhovany Tupaz¹, Mariano Asteasuain¹, Mabel Sánchez¹

1. *Planta Piloto de Ingeniería Química (CONICET-UNS), Camino La Carrindanga km 7, 8000, Bahía Blanca, Argentina. jtupazpantoja@plapiqui.edu.ar*

Introduction

The problem of state estimation in nonlinear processes has been covered extensively in the past. Typical examples of traditional chemical systems in which these problems arise are polymerization processes.

A widespread state estimation technique in process control is the Extended Kalman Filter. In spite of its popularity, this strategy may present problems in the case of highly nonlinear systems. The Unscented Kalman Filter (UKF) has been developed for this type of processes. It is based on a mechanism that propagates the mean and covariance of a random variable through a nonlinear transformation.¹

Because the presence of outliers distorts variable estimates, robust estimators are devised that produce reliable estimates, not only when data follow a given distribution exactly, but also when this happens only approximately due to the presence of outliers.²

The aims of this paper is to compare the performance of different M-estimators in the framework of the UKF when they are applied to a copolymerization process.³

Experimental Part

The estimation strategy is a robust derivative-free algorithm that can handle measurement outliers. At first a nonlinear regression model is built combining the measurement model and the relationships between the true states and their predictions. This regression problem is solved using the concepts of Robust Statistics. The weights of each variable are implicitly calculated initially. Then, the weight matrix is used to reformulate the covariance matrixes involved in the conventional UKF. The performance of three different M-estimators is analyzed: Huber (Hub), Welsch (Wel) and Correntropy (Cor).⁴ The first one is a monotone estimator, and also the most commonly used for filtering. The other two are redescending estimators.

The process selected as case study is the copolymerization of methyl methacrylate (MMA) and vinyl acetate (VA) in a continuous stirred tank reactor with a recycle loop. Five variables are measured with a sampling interval of 5min. Some observations are contaminated with outliers.

Results and Discussions

Fig. 1, shows the weight-average molecular weight (Mw) measurements and the estimates obtained when each M-estimator is applied. It is observed that estimates are close to the true variable value in the presence of outliers. Also estimators still provide good estimates when outliers are absent. In Table 1, the Mean Square Errors (MSE) of the estimates are shown. It can be seen that the MSEs for the redescending estimators are lower than the one achieved applying the Huber estimator.

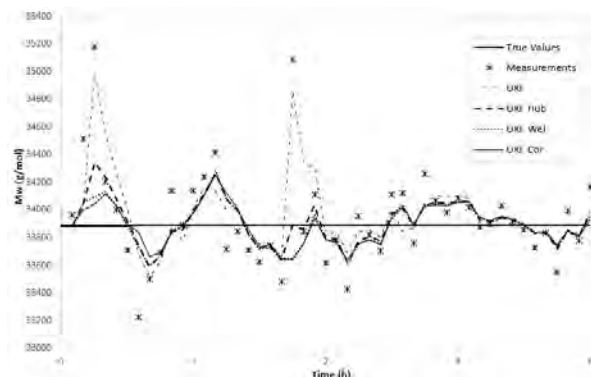


Figure 1. Measurements and estimates of Mw vs time.

Table 1. MSE of Mw in each M-estimators.

M-estimator	MSE of Mw
UKF	8,32E+04
UKF Hub	2,68E+04
UKF Wel	2,34E+04
UKF Cor	1,99E+04

Conclusions

Redescending M-estimators improve the estimation performance in comparison to the one obtained using monotone estimators.

References

1. Julier, J.; Uhlmann, J. K. Proceeding of SPIE. 1997.
2. Maronna, R.; Martin, R. D.; Yohai, V. Robust Statistics: Theory and Methods, John Wiley and Sons Ltd, Chichester. 2006.
3. Congalidis, J. P.; Richards, J.; Ray, W. H. AIChE J. 1989, 35, 891.
4. Llanos, C. E.; Sánchez, M. C.; Maronna, R. Ind. Eng. Chem. Res. 2015, 54, 18, 5096.



FORCING RADICAL COPOLYMERIZATION REACTIONS TO DESIGN THE PROPERTIES OF MULTICOMPONENT POLYMER SYSTEMS

C.F. Jasso-Gastinel¹, A.H. Arnez-Prado¹, F.J. Rivera-Gálvez¹, L.O. Sahagún-Aguilar¹, F.J. Aranda-García¹, M.A. López-Manchado³, M.E. Hernández-Hernández¹, and L.J. González-Ortiz²-

1. Chemical Eng Department, CUCEI, Universidad de Guadalajara, Blvd. Gral. Marcelino García Barragán 1421, Guadalajara Jalisco, MÉXICO carlos.jasso@cucei.udg.mx
2. Chemistry Department, CUCEI, Universidad de Guadalajara, Blvd. Gral. Marcelino García Barragán 1421, Guadalajara Jalisco, MÉXICO
3. ICTP, CSIC Instituto de C. y T. de Polímeros, Juan de la Cierva 3, Madrid 6, España

Introduction

To optimize the contribution of each component in copolymers, the comonomers can be feeded using a semicontinuous process varying feed composition to force the instantaneous composition of the chains being synthesized. Forming significant amounts of chains rich in comonomer A, and chains rich in comonomer B, the properties contribution of each component can be enhanced. That approach can even be applied to three component polymers feeding sequentially two pairs of comonomers with one concurrent component.

Experimental Part

Styrene (S), butyl acrylate (BA), and 4-vinylbenzyl chloride (VBC) (for the terpolymers) were used as monomers in a 4 L glass reactor at 72°C, stirring the emulsion system at 400 rpm. Potassium persulfate was used as initiator. For the latexes, first a polystyrene (PS) seed was prepared forming a latex containing 20 wt % of solids. Several different feeding schemes were used for the synthesis of 50/50 S/BA (Linear [Li], parabolic [Pa], or V monomer feeding profiles) and 25/60/15 BA/S/VBC wt % polymeric materials by means of a seeded semicontinuous emulsion process. For the polymeric materials, chemical characterization was done by 1H-NMR (Varian Gemini 2000); for mechanical testing, samples were prepared by compression molding (Schwabenthan polystat 200T). Stress-strain measurements were performed at several temperatures (ASTM D638, samples Type IV, crosshead speed: 0.0083 cm/s; United Universal testing machine SFM10. Mechanodynamic tests were carried out as a function of temperature (DMA, ASTM D-5023, three point bending clamp, 1 Hz, heating rate: 1.5 °C/min; TA Instruments Q800. Sample microscopic observations were performed by TEM, SEM or AFM.

Results and Discussions

In Figure 1 a) histograms showing the distribution of the composition of S/BA copolymer chains are presented for four different feeding schemes. Basically, the copolymer chains that are rich in S will contribute significantly to Young or storage modulus ($S \approx 0.75$ or higher); for chains composition that are rich in BA ($S \approx 0.25$ or lower), the major contribution will be for deformation capacity. Globally, a histogram delineates a specific

stress- strain curve. In Figure 1 b) two feeding schemes relatively show high modulus with moderate deformation, while the other two (PaS/PaBA and VS/VBA) show low modulus with very high deformation capacity. For 3 component systems, it was found that the feeding order sequence of the comonomer pairs influences the final properties, due to their differences in relative reactivities

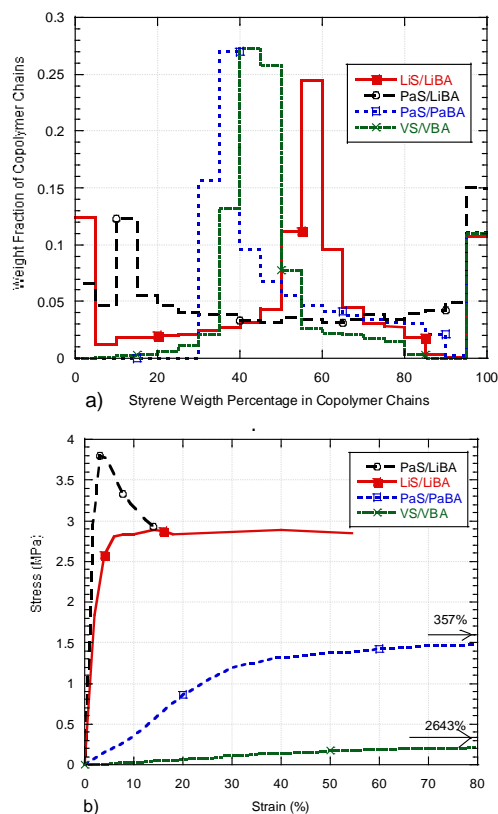


Figure 1. a) Weight fraction spectrum of copolymer chains composition for several forced gradient materials of 50/50 w/w. System S/BA. b) Tensile behavior of those materials at 25 °C.

Conclusions

Varying feeding schemes of semicontinuous processes, the properties of 2 and 3 component polymers can be designed.



MATHEMATICAL MODEL FOR THE SYNTHESIS OF THERMOSETTING POLYMERS BASED ON EPOXY RESINS

Emilio Berkenwald¹, Marisa Spontón², Verónica Nicolau², Diana Estenoz²

1. Department of Chemical Engineering, Instituto Tecnológico de Buenos Aires (ITBA), Av. Madero 399, C.P.1106, Buenos Aires, Argentina, ebk@itba.edu.ar
2. Instituto de Desarrollo Tecnológico para la Industria Química, INTEC (Universidad Nacional del Litoral - CONICET), Güemes 3450, C.P. 3000, Santa Fe, Argentina, destenoz@santafe-conicet.gov.ar

Introduction

The objective of this work is to develop a mathematical model for the curing process that predicts the evolution of molecular structure, gel point and main reaction variables (concentration of reagents and products) along the process as well as structure-properties relations for the prediction of quality variables.

A comprehensive mathematical model is presented. The model is based on general kinetics of an epoxy-amine resin curing process, considering monomers of different functionality and reactivity. The model allows relating the time of cure to the main reaction variables, as well as polymer molecular characteristics and physical properties and may be used to optimize and control the chemical synthesis of epoxy resins. The model is validated and adjusted using experimental data for the synthesis of epoxy-amine resins.

Experimental Work

Several thermosetting polymers based on epoxy-amine resins were prepared by curing diglycidyl ether of bisphenol A (DGEBA) with linear polyether-diamines in stoichiometric conditions. For the reactions, three polyether-diamines with different molecular weights (230, 400 and 2000 g/mol) were used.

The crosslinking reactions were carried out at 80 °C for 2 h and 125 °C for 2 h. Samples were taken along the reaction in order to measure conversion by FT-IR spectroscopy. Average molecular weights until gel point were determined by SEC, heat of reaction (ΔH^p) by DSC and density by gravimetry.

Final materials were characterized by DMTA to obtain the glass transition temperature (T_g), flexural modulus (E') and crosslink density (M_c).

Mathematical Model

The mathematical model considers both autocatalytic and non-catalytic mechanisms for a stepwise polymerization.

The model consists of three interdependent modules: the *Global Module*, predicting the evolution of the chemical species concentrations with reaction time; the *Network Properties Module*, based on the recursive nature of the polymerization reaction^{1,2} as well as laws of probability and expectation, which quantifies the evolution of the network average molecular weights and gel point; and the *Physical Properties Module*, predicting the mechanical and thermal properties of the cured resin, such as the elastic modulus and glass transition temperature.

The model consists of a system of ordinary differential equations and non-linear equations, which were programmed and solved in MATLAB v8.3 using Runge-Kutta and multivariate Newton-Raphson numerical routines.

Results and Discussions

The model parameters are adjusted and validated using the experimental results by least squares minimization method using a random search algorithm. A very good agreement between predictions and measured variables is observed.

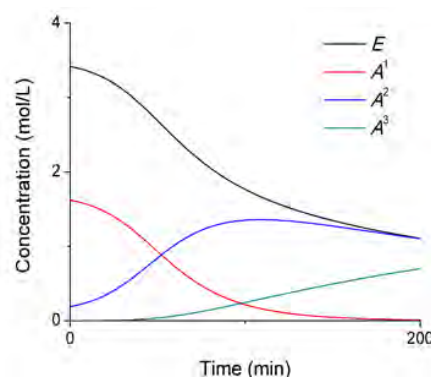


Figure 1. Evolution of functional groups: epoxy primary, secondary tertiary amine.

The model can be used to theoretically evaluate the influence of reaction conditions as well as monomer structure on the gel point and properties of the obtained materials.

Conclusions

A mathematical model for the synthesis of thermosetting polymers based on epoxy resins was presented. The model allows estimating the evolution of the reacting chemical species, as well as network characteristics and physical properties of the obtained materials.

References

1. D. R. Miller, C. W. Macosko, *Macromolecules*, 2, 9, 1978.
2. D. R. Miller, C. W. Macosko., *Macromolecular Theory and Simulations*, 13, 8, 1976.



SENSITIVITY ANALYSIS FOR A SYSTEM OF TERPOLYMERIZATION

 Oscar Meza Díaz¹, Juan Carlos Tapia Picazo¹

 1. Department of Chemical and Biochemical Engineering, Technological Institute of Aguascalientes, Av. Adolfo López Mateos No. 182 Ote. Fracc. Gens, C.P 20256, Aguascalientes, Ags, Mexico. omeza.diaz@gmail.com

Introduction

In the high technology area, the carbon fibers (CF) play a very important role in aerospace, automotive industry, and defense; because of the ability to withstand high temperatures, mechanical and chemical resistance, and high lightness. Although a CF precursor widely used is polyacrylonitrile (PAN), it needs to improve its properties through the incorporation of acid comonomer. Besides, the final quality of CF depends of copolymer composition and reactivity ration.¹ In this case; the terpolymer system is constituted for: Acrylonitrile (AN), Vinyl Acetate (VA) and Itaconic Acid (IA); which it offers good qualities to be precursor of CF due to the specific characteristics of each monomer. Due to commercial importance of polymer precursor production of CF, is fundamental the modeling, analysis and optimization of this system for identify good operation conditions, try predicting quality of polymer, reducing cost, etc. Models of solution terpolymerization reactors are scarce and exhibit highly nonlinear behavior because the complex kinetics of the polymerization reaction.² Carry out a sensitivity analysis, allow find values of some important variables in the CF industry, and view the behavior of reaction model. This work is focused first, obtain solution polymerization model for continuous stirred tank reactor (CSTR); including Charge-Transfer Complex (CTC) in the kinetic mechanism, because of their training in terpolymerization system. And second, make a sensitivity analysis over obtained model.

Experimental Part

Methodology to obtain-solution model

The CSTR model was obtained, by converting to dimensionless variables, each terms in the expressions of mass and energy balances; the object of this methodology given by Hamer³, is facilitate the analytic solution of CSTR model.

CTC formation and obtaining constant rate of complex

CTC formation was verified using UV-Vis, this technique consist it comprises preparing a solution of one of the monomers in low concentration, while for the second monomers was prepared various solution at different concentrations.⁴ The absorption spectrum of each of the solutions was obtained, for obtain the complex absorption spectrum; mixing 2ml of solution with constant concentration with 2ml of the other monomer solution, and get the spectrum of the mix; the operation is repeated with the other solutions. For obtaining the spectrum of the complex; spectra of monomers were subtracted from spectrum of the mixture. For obtain complex's rate constant, it was used the model of

simultaneous participation of free monomers and complexes⁵ which considers both participation of free monomers and CTC, polymerizing independently of each other. The equation (1) and (2) both are straight line equation where the value of A(X) and F(X) can be calculated by linear regression.

$$\frac{v_{br}}{[M_1]} = A(X) + A(X)F(X)[M_1] \text{ Eq. (1)}$$

$$F(X) = K \left(\frac{k_{1c1}}{k_{12}} + \frac{k_{2c1}}{k_{21}} X \right) \text{ Eq. (2)}$$

Where X its monomers ratio, v_{br} its overall rate, K, equilibrium constant and k_{ic1} it's the CTC constant rate.

Results and Discussions

The Fig. 1 its one of the absorption spectrum for the complex formed between AN and VA, the complex was absorbance between 294 and 297 nm, the technique⁴ only it suggests that the increase in absorbance is signal complex formation. Therefore there is a CTC formed.

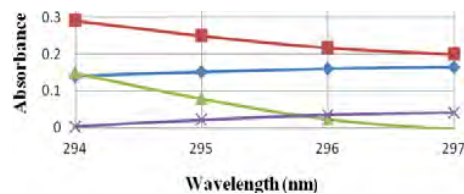


Figure 1. Absorption spectrum: blue line (AN), purple line (VA), mixing red line, green line complex.

Conclusions

In the terpolymerization system only there was evidence of CTC formation between: AN-VA and VA-IA, in the case of AN-IA the spectrum of the mixture no increase in absorbance, therefore complex cant formed.

References

1. Devasia, R.; Nair, C.P. R; Ninan, K.N.. *European Polymer Journal* 2002, 38, 2004.
2. Srour, M.H.; Gomes, V.G.; Altarawneh, I.S.; Romagnoli, J.A. *Chemical Engineering Science* 2009, 64, 2076.
3. Hamer, J.W; Akramov, T.A.; Ray, W.H. *Chemical Engineering Science* 1981, 36, 1897-1914.
4. Bates, F.; Baker, G. *Macromolecules*, 1983, 16:4 708.
5. Braun, D.; Hu F. *Polymer*, 2004, 45, 63.



COMPARISON OF RHEOLOGICAL PROPERTIES AND IZOD IMPACT RESISTANCE OF PPE/HIPS/SBS BLENDS AND ABS

Erika I. López Martínez^{1*}, Juan A. Arteaga-Bustillos², Mónica E. Mendoza-Duarte¹, Alejandro Vega-Rios¹, Claudia A. Hernández-Escobar¹, E. Armando Zaragoza-Contreras¹, Sergio G. Flores-Gallardo^{1*---}

1. Centro de Investigación en Materiales Avanzados S.C., Miguel de Cervantes 120, C.P. 31136, Chihuahua, Chih. México erika.lopez@cimav.edu.mx, sergio.flores@cimav.edu.mx
2. Universidad Autónoma de Chihuahua, Circuito Universitario s/n, C.P. 31125, Chihuahua, Chih. México.

Introduction

During the last sixty years blending of dissimilar polymers has been a major path to tailor materials with new properties in industry. Depending on the structure and the nature of the dispersed phase in a polymer blend, a wide spectrum of properties can be tailored. Due to the fact that an already existing range of base polymers is used, a large variety of new high-capacity polymers is readily and economically available. The highest market value and the strongest growth rate are predicted for blends based on both polycarbonate (PC) and poly(2,6-dimethyl-1,4-phenylene ether) also referred as polyphenylene ether (PPE). Since PPE and polystyrene (PS) are completely miscible at all molecular weights and concentration ranges, PS or its derivatives (such as high-impact polystyrene (HIPS), styrene-butadiene-styrene (SBS) block copolymers) have been used to improve the processability and toughness of pure PPE. The aim of this work is to evaluate if the PPE/HIPS/SBS blends can compete with the rheological and Izod impact resistance of Acrylonitrile Butadiene Styrene (ABS). ABS is the preferred engineering plastic when it comes to dealing with automotive applications because of its heat and UV resistance, good processability and Impact strength.

Experimental Part

Blends were prepared by using a Brabender Plasticorder internal mixer at a rotor speed of 100 rpm, 280°C and cam blades. PPE and HIPS were first added to the mixer and were allowed to soften. Thereafter, the block copolymer was added and mixed for 3 min. ABS was prepared under the same conditions than the PPE/HIPS blends. The specimens for rheological (Rheometry and DMA) and mechanical (Izod Resistance) measurements were obtained by injection molding at 130 psi of pressure and 310°C.

Results and Discussions

Summary of blends composition (w/w/w) and Izod impact test results are shown in Table 1. In general terms, when increasing the SBS content in the PPE/HIPS blends, the impact resistance is improved because of the toughening effect of elastomers that act as in-situ reinforcing agents since the mode of action of the rubber particles consists generally in initiating deformation mechanism

(crazing, shear failure), which allow high dissipation of energy. The PPE/HIPS blends prepared presented higher impact resistance than ABS.

Table 1. Blends prepared and Izod Impact Resistance obtained

SAMPLE	PPE (wt%)	HIPS (wt%)	SBS (wt%)	Izod Impact Resistance (kJ/m ²)
ABS	-	-	-	19.67
PPE/HIPS	77.77	22.23	-	22.40
PPE/HIPS/SBS416-6%	73.12	20.88	6	25.81
PPE/HIPS/SBS416-12%	68.45	19.55	12	27.81

There are a relationship between rheological properties and the morphology of polymer blends. The elasticity presented at low frequencies plays a role in the phase structure. A higher elasticity is presented, higher tendency of forming a continuous phase it would have. PPE/HIPS blends showed higher elasticity and thermo-mechanical stability than ABS.

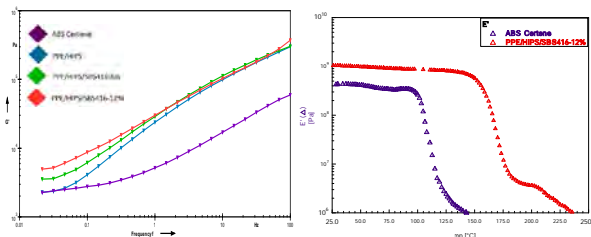


Figure 1. Storage modulus of the blends by Frequency and Temperature Sweep.

Conclusions

The compounding PPE/HIPS and PPE/HIPS/SBS416 blends presented higher Izod-Impact resistance and rheological properties (thermomechanical stability and elasticity) than ABS.

References

1. Adhikari R.; Nepal J. of Science and Technology 2011, 12, 149.
2. Zhang et al.; Composite Science and Technology 2013, 86,122.
3. Puskas J.E. et al.; Polymer 2007,48, 590.



EFFECT THE DEPOLYMERIZATION OF THERMOPLASTIC STARCH (TPS) FILMS OBTAINED BY EXTRUSION TWIN SCREW

Mayela Casas¹, Francisco Rodríguez¹, Gustavo Soria¹, Juan Contreras²

1. *Polymers Processing Department, Centro de Investigación en Química Aplicada, CP 25294, Saltillo-Coah, Mexico. mayela700@hotmail.com*
2. *Food Research Department, School of Chemistry, University Autonomous of Coahuila, CP 25280, Saltillo, Coahuila, Mexico.*

Introduction

Starch is a reserve polymer, formed by two large polymeric chains, amylopectin 100-400X10⁶ g/mol and amylose 0.2-2X10⁶ g/mol¹. One technique for obtaining TPS films is through twin-screw extrusion, where the starch is gelatinized in presence of heat, a plasticizer such as e.g. glycerol and high shear is result a thermoplastic material. It is well known that polymers may degrade upon combined heating and shearing but, in the case of TPS, less is know about the detailed mechanisms involved and how to control the depolymerization. Some parameters that may be participating in a depolymerization TPS would screw speed and feed flow rate material on the residence time. The main objective of this work was to evaluate the effect of depolymerization of TPS on the residence time in the extruder and physical properties of the film.

Experimental Part

For obtaining the film a double screw extruder (ZSK30, screw diameter $D=24$ mm, length $L=28D$) with a 150 mm wide film die. The extruder was configured with nine zones (z): The temperatures control were z-1,2= 70 °C where a suspension the a starch, glycerin and water was fed. In the Z3-Z8=90 °C, Z9= 80 °C die section. The feed rates the suspension evaluated were 3.5 and 9.7 kg/h and screw speed of 50,100 and 150 rpm. The obtained films were placed in glass supports dried 20 h at 60 °C. The film was characterized by water absorption index (WAI) and water solubility index (WSI)³. The depolymerization of the film was evaluated by size exclusion chromatography (SEC). A sample of 20 mg/mL were dissolved in 0.5M NaOH, eluted through a Sepharose CL-2B column using 0.01M NaOH a flow rate of 1 mL/min, volume fractions of 2 mL. Fractions were analyzed by total sugars.

Results and Discussions

The TPS films, obtained at a flow of 3.5 kg/h had higher WSI values that films obtained at a flow of 9.7 kg/h Table 1. Increasing the screw speed there is an increase in the WAI and a decrease in the WSI, due to a decrease in residence time of the material in the extruder.

Method	Sample (outflow-kg/h)	Screw speed (rpm)	Residence time (min)	WAI	WSI	Relative loss of plasticizer (%)
Extrusion	TPS-(3.5)	50	5	4.86	0.35	84
	TPS-(3.5)	100	2.3	4.66	0.26	59
	TPS-(3.5)	150	2.2	5.06	0.23	52
	TPS-(9.7)	50	2.13	4.42	0.28	64
	TPS-(9.7)	100	1.27	5.65	0.26	60
	TPS-(9.7)	150	1.19	6.07	0.20	41

Table 1. Obtaining TPS films extrusion via.

⁵ g/mol is observed Figure 1.

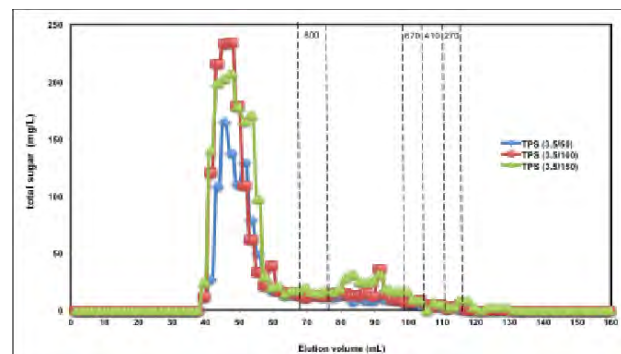


Figure 1. Profile chromatographic TPS films fractionated to CL-2B and analyzed by the technique of total sugars.

Conclusions

The films obtained via extrusion at high shear stresses produce a starch depolymerization. Which affects physical properties of TPS, increasing plasticizer migration to the surface due to this formation of polymer chains of less molecular weight.

Acknowledgment: Jesús Rodríguez, Sergio Zertuche, José López, Fabián Chávez

References

1. Bastioli, C., *Handbook of Biodegradable Polymers*, ed. R.T. Limited. 2005, UK: Rapra Technology Limited..
2. Li, M., Liu, P., Zou, W., Yu, L., Xie, F., Pu, H., Liu, H., Chen, L. Extrusion processing and characterization of edible starch films with different amylose contents. 2011, 106 (95-101).
3. Anderson, R.A., Conway, H.F., Peplinski, A.J., 1970. Gelatinization of corn grits by roll cooking, extrusion cooking and steaming. *Starch* 22, 130-135.



PROCESSING AND CHARACTERIZATION OF POLYETHYLENE TEREPHTHALATE AND HIGH DENSITY POLYETHYLENE COMPOSITES WITH AGAVE FIBERS

Erendira E. Covarrubias Flores¹, Rubén González Núñez¹, Milton O. Vázquez Lepe²

¹Departamento de Ingeniería Química, ²Departamento de Ingeniería de Proyectos. Universidad de Guadalajara, Centro Universitario de Ciencias Exactas e Ingenierías, Blvd. Marcelino García Barragán 1421, Guadalajara, Jalisco, 44430, MÉXICO. ereecf@gmail.com

Introduction

This work describes the study of processing and characterization of the mechanical properties of recycled polyethylene terephthalate (PET) and recycled high density polyethylene (HDPE) composites using agave fiber, adding a compatibilizer and a coupling agent to the mixture to modify its properties.¹ The PET and HDPE containers used in this study came from the Laboratory and Technological Development in Plastics Recycling (LIDETREP), which supports the solid residue management of the University of Guadalajara.

Experimental Phase

The materials are collected, separated and manually classified; then enter a milling, washing and drying process. To obtain the composite, the plastics and the compatibilizers are mixed in an extruder with a single screw at a maximum processing temperature of 250 °C. The mixtures contain 10%, 20%, 30% and 40% wt. of PET. After that, the materials are submitted to a second extrusion in which we add the coupling agent and the fiber in a proportion of 10% wt. at a maximum temperature of 200°C.² With the obtained granules the fluidity index is measured, differential scanning calorimetry analysis (DSC) and thermogravimetric analysis (TGA) are realized. The extruded material is submitted to a drying process at 60°C and finally it goes through a thermo-compression modeling process at 200°C to obtain test specimens of the established measures for the realization of the following mechanical tests: tensile properties, flexural properties and impact resistance.

Results and Discussions

From the composites without fiber; at the mechanical tests, the material shows a general increase on its tensile resistance and flexural resistance (Figure 1); contrary to the impact resistance (Figure 2) where we observe an important decrease in such property, according to the content of PET. This results in a more breakable and rigid material when we increase the amount of PET in the mixture. From the thermogravimetric analysis of the polymeric matrix, we know that the highest processing temperature is of 375°C for PET, whereas for HDPE is 400°C, because of this, the selected temperature doesn't cause any thermal deterioration in the materials.

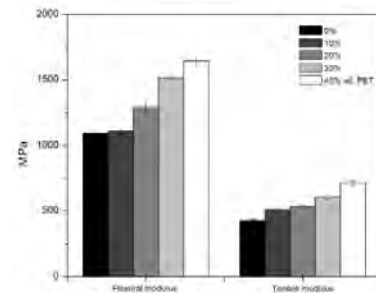


Figure 1. Properties of flexural and tensile without agave fiber or compatibilizer added to the composite.

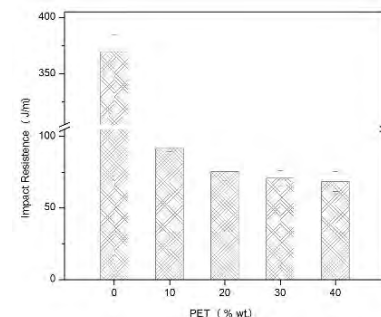


Figure 2. Property of impact resistance without agave fiber or compatibilizer added to the composite.

Conclusions

In the present study, we show the advances on the mechanical behavior of the recycled PET/HDPE composites. By DSC characterization we observed that the melting temperature of the polymeric matrix is within the processing range of temperatures. On the mechanical properties, the tensile modulus increases up to 67% and the flexural modulus up to 50% with the highest amount of PET. However impact resistance decreased considerably when increasing the amount of PET in the mixture.

Acknowledgment: To the National Council of Science and Technology (CONACYT) scholarship 330576.

References

1. Pracella M., Lorenzo R., Donatella C., Andrzej G. *Macromolecular Chemistry and Physics* 2002, 203, 1473–1485.
2. Lei Y., Qinglin W. *Bioresource Technology* 2010, 101, 3665–3671.



ANÁLISIS DE UN SISTEMA DE OBTENCIÓN DE FIBRA DE CARBÓN DE BAJA PUREZA

Daniel Alcalá Sánchez ¹, Juan Carlos Tapia Picazo ¹

1. Instituto Tecnológico de Aguascalientes, Av. Adolfo López Mateos #1801 Fracc. Bona Gens, 20256, Aguascalientes, Aguascalientes, México. daniel_hc195s@hotmail.com

Introducción

Las fibras de carbón (FC) deben sus altas prestaciones a sus excelentes propiedades mecánicas que dependen fuertemente de la calidad de la fibra que se utiliza para obtenerla, conocida como fibra precursora.¹ El elevado costo de producción de estos materiales les hace poco accesibles, por tanto, diversos estudios son enfocados a reducir tales costos. Emplear como precursores fibras de grado textil puede ser una opción para reducir los costos de procesamiento.² El presente trabajo evalúa un polímero desarrollado a base de acrilonitrilo-acrilato de metilo (AN-AM) como un precursor de FC de baja pureza (fibras estabilizadas). Propiedades físicas, mecánicas y térmicas de fibras obtenidas son comparadas con fibras precursoras obtenidas a partir de un polímero acrílico comercial.

Parte Experimental

Un polímero a base de AN-AM, fue procesado en un sistema de extrusión en húmedo para ser convertido en fibra precursora (FPRE). FPRE se caracterizó física y mecánicamente. Muestras de FPRE se sometieron a procesos de estabilización térmica durante 20 min a 200 (PRE2), 220 (PRE3) y 200+220°C (PRE4). FTIR se aplicó a FPRE antes y después de la estabilización térmica. Un polímero comercial a base de acrilonitrilo-acetato de vinilo fue convertido a fibra precursora (FCOM) y se aplicaron los mismos procedimientos que FPRE.

Resultados y Discusiones

La Fig. 1 muestra los resultados de la caracterización de FPRE y FCOM. Las diferencias se atribuyen principalmente a los componentes del polímero y la interacción entre ellos durante el proceso de extrusión.³ La Fig.2 muestra espectros FTIR de FPRE y FCOM a diferentes temperaturas de tratamiento. Los cambios en las intensidades de los picos de los grupos C≡N a 2245 cm⁻¹, muestran reducción con el incremento de la temperatura; los picos en las bandas características para los grupos C=O y C=C a 1735 cm⁻¹ y 1600 cm⁻¹ respectivamente, incrementan su intensidad mientras la temperatura aumenta. En FPRE, es más notoria la reducción en la intensidad de los picos en las bandas características de los enlaces C≡N. En FCOM, la formación de los enlaces C=O es más notoria que los enlaces C=C, ya que el proceso de oxidación se está llevando a cabo de manera rápida respecto a la ciclización de la estructura de la fibra. En las muestras a partir de FPRE, la formación de los enlaces C=C es más notoria que la formación de los enlaces C=O, dando como resultado una ciclización de la estructura en menor tiempo.

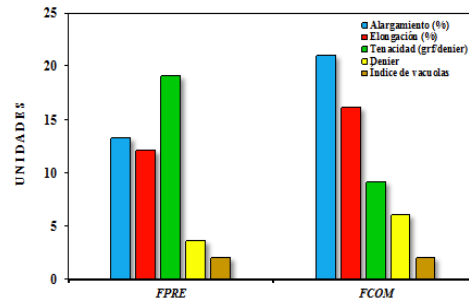


Figura 1. Caracterización de fibras precursoras FPRE vs FCOM

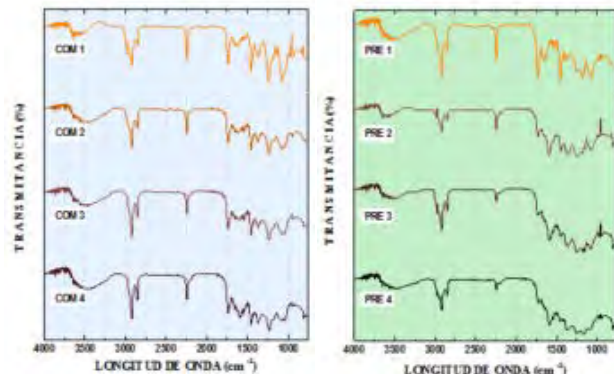


Figura 2. FTIR de FPRE y FCOM en proceso de estabilización, a 0, 200, 220 y 200+220 °C.

Conclusiones

Un nuevo polímero a base de acrilonitrilo-acrilato de metilo promete ser un precursor competitivo para el desarrollo de fibras de carbón ya que con mayor velocidad de estabilización y con mejores propiedades mecánicas que un polímero acrílico comercial las cuales pueden ayudar a robustecer un proceso general de fibras carbón de alta calidad y bajo costo.

Referencias

1. Wangxi, Z.; Jie, L.; Gang, W. Carbon 2003, 41, 2805
2. Eslami, R.; Raissi, S Engineering and Technology 2009, 50, 430
3. Zhao, J.; Zhang, Y.; Dong, R. Polymer 2008, 47, Part B, 261.



MIXED MATRIX MEMBRANES BASED ON POLYSULFONE AND MODIFIED CLINOPTILOLITE ZEOLITE: STUDY OF THERMAL AND GAS PERMEATION PROPERTIES

Gema C. Hernández Silva¹, Griselda Castruita de León^{2*}, Sandra P. García Rodríguez³, H. Iván Meléndez Ortiz²

1. Facultad de Ciencias Químicas UAdeC, Ing. J. Cárdenas Valdés, 25280, Saltillo, Coahuila, México.

2. CONACYT-Centro de Investigación en Química Aplicada, Blvd. Enrique Reyna 140, 25294, Saltillo, Coahuila, México.

* griselda.castruita@ciqa.edu.mx

3. Centro de Investigación en Química Aplicada, Blvd. Enrique Reyna 140, 25294, Saltillo, Coahuila, México.

Introduction

The use of selective membranes for removing CO₂ and other gases from natural gas is a developing emerging technology. Polymeric membranes have shown interesting gas separation properties [1]. An attractive option to enhance the gas separation is through polymeric-inorganic systems to form mixed matrix membranes (MMM). The combination of processability of polymers and the separation properties of inorganic materials allows an improvement on the physicochemical properties and gas permselectivity of membranes [2]. Natural zeolite, particularly clinoptilolite, is highly gas permeable and CO₂ selective. The aim of this work was the investigation of the thermal properties and membrane performance for separation of CO₂ from CH₄ of MMM composed of polysulfone (Psu) and clinoptilolite zeolite previously enriched with different cations (Ca²⁺, Na⁺ and K⁺) by ionic interchange.

Experimental Part

MMM based on Psu and modified clinoptilolite were prepared by casting: A Psu solution (13 wt%) in CHCl₃ was prepared. Different zeolite content (7.5; 12.5 wt % with respect to polymer weight) was added to this solution. Zeolite was dispersed using an ultrasonic treatment: 45 min using an ultrasonic bath and 8 min using an ultrasonic processor. This mixture was homogenized by magnetic stirring during 4 h. Mixture polymer-zeolite was poured into a glass mold allowing the evaporation of solvent at room temperature. TGA and DSC analyses were carried out under inert atmosphere. Gas permeation properties were studied using a gas mixture of CH₄/CO₂ 95/5 mol%. An upstream pressure of 150 psi was assessed.

Results and Discussions

Figure 1 shows the TGA thermograms of membranes. All membranes exhibited similar degradation steps starting at 500°C. The remaining weight agrees with the zeolite content in the membrane. Figure inset indicates the glass transition temperature of membranes (T_g). T_g values increased slightly with the presence of zeolite. Higher T_g value was obtained at higher zeolite content. Table 1 shows the permeation properties of membranes. MMM exhibited an increase on the CO₂ permeability in comparison with Psu membrane. Significant increment on t was appreciated in MMM using clinoptilolite zeolite modified with Ca²⁺ cations.

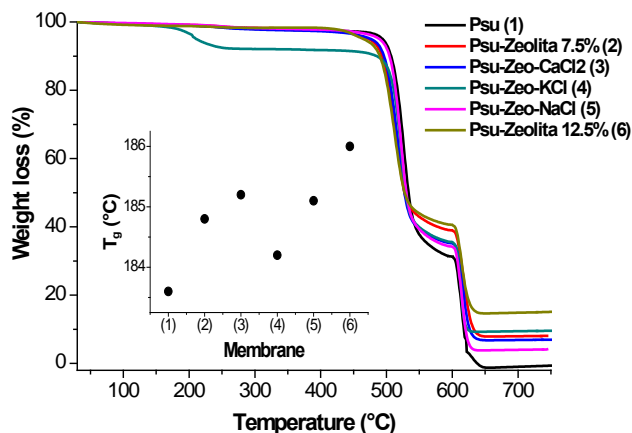


Figure 1. Thermal properties of membranes by DSC and TGA.

Table 1. Gas permeation properties of membranes.

Membrane	CO ₂ Permeability (barrer)	CH ₄ Permeability (barrer)
Psu	6.5	0.1
Psu-Zeolita 7.5%	11.8	0.3
Psu-Zeo-CaCl ₂	40.9	0.4
Psu-Zeo-KCl	9.1	0.2
Psu-Zeo-NaCl	9.3	0.1

Conclusions

The presence of clinoptilolite zeolite in MMM improved the permeability of CO₂, mostly those membranes prepared with 7.5 wt% of zeolite enriched with Ca²⁺ cations.

Acknowledgment: Thanking to CIQA for financial support (project 6314) and Cátedras-CONAYT program. We are grateful to B. Puente, G. Méndez, J. Cepeda and A. Espinosa for their technical assistance.

References

1. Yampolskii Y. *Macromolecules* 2012, 45, 329.
2. M. Rezakazemi, et.al. *Prog. Polym. Sci.* 2014, 39, 817.



CONDUCTIVE MEMBRANES BASED ON COMPOSITE POLYMERS FOR ENERGY APPLICATIONS

Vicente Compañ Moreno

Dpto. Termodinámica Aplicada. Escuela Técnica Superior de Ingenieros Industriales (ETSII). Universidad Politécnica de Valencia. Camino de Vera s/n 46022-Valencia (Spain). E-mail: vicommo@ter.upv.es

Introduction

The demand for clean and efficient sources of energy in the future energy scenario have driven in recent years the development of alternative technologies to eliminate or reduce oil dependency and environmentally friendly power sources for many applications including transportation, distributed power and portable systems. In this sense, proton exchange membranes for fuel cells and Lithium-Ion batteries are an emerging technology that has focused interest in both basic research and technological development. However, important scientific, technical and economical problems need to be solved before achieving mass commercialization of proton exchange membranes for fuel cells application with hydrogen and direct methanol as feed for fuel cells applications, (PEMFCs) and (DMFCs), respectively^{1,2}. In the case of fuel cells, to achieve acceptance of this technology in a general framework, combined efforts are needed in different aspects such as membranes, electrodes, manufacture and assembly of all of them, through standardized integration systems and accepted by users. In this work the use of new strategies for the preparation of proton exchange membranes with low cost and higher durability and performances is proposed³⁻⁵.

To achieve this objective, we have synthesized and characterized proton exchange membranes below three lines of action:

- 1) Research and development of new nanofiber reinforced polymer membranes based on Nafion/PVA³⁻⁶, SPEEK/PVA and SPEEK/PVB^{7,8}, the use of Ionic Liquids (ILs)⁹⁻¹¹. Metal-organic frameworks (MOFs)¹²⁻¹³ and Graphene¹⁴⁻¹⁷ for use as a separator between the anode and cathode for Fuel Cells application, (PEMFC and DMFC), able to work at temperatures within the range 100 -160 °C and as polymer-functionalized graphene oxide hybrid membranes for vanadium redox flow battery¹⁷.
- 2) Detailed analysis of the characterization and optimization of advanced structures for application in the membrane-electrode assemblies (MEAs), through studies of the morphology, thermal, chemical and mechanical properties, as well as the proton conductivity.
- 3) In-situ evaluation of the efficiency, delivered power and durability of the assemblies obtained with our membranes in a single fuel cells system with the intention to build in a near future a stacks for low power equipment (about 250 W).

The overlapping of these three strategies may be a viable alternative for low power equipment, such as portable electronic devices, electric wheelchairs, emergency systems, etc.

The electrospinning technique, in which our group could be considered pioneer³⁻⁸, at least in Spain, has worked for the last 8 years in the development of new composite membranes for application in PEMFC and DMFC. The experience gained here will allow us to explore the possibility of producing nanofibers of technical polymers that will be incorporated as reinforcement in the proton exchange membranes. The incorporation or encapsulation in the electrospun nanofibers of different compounds such as metal-organic frameworks (MOFs) and ionic liquids or mixtures of them. This will permit us to build new membrane-electrode assemblies and evaluate the efficiency and stability of our novel

membrane structures and catalysts (new platinum-metal alloys). Thus, our study addresses the development of new membranes of low cost materials and high efficiency, with improved mechanical properties and chemical stability in the temperature range between 100 and 160 °C, for the construction of fuel cell stacks, optimizing membrane-electrode assemblies. With the new membrane materials we expect to surpass the current state of art and technology in terms of durability, efficiency and cost.

Acknowledgment: This research has been supported by the ENE/2015-69203-R. project, granted by the Ministerio de Economía y Competitividad (MINECO), Spain.

References

1. Li Q, He R, Jensen JO, Bjerrum NJ. Approaches and recent development of polymer electrolyte membranes for fuel cells operating above 100°C Chem Mater 2003; 15:4896-4915.
2. Neburchilov V, Martin J, Wang H, Zhang J. A review of polymer electrolyte membranes for Direct methanol fuel cells. J. Power Sources 2007; 169: 221-238.
3. Sergio Mollá, V. Compañ, Journal Power Sources . 196, (2011) 2699-2708.
4. S. Mollá, S. Luis, J. Prats, V. Compañ. Fuel Cells. 11, (6) (2011) 897-906.
5. Sergio Mollá; Vicente Compañ-Moreno; Enrique Giménez; J. Alberto Blazquez; Idoia Urdanpilleta. International Journal of Hydrogen Energy. 36 (2011) 9886-9895.
6. Sergio Mollá, V. Compañ. Journal Membrane Science. 372(2011) 191-20010.
7. S. Mollá, V. Compañ. International Journal of Hydrogen Energy. 39, (2014) 5121-5136.12.
8. S. Mollá, V. Compañ Nanocomposites SPEEK-based membranes for Direct Methanol Fuel Cells at intermediate temperatures. Journal of Membrane Science, 492, (2015) 123-136.
9. Abel Garcia-Bernabé, Vicente Compañ, M. Isabel Burguete, Eduardo García-Verdugo, Naima Karbass, and Evaristo Riande. Journal Physical Chemistry. C, Vol. 114 (2010) 7030-7037
10. Vicente Compañ, Sergio Molla, Eduardo García-Verdugo, Santiago V. Luis, M. Isabel Burguete. Journal of Non-Crystalline Solids. Vol. 358 (9) (2012), 1228-1237.
11. B. Altava, V. Compañ, A. Andrio, L. F. del Castillo, S. Mollá, M. I. Burguete, E. García-Verdugo, S. V. Luis. Conductive Films Based on Composite Polymers Containing Ionic Liquids Absorbed on -Crosslinked Polymeric Ionic-Like Liquids (SILLPs). Polymer 72, (2015),69-81.
12. Ren Y, Chia G H, Gao Z. Nano Today 8 (2013) 577-597
13. Taylor J. M., Dawson K. W., Shimizu G.KH. J Am. Chem. Soc. 135 (2013) 1193-1196.
14. Liu, Z., Boachao G, Kexun Li, Kan Huang. Fuel 176 (2016) 173-180.
15. Amin Taheri Najafabadi A.T., Norvin Ng, Elöd Gyenge. Biosensors and Bioelectronics 81 (2016)103-110.
16. Quesnel E., Roux F., Emieux F., et al. 2D Materials. 2 (2015) 030204 pages 1-16
17. Li Cao, Lei Kong, Lingqian Kong, Xingxiang Zhang, Haifeng Shi. Journal Power Sources 299 (2015) 255-264.



Gas separation properties of unsupported CMC membranes from blends of high temperature rigid aromatic polymers

José Manuel Pérez Francisco¹, José Luis Santiago García¹, María Isabel Loría Bastarrachea¹, Manuel Aguilar Vega¹

1. Unidad de Materiales, Centro de Investigación Científica de Yucatán, A.C., Calle 43, No. 130, C.P., 97200 Mérida, Yucatán, México. *mjav@cicy.mx*

Introduction

Membrane technology has shown a remarkable development during the last three decades for gas separation processes¹. Within this technology, carbon molecular sieve (CMS) membranes in gas separations offer an outstanding relationship of permeability and selectivity for different gas pairs. CMS membranes are obtained from pyrolysis/carbonization of polymeric membranes² and typically, two types of pores are formed; namely, micropores and ultramicropores, related to high permeability and high selectivity for different gas pairs, respectively. In the present work CMS membranes from polyimide PI DPPTD-MIMA (PI), polybenzimidazole (PBI) and their blends are reported. The effects of composition, microstructure and gas separation performance on CMSM's are investigated.

Experimental Part

Polymeric dense membranes were obtained from pristine polymers and different compositions of PI/PBI (87.5/12.5, 75/25, 50/50 and 25/75 wt%) by the casting method. CMS membranes were pyrolyzed at 600°C under UHP argon flow, following a method reported by Ning and Koros³. Wide angle X-ray diffraction (WAXD) measurements were performed on CMSM using a SIEMENS 5000 X-ray diffractometer with CuK α radiation (wavelength 1.54 Å). Gas transport properties were determined by a variable-pressure constant-volume method at different temperatures and 2 atm upstream pressure for He, O₂, N₂, CH₄ and CO₂.

Results and Discussions

Table 1. CMSM's pure gas permeability coefficients at 35°C and 2 atm upstream pressure

CMSM	Permeability (Barrer)					Ideal selectivity	
	He	O ₂	N ₂	CH ₄	CO ₂	α_{O_2/N_2}	α_{CO_2/CH_4}
PI100-600	820	118	14.0	7.3	431	8.5	59.4
PI87.5-600	524	98	12.2	7.0	359	8.1	51.0
PI75-600	455	39	4.8	3.4	109	8.1	31.7
PI50-600	192	24	4.3	3.3	83	5.7	25.2
PI25-600	186	27	3.6	3.2	97	7.6	30.7
PBI-600	147	7.7	1.8	1.0	23	4.4	23.4

Table 1 shows that permeability coefficients increase for pure gases and ideal selectivity for different gas pairs when PBI concentration decrease in membrane precursors. Diffraction

patterns show two maxima in d-spacing obtained by Bragg's law ($n\lambda=2d \sin \theta$): the first between 6.17 - 6.37 Å and the second located on ~4 Å. In CMS blend membranes the intensity of each maximum in d-spacing show a variation related with the concentration of PBI in the membrane precursors. The excellent relationship between permeability and selectivity causes that several CMS membranes in this study surpass separation performance trade-off for several industrially interesting gas pairs (CO₂/CH₄ and O₂/N₂) as is shown in Figure 1.

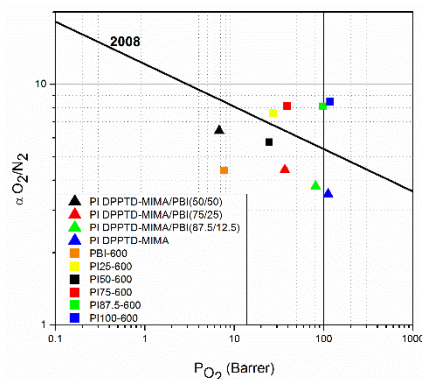


Figure 1. O₂/N₂ polymeric PI/PBI precursors separation performance and that of the corresponding CMS membranes with respect to trade-off line

Gas permeability coefficients for these CMS membranes increase with temperature following an Arrhenius type behavior. It was found that gas permeation activation energy increases with gas molecular kinetic diameter and with increasing PBI concentration in polymeric precursor.

Conclusions

The presence of PBI in polymeric precursor membranes decrease gas permeability coefficients and gas pair selectivity in CMS membranes, even though some of them remain above or close to the upper bound limit performance of increasing permeability and selectivity.

Acknowledgment: This work was supported by the CONACYT under grant 354777.

References

1. Saufi, S.M.; Ismail, A.F. Carbon 2004, 42, 241.
2. Suda, H.; Haraya, K. J. Phys. Chem. Part B. 1997, 101 3988.
3. Ning, X.; Koros, W.J. Carbon 2014, 66 511.



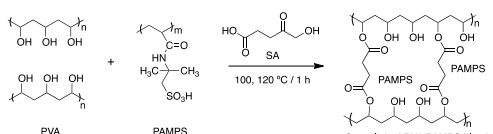
BIODIESEL PRODUCTION FROM SOYBEAN OIL BY CROSSLINKED PVA/PAMPS BLENDS CATALYTIC MEMBRANES

Maria Ortencia González-Díaz¹, Zazil Corzo-González², Maria I. Loria-Bastarrachea², Manuel Aguilar-Vega²

1. CONACYT - Laboratorio de membranas, Unidad de Materiales, Centro de Investigación Científica de Yucatán, A.C., Calle 43 No. 130, Chuburná de Hidalgo, 97200, Mérida Yucatán, México maria.gonzalez@cicy.mx
2. Laboratorio de membranas, Unidad de Materiales, Centro de Investigación Científica de Yucatán, A.C., Calle 43 No. 130, Chuburná de Hidalgo, 97200, Mérida Yucatán, México

Introduction

The development of catalytic membranes as heterogeneous catalysts provides an opportunity to reduce the cost of biodiesel production, as well as being environmentally and eliminating the catalyst separation step [1]. Membrane catalysts can be obtained by polymer modification or blending a good film-forming polymer, such as poly(vinyl alcohol) (PVA), with other active components [2]. Here we report the preparation of new catalytic PVA membranes blended with different ratios of poly (2-acrylamido-2-1-propanesulfonic acid) (PAMPS) crosslinked with succinic acid (SA) (see scheme 1). We also present the catalytic performance of the PVA/PAMPS membranes for the biodiesel production by transesterification of soybean oil in the presence of methanol.



Scheme 1. Crosslinking scheme of PVA/PAMPS blends with SA

Experimental Part

Membranes were prepared by casting a 6% (wt/v) solution of PVA/PAMPS blend in water. The selected blending ratios were 10, 20 and 30 wt% of PAMPS. The membranes were heated at 100 and 120 °C for 1 h under vacuum to crosslink the membrane and were characterized by FTIR. Swelling was determined gravimetrically and ion exchange capacity (IEC) was measured using an acid/base titration method. The transesterification reaction was carried out in a series of 12 mL screw-cap vials under stirring at 60 °C. Each vial was loaded with PVA/PAMPS membrane (equivalent to 0.068 mmol/g oil) and 6 mL of MeOH. Then, they were swelled in MeOH for 24 h. The reaction was started with the addition of 0.5 mL of vegetable oil. Biodiesel conversion was monitored periodically by ¹H-NMR.

Results and Discussions

Fig. 1 presents IEC and % methanol swelling of the PVA/PAMPS membranes cross-linked with 5% of SA at 120 °C and with 10% of SA at 100 °C, which presented a good balance between swelling properties, weight loss and stability in MeOH and soybean oil. The acidity and swelling of the membranes increase significantly with increasing PAMPS content present and cross-linked temperature. Fig. 2 shows the results of the transesterification reaction. It can be seen that, with the 80:20 and 70:30 PVA/PAMPS membranes crosslinked at 120 °C, less than 10 % biodiesel conversion was

obtained in 360 h. On the other hand, conversion increased considerably in the reaction catalyzed by the membranes crosslinked at 100 °C, reaching 94 and 93% respectively, and it remained stable at 94%.

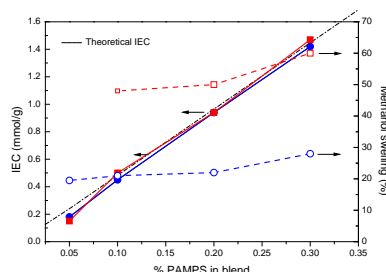


Fig. 1. IEC of PVA/PAMPS membrane with different blend ratio cross-linked (●) with 5 % SA at 120 °C for 1 h; (■) with 10 % SA at 100 °C. Methanol swelling of membrane cross-linked (○) with 5 % SA at 120 °C and (□) with 10 % SA at 100 °C

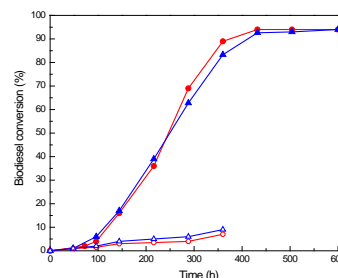


Fig. 2. Catalytic activity of PVA/PAMPS membranes (○) 80:20, (Δ) 70:30 crosslinked with 5% SA at 120 °C and (●) 80:20, (▲) 70:30 crosslinked with 10 % SA at 100 °C.

Conclusions

Catalytic activity for triglycerides of these membranes depends strongly on the crosslinking degree and on acid groups concentration. The best balance on catalytic activity and stability was found in PVA/PAMPS membranes crosslinked with 10 % of SA at 100 °C, which presented high catalytic activity with conversion to methyl esters between 90-94 %.

Acknowledgment: Catedras Conacyt and LANNBIO Cinvestav-Mérida

References

1. Casimiro, M.H.; Silva, A.G.; Alvarez, R.; Ferreira, L.M.; Ramos, A.M.; Vital, J.; Radiat. Phys. Chem. 2014, 94, 171.
2. Zhu, M.; He, B.; Shi, W.; Feng, Y.; Ding, J.; Li, J.; Zeng, F.; Fuel 2010, 89, 2299.



SYNTHESIS OF NEW CROSSLINKED FLUORINE-CONTAINING POLYNORBORNENE DICARBOXIMIDE

Ivette Aranda-Suárez¹, Arlette A. Santiago², Mercedes Gabriela Téllez Arias³, Joel Vargas¹

1. Instituto de Investigaciones en Materiales, Unidad Morelia, Universidad Nacional Autónoma de México, Antigua Carretera a Pátzcuaro No. 8701, Col. Ex Hacienda de San José de la Huerta, C.P. 58190, Morelia, Michoacán, México. jvargas@iim.unam.mx
2. Escuela Nacional de Estudios Superiores, Unidad Morelia, Universidad Nacional Autónoma de México, Antigua Carretera a Pátzcuaro No. 8701, Col. Ex Hacienda de San José de la Huerta, C.P. 58190, Morelia, Michoacán, México.
3. Facultad de Ingeniería Química, Universidad Michoacana de San Nicolás de Hidalgo, Morelia, Michoacán, C.P. 58060, México.

Introduction

In the last two decades, the use of engineering polymer membranes for gas separation has received a widespread attention. Currently, commercially available polymers for this purpose are glassy polymers, such as polysulfones, cellulose acetates and polyimides which offer high common solvent solubility, have good thermal and mechanical properties as well as excellent intrinsic CO₂/CH₄ separation properties.¹ Despite these attractive features, polymeric membrane performance is limited and challenged by plasticization. To enhance plasticization resistance, thermally and chemically crosslinked polymeric membranes have been developed for the separation of the more condensable gases.²

Experimental Part

Synthesis of monomer 1: An amount of norbornene-5,6 dicarboxylic anhydride (NDA) (1 g, 6 mmol) and 1.5 g (3 mmol) of 4,4'-(Hexafluoroisopropylidene)bis(*p*-phenyleneoxy)dianiline was dissolved in 30 mL of dichloromethane. The reaction was maintained at reflux for 2 h and then cooled to room temperature. The precipitate was recovered by filtration and dried. The obtained amic acid and anhydrous sodium acetate (2.2 g, 26.8 mmol) were dissolved in 30 mL of acetic anhydride, heated at 60–70 °C for 12 h and then cooled. The solid obtained is filtered and recrystallized from ethanol. The monomer 1 is white. Monomer 2 was synthesized according to the procedure previously reported.³

Synthesis of polymer 3: Monomer 1 (2.6385x10⁻³ g, 3.2545x10⁻³ mmol), monomer 2 (0.2 g, 0.6509 mmol), cis-1,4-Diacetoxy-2-butene ATC (2.2526x10⁻⁴ g, 1.3083x10⁻³ mmol) and Grubbs Catalyst, 2nd Generation (5.5647x10⁻⁴ g, 6.5547x10⁻⁴ mmol) were stirred in 5 mL of 1,2-dichloroethane at 45 °C for 24 h and then precipitated in excess methanol (Figure 1). The obtained polymer was soluble in chloroform.

Results and Discussions

4,4'-(Hexafluoroisopropylidene)bis(*p*-phenyleneoxy)dianiline reacted with NDA to the corresponding amic acid which was cyclized to imide using acetic anhydride as dehydrating agent. ¹H-NMR spectrum confirmed monomer structure and purity.

The crosslinked polymer 3 has a higher *T_g* (238 °C) in comparison with that of the uncrosslinked polymer obtained from monomer 2 (179 °C).

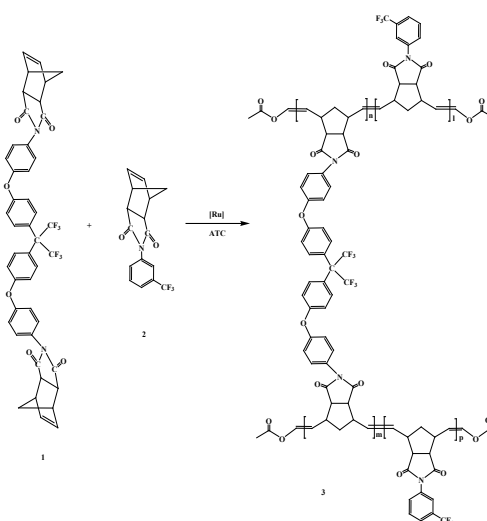


Figure 1. Synthesis of crosslinked polymer via ring-opening metathesis polymerization (ROMP).

Conclusions

The controlled chemical crosslinking via ROMP is an effective tool to improved the thermal as well as the mechanical properties of polynorbornene derivatives.

Acknowledgment: We thank CONACyT for generous support with contract 239947. Financial support from DGAPA-UNAM PAPIIT through the Project IA102115 is gratefully acknowledged.

References

1. Kraftschik, B.; Koros, W.J. *J Membr Sci* 2013;428:608.
2. Eguchi, H.; Kim, D.J.; Koros, W.J. *Polymer* 2015;58:121.
3. Cruz-Morales, J. A.; Vargas, J.; Santiago, A. A.; Vásquez-García, S. R.; Tlenkopatchev, M. A.; de Lys, T.; López-González, M. *High Performance Polymers*, 2016, en prensa.

ANTIFOULING ASYMMETRIC MEMBRANES: EFFECT OF COAGULATION BATH IN S-PPS FORMATION AND PROPERTIES

Marcial Yam¹, José Santiago¹, María Loría¹, Santiago Duarte¹, Francisco Ruiz², Manuel Aguilar¹.

1. Materials Unit Scientific Research Center of Yucatan, A.C., Address: Calle 43, ZIP code: 97205, City: Merida, Yucatan Country: Mexico. Email: mjav@cicy.mx
2. Departamento de Ingenierías y de Ingeniería y Ciencias Químicas, Universidad Iberoamericana, Prol. Paseo de la Reforma No. 880, Lomas de Santa Fe, México D. F. 01219

Introduction

Polyphenylsulfone PPS is widely used due to their high chemical, thermal and mechanical resistance. PPS could be used to prepare asymmetric membranes for microfiltration, MF, ultrafiltration, UF, Nanofiltration, NF and reverse osmosis, RO. This type of membranes shows a tendency to fouling due to its hydrophobic nature. An alternative to reduce PPS fouling is sulfonation, by trimethylsilyl chorosulfonate (TMSCIS)^{1,2}. The introduction of sulfonic groups in the main chain increases S-PPS hydrophilicity and enhances antifouling properties, permeate flux and selectivity; therefore; increases the cycle life of the asymmetric membranes. S-PPS asymmetric membranes are prepared through coagulation baths with non-solvents by phase immersion which allows the growth and development of porous structures with antifouling capacity. In this work S-PPS asymmetric UF membranes were obtained with three sulfonation degrees, SD (table 1). The linearized cloud point³ and the ternary phase diagrams were obtained from the cloud points data⁴, for polyphenylsulfone, PPS and sulfonated polyphenylsulfone, S-PPS. Two different coagulation baths were tested: acetone/isopropanol and acetic acid-NaHCO₃/isopropanol. The effect of PPS sulfonation degree, SD and coagulation bath on morphology and structure formation of the asymmetric membranes was studied as well as the antifouling capacity.

Table 1, Corresponding ratios of TMSCIS /polymer units in the reaction and SD determined for PPS at room temperature reaction in TCE.

Polymer code	Sulfonation agent(mL)/PPS (g)	PPS Sulfonation degree of polymer (%)
S-PPS-00	0.0	0
S-PPS-01	0.61	21
S-PPS-02	0.95	33
S-PPS-03	1.56	50

Experimental Part

9.6 gr de PPS was dissolved in 1,1,2,2 tetrachloethane, TCE, by addition of TMSCIS, under anhydrous conditions and nitrogen atmosphere at room temperature for 48 hours. The methods used for PPSU and S-PPS characterization and asymmetric membranes were FTIR, TGA, ¹H-RMN, SEM, CA, Porosity. The antifouling performance of PPS and S-PPS asymmetric membranes were determined by the follow equations:

$$FRR (\%) = \frac{J_{w1} - J_{w2}}{J_{w1}} \times 100; \quad R_r (\%) = \frac{J_{w2}}{J_{w1}} \times 100;$$

$$R (\%) = \left(1 - \frac{C_p}{C_f}\right) \times 100.$$

Using Bovine Serum Albumin, BSA, to determine the fouling capacity in a dead-end high pressure cell HP4750.

Results and Discussions

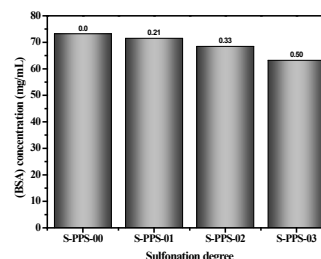


Figure 1. BSA static absorption, PSA, tests in PPS and S-PPS asymmetric membranes obtained from AA-NaHCO₃/isopropanol coagulation bath shows a decreasing fouling effect as SD increases in PPS.

Table 2. Porosity, medium pore radio, and fouling properties of PPS and S-PPS asymmetric membranes.

Membrane code	ε (%)	r _m (nm)	Rejection (%)	FRR (%)	R _r (%)
S-PPS-00	67.6 ± 2.1	0.1	20.8	41.7	22.3
S-PPS-01	70.4 ± 0.7	2.3	27.8	47.5	35.8
S-PPS-02	46.7 ± 3.0	4.5	16.4	63.9	57.9
S-PPS-03	51.7 ± 1.8	0.2	59.2	70.0	56.1

The results indicate that rejection, R (%) increase with SD as well as flux recovery ratio FRR and R_r. FRR and R_r results indicate that PSA diminish with increased SD and indication of boundary layer formation on the surface weakening protein absorption in the membrane.

Conclusions: S-PPS with three different SD: 21, 33 and 50 % in a controlled reaction using 1, 1, 2, 2, TCE and TMSCIS.. S-PPS UF asymmetric membranes were successfully developed from polymeric solution in acetic acid-NaHCO₃/isopropanol coagulation bath. This bath allows a better control for nucleation and growth pores avoiding the macrovoids formation in all S-PPSU. The resultant S-PPS asymmetric membranes show increasing antifouling properties as SD increases due to higher hydrophilicity and weakening protein absorption.

Acknowledgment: the authors are gratefully acknowledged by the financial support from CONACYT, through the grant no.344563. CICY for allow to pursue my doctoral studies.

References

1. A. Dyck, D. Fritsch, and S. P. Nunes. *J. Appl. Polym. Sci.* 2002, 86, 2820.
2. E. Parceró, R. Herrera, and S. P. Nunes. *Memb. Sci.*, 2006, 285, 206.
3. J. C. Jansen, S. et. al., *Memb. Sci.*, 2013, 447, 117.
4. R. M. Boom and C. A. Smolders. *Polymer*, 1993, 34, 2348..



EFFECT OF ADDING FERROUS SOLUTIONS ON CHEMICAL AND THERMAL STABILITY OF CHITOSAN MEMBRANES

Juan Carlos Castro Alcántara¹, Mariana Cerda Zorrilla¹, José Antonio Azamar Barrios¹

1. Centro de Investigación y de Estudios Avanzados del Instituto Politécnico Nacional, Unidad Mérida, Antigua Carretera a Progreso Km.6, Cordemex, 97310, Mérida, Yucatán, México. jiencarlos@gmail.com

Introduction

During the last three decades the chitosan has been studied and used as biomaterial for a wide variety of medical and industrial applications due to its properties like biocompatibility, non-toxicity and antimicrobial activity. There are reactive functional groups in the molecule of chitosan. Neutralization of chitosan materials by immersion into ethanol and NaOH solutions in order to improve its chemical stability has been reported.^{1,2} Furthermore, it has reported a positive effect on the stability of chitosan films by aggregation of glycerin.³ In this work the aggregation of ferrous solutions during the preparation of chitosan membranes as a novel method for increasing both the chemical stability and thermal stability of chitosan materials is studied.

Experimental Part

A 1% w/v chitosan of medium molecular weight solution in 5% v/v acetic acid solution was prepared (CS). A ferrous solution (FS) with 1 mM $(\text{NH}_4)_2\text{Fe}(\text{SO}_4)_2$, 1 mM NaCl and 0.4 M H_2SO_4 was prepared. Mixtures with concentrations shown in Table 1 were cast on petri dishes and then were dried at 50 °C in order to obtain the corresponding MQ, MQF and MQF-G membranes. After drying, a MQF membrane was neutralized by its immersion into 40% v/v ethanol solution for 10 minutes and then washed with deionized water, this membrane was abbreviated as MQF-E. Another MQF membrane was neutralized by its immersion into 0.1 M NaOH solution for 10 minutes and then washed with deionized water, this membrane was abbreviated as MQF-NaOH. UV-vis spectra of all membranes were obtained, using an A&E Co. UV16008 spectrophotometer, for up to 92 days. TGA analysis of MQ and MQF were performed with a TA Instruments Discovery.

Table 1. Volume percentages of the mixed solutions for membrane preparation.

Membrane	% CS	% FS	% Glycerin
MQ	100	0	0
MQF	98	2	0
MQF-G	95	2	3

Results and Discussions

Fig. 1 shows the changes in absorbance of the membranes versus time. Absorbance of MQF-G and MQF-NaOH membranes exhibit a growing trend. MQF-E presents the greatest variation in

absorbance. MQ is stable for up to 40 days and then starts to oxidize. MQF membrane has the less variation in the absorbance indicating that addition of ferrous solution extends the stability of chitosan membranes.

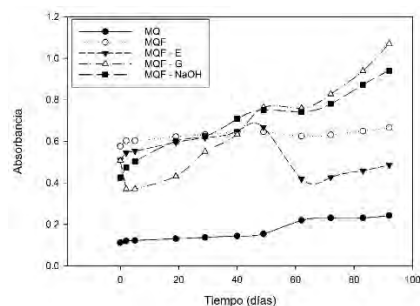


Figure 1. Absorbance at 304 nm of different membranes versus time elapsed from its preparation.

In Fig. 2 can be seen an increase in the thermal stability of the chitosan membranes due to aggregation of the ferrous solution, corresponding to an increase in the depolymerization temperature of about 100 °C.

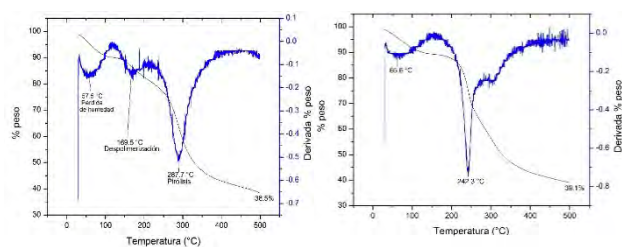


Figure 2. TGA and its first derivative of MQ (left) and MQF (right).

Conclusions

Aggregation of the ferrous solution to membranes of chitosan increases both chemical and thermal stability, since a decrease in the chemical reactivity and an increase in depolymerization temperature of MQF membranes was observed. An additional neutralization process is not necessary.

References

- He, Q.; Ao, Q.; Gong, Y.; Zhang, X. *J. Mater Sci* 2011, 22, 2791.
- Noriega, S. E.; Subramanian, A. *Int. J. Carbohydrate Chem* 2011, 13.
- Kim, K. M.; Son, J. H.; Hanna, M. *J. Food Sci. Eng.* 2006, 71, 119.



ADMET POLYMERIZATION USING GREEN CHEMISTRY

Taylor W. Gaines¹, Kathryn R. Williams¹, Kenneth B. Wagener^{1*}, Giovanni Rojas^{1,2*}

1. Butler Polymer Research Laboratory, Department of Chemistry, University of Florida, Gainesville, FL 32611-7200, USA
2. Universidad Icesi, Facultad de Ciencias Naturales, Departamento de Ciencias Químicas, Calle 18 No. 122 -135, Cali, Colombia grojas@icesi.edu.co

Introduction

A variety of complex materials have been created via ADMET polymerization, including various types of branched polyethylenes,^{1,4} and polyolefins functionalized with hydroxyls,⁵ carboxylics,⁶ phosphonics,⁷ halogens,⁸ to name a few. Many of these materials are synthesized in a precise manner in which functional groups are placed in exact locations along polymer backbones. Precision results from the selective ADMET reaction of symmetrical α,ω -diene monomers (**Figure 1**) using tolerant and robust catalysts. Effective control of polymerization conditions eliminates unintentional side reactions and defects, yielding precision materials. We now report the expansion of ADMET's versatility, using microwave irradiation, a technique synonymous with control.⁹

Experimental Part

The 1,9-decadiene monomer was purchased from Sigma-Aldrich and purified either by potassium mirror or by passing through a silica plug using hexanes as the solvent, followed by rotary evaporation. Monomers tricoso-1,22-diene-12-ol and undecyl-1,10-diene-6-ol were prepared by previously reported methods.⁵ Methylene chloride was obtained from a solvent system; 1,2-dichlorobenzene was stored over alumina for at least 24 hours prior to use.

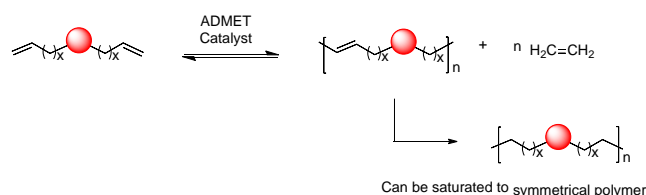


Figure 1. ADMET Polymerization and subsequent alkene saturation providing a precision polyolefin

Results and Discussions

We chose the CEM Discover S-Class microwave reactor, which is capable of either fixed-power with a specified maximum temperature, T_{max} , or fixed-temperature operation. Here, the fixed-power mode is referred to as “pulsed.” In pulsed mode the reactor irradiates the sample at the specified microwave power until the maximum temperature is reached; subsequently, the microwave power (at one-half the specified wattage) is applied intermittently to sustain T_{max} . In the fixed temperature mode, the programmed power level remains constant until the preset

temperature is reached. Then, the temperature is maintained by continuous irradiation at very low power (a few watts). The reactor also can be programmed for maximum pressure, sealing the reaction chamber; in this work the reaction vessel remains open for the removal of ethylene driving the reaction forward to polymer product.

Confirmation of microwave success is provided by ¹H-NMR evidence, where progress of the reaction is monitored in the 5-6 ppm region. The internal and external proton resonances of the terminal double bond in monomer are well separated at about 5 ppm (=CH₂) and 5.8 ppm (=CH-), while those for internal alkenes occur at 5.4 ppm. Thus, during polymerization the multiplets at 5 and 5.8 ppm gradually disappear as the polymer resonance at 5.4 ppm grows, indicative of high-molecular weight polymer formation.

Conclusions

Microwave irradiation enhances ADMET polymerization of α,ω -dienes by shortening the time required to produce high molecular weight polymers of the step variety. The pulsed mode, which used higher power, provided a slight advantage. A variety of solvents, catalysts, and ethylene removal techniques can be used to synthesize polyolefins in a microwave reactor. No perceptible difference in reaction enhancement was observed for alcohol monomers; microwave reactors are viable for polymerizing both non-polar and polar substrates. Without question, microwave-assisted ADMET chemistry offers an advantage over the typical oil bath-heated polymerizations by essentially tripling molecular weights in the same time period.

References

1. Wagener, K. B.; Valenti, D.; Hahn, S. F. *Macromolecules* **1997**, *30*, 6688.
2. Sworen John, C.; Smith Jason, A.; Wagener Kenneth, B.; Baugh Lisa, S.; Rucker Steven, P. *J Am Chem Soc* **2003**, *125*, 2228.
3. Rojas, G.; Inci, B.; Wei, Y.; Wagener, K. B. *J. Am. Chem. Soc.* **2009**, *131*, 17376.
4. Inci, B.; Wagener Kenneth, B. *J Am Chem Soc* **2011**, *133*, 11872.
5. Valenti, D. J.; Wagener, K. B. *Macromolecules* **1998**, *31*, 2764.
6. Baughman, T. W.; Chan, C. D.; Winey, K. I.; Wagener, K. B. *Macromolecules (Washington, DC, U. S.)* **2007**, *40*, 6564.
7. Opper, K. L.; Fassbender, B.; Brunklaus, G.; Spiess, H. W.; Wagener, K. B. *Macromolecules (Washington, DC, U. S.)* **2009**, *42*, 4407.
8. Boz, E.; Wagener, K. B.; Ghosal, A.; Fu, R.; Alamo, R. G. *Macromolecules* **2006**, *39*, 4437.
9. Kappe, C. O.; Dallinger, D.; Murphree, S. S.; Editors *Practical Microwave Synthesis for Organic Chemists: Strategies, Instruments, and Protocols*, 2009



SYNTHESIS AND CHARACTERIZATION OF SILICON-CONTAINING AROMATIC POLY(AZOMETHINE)S. A STUDY OF MOLECULAR FLEXIBILITY

Claudio A. Terraza,¹ Luis H. Tagle,¹ Rene A. Hauyon,¹ Patricio A. Sobarzo,¹ Pablo A. Ortiz,¹ Alain Tundidor-Camba,¹ Carmen M. González-Henríquez²

¹ Pontificia Universidad Católica de Chile, Faculty of Chemistry, P.O. Box 306, Santiago, Chile (cterraza@uc.cl)

² Universidad Tecnológica Metropolitana, José Pedro Alessandri 1242, Ñuñoa, Santiago, Chile.

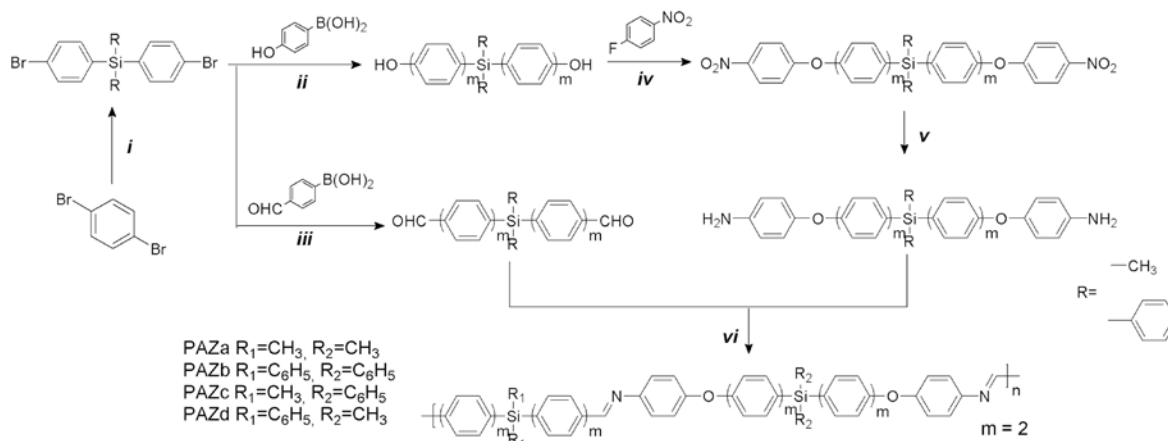
Introduction

The poly(azomethine)s (PAZs) also called poly(imine)s and poly Schiff bases have attracted the attention of many researchers in recent decades because of their excellent properties like high thermal stability, mechanical strength, electrical conductivity, non-linear optical activity, ability to form chelates and catalyst^{1,2}. PAZs containing various aromatic and/or aliphatic groups in the main chain have been investigated in optoelectronic devices as host materials, and as chemosensors because their acidochromic properties¹⁻⁴. However, PAZs have a drawback, and that is their low solubility in common organic solvents and high glass transition temperature, both factors contributing to a decrease in their processability. To solve this problem, different strategies have been used like the incorporation of flexible or non-planar moieties like oxyether and thioether function in the main chain and also bulky side groups to improve their processability. The

bromophenyl)diorganosilane with 4-formylphenylboronic acid, while the diamines were synthesized from bis-(4-bromophenyl)diorganosilane and 4-hydroxyphenylboronic acid. The obtained dibiphenol reacts with 1-fluoro-4-nitrobenzene to give the dinitro derivatives, to finally reduce them with hydrazine monohydrate using Pd/C as catalyst agent. The first two reactions were accomplished in nitrogen atmosphere which are summarized in Scheme 1. All compounds were characterized by FTIR, ¹H, ¹³C and ²⁹Si NMR spectroscopy and the results are in agreement with the proposed structures.

Results and Discussions

Thermal and optical properties of new PAZs were measured. The results suggest that these new polymers could be suitable Materials for advanced applications how host material in



incorporation of heteroatoms like Si in the main, can achieve a high solubility because of the longer and flexible C-Si bond⁵. In this work, we present the synthesis of new aromatic PAZs obtained from diamine (1a-b) and dialdehyde (2a-b) by polycondensation in solution. All monomers were synthesized with a central silicon atom, while diamines have the oxyether function incorporated to increase the polymers processability.

Experimental Part

The polymer synthesis was carried out by multiple synthetic steps. All monomers were synthesized from 1-4-dibromobenzene. The dialdehydes were synthesized by Suzuki-Cross coupling of bis-(4-

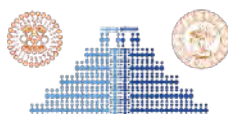
technological devices because their good thermal and optical behavior.

Acknowledgment:

All authors Acknowledge FONDECYT grant 1150157 to support.

References:

- ¹ *Polym. Rev.*, **44**, 131-173 (2004).
- ² *J. Mater. Chem.*, **20**, 937-944 (2010).
- ³ *Synt. Met.*, **160**, 2065-2076 (2010).
- ⁴ *Spectrochim. Acta Part A: Molecular and Biomolecular Spectroscopy*, **140**, 398-406 (2015).
- ⁵ *RSC Adv.*, **5**, 49132-49142 (2015).



A ROUTE TO PRECISE SUPRAMACROMOLECULAR CONSTRUCTS:
QUANTITATIVE MOLECULAR FISSION AND FUSION

George R. Newkome

1. *Departments of Polymer Science and Chemistry, The University of Akron, Akron, Ohio 44326, newkome@uakron.edu*

Abstract

One of the most interesting questions is - can supramacromolecular compounds be quantitatively made in precise manner each and every time. In fact, there are very few organic materials that are constructed from monomers in one-step *and* possess a perfect structure. In the nineties, our first attempts used <tpy-M²⁺-tpy> connectivity, where tpy = [2,2':6',2'']-terpyridine, but this methodology gave perfect metallo dendrimers but not quantitatively.¹ This then led to using simple, perfect simple polycarboxylates to be the counterions for different metalloconstructs,² possessing a very accurate size, shape, and structure. Thus, perfectly directed structural rigidity and diverse modes of different metal connectivity have given avenues to the construction of three-dimensional supramolecular materials predicated on similar, as well as dissimilar polytopic ligands.³⁻⁵ Progress from very simple ring structures, based on 120°- and 60°-juxtaposed *bisterpyridines*, led to a combination of multiple, building blocks, affording entrée to the quantitative synthesis of precise macromolecular architectures⁶ (Figures 1 and 2). The structural implications of reaction concentration on the assembly process will be introduced, especially based on forming labile coordinative bonds and resulting in the formation of thermodynamically favored products. The construction of novel 3D architectures will be demonstrated then the introduction of concept of molecular fission/fusion⁷ to lastly demonstrate how this leads to precise nano-scale polygons, generated in quantitative yields.^{8,9}

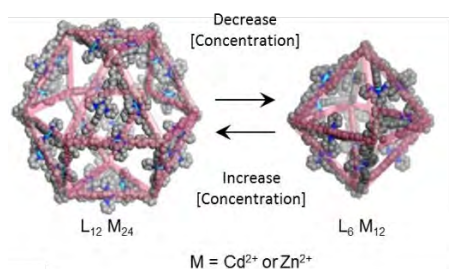


Figure 1. Dynamic equilibrium between a cuboctahedron ($L_{12}M_{24}$) and an octahedron (L_6M_{12}). A single, *tertrakisterpyridine* building block (L) self-assembles in the presence of an exact amount of metal (M) to give the Archimedean shapes.

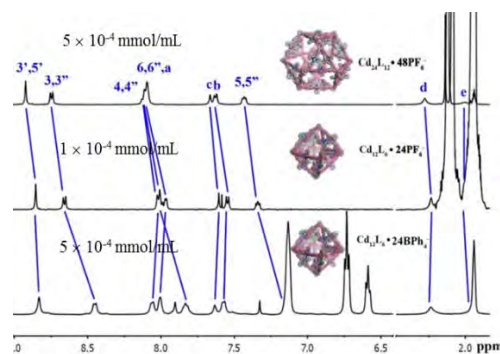
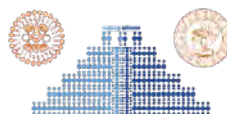


Figure 2. The stacked series of ¹H NMR spectra illustrates the change in architecture upon dilution of the cuboctahedron to give the octahedron. A change in counterion species is also observed to give the smaller octahedron construct.

Acknowledgment: The author is grateful to the National Science Foundation (GRN-CHE 1151991) for financial support.

References

1. Newkome, G. R.; Cardullo, F.; Constable, E. C.; Moorefield, C. N.; Thompson, A. M. W. C. *J. Chem. Soc., Chem. Commun.* 1993, 925.
2. Wang, P.; Moorefield, C. N.; Jeong, K.-U.; Hwang, S.-H.; Li, S.; Cheng, S. Z. D.; Newkome, G. R. *Adv. Mater.* 2008, 20, 1381.
3. Perera, S.; Li, X.; Soler, M.; Wesdemiotis, C.; Moorefield, C. N.; Newkome, G. R. *Chem. Commun.* 2011, 47, 4658.
4. Schultz, A.; Li, X.; McCusker, J. K.; Moorefield, C. N.; Castellano, F. N.; Wesdemiotis, C.; Newkome, G. R. *Chem. Eur. J.* 2012, 18, 11569.
5. Ludlow III, J. M.; Tominaga, M.; Chujo, Y.; Schultz, A.; Lu, X.; Xie, T.; Guo, K.; Moorefield, C. N.; Wesdemiotis, C.; Newkome, G. R. *Dalton Trans.* 2014, 43, 9604.
6. Lu, X.; Li, X.; Guo, K.; Xie, T.-Z.; Moorefield, C. N.; Wesdemiotis, C.; Newkome, G. R. *J. Am. Chem. Soc.* 2014, 136, 18149.
7. Xie, T.-Z.; Guo, K.; Guo, Z.; Gao, W.-Y.; Wojtas, L.; Ning, G.-H.; Huang, M.; Lu, X.; Li, J.-Y.; Liao, S.-Y.; Chen, Y.-S.; Moorefield, C. N.; Saunders, M. J.; Cheng, S. Z. D.; Wesdemiotis, C.; Newkome, G. R. *Angew. Chem. Int. Ed.* 2015, 54, 9224.
8. Newkome, G. R.; Moorefield, C. N. *Chem. Soc. Rev.* 2015, 44, 3954.
9. Ludlow III, J. M.; Newkome, G. R. *Progress in Heterocyclic Chemistry* 2016, doi:10.1016/bs.aihch.2016.04.008.



PHOTOCURING KINETICS OF A TERNARY ACRYLATE-THIOL-OXETANE SYSTEM

Ricardo Acosta Ortiz ¹, Darío Trujillo Arriaga², Omar Acosta Berlanga ³, Aida Esmeralda García Valdéz ³,

1. Centro de investigación en química aplicada, Blvd Enrique Reyna #140, 26294, Saltillo, Coahuila,

Mexico ricardo.acosta@ciga.edu.mx

2. Departamento de Ingeniería Química, Universidad de Sonora,

3. Facultad de Ciencias Químicas UAdeC, Blvd Venustiano Carranza e Ing. Jose Cardenas Valdez, Saltillo, Coahuila, Mexico

4. Centro de Investigación en Química Aplicada, Blvd Enrique Reyna #140, 26294, Saltillo, Coahuila, Mexico

Introduction

The need for rapid and efficient photocurable systems aimed for 3-D printing using the technique of stereolithography, have led to pursue the development of hybrid systems. By combining the features of two or more polymerizable systems is possible to obtain materials with tailorable properties. At the same time disadvantages like oxygen inhibition in the radical polymerization and lack of good mechanical properties can be overcome. For instance, the more utilized acrylates, polymerize very rapidly and the obtained polymers present good mechanical properties. However, the polyacrylates are fragile due to the highly cross-linked network characteristic of these materials. The introduction of a soft-phase can enhance the lack of toughness of the polyacrylates. The polythioethers derived from the thiol-ene photopolymerization can fulfill this role of soft-phase due to their flexibility and low T_g. Moreover, the highly reactive oxetanes and the excellent mechanical properties of the polyethers derived from them, can enhance the properties of the final copolymer. Thus, in this work was investigated the effect of concurrently photopolymerizing a ternary system including acrylates, oxetanes and multifunctional thiols.

Experimental Part:

The oxetane monomer OXT 121 whose chemical name is 1,4-Bis[(3-ethyl-3-oxetanyl)methoxy]methyl]benzene, and the acrylate bisphenol F ethoxylate (2 EO/phenol) diacrylate (BFDA) were kindly donated by Nagase Co. The curing agent ALA4 was prepared according to a previously reported method [1]. The tetrafunctional thiol pentaerythritol tetrakis (3-mercaptopropionate (PTKMP)) was purchased from Sigma-Aldrich. Kinetics of photopolymerization were determined by real-time FTIR spectroscopy (RT-FTIR). The photocurable formulations were irradiated inside the compartment of the IR spectrometer with a UV light intensity of 40 mW/cm² and 85 °C. This temperature was achieved using a Pike technologies heat solid transmission cell. The bands at 2570 cm⁻¹ corresponding to the thiol groups, at 1646 cm⁻¹ characteristics of the double bond of the acrylates and 827 cm⁻¹ for the oxetane rings were monitored simultaneously.

Result and Discussion

Figure 1 depicts the conversion profiles for each functional group, namely, acrylates, oxetanes and thiol groups. It is observed that both the acrylates and the oxetanes displayed analogue photopolymerization rate (slope of the curves) which denote a high reactivity, achieving conversions of 75 and 65 % respectively in 50 seconds. The thiols groups showed lower photopolymerization rates and also lower conversion (52 %) after 200 seconds.

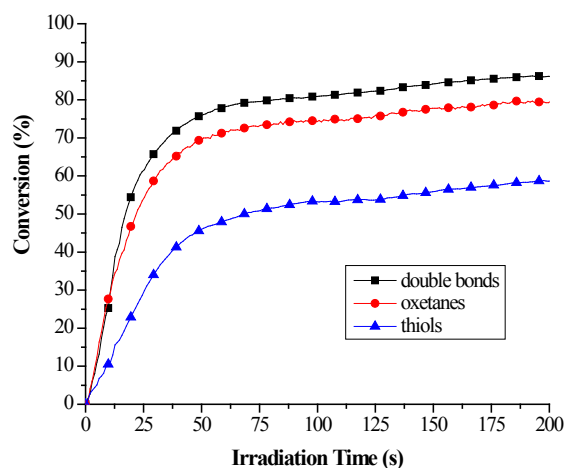


Fig.1 Comparison of conversion profiles of the photocurable formulation of OXT 121, PTKMP and BFDA.

Conclusion

A highly reactive ternary photocurable systems was developed. . The formed thioether groups attacked the acrylates by a nucleophilic thiol-Michael addition and also the oxetanes, to induce their anionic polymerization producing a polyether- polyacrylate- polythioether.

References

1. Ricardo Acosta Ortiz, Aida Esmeralda Garcia Valdez, Ana Gabriela Navarro Tovar, Adrian Alejandro Hilario de la Cruz, Luis Fernando Gonzalez Sanchez, Justo Horacio Trejo Garcia, Jorge Felix Espinoza Muñoz, Marco Sangermano; Development of a photocurable epoxy-amine/thiol-ene system. *Journal of Polymer Research*, 2014, 21, 504



ETHYLENE POLYMERIZATION WITH MONOMETALIC ZIRCONOCENE HYDRIDE CATALYSTS

María Teresa Córdova¹, Maricela García¹, Odilia Pérez^{1*}

1. Centro de Investigación en Química Aplicada, Blvd. Enrique Reyna Hermosillo 140, 25253, Saltillo, México. odilia.perez@ciqa.edu.mx

Introduction

Pentamethylzirconocene dihydride ($Cp_2^*ZrH_2$) was reported by Bercaw since 1970 as intermediate specie in organic syntheses. This complex was also used as selective reducing agent of CO ligands, and also in homogeneous hydrogenation catalysis.^{1,2} Though $Cp_2^*ZrH_2$ contains the appropriate chemical features of metallocene complexes it has not been used as polymeric catalyst. In this work we studied the ethylene polymerization in homogeneous phase, using the monometalic $Cp_2^*ZrH_2$ activated with $B(C_6F_5)_3$, at several polymerization conditions, which showed high activities and high density polyethylene (HDPE) of high M_w . The monometalic catalytic specie exhibited different kinetic behavior in the ethylene polymerizations, compared with bimetallic hydrides or classical metallocene catalysts.

Experimental Part

Polymerizations were carried out in a 600 mL stainless steel reactor, varying temperature (30, 50 and 70 °C), solvents (hexane, heptane and its mixtures), setting up boron/Zr ratio to B/Zr = 5, agitation to 500 rpm and reaction time of 30 min. Zirconium concentration was established at 1.7×10^{-6} mol for all the reactions, and 0.5 mmol of triisobutylaluminium (TIBAL) were used as scavenger for 150 ml of solvent. The catalytic activity of the $Cp_2^*ZrH_2/B(C_6F_5)_3$ system for each experiment, was calculated dividing the polymer amount obtained in grams, between mol of Zr added to the reactor, and time of polymerization. Molar mass (M_w) and molar mass distribution (\bar{D}) of the polymers were determined by gel permeation chromatography (GPC) at high temperature, and the morphology of the polyethylenes was analyzed by scanning electronic microscopy (SEM).

Results and Discussions

Table 1 shows the results of the ethylene polymerizations with the $Cp_2^*ZrH_2/B(C_6F_5)_3$ system, where high activities were obtained at different reaction conditions. The catalytic system led to higher M_w of the polymers and activities, at 30 °C, what could be related to the higher stability of the catalyst at this temperature. Solvent and mixture of solvents affected the dispersity of the molar masses (\bar{D}) produced in the polymers, where different ionic pairs of the catalytic system could have been formed between the zirconocene dihydride [$Cp_2^*ZrH_2$] and the co-catalyst [$B(C_6F_5)_3$],

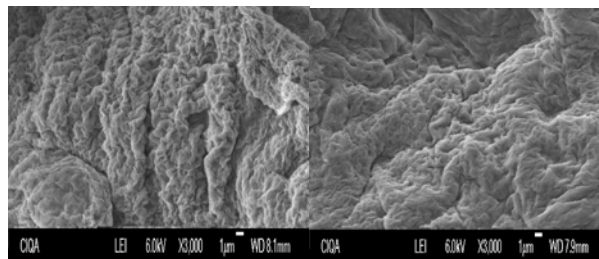


Figure 1. SEM microscopies of HDPE obtained with $Cp_2^*ZrH_2/B(C_6F_5)_3$ system left (Exp. 1), right (Exp. 3).

because their solubility. Ethylene pressure was set at 42 psi, in order to compare the temperature effect and kind of solvent, however, one experiment at 65 psi of ethylene was carried out, where an increase of the activity, close to 50 %, was observed, as well as higher M_w of the polyethylene. HDPE showed morphology, similar to polymers formed in heterogeneous phase.

Table 1. Polymerization reactions of ethylene with $Cp_2^*ZrH_2$

Exp	T (°C)	P (psi)	Solvent (Hex:Hep)	Activity KgPE/molZr	M_w (10^{-3})	\bar{D}
1	30	42	Hex	1108	460	5.0
2	30	65	Hex	3322	805	3.9
3	30	42	1:1	1895	502	4.4
4	30	42	2:1	1848	621	8.3
5	50	42	Hex	1991	493	3.9
6	70	42	Hex	858	143	2.4

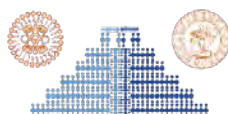
Conclusions

The monometalic catalytic system $Cp_2^*ZrH_2/B(C_6F_5)_3$ produced HDPE with high activity and high M_w , of good morphology, comparable to polymers produced with heterogeneous systems.

Acknowledgment: To CONACYT, project 167901, Myriam Lozano, Ma. Guadalupe Méndez and Josefina Zamora for polymer characterizations.

References

- Paul J. Chirik, Michael W. Day, and John E. Bercaw, *Organometallics*, 1999, 18, 1873-1881.
- J.M. Manriquez, D.R. McAlister, R.D. Sanner, and J.E. Bercaw, *J. Am. Chem. Soc.*, 1978, 100, 9, 2716-2724.



SÍNTESIS Y CARACTERIZACIÓN DE POLIMETACRILATO DE 4-(2-TIOFENIL) BENCILO

Felipe Gallardo¹, Juan Pablo Soto¹, Juliet Aristizabal¹, Juan Carlos Ahumada¹, Cindy Escalona¹, Víctor Rojas¹

1. Laboratorio de Química Orgánica 1, Instituto de Química, Pontificia Universidad Católica de Valparaíso, Avenida Universidad 330, Curauma, 2340025, Valparaíso, Chile. felipe.gallardo.v@gmail.com.

Introducción

La combinación de polímeros de adición con moléculas conjugadas promueve la obtención de macromoléculas que incorporan las propiedades que ambos poseen, por ejemplo podemos mencionar el aumento de la solubilidad, estabilidad y procesamiento, destacando en este campo la combinación PEDOT:PSS¹. En la continua búsqueda de materiales con propiedades similares es que se han propuesto funcionalizaciones de matrices poliméricas de adición con grupos potencialmente electropolimerizables, para estudiar sus propiedades térmicas y electroquímicas^{2,3}. En este trabajo se presenta la síntesis y caracterización del polimetacrilato de 4-(2-tiofenil)benzilo y el estudio de las propiedades térmicas y electroquímicas del material resultante.

Desarrollo Experimental

La síntesis del monómero se realizó a través de cuatro pasos de reacción, el primero fue la protección del grupo hidroxilo utilizando 3,4-dihidro-2H-pirano, obteniendo el éter THP. Posteriormente, se realizó el acoplamiento de Kumada, empleando el 2-bromotiofeno, para obtener el 4-(2-tiofenil) éter THP, para a continuación realizar la desprotección del grupo hidroxilo. Finalmente se hizo una esterificación de Steglich para la obtención del monómero. La polimerización se realizó con peróxido de benzoilo a 80°C, durante 5 horas utilizando tolueno como solvente, una vez finalizado se agregó metanol y se filtró a vacío, obteniendo un sólido de color amarillo. El monómero y polímero, al igual que los productos de la ruta de síntesis expuesta en la figura 1, fueron caracterizados mediante espectroscopia FTIR y RMN. Finalmente las propiedades térmicas del polímero fueron estudiadas empleando calorimetría diferencial de barrido (DSC).

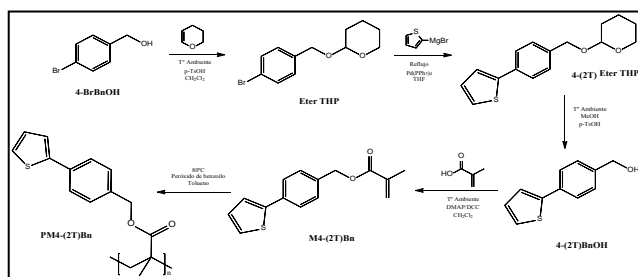


Figura 1. Ruta de síntesis para la obtención del PM4-(2T)Bn.

Resultados y Discusiones

En la figura 2 se observa la comparación de los espectros FTIR del monómero y polímero, donde se comprueba la presencia del grupo carbonilo (1716 y 1724 cm⁻¹) y enlace C-O (1156 y 1140 cm⁻¹), por otra parte, la banda correspondiente a C=C solo está

presente en el monómero (1624 cm⁻¹) y se observa una mayor contribución de las bandas presentes en el espectro del polímero.

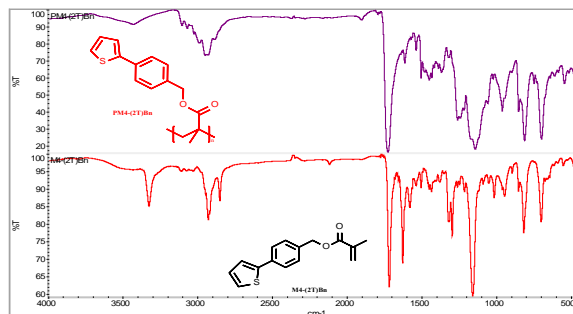


Figura 2. Espectros FTIR de M4-(2T)Bn y PM4-(2T)Bn en KBr.

En el espectro de RMN ¹H del polímero se observa la presencia de los protones correspondientes al grupo CH₂ que está unido al oxígeno del éster (δ=4.85 ppm), además la señal del grupo metil del polimetacrilato aparece a δ=0.74 y 0.99 ppm, lo que indica que el polímero presenta tacticidad (sindiotáctico y atáctico). Por otra parte a δ=1.84 ppm se observa la contribución correspondiente al grupo CH₂ del polimetacrilato. Por su parte, en el espectro RMN de ¹³C se observa la aparición de la señal correspondiente al grupo metil (δ=18.3 ppm), al grupo carbonilo (δ=167 ppm), al carbono cuaternario del metacrilato (δ=45 ppm) y al grupo CH₂ (δ=66.4 ppm) que está unido al oxígeno del éster. La zona aromática de los espectros antes mencionados son similares para el monómero y polímero, siendo su única diferencia el aumento de las contribuciones en el segundo de ellos. Finalmente el termograma de DSC muestra que el polímero es termoestable en un rango de 200 °C, no presentando transición vítrea ni de fusión.

Conclusiones

Se logró sintetizar de forma satisfactoria el PM4-(2T)Bn, el cual fue caracterizado mediante IR, RMN ¹H y ¹³C. Además se realizó un estudio de sus propiedades térmicas mediante DSC, cuyo resultado arrojó que la macromolécula presenta un comportamiento termoestable.

Agradecimientos: Los autores agradecen a: Beca CONICYT 21150662; A la Vicerrectoría de Investigación y Estudios Avanzados de la PUCV por las Becas de Arancel y Mantenimiento.

Referencias

- Ouyang J, Chu C-W, Chen F-C, Xu Q, Yang Y. Adv Funct Mater. 2005;15(2):203-8.
- Hu Z, Fu B, Aiyar A, Reichman E. J Polym Sci Part Polym Chem. 2012;50(2):199-206.
- Barik S, Valiyaveetil S. Macromolecules. 2008;41(17):6376-86.

CONTROLLED SYNTHESIS OF α,ω -TELECHELIC PDMS

M. Soledad Lencina¹, Viviana Hanazumi², Leonardo Redondo², Camila Müller²,
Daniel Vega¹ Mario Ninago², Andrés Ciolino², Marcelo Villar²

¹Instituto de Física del Sur, (IFISUR, UNS-CONICET), Universidad Nacional del Sur, Av. Alem 1253, (8000) Bahía Blanca, Argentina

²Planta Piloto de Ingeniería Química (PLAPIQUI; UNS-CONICET), Camino “La Carrindanga” Km 7, (800) Bahía Blanca, Argentina.

Introduction

One of the goals of polymer chemistry is developing new synthetic pathways for the controlled synthesis of polymers with predictable, well-defined structures. Living anionic polymerization provides one of the best methodologies for synthesizing complex macromolecular structures such as block or graft copolymers, stars and functional macromolecules¹. Among them, the synthesis of telechelic polymers is of interest because these kind of macromolecules allow synthesizing model polymer networks, whose mechanical and rheological properties provides the key to design “tailor-made” engineering materials. In this work we report the synthesis of α,ω -vinyl terminated PDMS (B2V) by employing a novel bifunctional initiator. The synthesis involves high-vacuum anionic polymerization techniques and the sequential addition of specific reagents, starting from commercial diglycidylether terminated poly(dimethylsiloxane) (PDMS-DGE). The final reaction product was characterized by conventional analytical techniques, such as SEC, ¹H-NMR and FTIR.

Experimental Part

Reagents were purified under high-vacuum, by employing standard procedures². The initiator, *sec*-butyllithium (*sec*-Bu⁻Li⁺) was freshly synthesized from *sec*-butylchloride and lithium metal. Vacuum-sealed ampoules from commercial diphenylethylene (DPE), PDMS-DGE, and hexamethyl(cyclotrisiloxane) monomer (D₃) were obtained. Cyclohexane (CH) and tetrahydrofuran (THF) were employed for D₃ polymerization. Chlorodimethylvinyl silane (CDMS) and well-degassed methanol were employed as terminating agents. The main polymerization reactor was designed by employing glass-blowing techniques. Vacuum-sealed ampoules of reagents were attached to the main reactor, connected to the vacuum line and checked for pinholes. Then, purified CH was distilled. The reactor was detached from the vacuum line by heat-sealing procedures, and DFE ampoule was broken. After that, *sec*-Bu⁻Li⁺ was added and the reaction was left to proceed during 3 h in order to obtain the corresponding adduct. After that, PDMS-DGE ampoule was broken to promote oxyraning opening at both ends. After 24 h, D₃ ampoule was added. The reaction was left to proceed during 20 h at room temperature, and then THF ampoule was broken to promote polymerization. A sample ampoule was taken after 24 h, and the reaction product was precipitated in cold methanol (B2OH). After that, the CDMS ampoule from the main polymerization reactor was broken. The resulting polymer was precipitated in methanol, washed with 10 wt% aqueous sodium bicarbonate solution, extracted with

water/ether, and precipitated in cold methanol. The resulting polymers were characterized by conventional techniques, such as SEC, ¹H-NMR, and FTIR.

Results and Discussions

Figure 1 show the SEC chromatographs for B2OH and B2V, together with the results obtained for the molar mass distributions.

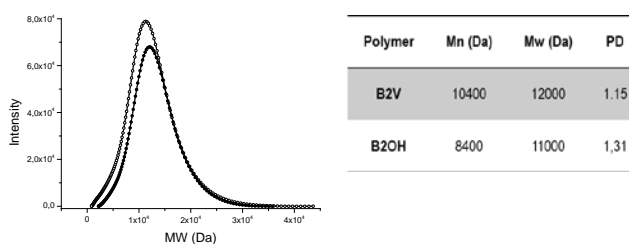


Figure 1. SEC results for B2V (●) and B2OH (○).

Figure 2 shows the FTIR spectra for both, B2V and B2OH polymers.

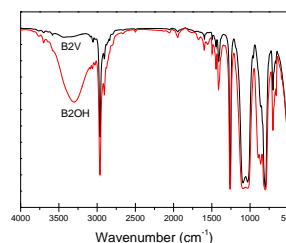


Figure 2. FTIR spectra for B2V (black line) and B2OH (red line).

The main difference is the prominent O-H stretching band above 3,000 cm⁻¹, which is observed in B2OH spectrum but results absent in B2V.

Conclusions

A controlled method for synthesizing α,ω -vinyl terminated PDMS was developed by employing controlled anionic polymerization (high-vacuum techniques). Further characterization of the resulting polymer is on the way.

References

- Quirk, R. P., Yoo, T., Lee, Y., Kim, J., Lee, B. Adv. Polym Sci. 2000, 153, 69.
- Hadjichristids, N., Iatrou, H., Pispas, S., Pitsikalis, M. J. Polym. Sci. Part A: Polym. Chem. 2000, 38, 3211.



ANALYSIS OF LOW MOLECULAR WEIGHT POLYMERS USING LATEST ADVANCED MULTI-DETECTOR GPC SYSTEMS

Mark R. Potheary¹, Edna Alvarez²---

1. Malvern Instruments Inc., 4802 North Sam Houston Parkway, Houston Texas, 77086, USA. Mark.potheary@malvern.com
2. Malvern Instruments Inc., Hermosillo 22, Col. Roma Sur, 06760, Mexico, D.F. edna.alvarez@malvern.com

Introduction

Gel-permeation chromatography (GPC) is the most widely used tool for the measurement of molecular weight and molecular weight distribution of natural and synthetic polymers. Advanced detectors such as light scattering are increasingly used to overcome the limitations of conventional GPC measurements and offer *absolute* molecular weight. A viscometer measures intrinsic viscosity, a key structure factor that can be used to calculate branching levels and can be combined with molecular weight data to calculate hydrodynamic radius. In combination these data allow detailed structural information of a polymer to be generated in a single GPC measurement which can be compared with other samples in Mark-Houwink plots. This can be used to study substitution or branching levels.

Among the practical challenges when making light scattering measurements is sensitivity to the light scattered by the sample. Sensitivity is limited by a polymer's molecular weight, concentration and dn/dc . In the development of novel polymers, limitations in any of these areas are common. For instance, drug delivery polymers such as PLGA often have low dn/dc , while coating polymers such as epoxies and smaller components such as polyols can have extremely low molecular weight. Of course, many polymers, particularly during their early development are only available in limited quantities, which restricts the amount of material that can be loaded on to the column.

Experimental Part

Various polymers including polyols, PLGA, and cellulose derivatives were separated using OMNISEC (Malvern

Instruments). Samples were separated in THF with 2 T6000M columns, or in chloroform with 2 x C6000M columns, or in 0.1M sodium sulphate over 2 x A6000M columns, respectively.

Results and Discussions

Accurate molecular weights were measured with high repeatability. The data achieved allowed the different PLGA polymers to be compared to monitor the trend in intrinsic viscosity with composition (figure 1).

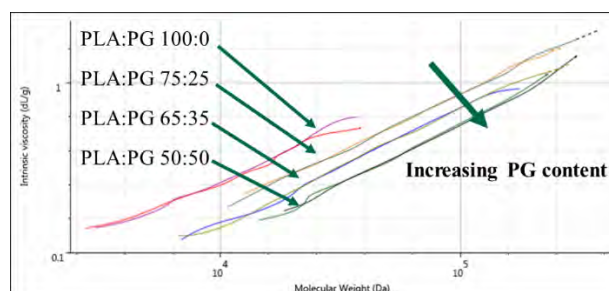


Figure 1. Overlaid Mark-Houwink Plots for multiple PLGA samples.

Conclusions

The light scattering and refractive index sensitivity of OMNISEC enable absolute molecular weight measurements of polymers that were previously not measurable with light scattering. This opens up a new range of applications to these measurements. In particular, quality measurements of drug delivery polymers such as PLGA are now possible as well as samples with extremely low molecular weights such as polyols and epoxies.

NANOSTRUCTURING AND SURFACE FUNCTIONALIZATION OF POLYMERS BY GASEOUS PLASMA TREATMENT FOR BIOMEDICAL APPLICATIONS

Alenka Vesel¹, Ita Junkar², Karin Stana Kleinschek³, Miran Mozetič^{1,2}

1. Jozef Stefan Institute, Jamova cesta 39, 1000, Ljubljana, Slovenia. miran.mozetic@ijs.si
2. Centre of Excellence for Polymer materials, Hajdrihova 19, 1000, Ljubljana, Slovenia.
3. Institute of Engineering Materials and Design, University of Maribor, Smetanova ulica 17, 2000, Maribor, Slovenia.

Introduction

Surface properties of polymer materials such as morphology, wettability and biocompatibility should be adapted to requirements of a specific application. Although different techniques for tailoring the properties have been invented non-equilibrium gaseous plasma treatments are often superior due to reliability, ability of treatment on industrial scale and ecological reasons. The surface of a polymer material is often saturated with preferred functional groups upon plasma treatment even in a fraction of a second. Prolonged treatment often leads to nano-structuring of originally smooth surfaces what is beneficial in cases where extreme surface finish in terms of wettability is required. Plasma treatment has been applied successfully for both fibrous¹ and planar² polymers.

Experimental Part

Non-equilibrium gaseous plasma is created at atmospheric or low pressure. The atmospheric pressure plasma is usually one or two-dimensional while uniform low pressure plasma is easily sustained in large three-dimensional chambers so it is particularly suitable for treatment of three-dimensional objects of complex shape. In both cases the gas temperature is usually close to RT, but the chemical reactivity is as high as if the gas were heated to thousands °C. The chemical reactivity is predominantly due to molecular radicals that are created by electron-impact dissociation of parent molecules. Figure 1 represents typical plasma at about 1 mbar where the density of neutral oxygen atoms is $1 \times 10^{22} \text{ m}^{-3}$.

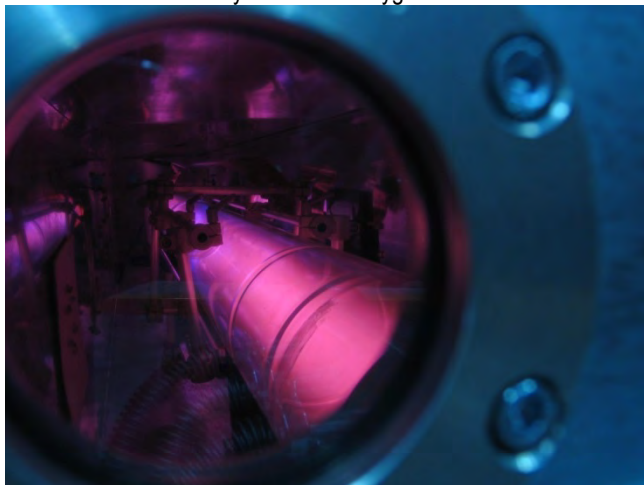


Figure 1. Non-equilibrium gaseous plasma in a 4 m long reactor

Results and Discussions

Brief treatment with oxygen plasma is applied for functionalization of the polymer surface with polar groups and thus increasing wettability. The contact angle of a water drop on smooth polymers is rarely below 20°. In order to make the polymer super-hydrophilic nano-structured morphology is required. Such an effect is presented in Figure 2 and is obtained by treatment of a polymer for several 10 s. The same material is made super-hydrophobic by subsequently treatment with fluorine-containing gas, typically CF₄.

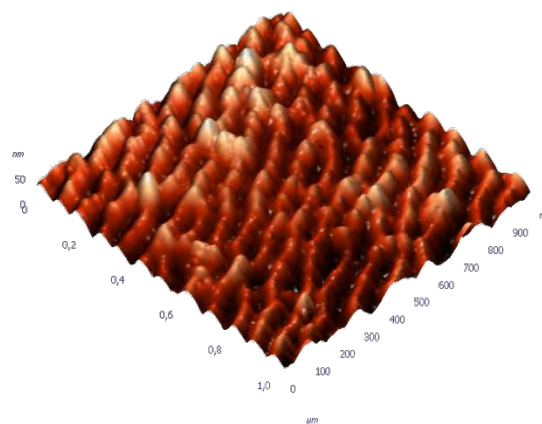


Figure 2. AFM image of originally smooth PET surface

Conclusions

Combination of polymer morphology and surface functional groups improves the biocompatibility of polymers. The effect is beneficial for tailored conformation of adsorbed proteins, proliferation of biological cells and prevention of blood platelet adhesion and activation so it is used for treatment of scaffolds as well as cardiovascular implants.

Acknowledgment: ARRS P2-0082

References

1. Gorjanc, M.; Mozetič, M. *Modification of fibrous polymers by gaseous plasma: principles, techniques and applications* 2014, Lambert Academic Publishing.
2. Vesel, A.; Mozetič, M. *Plasma-assisted polymer surface modifications. Printing on polymers*. Ed. Izdebska, J and Thomas, S 2016, Elsevier

PARTICLE SIZE DISTRIBUTION BY CAPILLARY HYDRODYNAMIC FRACTIONATION: A NEW APPROACH BASED ON MULTI-WAVELENGTH UV DETECTION

Luis A. Clementi^{1,2}, Miren Aguirre³, José R. Leiza³, Luis M. Gugliotta¹, Jorge R. Vega^{1,2}

1. INTEC (UNL, CONICET), Güemes 3450, 3000, Santa Fe, Argentina. laclementi@santafe-conicet.gov.ar
2. Fac. Reg. Santa Fe (UTN), Lavaisse 610, 3000, Santa Fe, Argentina. jvega@santafe-conicet.gov.ar
3. POLYMAT (Univ. of the Basque Country), Av. Tolosa 72, 20018, San Sebastian, España, jrleiza@ehu.es

Introduction

The particle size distribution (PSD) of a polymer latex can importantly influence several properties such as the rheological behaviors, the chemical stabilities, the coagulation processes, and the diffusion rates of the final product.

There are several techniques for estimating the PSD of a latex.¹ In capillary hydrodynamic fractionation (CHDF), the particles are fractionated according to size inside a capillary. A single-wavelength UV-spectrometer is often used for measuring the particle concentration of each eluted fraction.² Unfortunately, CHDF exhibits several drawbacks: i) it requires a calibration; ii) the particle refractive index must be known; and iii) it exhibits instrumental broadening. As a consequence, the PSDs estimated by CHDF typically exhibits meaningful errors.³

A new approach is here proposed for estimating the PSD of a latex by CHDF with UV detection collected at several wavelengths. The new method is evaluated on the basis of three polystyrene (PS) latexes that exhibit PSDs with different sizes and shapes.

The Proposed Method

Consider a discrete fractogram, $\tau(t_i, \lambda_j)$, at sampling times t_i ($i=1, \dots, I$) and wavelengths λ_j ($j=1, \dots, J$). At each t_i , $\tau(t_i, \lambda_j) = \tau_i(\lambda_j)$ can be used for estimating: (i) the instantaneous number PSD present in the detector cell, $f_i(D_i)$, and (ii) the instantaneous particle concentration, c_i , by solving a light scattering inverse problem.¹ Then, from $f_i(D_i)$ and c_i , the global PSD can be calculated as:

$$f(D_i) = \sum_{i=1}^I c_i \times f_i(D_i)$$

Experimental Part

Three PS latexes, L₁, L₂, and L₃, were analyzed by CHDF with simultaneous UV detection at 220nm, 240nm, 260nm, and 280nm. At each t_i , $f_i(D_i)$ and c_i , were estimated from $\tau(t_i, \lambda_j)$ through a general regression neural network (GRNN) previously trained on the basis of simulated data.⁴

All samples were also characterized by dynamic light scattering (DLS), disk centrifuge photodensitometry (DCP), and the standard CHDF with single wavelength detection at 220 nm.

Results and Discussions

Figure 1 shows the PSDs estimated through the proposed method, by DLS, and by the standard CHDF with single wavelength

detection. Table 1 presents the average diameter, \bar{D} , and the standard deviation, σ , of all PSDs. For bimodal PSDs, \bar{D} , σ and the weight fraction, w_i , were calculated for each individual mode. Compared to DLS and the standard CHDF, the proposed method mostly produced PSDs estimates closer to DCP (which is assumed as the reference technique to estimate PSDs).

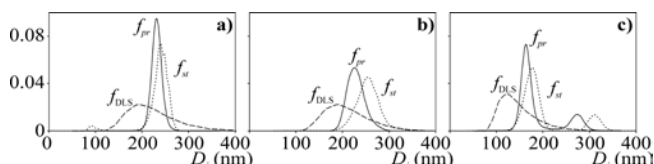


Figure 1. PSDs estimated by: the proposed method (f_{pr}), DLS (f_{DLS}), and the standard CHDF (f_{st}) for: a) L₁, b) L₂, and c) L₃.

Table 1: Average diameter, \bar{D} , standard deviation, σ , and weight fraction, w_i , of each estimated PSD.

		DCP	DLS	Standard CHDF	Proposed method
L ₁	\bar{D} (nm)	243	221	239	234
	σ (nm)	8.9	51.0	14.3	11.5
L ₂	\bar{D} (nm)	235	212	255	235
	σ	29.1	50.7	25.0	20.7
L ₃	\bar{D} (nm)	151	147	175	166
	Mode 1 σ (nm)	8.9	40.8	15.7	13.7
	w_i (%)	50	100	44.2	47.5
	Mode 2 \bar{D} (nm)	285	-	311	272
	Mode 2 σ (nm)	19.5	-	13.7	16.3
	w_i (%)	50	-	55.8	52.5

Conclusions

The proposed method is quite simple and proved to accurately estimate both unimodal and bimodal PSDs. Some advantages of the method are: i) no calibration is required; ii) the instrumental broadening is automatically corrected for; and iii) the injection of the marker solution is not necessary. However, a simultaneous multi-wavelength UV detection is required.

Acknowledgment: To CONICET, UNL and UTN.

References

1. Gugliotta L.; Clementi L.; Vega J.; Transworld Res. Net., Kerala, 2010.
2. DosRamos G.; Silebi C. J. Coll. In. Sci., 1990, 135, 165.
3. Clementi L., Artetxe Z., Aguirreurreta Z., Aguirre A., Leiza J., Gugliotta L., Vega J. Particuology, 2014, 17, 97.
4. Specht D. IEEE Trans. Neural Net. 1991, 2(6), 568.



ON-LINE MONITORING OF THE SYNTHESIS OF N,N-DIMETHYLACRYLAMIDE HYDROGELS BY UV-SPECTROMETRY

Valeria, S. Garcia¹, Luis A. Clementi^{1,2}, Carolina G. Gutierrez¹, Luciana Vera-Candioti³, Veronica V.G. Gonzalez¹, Luis M. Gugliotta¹

1. INTEC (UNL, CONICET), Guemes 3450, 3000, Santa Fe, Argentina. lgug@intec.unl.edu.ar
2. Fac. Reg. Santa Fe (UTN), Lavaise 610, 3000, Santa Fe, Argentina. laclementi@santafe-conicet.gov.ar
3. Fac. de Bioquímica y Cs. Biológicas (UNL), Ciudad Univ., 3000, Santa Fe, Argentina. Informes@fcb.unl.edu.ar

Introduction

Hydrogels are polymeric materials constituted by a tridimensional network of highly crosslinked polymeric chains. Main application of hydrogels are as absorbents, membranes, coatings, catalytic supports, fragmentation of biopolymers, drug delivery systems, and sensors.¹⁻³

The internal structure of hydrogels is of great importance since it influences some of its final properties. In general, the internal structure of an hydrogel is mainly defined along the reaction. Unfortunately, only few methods have been reported for monitoring the synthesis of hydrogels, and are based on complicated techniques.^{4,5}

In this work, the UV spectrometry technique is studied as a way of monitoring the synthesis of *N,N*-dimethylacrylamide (DMA) hydrogels. For comparison purposes, independent estimation of monomer conversion and free double bounds along the polymerization were also performed.

Experimental Part

Eight DMA hydrogels were synthesized employing different amounts of *N,N*-methyl-bis-acrylamide (BIS: 0%, 0.5%, 2% and 4%) as crosslinker, and varied solid contents (5% and 10%). Each reaction was carried out inside an UV spectrometer cell in order to measure the turbidity, τ , of the reaction medium along time at a wavelength of 430 nm. Also, for all reactions with 10% solid contents, samples were taken every 30 seconds and the conversion, x , was measured. Finally, for reactions with 10% solid content and 2% and 4% of BIS, the free double bonds of the crosslinker, c , were determined through a method based on titration with iodine. All the obtained measurements are presented in Figures 1 and 2.

Results and Discussions

From Fig. 1 it can be see that the BIS percentage strongly influences the shape of τ measurements. As the percentage of BIS increases, the baseline of τ also increases and the resulting peak becomes narrower. From Figure 2, it is clear that the final conversion x can be detected when the baseline of the τ measurement is reached. Additionally, from Figures 2c and 2d, the descendent zone of the τ curve indicates an acceleration of crosslinking, as it can be seen from the free double bounds evolution. In the cases of 0% of BIS (where no crosslinking exist),

the descendent zone in the τ curve could be explained by the entanglement of the polymeric chains.

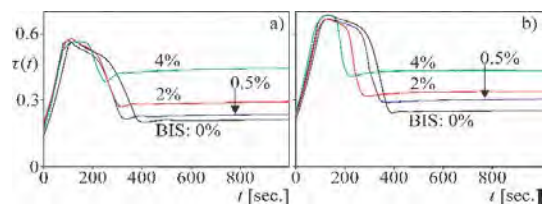


Figure 1. Turbidity measurements for solid content of 5% (a) and 10% (b), and BIS percentage of 0%, 0.5%, 2% and 4%.

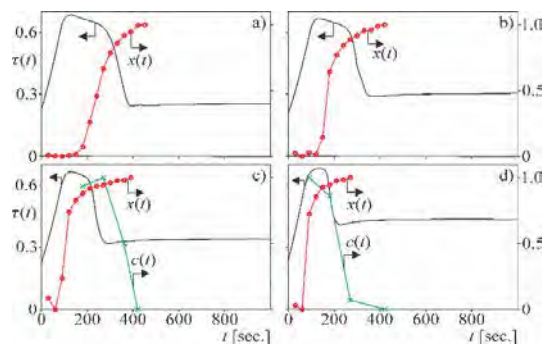


Figure 2. Turbidity measurements, conversions x and free double bounds, for solid content of 10% and BIS of 0% (a), 0.5% (b), 2% (c), and 4% (d).

Conclusions

Turbidity measurements exhibited a high sensitivity to changes in both the polymerization rate, and the solid content. In addition, some results suggest that crosslinking may be also characterized by this technique. As a conclusion, UV-spectrometry may be a potential technique for monitoring the synthesis of hydrogels.

Acknowledgment: To CONICET, UNL and UTN for the financial support.

References

1. De Rossi D.; Kajiwara K.; Osada Y.; Yamauchi A. *Plenum Press*, New York, 1991.
2. De Loos M.; Feringa B.; Van Esch J. *Europ. Journal Org. Chem.* 2005, 17, 3615.
3. Calo E.; Khutoryanskiy V. *Europ. Polym. Journal*, 2015, 65, 252.
4. Weng L.; Zhou X.; Zhang X.; Zhang L. *Polymer*, 2002, 43, 6761.
5. Norisuye T.; Shibayama M.; Nomura S. *Polymer*, 1998, 39, 2769.



Thermal Behavior and Morphological Characterization of LDPE/LLDPE and LDPE/mLLDPE Binary Blends

Dinorah I. Rodríguez Otamendi, Javier Gudiño Rivera, Rubén Saldívar Guerrero

Centro de Investigación en Química Aplicada, Blvd. Enrique Reyna Herosillo No. 140, Colonia San José de los Cerritos, Saltillo, Coah. C.P. 25294, javier.gudino@ciqa.edu.mx

Introduction

Binary blends of low density polyethylene (LDPE) with Ziegler-Natta (LLDPE), and Metallocene linear low density (mLLDPE) polyethylenes are used extensively in the manufacturing of commercial films. The LLDPE resins manufactured by Ziegler-Natta catalysts are lightly branched with broad molecular weight distributions (MWD)¹, while LLDPE resins catalyzed by Metallocenes have more orderly arrangement of branches with narrow MWDs². In this work we prepared LDPE/LLDPE, and LDPE/mLLDPE blends in order to observe changes in their thermal behavior, and morphology with the composition of both components.

Experimental Part

LDPE/LLDPE and LDPE/mLLDPE blends were prepared in a twin screw extruder. The thermal behavior was studied with a DSC Calorimeter, from 30 to 180 °C with a temperature ramp of 5°C/min in a nitrogen atmosphere. For morphological characterization 20x10x0.7 mm plates were prepared and crystallized in a heating plate employing the same conditions as DSC. These specimens were analyzed by WAXD in a Diffractometer with a 2 to 80° scan interval in 2θ with a 0.02°/s velocity using Cu Kα radiation at λ= 1.5406 Å. For the SAXS study a diffractometer was used with an operating range of 0.5-25° in 2θ at room temperature.

Results and Discussions

Fig. 1 shows the endotherms of fusion of each blend. For LDPE/LLDPE blends we observe multiple endotherms at different compositions, and with a higher content of LDPE it is favored the low temperature melting endotherm, whereas in LDPE/mLLDPE blends it is favored the formation of a main crystalline population, and as a result it is observed a wider endotherm of fusion. In Fig. 2 we observe the X-ray diffraction patterns of the blends. The presence of four main peaks can be observed in both types of blends. These peaks correspond to the crystallographic planes (110), (200), (310) and (220) which are related to an orthorhombic structure³. In LDPE/LLDPE blends with a higher content of LDPE we observe an increase in the intensity of the (110) peak, and a decrease in the peaks (310) and (220). In LDPE/mLLDPE blends we observe and increase in the intensity of the peaks at (310) and (220) with a higher content of mLLDPE. In the X-ray dispersion patterns of the blends (not shown here) it is observed the formation of two well-defined lamellar stacks for blends with a 30% wt of LDPE content, whereas for the rest of blends this pattern occurs in a lower extent.

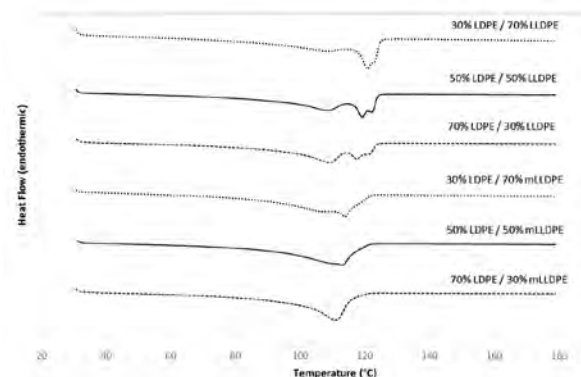


Figure 1. DSC scans of the binary blends during the heating process.

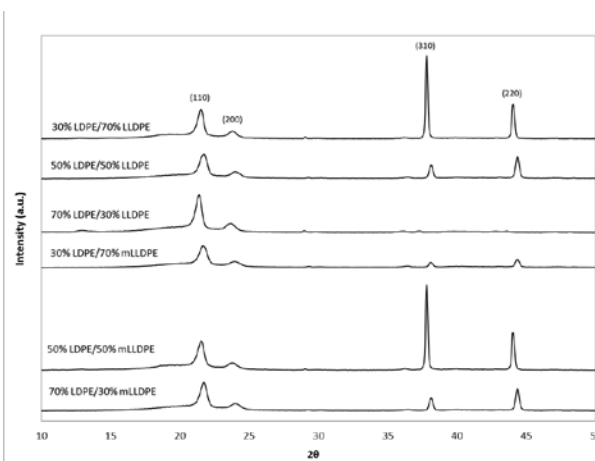


Figure 2. WAXD patterns of the binary blends.

Conclusions

The thermal behavior changes with the type of LLDPE, and with an increase in the content of LDPE the crystalline structure of the blend change to a less ordered structure due to a higher content of long chain branches.

Acknowledgment: To M.C. Marco Antonio de Jesús Téllez from CIQA Saltillo for his help in the morphological characterization.

References

1. Peacock A.J., *Handbook of Polyethylenes*, Marcel Dekker, 2000.
2. Furukawa, T; Sato, H; Kita, Y; Matsukawa, K; Yamaguchi, H; Ochiai, S; Siesler, H.W.; Ozaki, Y. *Polymer Journal*. 2006, 38, 1127.
3. Clark E.S. *Unit Cell Information on Some Important Polymers*. Ch. 38.

EXPERIMENTAL AND NUMERICAL STUDY OF ETHANOL DIFFUSION IN POLYOXYMETHYLENE INJECTION-MOLDED PARTS

Diana Amaya ¹, Jorge Medina ², Camilo Cruz ³

1. Universidad de los Andes, Cra 1 No. 18A-12, 111711, Bogotá, Colombia dm.amaya48@uniandes.edu.co
2. Universidad de los Andes, Cra 1 No. 18A-12, 111711, Bogotá, Colombia
3. Industrial partner, Consumer Goods and Automotive Sector, Stuttgart, Germany.

Introduction

Injection molded samples of polyoxymethylene copolymer (POM-C) have been characterized dry as molded and after conditioning in ethanol at 50, 70 and 120°C for a range of time up to 484 h. The results reveal a decrement in tensile and impact properties. All conditioned samples showed a time dependent weight increment which could be characterized as Fickian diffusion process with a temperature dependent diffusion coefficient. A 3D-simulation was carried out in ABAQUS to mimic the experimental conditioning carried out in the injection-molded specimens in order to validate the hypothesis of 1D diffusion used to identify the parameters of the diffusion model.

Experimental Part

At 50°C samples were put into a Julabo ® thermal bath which were placed in glass bottles filled with ethanol. The heating media was water at 50.0 ± 0.1°C. This conditioning was up to 484h. At 70 and 120°C samples were put into a Parr ® reactor No. 4578 filled with ethanol. These conditionings were out up to 274h and 148h respectively. In all these ageing tests, the samples were stacked vertically in such way that the fluid had access to all surfaces of each one. On removal from the conditioning container (thermal bath or reactor according to temperature case) the fluid in surface sample was removed with tissue and then they were immediately weighed. A digital balance Mettler Toledo No. AB204 with an operating range between 0 and 210 ± 0.0001g was used to measure sample weights. Each data point presented in the following is the average of measurements on 10 individual samples. Uniaxial tension tests were conducted on an Instron 3367 machine according to ASTM D638-14. Impact tests were conducted on an Impact tester TMI No. 43-1 according to ASTM D256-10. Fickian diffusion simulation was carried out in ABAQUS/Implicit using a 3D model. Moisture boundary conditions were applied to the whole body of sample.

Results and Discussions

The following results are only shown for tensile unstrained specimens at 70°C. Fig. 1 shows Fickian behavior for the 3 methods: experimental, analytical and computational. Diffusion coefficients from all samples follow the Arrhenius behavior as a function of temperature. Ethanol diffusion is similar at 50 and 70°C for all samples. Although at 120°C diffusion is affected significantly by temperature since all samples reached saturation much quicker. Table 1 shows the identified Fickian diffusion

parameters, which were introduced in ABAQUS in order to reach a numerical approach.

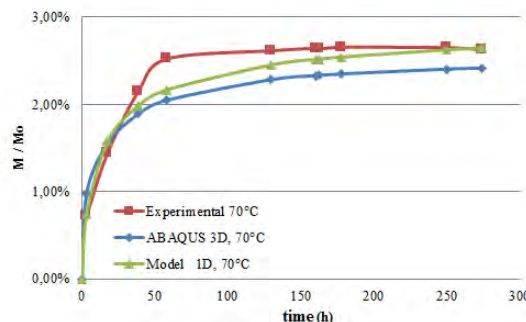


Figure 1. Fickian analysis of tensile unstrained samples weight gain after ageing in ethanol at 70°C

Table 1. Fickian diffusion identified parameters for tensile unstrained specimens at 70°C.

Identified diffusion coefficient of ethanol in POM-C (m ² /s)	Identified saturation concentration of ethanol (g ethanol / g dry POM)
8,7221×10 ⁻¹²	20,5883

Conclusions

This study revealed significant changes in mechanical properties and crystallinity of POM-C due to ageing in ethanol at 50, 70 and 120°C. Weight increment followed Fickian diffusion process for all ageing tests. The dependence of diffusion with temperature was proved; noting that at 120°C ethanol diffusion through this polymer was greater than other ageing conditions. In addition, at this condition, mechanical properties decayed dramatically due to its ductile behavior. Therefore, it is not recommendable to operate at this regime in automotive applications.

Acknowledgment: Robert Bosch GmbH, Germany, Chemical Engineering Department from Universidad de los Andes.

References

- [1] J. Kajio and M. Hedenqvist, "Ageing properties of polyamide-12 pipes exposed to fuels with and without ethanol," *Polymer Degradation and Stability*, p. 1846–1854, 26 July 2008.
- [2] J. Thomason and J. Ali, "The dimensional stability of glass–fibre reinforced polyamide 66 during hydrolysis conditioning," *Composites: Part A*, no. 40, p. 625–634, 22 February 2009.
- [3] K. Kallio and M. Hedenqvist, "Ageing properties of car fuel-lines; accelerated testing in "close-to-real" service conditions," *Polymer Testing*, no. 29, pp. 41–48, 2010.



ESR SPECTROSCOPY IN THE IDENTIFICATION OF FREE RADICALS GENERATED BY DIFFERENT CURING MODES IN A DENTAL RESIN CEMENT

Bruno Luiz Santana Vicentin¹, Eduardo Di Mauro¹

1. Departamento de Física, Universidade Estadual de Londrina, Rodovia PR 445 Km 380, Campus Universitário. 86.057-970, Londrina, PR, Brazil dimauro@uel.br

Introduction

In clinical situations of extensive coronary destruction the use of a retentive system for the tooth restorative material is required. The post-and-core technique currently is the recommended protocol in tooth restoration to cement the post into the root canal. In the post cementation procedure, the root canal is filled with resin cement and thus the post is introduced into the canal keeping a small part of it out of the root canal to perform the external restoration^[1]. In order to guarantee that the cement gets polymerized in all the extension of the post, dual cure resin cements have been developed associating light irradiation (photo-cure) to chemical initiation (self-cure), ensuring polymerization at deepest points of the restoration where radiation cannot excite camphoroquinone^[1]. The free radicals generated by photo-cure were studied in a resin composite by Fontes et al (2014)^[2]. This research was conducted to identify the free radicals responsible for the chain reaction of the self-cure.

Experimental Part

Samples of dual cure resin cement from Allcem (FGM, Joinville, Brazil) in the color shade A1 were examined by X-band ESR. The irradiation of the cement with the blue visible light was produced by a LED (Ultra Blue, DabiAtlante, Ribeirão Preto, Brazil) with a potency of 492 mW/cm². The resin cement samples were separated in two major groups: irradiated for 40 s and not-irradiated. The X-band (~9 GHz) EPR spectra were obtained with a JEOL JES-PE-3X spectrometer at room temperature using 1 mW microwave power, 0.40 mT modulation amplitude, and 100 kHz. The samples were placed in a 2 × 2 mm Teflon mold. The data treatment was performed with OriginLab software, and simulations were achieved using the WinEPR (Bruker) software.

Results and Discussions

The model for the photo-initiation is well described by Truffier-Boutry et al (2003)^[3]. According to authors there are two paramagnetic species forming the EPR spectrum, RI (CH₃-C^{*}-CH₂) and RII (CH₂-C^{*}-CH₂). Figure 1 shows the X-band ESR spectra of photo-cured and self-cured samples of a dual cured dental resin cement. It can be seen that the spectra presents same number of lines, same line-width and g values. The simulated EPR spectrum shows that the hyperfine coupling constants are the same for both samples. Figure 2 shows the simulations for Radical I and Radical II, with the superposition of the sum of the simulated spectrum with the experiment for the self-cured sample. Comparing with the radical species studied by Fontes et al (2014)^[2] for the photo-cure we can say that the

radical species generated in the self-cure are the same and are simultaneously present in the sample and occur independently of the polymerization protocol.

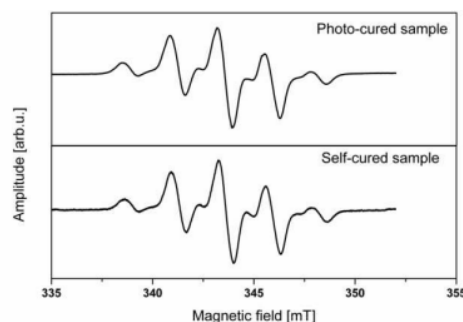


Figure 1. ESR spectrum of photo-cured and self-cured samples.

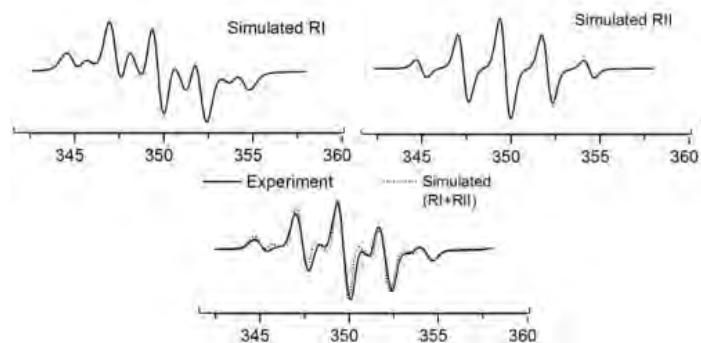


Figure 2. Simulations for Radical I and Radical II. Sum of simulations superposed to the experiment for the self-cured sample.

Conclusions

There are two paramagnetic species forming the EPR spectrum, RI (CH₃-C^{*}-CH₂) and RII (CH₂-C^{*}-CH₂), independently the mode of cure.

Acknowledgments: Authors thanks to FGM MateriaisDentários for providing samples of dual cure resin cement AllCem.

References

1. Vicentin, B.L.S.; Salomão, F.M.; Hoepfner, M.G.; Di Mauro, E. *Appl. Magn. Reson.* 2016, 47, 211.
2. Fontes, A.S.; Vicentin, B.L.S.; Valezi, D.F.; Costa, M.F.; Sano, W.; Di Mauro, E. *Appl. Magn. Reson.* 2014, 44, 681.
3. Truffier-Boutry, D.; Gallez, X.A.; Demoustier-Champagne, S.; Devaux, J.; Mestdagh, M.; Champagne, B.; Leloup, G. *J. Polym. Sci. A Polym. Chem.* 2003, 41, 1691.

MICRO-RAMAN ANALYSIS OF THE ALPHA RADIATION EFFECT ON THE POLY ALLYL DIGLYCOL CARBONATE.

Mariana Cerda Zorrilla¹, Juan Carlos Castro Alcántara¹, José Antonio Azamar Barrios¹, Guillermo C. Espinosa García²

1. Centro de Investigación y Estudios Avanzados del Instituto Politécnico Nacional, Unidad Mérida, Antigua Carretera a Progreso Km.6, Cordemex, 97310, Mérida Yucatán, México. marianacz.esr@gmail.com
2. Instituto de Física. Universidad Nacional Autónoma de México. Circuito de la Investigación Científica, Ciudad Universitaria. 04520, México, D.F.

Introduction

Poly allyl diglycol carbonate (PADC or CR-39) is a thermosetting polymer which it is widely used for the detection of ionizing particles by the nuclear tracks in solid method.¹ This being one of the most sensitive polymeric detectors by nuclear track, and because the response of the material to radiation depends on the material properties, information about the structure and the track formation process is of great importance for the development of new polymeric detectors with a sensitive and controllable threshold detection, which has led to the search of new methods of characterization and analysis to detectors particularly the PADC. In this work the Micro-Raman analysis for the polymeric detector CR-39 in response to alpha radiation is shown.

Experimental Part

CR-39 LANTRACK (TR) with a 950 μm thickness was used as detecting material. An emitter source of alpha particles of 5.15 MeV was selected as track generator radioactive source. The exposure was made in air. The detectors were chemically etched under the same conditions following the very well established procedure, in 6.25 M KOH solution at $60 \pm 1^\circ\text{C}$.² The detectors were washed and dried with the same process and conditions. After these procedures, the detectors were analyzed with the Micro-Raman Thermo Scientific DXR (IF-UNAM) with a 532 nm laser, and the spectra were analyzed with the OMNIC 8.1 Thermo Fisher Scientific Inc. software.

Results and Discussions

The inset of Fig. 1 shows the imagen of a CR-39 irradiated and their revealed tracks, after being irradiated and chemically treated. Outside and Inside the Raman spectrum track was taken as shown in Fig. 1. The Raman intensities of all the functional groups within the polymeric structure decrease of a uniform way inside the track. Because to this decrease, to make a track mapping by the Micro-Raman technique regarding intensities is obtained a 3D track representation such as in the Fig. 2.



Figure 1. Raman spectrum inside and outside of the track.

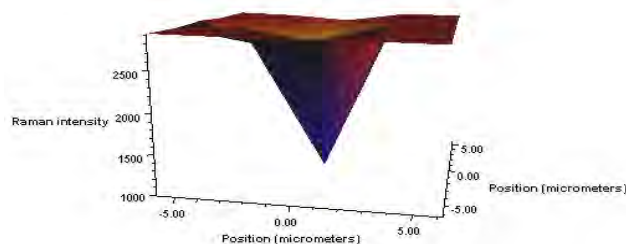


Figure 2. 3-D representation of the nuclear track.

Conclusions

The Micro-Raman analysis to the PADC detector shows decreasing intensities of the functional groups, but not the breaking of the monomer, because of this with the Raman analysis is observed the change in the polymeric structure both spectral and morphological level, to have a three-dimensional representation associated to the intensity change.

Acknowledgment: Cristina Zorrilla Cangas (*Micro-Raman, IF-UNAM*), José I. Golzarri (IF-UNAM), LANNBIO CINVESTAV Mérida, UNAM-DGAPA-PAPIIT IN-103316.

References:

1. Gianluca., Handbook thermoset plastics . USA: Elsevier., 2013.
2. Espinosa, G., Gammage, R., Golzarri, J. & Castaño, V.. Int. J. Polym. Mater., 1998, 40, 87.

INESTABILIDADES ELÁSTICAS DE FILMS METÁLICOS SOBRE SUSTRATOS POLIMÉRICOS

Diana C. Agudelo ¹, Daniel A. Vega ², Marcelo A. Villar ¹

1. Planta Piloto de Ingeniería Química, PLAPIQUI (UNS-CONICET), Camino La Carrindanga km. 7, (8000) Bahía Blanca, Argentina. cagudelomora@plapiqui.edu.ar
2. Instituto de Física del Sur, INFISUR (UNS-CONICET), Av. Alem 1253, (8000) Bahía Blanca, Argentina.

Introducción

El estudio sobre la formación de inestabilidades elásticas (arrugas) ha tomado gran interés, en las últimas dos décadas, debido a las numerosas aplicaciones posibles de estos mecanismos auto-organizables que pueden crear diversos tipos de patrones superficiales en todas las escalas.¹ En particular, las investigaciones sobre películas de redes poliméricas son interesantes por el control de sus propiedades finales mediante la variación de su estructura molecular, lo que las hace óptimas en aplicaciones como sensores, dispositivos de microfluidos, revestimientos sensibles, sustratos para cultivo de tejidos, bio-adhesivos y metrología de materiales elásticos.² En este trabajo se estudió la influencia de la funcionalidad del punto de entrecruzamiento sobre la formación de inestabilidades elásticas (arrugas) en películas de oro empleando redes modelo de poli(dimetilsiloxano).

Experimental

Se obtuvieron redes modelos de poli(dimetilsiloxano) (PDMS) por reacción de hidrosilación entre α,ω -divinilpolidimetilsiloxano (B₂), y entrecruzantes de funcionalidad 3 (feniltris(dimetilsiloxi)silano, A₃) y 4 (tetrakis(dimetil-siloxi)silano, A₄) (United Chemical Technologies, Inc.) puros, y mezclas de los mismos en diferentes proporciones. Los reactivos fueron pesados, mezclados mecánicamente y desgasificados bajo vacío. Se sumergieron placas de vidrio dentro de cada una de las mezclas durante 5 segundos y las placas recubiertas fueron colocadas en una estufa a 60 °C durante 8 horas. Una vez curadas, las muestras fueron recubiertas con una película de oro de aproximadamente 90 nm de espesor mediante deposición del metal en una atmósfera de Argón. Los sistemas fueron hinchados con diferentes solventes para la generación de inestabilidades elásticas (buckling). Mediante el uso de microscopía óptica se midió la longitud de onda de las ondulaciones obtenidas en la capa de oro.

Resultados y Discusión

En una etapa inicial, el hinchamiento de las redes de PDMS promueve la formación de inestabilidades elásticas en la superficie del oro, formando patrones de ondulaciones altamente desordenados. La interacción entre las ondulaciones induce la difusión

y aniquilación de defectos reduciendo el exceso de energía elástica almacenada en la estructura.

Las propiedades de las redes modelo de PDMS se ven notoriamente afectadas por la funcionalidad del entrecruzante (f). Un aumento en f genera redes con mayor módulo elástico y mayor fracción en volumen de polímero en la red hinchada en equilibrio debido al aumento en la concentración de cadenas elásticamente activas en la red. Por lo tanto, a medida que aumenta f se obtiene un incremento en el módulo elástico de las redes, y por ende, en la longitud de onda del patrón generado en la lámina de oro (Figura 1).

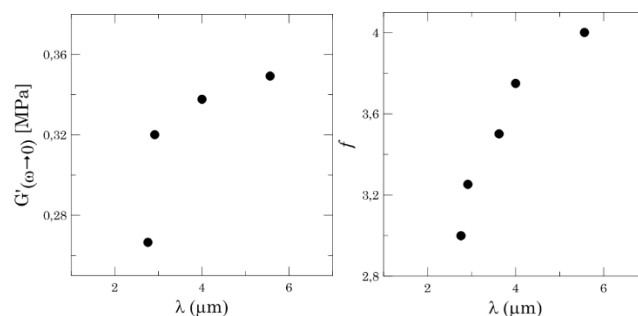


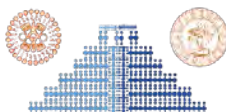
Figura 1. Módulo de almacenamiento de equilibrio a baja frecuencia para redes modelo de PDMS (izq.) y funcionalidad promedio del punto de entrecruzamiento (der.) en función de la longitud de onda de las inestabilidades elásticas generadas en las redes de PDMS recubiertas con una película de oro.

Conclusiones

Se obtuvieron inestabilidades elásticas en redes modelo de PDMS recubiertas con una película de oro, mediante hinchamiento con aceite de silicona. Se observó un aumento en la longitud de onda a medida que aumenta la funcionalidad del punto de entrecruzamiento en acuerdo cualitativo con las predicciones de modelos teóricos

Agradecimientos: Los autores agradecen al Consejo Nacional de Investigaciones Científicas y Técnicas (CONICET) y a la Universidad Nacional del Sur (UNS) por el apoyo brindado para la realización de este trabajo.

Referencias



MICRO AND NANO MOLECULARLY IMPRINTED POLYMERS (MIPs) FOR TO PRECONCENTRATED ORGANIC TARGET MOLECULES AND FOR TO BE USED AS RECEPTORS IN ELISA TEST

***Eduardo Pereira**¹, **César Cáceres**¹, **Yadiris García**¹, **Ewa Moczko**², **Bernabé L. Rivas**¹, **Sergey A. Piletsky**³

1. Faculty of Chemical Sciences, University of Concepción, P.O. BOX 160-C, Concepción, Chile, epereira@udec.cl
2. Department of Environmental Chemistry, Faculty of Sciences, Universidad Católica de la SSMMA Concepción, Alonso de Ribera 2850, Concepción, Chile
3. Chemistry Department, College of Science and Engineering, University of Leicester, UK

Introduction

Recently, new classes of organic pollutants including poly-aromatic hydrocarbons (PAHs), antibiotics, endocrine disrupting compounds (EDCs), pharmaceuticals, and personal care products (PPCPs), in very low concentration, part-pertrillion (ppt) range, have been identified. On the other hand, Forensic Chemistry is an area of the chemistry devoted to the analysis of several substances, most of them organic molecules, that might be important or might have been used in the commission of a crime. Moreover, the enzyme-linked immunosorbent assay (ELISA) is used for quantitative determination of the analytes. The disadvantages of this technology are the low stability of reagents, the need for refrigerated transport and storage, batch-to-batch (or clone-to-clone) variability, and the high cost of producing antibodies are often cited as problems¹.

In this work we have developed materials and nanomaterials based on molecularly imprinted polymers having high capability and selectivity of molecular recognition with ability to be used in the solid phase extraction, analytical detection and quantitative diagnosis assay of target organic molecules from environmental and forensic samples².

Experimental Part

MIPs and NanoMIPs were synthesized following the non-covalent strategy, using the target molecules as templates. The target molecules include bisphenol-A and progesterone, as well as, some organic analytes coming from organic gunshot residues, such as, diphenylamine. The tested variables were the monomer ratio, nature of solvent, ratio between solvent and co-monomer mix, crosslinker/co-monomer ratio and template/co-monomers ratio. Some of these variables were evaluated by using multivariate analysis and experimental design in order to establish the critical factors that affect the sorption capacity and the selectivity. The sorption capacity of target organic molecules was studied in batch method and the sorption mechanism was studied through the adsorption isotherm and kinetics assays. The synthesis of NanoMIPs for the detection of biotin and melamine were conducted using the solid phase approach² (see figure 1). The sensitivity and selectivity of the NanoMIPs were evaluated in ELISA test by immobilizing them in microplates. Then the analysis is based on a competitive assay between the free analytes and analytes labelled with HRP.

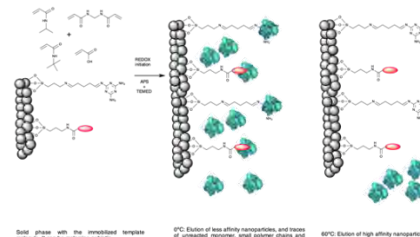


Figure 1. Scheme of the synthesis of NanoMIPs using the solid phase approach²

Results and Discussions

Through radical polymerization, a set of MIPs based on 1-vinyl-2-pyrrolidone and 1-vinylimidazol monomers were obtained with yields around 80 %. These were characterized through FT-IR and SEM. The MIPs shows high retention capacity for diphenylamine bisphenol-A and progesterone compared with the respective NIPs (Non Imprinted Polymers). The ELISA test shows good results for nanoMIPs made in water for biotin but bad results for melamine. This problem was fixed using the nanoMIPs made for melamine but synthesized in organic media with shield of polyethyleneglicol (see figure 2).

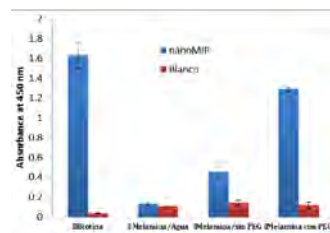


Figure 2. Absorbance capacity of HRP-Biotin and HRP-Melamine for the nanoMIPs in ELISA Test.

Acknowledgment: The authors thank gratefully to research project FONDECYT No 1160942 and to CONICICYT grant No 21110603

References

1. C. Cáceres, F. Canfarotta, I. Chianella, E. Pereira, E. Moczko, C. Esen, A. Guerreiro, E. Piletska, M. J. Whitcombe and S. A. Piletsky. *Analyst*, 2016, 141, 1405
2. Chianella, I.; Guerreiro, A.; Moczko E.; Caygill S.; Piletska E.; De Vargas Sansalvador I.; Whitcombe M.; Piletsky S. *Anal. Chem.* 2013, 85, 8462–8468

CONDUCTIVIDAD IÓNICA EN POLÍMEROS COMPOSITOS CONTENIENDO SALES DE LITIO BASADOS EN LÍQUIDOS IÓNICOS SOPORTADOS

Abel García-Bernabé¹, Eduardo García-Verdugo², Santiago V. Luis², Vicente Compañ¹

1. Departamento de Termodinámica Aplicada. Universidad Politécnica de Valencia. Camino de Vera s/n 46022-Valencia (España) vicommo@upv.ter.es

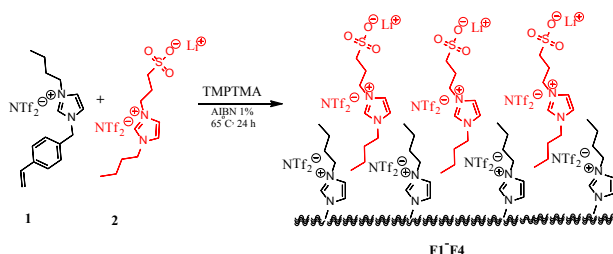
2. Departamento de Química Inorgánica y Orgánica. Universidad Jaume I. Avda. Sos Baynat s/n Castellón de la Plana 12071 (España) luis@uji.es

Introducción

Los líquidos iónicos soportados son macromoléculas con interesantes propiedades¹ y aplicaciones² debido a la combinación de las propiedades de los líquidos iónicos y de las macromoléculas. Una de interesante propiedad es la alta conductividad iónica de estos materiales. Recientemente en nuestro grupo de investigación hemos abordado el estudio del transporte iónico en varios líquidos iónicos soportados (SILLPs)^{3,4,5,6}. En esta comunicación estudiamos el transporte iónico de cuatro SILLPs basado en 1-butilimidazol conteniendo sales de litio absorbidas en la estructura macromolecular.

Parte experimental

Los SILLPs analizados derivan de la polimerización de un monómero estirénico conteniendo el grupo 1-butilimidazolio entrecruzado con trimetacrilato (TMPTMA). Además se añadió en la macromolécula una sal de litio con estructura de líquido iónico.



Esquema 1. Preparación de los SILLPs

Tabla 1. Composición de los SILLPs

SILLPs	% TMPTMA	% 1	% 2
F1	11.1	44.45	44.45
F2	5.2	47.4	47.4
F3	16.5	67.0	16.5
F4	8.1	73.5	18.4

Las medidas de impedancia se realizaron utilizando el espectrómetro dieléctrico de banda ancha Novocontrol. El rango de frecuencia fue de 10^{-1} a 3×10^6 Hz. Los espectros se midieron isotérmicamente desde 20°C a 120°C en saltos de 10°C.

Resultados y Discusión

En la figura a se muestran los diagramas de Bode de los cuatro SILLPs a 30 y 100°C. En estos diagramas se observa dos máximos en el ángulo de fase (φ), y para cada uno de ellos se obtiene un plateau en el módulo de la conductividad compleja. Cada plateau se corresponde con un proceso de transporte iónico caracterizado por la conductividad DC (σ_{DC}) y que se asocia a la

movilidad de un ión en la matriz polimérica. La movilidad del anión NTf_2^- es más alta que el catión litio, por lo que el valor de la conductividad DC de NTf_2^- se observa a frecuencias altas.³ La movilidad de un ión en la matriz polimérica. La movilidad del anión NTf_2^- es más alta que el catión litio, por lo que el valor de la conductividad DC de NTf_2^- se observa a frecuencias altas.³

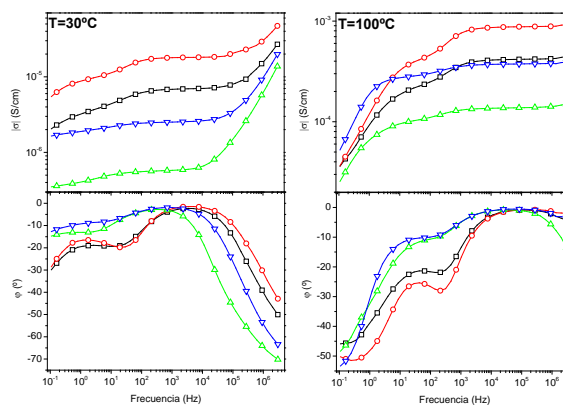


Figura 1. Diagrama de Bode a 30°C y 100°C. F1 (∇ , negro), F2 ($-$, rojo), F3 (8, verde) y F4 (X, azul)

Conclusiones

Los resultados experimentales de las medidas de impedancia de los cuatro SILLPs analizados muestran el transporte iónico de las dos especies absorbidas: la movilidad de los aniones NTf_2^- y la de los cationes Li^+ .

Agradecimientos: Este trabajo ha sido financiado por los proyectos ENE/2011-24761, CTO2011-28903-C02-01 y PROMETE02012/020

Referencias

1. Ueki, T.; Watanabe M. *Macromolecules* 2008, 41, 3739.
2. Lua J.; Yana F.; Texter J. *Progress in Polymer Science* 2009, 34, 431.
3. García-Bernabé A.; Compañ V.; Burguete MI.; García-Verdugo E.; Karbass N.; Luis SV. *J. Phys. Chem. C* 2010, 114, 7030.
4. Sans V.; Karbass N.; Burguete MI.; Compañ V.; García-Verdugo E.; Luis SV.; Pawlak M. *Chem. Eur. J.* 2011, 17, 1894.
5. Compañ V.; Molla S.; García-Verdugo E.; Luis SV.; Burguete MI. *J. Non-Crystalline Solids* 2012, 358, 1228.
6. Altava B.; Compañ V.; Andrio A.; del Castillo LF.; Molla S.; Burguete MI.; García-Verdugo E.; Luis SV. *Polymer*, 2015, 72, 69.

BLEACHING ON PLASTICIZED PVC FORMULATIONS EXPOSED TO NATURAL WEATHERING

González-Falcón Elizabeth¹, Sánchez-Peña M. Judith¹, Arellano Martín², González-Ortiz Luis J.¹

1. Departamento de Química, Centro Universitario de Ciencias Exactas e Ingenierías, Boulevard Marcelino García Barragán #1421 C.P. 44430, Guadalajara, Jalisco. México.
 2. Departamento de Ingeniería Química, Centro Universitario de Ciencias Exactas e Ingenierías, Boulevard Marcelino García Barragán #1421 C.P. 44430, Guadalajara, Jalisco. México
- e-mail contact: ljglez@yahoo.com

Introduction

The degrading behavior of industrial type plasticized PVC formulations exposed to natural weathering is complex and it is not completely understood. However, it is usually recognized that it depends, among others factors, on: oxygen and humidity presence and, light irradiation (type and intensity)¹. The bleaching phenomena has been reported for non-plasticized PVC formulations². Besides, considering purely theoretical approaches, a wide set of partially connected reactions have been proposed³. However, this phenomena has not been studied experimentally in plasticized formulations. Thus, the evolution of the concentration of the different polyenes (6 ≤ n ≤ 20) contained in plasticized PVC formulations is reported here, which were exposed to 9 different outdoors conditions.

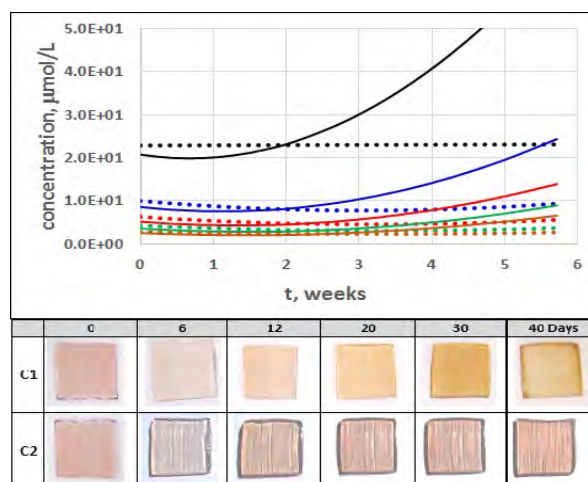
Experimental Part

The samples to be degraded were prepared as follows: (a) dry blending the components, (b) pelletizing the dry-blend (twin-screw extruder Leistritz 276L/32D) and, (c) extruding the pellets (to obtain ribbons). In all formulations, the DEHP/ESO ratio was 45/3 (phr/phr) and the total content of stearates was 1.0 phr, considering the following CaSt₂/ZnSt₂ ratios: 0.0/1.0, 0.2/0.8, 0.4/0.6, 0.6/0.4, 0.8/0.2 and, 1.0/0.0. The samples were exposed to natural weathering to 9 different conditions; the maximum degradation time was 40 days. The concentration of polyenes was determined by UV-visible spectroscopy (Cintra 6 GBC).

Results and Discussions

To analyze the combined effect of temperature (296±5 K vs 290±4 K) and UV irradiation level (0.085±0.012 W/m² vs 0.067±0.005W/m²), in the Figure 1 the polyene accumulation behavior and visual appearance of formulation F1 (CaSt₂/ZnSt₂:1/0) is presented. There, it can be noticed that a small increasing of such factors (ΔT(%)=2% and ΔUV(%)=27%) produce an important increment on both phenomena, the bleaching (decrement on polyene

concentration starting the outdoors exposition) and the polyene accumulation (dominating process at longer times), which could be occurring simultaneously in formulation. The discoloration of PVC samples can also be appreciated



in Figure 1.

Figure 1. Polyene accumulation behavior and visual appearance for F1 (CaSt₂/ZnSt₂: 1/0) degraded at the environmental conditions: C1 (—) o C2 (....).

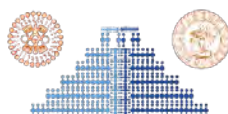
Conclusions

Even though, the studied factors were slightly modified, their effect was considerable in several cases, being remarkable the stabilizing effect of the presence of “liquid water” over samples.

Acknowledgment: EGF thanks to CONACyT for her scholarship # 249090.

References

1. Jakubowicz, I., Yarahmadi, N. & Gevert, T. Polym. Degrad. Stab. 1999, 66, 415.
2. Gardette, J.-L. & Lemaire, J. J. Vinyl Addit. Technol. 1993, 15, 113.
3. Nagy, T. T., Kelen, T., Turcsanyi, B. & Tudos, F. 1977, 15, 853.



THE EFFECT OF ADDITION OF VEGETABLE OIL IN THE HYDROPHOBIC BEHAVIOR OF WATERBORNE POLYURETHANE

Gabriela Miranda ¹, Wesley Monteiro ¹, Cláudia dos Santos ², Rosane Ligabue ^{1,2}

1. Graduation Program in Materials Engineering and Technology, PUCRS, Building 30. Partenon. 90619-900, Porto Alegre, RS, Brazil.
2. School of Chemistry, PUCRS, Building 12. Partenon. 90619-900, Porto Alegre, RS, Brazil.
3. Email: gabriela.messias@acad.pucrs.br

Introduction

The vegetables oils are interesting alternatives for chemical industry because they are natural materials from renewable source. They can be used in the polyols synthesis (increasing the biodegradability)¹ and as natural plasticizer². The addition the oils into waterborne polyurethanes resins (WPU) can lead the an increase of hydrophobicity of these systems due the apolar characteristics of the oils. The present work aims to evaluate the effect of addition of different commercial vegetable oils (canola and linseed oil), in order to improve the water resistance of coatings obtained from WPU.

Experimental Part

The commercial oils (canola – OC or linseed – OL) were added in 1%w/w in the commercial WPU (37% solids content) under stirring (300rpm). In other experiment, the oils were emulsified by stirring (7500rpm, 2h) in an Ultra-Turrax emulsificator (Multitec IKA®T25) before the addition in the WPU. Two systems for each oil were obtained: WPU+oil (named as system 1); WPU+oil emulsified (named as system 2). The films were obtained from WPU+oil systems with a Bird applicator (wet thickness of 700µm) and characterized by Differential Scanning Calorimetry technique (DSC - Q20, TA Instruments) from -90°C a 200°C at a heating/cooling rate of 10°C.min⁻¹. The hydrolysis resistance of the films (15x15x2mm) was evaluated by immersion test in 30 mL of pure water for 72h.

Results and Discussions

The table 1 presented the values of glass transition temperature (T_g) for WPUOC, WPUOL and WPU (without oil). The addition of the oils not changed significantly the glass transition temperature.

Table 1. Values of T_g (°C) for WPUOL and WPUOC films.

	WPU	WPUOC1	WPUOC2	WPUOL1	WPUOL2
T _g (°C)	-39,4	-40,6	-39	-42,8	-35,9

The figure 1 presents the absorbed water content (% swelling) for WPUOC and WPUOL films and for WPU pristine.

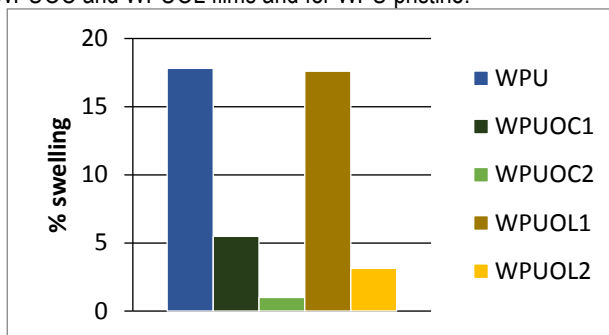


Figure 1. Swelling (%) behaviour of WPUOC, WPUOL and WPU pristine films.

The oil addition emulsified (WPUOC2 and WPUOL2) led to the best water resistance results with swelling of 0,99% and 3,14%, respectively. These results show that the emulsified oils have a better interaction with polyurethane matrix, changing the hydrophobic behavior of coating.

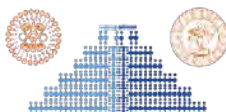
Conclusions

The addition of emulsified oil (WPUOL2 and WPUOC2) led the greatest effect on hydrophobic behavior of the WPU. The addition of emulsified oil led the a significant improve in the water resistance of the WPU. Furthermore, the addition of 1% of oil acts as a barrier agent and no as plasticizer.

Acknowledgment: CNPq, CAPES, PUCRS and Nokxeller Microdispersions by donation of raw materials.

References

1. Lligadas, G.; Ronda, J.; Galia, M.; Cádiz, V. *Materials Today* 2013, 16, 9, 337-343.
2. Madaleno, E.; Rosa, D.; Zawadzki, S.; Pedrozo, T.; Ramos, L. *Polímeros: Ciência e Tecnologia* 2009, 19, 4, 263- 270.
3. Kong, X.; Liu, G.; Curtis, J. M. *European Polymer Journal* 2012, 48, 2097-2106.
4. Viera, M.; Silva, M.; Santos, L.; Beppu, M. *European Polymer Journal* 2011, 47, 254-263.



PREPARATION AND CHARACTERIZATION OF POLYMER POLOXAMER P-407 FUNCTIONALIZED WITH ESTERS DERIVED OF CITRIC ACID

José Eduardo Hernández Torres¹, Ernesto Rivera Becerril¹, Gerardo Pérez Hernández¹

1. Universidad Autónoma Metropolitana Unidad Cuajimalpa, Vasco de Quiroga #4871, Col. Santa Fe, Del. Cuajimalpa, 05348. México D. F. México eduardotorreshd@gmail.com

Introduction

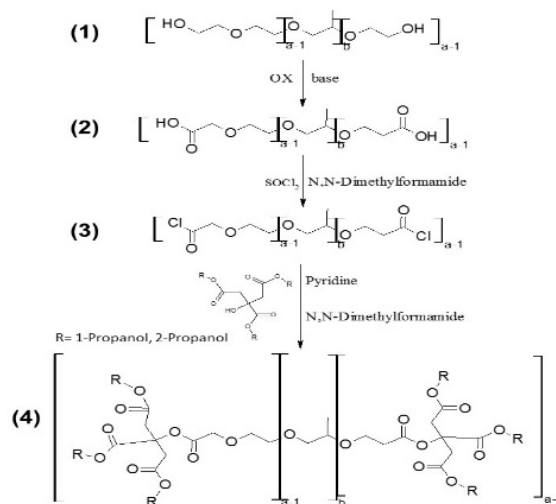
Poloxamer is a copolymer composed of three nonionic block, formed by a central hydrophobic chain, flanked by two hydrophilic chains, α - ω -hydroxy-hidroxi-poli-(oxyethylene)_a-poly (oxypropylene)_b-poly (oxyethylene)_a. Poloxamer P-407 is widely used as a vehicle or drug matrix due to their physicochemical properties to generate a modified release.¹ In addition, citric acid has been incorporated in pharmaceutical applications as nanostructured carrier² and precursor of new materials.³ Given these properties of the poloxamer and citric acid, the objective of this work was functionalizing the hydroxyl group of poloxamer polymer P-407 with esters derived from citric acid, which will generate a new material with potential application in confinement and release of drugs.

Experimental Part

Compound (2) it was obtained by oxidation of compound (1) with KMnO₄ in basic medium. Compound (3) it was synthesized by chlorinating the compound (2) with chloride thionyl (SOCl₂) and N, N-dimethylformamide as a catalyst. Compound (4) was obtained from the compound (3) and the ester derivatives of citric acid in dimethylformamide as a solvent and pyridine as catalyst. The ester derivatives of citric acid were synthesized using citric acid, together with the corresponding alcohol (1-propanol and 2-propanol), with sulfuric acid as catalyst under reflux conditions. The characterization of the compounds obtained were determined using FTIR instruments (Brucker Tensor 27) and NMR (FT-NMR (60 MHz) ANASAZI).

Results and Discussions

Scheme 1 shows the sequence of the compounds obtained. Compound (2) had a yield of 80%, and was as a white solid. Compound (3) it was obtained as a light yellow solid with 30% yield. Compounds (4) had a semisolid, yellowish, for the case of compound (4) with the ester derivative with 1-propanol yield was 50%, while the product of the ester derivative of 2-propanol was 40%. The results of the characterization of the compounds shown in Table 1.



Scheme 1. Synthesis of compound (4).

Table 1. Signals characteristic of the compounds obtained.

Compound	FTIR (cm ⁻¹)	RMN ¹ H (ppm)	RMN ¹³ C (ppm)
(2)	3420,1677, 1609, 1468	1.16,1.24, 4.16, 4.79, 4.88, 4.95	17.64,75.90,80.23, 173.08, 173.37
(3)	3499,2972, 2884,1736, 1468,664	1.04,1.12, 4.75, 4.83, 4.93	17.23,39.28,77.39, 79.35, 164.74
(4) R= 1-Propanol	2968,1735, 1387,1092	0.75,0.91,1.52,2. 81,3.46,3.86	10.62,17.27,42.86, 171.66,167.39
(4) R= 2-Propanol	2873,1732, 1380,1100	0.89,1.05,2.70,2. 93,3.20,3.35, 4.7	21.61,17.32,43.58, 36.46,162.77, 169.04, 172.68

Conclusions

A new material (4) according to the spectroscopic characterization, which may be a potential for the containment system and modified drug release was obtained.

References

- Gaster, J.; Fink, H. P.; Pinnow, M. *Composites* 2006, 37, Part A, 1796.
- Ljungberg, N.; Cavaille, J. Y., Heux, L. *Polymer* 2006, 47, 6285.
- Amash, A.; Zugenmaier, P. *Polymer* 2000, 41, 1589.

MODIFICATION OF THE DEGREE OF CRYSTALLINITY OF POLY-3-HYDROXYBUTYRATE POWDER BY MEANS OF PLASMA TREATMENT

Samuel V.O. da Silva¹, Tobias Hartmann², Renata A. Simão¹, Lothar Kroll²

1. Federal University of Rio de Janeiro, Departamento de Engenharia Metalúrgica e de Materiais, Centro de Tecnologia, bloco F, sala F-211, ZIP 21941-972, Rio de Janeiro, Brazil. samuca@ufrj.br, rasimao@poli.ufrj.br
2. Technische Universität Chemnitz, Department of Lightweight Structures and Polymer Technology, Reichenhainer Str. 31/33, 09126, Chemnitz, Germany
tobias.hartmann@mb.tu-chemnitz.de, lothar.kroll@mb.tu-chemnitz.de

Introduction

The steadily increasing demand for polymeric materials for daily use in the last decades has caused serious concerns related to the space needed in landfills and the contribution to soil, air and water pollution in the long run.¹ These concerns have paved the way for the rising importance of biodegradable polymers in the industry.² Polyhydroxyalkanoates (PHA) are important biogenic representatives of this class of biodegradable polymers.³ The PHA-derivative Poly-(R)3-hydroxybutyrate (P3HB) is currently in the focus of research. It displays a number of properties comparable to petroleum-based polymers (especially polypropylene) as high melting temperature (180°C) and high tensile strength (35 MPa). However, pure P3HB has had only limited use mainly because of its intrinsic brittleness deriving from its high grade of crystallinity.⁴ There are different approaches to reduce or inhibit the crystallization process.⁵ Beside efforts in compounding P3HB with plasticizers or nucleating agents for controlling the degree of crystallinity and for improving flexibility in the final product, in the present work, there is a novel approach to influence the degree of crystallinity by plasma treatment of pure native P3HB powder.

Experimental Part

Non-commercial neat and native Biomer® P3HB was treated by inductive radio frequency (RF) plasma of acetic acid (HOAc) and air (ATM). Plasma treatment was carried out in an in-house built reactor, duration was 60 minutes with an applied power of 60 W. The reactor comprised of a revolving sample container inside a glass tube surrounded by a metallic coil and an impedance coupling circuit. Influences on the degree of crystallinity were characterized by XRD and DSC analyses. A relation between the area under the diffraction peaks (I_c) and the area under the amorphous halo (I_a) with a constant of proportionality ($k = 0.96 \pm 0.03$ for P3HB) are used to determine the degree of crystallinity using the XRD spectra [Eq. (1)], while a ratio between the enthalpy of fusion of the sample ($\Delta H_{f\text{Sample}}$) and the latent heat of fusion of 100% crystalline P3HB ($\Delta H_{f^\circ\text{PHB}} = 146 \text{ J/g}$)⁶ can be used to ascertain the degree of crystallinity with the aid of DSC analysis [Eq. (2)].

$$X_c = [(I_c) / (I_c + kI_a)] \times 100\% \quad \text{Eq.(1)}$$

$$X_c = (\Delta H_{f\text{Sample}} / \Delta H_{f^\circ\text{PHB}}) \times 100\% \quad \text{Eq.(2)}$$

Results and Discussions

Both treatments were able to reduce the crystallinity of P3HB. The treatment performed with HOAc plasma exhibited lower contribution from the amorphous phase as well as lower diffraction peaks, while the degree of crystallinity obtained as the ratio between enthalpy of fusions for the test sample, the HOAc plasma and the ATM plasma treated samples was 58.68%, 56.34% and 54.01%, respectively.

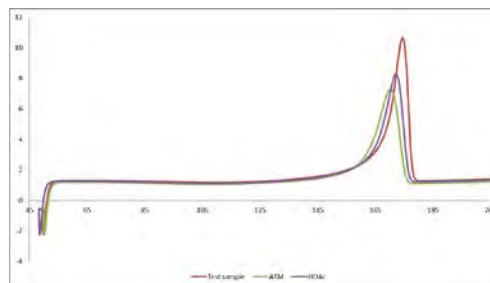


Figure 1. DSC results showing the decrease of the enthalpy of fusion for both treatments.

Conclusions

Plasma treatment is a feasible mean of lowering the degree of crystallinity of P3HB, but ATM seems to be a better candidate at reducing the crystallinity of the polymer as it does not affect amorphous phase as much as HOAc. Several further treatments are currently in the evaluation and characterization state. These results will be ready to publish in my presentation.

References

1. Shah, A.A. *et al. Biotechnology Advances* 2008, 26, 246.
2. Derraik, J.G.B. *Marine Pollution Bulletin* 2002, 44, 842.
3. Nair, L.S., Laurencin, C.T. *Prog. Polym. Sci.* 2007, 32, 762.
4. El-Hadi, A *et al. Polymer Testing* 2002, 21, 665.
5. Mohanty, A.K. *et al. Macromol. Mater. Eng* 200, 276, 1.
6. Barham, P.J. *et al. Journal of Materials Science* 1984, 19, 2781.

EFFECT OF PLASMA TREATMENT ON HYDROPHOBICITY OF PAPER

Jennifer Flórez Cristancho¹, Renata Antoun Simão¹-

1. DMM-PEMM/COPPE/UFRRJ Programa De Engenharia Metalúrgica E De Materiais Cid. Universitária-Centro de Tecnologia – Bloco F, Ilha do Fundão – Rio de Janeiro, 21941-972 jenniferflorez@metalmat.ufrrj.br

Introduction

Paper surface can be modified by RF plasma treatment, without the aid of conventional chemical agents, thus avoiding any environmental concerns². The surface of paper can undergo several physical and chemical alterations when modified by plasma, improving or providing properties of the paper. In this study, sulfur Hexafluoride (SF₆) plasma treatment was applied on commercial A4 paper plasma, under specific experimental conditions of pressure and power, in order to increase its hydrophobic character. The treated and untreated paper samples were characterized by contact angle measurements and FTIR.

Experimental Part

The plasma treatment was performed with an applied power of 60 W during 20 min at $1,1 \times 10^{-1}$ mbar. The influence of the plasma on the hydrophobicity of paper surface was determined from water contact angle measurements using a NRL A-100-00 RAME-HART Goniometer. Absorbance-Fourier Transform Infrared spectroscopy (FTIR) was used to identify the chemical linkages on the plasma functionalized paper surface. The spectra was obtained in the range of 600 to 4000 cm⁻¹ with a NICOLET 6700 spectrophotometer from THERMO SCIENTIFIC.

Results and Discussions

The plasma treatment of the paper sample induced an increase from 80° to 110° of the contact angle of a drop of water. This behavior is presented in the Fig. 1, and could be attributed to fluorine atoms reacting on the surface of paper, obtaining a significant decrease in the wettability and a decrease of the absorption kinetics.

Figure 2, illustrates the differences between bands of untreated and treated paper samples. The main difference between both samples was observed in the decrease of height at the peaks 872 cm⁻¹ (C-O-C) in plane symmetric, 1026 (C-O) stretching vibrations of primary alcohol, 1055 cm⁻¹ (C-O) stretching of secondary alcohol and a clear modification in form of the peak at 1417cm⁻¹, such that treated paper has a unique and better defined peak.

As regards to the region 2600 to 1600 cm⁻¹ corresponding to fingerprint of cellulose, (C-O-H) in-plane bending vibrations, (C-O-C) stretching of the β-(1-4)-glycosidic linkage, remain the same.



Figure 1. Drop of water on a paper sample: a) wetting surface and b) non-wetting surface (hydrophobic).

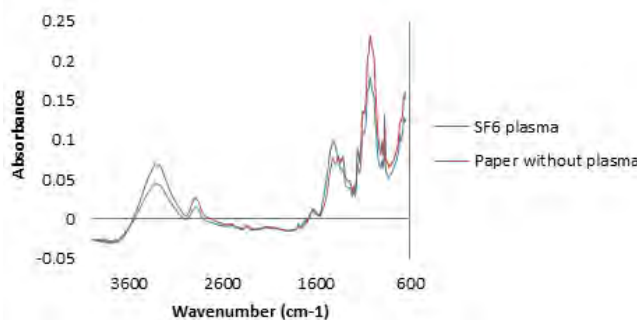


Figure 2. Comparative FTIR spectrum of untreated and treated paper samples.

Conclusions

Preliminary characterizations indicate surface modification by plasma treatment obtains significant results with an increase on hydrophobicity of paper. This process is simple, but very effective, and may replace hazardous chemical agents as functional group inducing medium, avoiding the possible formation of by-products and wastes.

Acknowledgment: CNPq

References

1. Jonhed A. Dissertation Karlstad University Studies 2006, 42.
2. Gaiolas C, et al. *Industrial Crops and products* 2013, 43, 114.
3. Sahin H. *Applied Surface Science* 2013, 265, 558.
4. Hajji L, et al. *Microchemical Journal* 2016, 124, 646.

PLASMA SPUTTERING OF Cu ON POLYETHYLENE

M. R. Mejía-Cuero^{1,2}, E. Colín-Orozco¹, M. G. Olayo-González², G. J. Cruz-Cruz²,
 R. Valdivia-Barrientos³, J. C. Palacios-González¹, I. Martínez-Cienfuegos¹

1. Facultad de Ingeniería, Universidad Autónoma del Estado de México, Cerro de Coatepec s/n, Ciudad Universitaria, Toluca, CP 50130, México. ecolino@uaemex.mx; rairam_mej@yahoo.com.mx
2. Departamento de Física, Instituto Nacional de Investigaciones Nucleares, Carr. México-Toluca, Km 36.5, Ocoyoacac, Edo. de México CP 52750, México.
3. Departamento de Estudios del Ambiente, Instituto Nacional de Investigaciones Nucleares, Carr. México-Toluca, Km 36.5, Ocoyoacac, Edo. de México CP 52750, México.

Introduction

Polyethylene (PE) is the simplest organic polymer made only with -CH₂- groups with properties as low conductivity and hydrophobicity. As PE almost does not interact with the surrounding medium, it is difficult to combine it with metals without degrading the polymer. One way to do this without degradation is by sputtering in which the metal is eroded by the impact of different energy particles such as ions, neutral atoms and electrons; and the eroded particles are deposited on PE forming layers with controlled thicknesses¹. The combination modifies the superficial properties of PE increasing the conductivity, optical properties and hydrophilicity. In this work, combinations of Cu on PE by plasma sputtering are studied.

Experimental Part

Cu deposition on PE substrates were obtained by the magnetron sputtering technique on an Intercovamex system, using a Cu target with 99.99% purity with different deposition time, 4 and 8 min. To analyze the morphological and structural properties of Cu on PE, the materials were characterized by FTIR, SEM, XRD, electrical conductivity and contact angle.

Results and Discussions

Figure 1 shows the SEM images for PE with deposition of Cu for two different deposition time, 4 min for PECu1 and 8 min for PECu2. These images demonstrate that Cu present homogeneous layers with thickness of 16.7 μm for PECu1 and 34.2 μm for PECu2. In this case, the thickness is directly related with the depositions time.

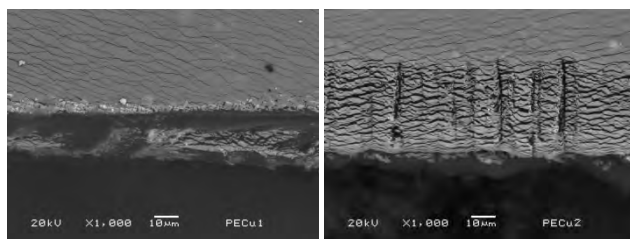


Figure 1. Micrographs of PE, PECu1 y PECu2.

Figure 2 shows the FTIR spectra of PE, and PE with Cu named PECu1 and PECu2. All the spectra contain the characteristic absorption bands of -C-H (2914, 2849 and 720 cm⁻¹) and -C-C-

(1472 cm⁻¹)^{2,3}, typical for PE. Additionally, PECu1 and PECu2 present the band of Cu-O (668 and 730 cm⁻¹) due to the copper deposition.

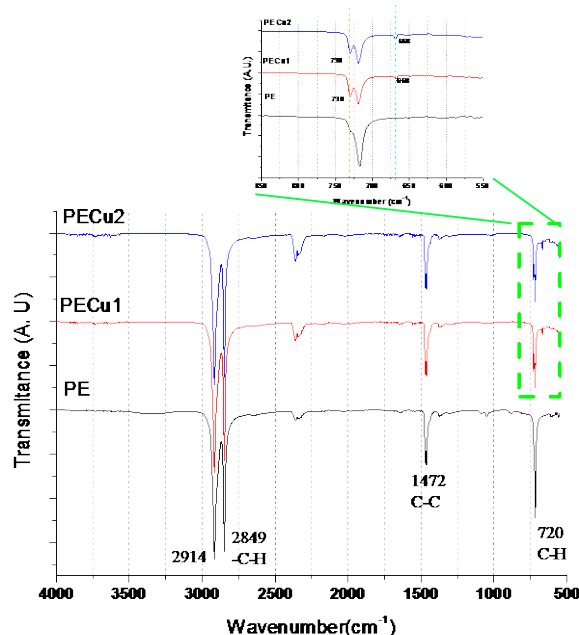


Figure 2. FTIR of PE, PECu1 y PECu2.

Conclusions

Copper particles were formed on polyethylene substrate by RF magnetron sputtering technique. SEM microstructure analysis indicated the formation of homogenous layers and different deposition thickness. This thickness is directly related with the deposition time. Further analysis will be related with the effect of the applied power and the distance between substrate and copper target.

References

1. Kelly, P.J.; Amell, R.D. Vacuum 2000, 159-172.
2. Gaddsdén, J.A. Infrared Spectra of Minerals and Related Inorganic Compound, 1st ed., Butterworth, London, 1975
3. Nyquist, R.A.; Kagel, R.O. Infrared Spectra of Inorganic Compounds, Academic Press, 1971.

PREPARATION OF GRAPHENE OXIDE BY HUMMERS METHOD WITH A NEW EXFOLIATION TECHNIQUE

Luis A. Maccllesh del pino Perez, Tomas Lozano*, Luisiana Morales-Zamudio

Instituto Tecnológico de Ciudad Madero, Av. 1 de Mayo s/n Col. Los Mangos, Cd. Madero Tamps. C.P. 89440

This study describes the synthesis of graphene oxide by modified Hummers method using a colloidal solution as exfoliation promoter, the ultrasonication step is eliminated resulting in less synthesis time and a material with properties favorable to be made functional. The samples were characterized by several analysis methods such as FTIR (Fourier Transform Infrared Spectroscopy), Raman spectroscopy and XRD (X-Ray Diffraction). All these analysis show the material obtained using an electrolyte is graphene oxide with a selectivity to epoxy groups. The synergy between graphite oxide and the saline solution causes repulsion and attraction forces which are explained by DLVO (Derjaguin-Landau-Verwey-Overbeek) theory of colloids. These effects are responsible for the exfoliation of graphene oxide.

Experimental Part

The graphene oxide was synthesized according to the Modified Hummer's method^[1]. The obtained solution pH was between 0-1.

Saline washes

To neutralize the solution successive washes are necessary, in this step is used the saline solution. Washing was performed by centrifugation with 1.5 liters of saline solution this amount of solution enough for the washing of 5 grams of graphite oxide. Slater^[2] studied the stability of hydrogen peroxide and reported in solution with low pH, the hydrogen peroxide is stable, but when pH increase above 5 the hydrogen peroxide molecule it begin to decompose, when a basic pH 6 to 7 was reached, almost all hydrogen peroxide was dissociated, the material was washed with 500 ml of deionized water to remove any salt remainder in the graphene oxide solution. The exfoliation is done during washes with saline solution, the effect cause an increment in the basal distance from graphite oxide, and it turning into graphene oxide. After centrifugation isopropanol was added to the solution until reach 1 liter, because the isopropanol possess a smaller dipole moment^[19] than water, this property allow to the graphene oxide's sheets get relaxed in the suspension, avoiding deformation in the sheets during the dried. The isopropanol reduces the drying time. The solution was dried at 60°C in air for 2 days. The obtained GO sample was kept in a desiccator for later use.

Results and Discussions

The Figure 1 shows the X-Ray patterns of GO-S, GO-U and graphite oxide. These peaks belong to the graphene oxide characteristics signals^[3,4]. The number of sheets of graphite was calculated with Bragg's equation and it corresponds to $n = 7.2$. The GO-S (by saline solution) shows a broad peak around $2\theta = 11.3^\circ$, the peak's amplitude

indicates that the material is losing its tridimensional structure due to oxidation and exfoliation. It also brings information about the number of sheets in that tridimensional structure. The number of sheets that compose the tridimensional structure of GO-S (n was 2.45) and a value of 4.17 for GO-U sheets (by sonification step). This is the reason why the GO-S patterns shows a broad peak and with lower intensity than GO-U. The graphite oxide shows a structure with less basal distance and it has more sheets (7.2) in its structure than the other two structures.

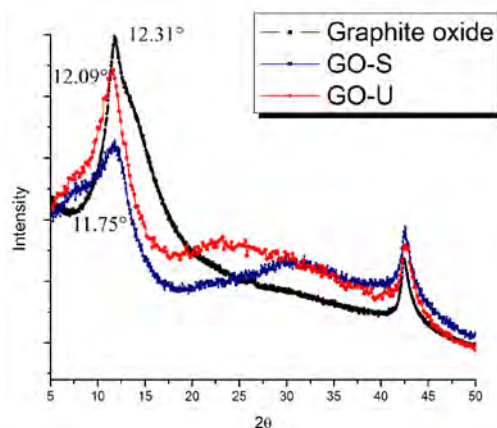


Figure 1. DRX patterns of GO-S, GO-U and Graphite oxide

Conclusions

The proposed approach using saline solution, is feasible and repeatable, allowing increased production of graphene oxide in less time avoiding the use of ultrasound treatment.

References

1. Jianguo, Song; Xinzhi, Wang; Chang, Tang, Chang Journal of Nanomaterials, 2014, ID 276143, 6
2. Trabal. Boletín del Instituto de Investigación Textil y de Cooperación Industrial, 1974, nº 59, p. 7-17 ISSN:1131-6756.
3. Vorrada Loryuenyong, KritTotevimam, Passkom Eimburanaprat, Wachai Boonchompoo, Achanai Buasri. Advance in Materials Science and engineering volume 2013, Article ID 923403.
4. Gilje, S.; Han.; Wang, M.; K.L.; Kaner, R. B. "A chemical route to graphene for device applications". Nano letters 2007,7,1-6. Supporting information.



FORMACIÓN INICIAL DE LA CADENA DE POLYINDOFENOL USANDO PERÓXIDO DE HIDRÓGENO (H₂O₂) PARA OXIDAR PARAFENILENDIAMINA (C₆H₈N₂)

Rosaura Vanessa Albino-Andrade¹, Juan Horacio Pacheco-Sánchez².

División de Estudios de Posgrados e Investigación, Instituto Tecnológico de Toluca, Metepec, CP 52149, Edo. Méx., México Tel: 722-208-7200 ext. 3211; E-mail: Rosauara.Vanessa@hotmail.com, hpacheco@ittoluca.edu.mx.

Introduction

Un método para la coloración de la fibra capilar es el teñido permanente, esta reacción es por medio de oxidaciones de acopladores primarios derivados de aminas, en donde la primera fase es la formación del ion Diiminium, la segunda fase es el acoplamiento de los iones¹ y la última fase es formación del polímero polyindofenol². Uno de los principales acopladores usados industrialmente es la parafenilendiamina (C₆H₈N₂). En este trabajo se estudia la formación del ion diiminium parafenilendiamina. La oxidación de la parafenilendiamina (C₆H₈N₂) se efectúa usando como oxidante al peróxido de hidrógeno (H₂O₂). La interacción entre estas dos moléculas se lleva a cabo por medio de DTF con el programa de cómputo DMol³. Estudios previos de esta reacción no han reportado la energía de interacción ni han descrito exactamente que compuestos se pueden formar.

Metodología

Se aplicó una optimización de geometría DFT-DMol³ all electrón a la interacción entre una molécula de parafenilendiamina (C₆H₈N₂) y una de peróxido de hidrógeno (H₂O₂). La primera prueba se efectuó con el funcional LDA-PWC, la segunda con el funcional GGA-PW91, la tercera con el funcional m-GGA-MOG-L, spin unrestricted, conjunto de bases dnd, simetría C₁. La geometría de entrada que se utilizó para esta interacción es la observada en la fig.1

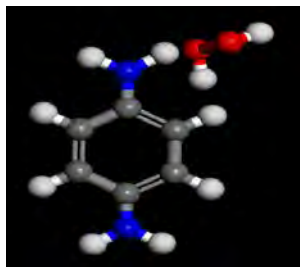


Figura 1. Geometría de entrada en la interacción de moléculas.

Resultados y conclusiones

La geometría de entrada en la figura 1 se obtuvo después de probar por ensayo y error muchas otras geometrías optimizadas. La interacción de las moléculas para la formación de ion

diiminium parafenilendiamina depende de la geometría de interacción, ya que el oxígeno es más electronegativo que el nitrógeno por lo cual a una distancia adecuada del oxígeno en el enlace N-H es capaz de ser roto por la fuerza del oxígeno, para que el oxígeno no entre en interacción con la molécula parafenilendiamina y solo provoque un estado de excitación en uno de los enlaces de N-H y sea capaz de romperlo³. Para esto fue necesario encontrar la posición geométrica adecuada utilizando los métodos LDA y GGA, los cuales no convergen y sugieren el uso de smearing. En vez de aplicar smearing se procedió a utilizar m-GGA dando una energía en la optimización de geometría de la molécula de -494.557370 Ha. Esta es la energía que se tiene de la oxidación de parafenilendiamina (C₆H₈N₂).

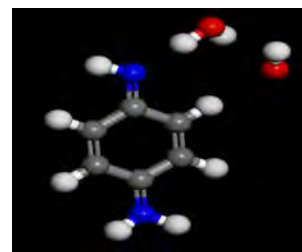


Figura 2. Molécula-ion diiminium parafenilendiamina.

Conclusion

La formación del ion diiminium parafenilendiamina, se logró solo con una interacción (1:1), esta oxidación es demasiado inestable ya que si alteramos la geometría se puede obtener una reacción indeseada, este es el primer camino para la formación del polyndofenol, se continúa con el estudio y se espera conseguir una comprensión teórica más completa de su formación.

Agradecimiento

Este trabajo se ha desarrollado con el soporte del proyecto DGEST-TecNM: IDCA 17452, clave ITTOL-CA-7

Referencias

1. Robbins C., Chemical and Physical of Human Hair, 4th ed. 314 (2001).
2. Brody, F.; Burns, M. J. Soc. Cosmet. Chem. 19: 361 (1968).
3. Morrison R., Neylson R., Química Organica, 5th ed. 214 (1900)

BIODEGRADABLE POLYURETHANES BASED ON PCL AND COUMARIN WITH PHOTOREVERSIBLE BEHAVIOUR

Castor Salgado¹, Marina P. Arrieta¹, Marta Fernández-García¹, Laura Peponi¹, Daniel López¹

1. Instituto de Ciencia y Tecnología de Polímeros, ICTP-CSIC, calle Juan de la Cierva 3, 28006 Madrid, Spain

daniel.l.g@csic.es

Introduction

Coumarins are interest molecules since they are able to experiment photodimerization via [2+2] photocycloaddition stimulated by UV irradiation.¹ The introduction of different proportion of coumarins into biodegradable polymers, such as poly(ϵ -caprolactone) (PCL),² with different molecular weights to further synthesize poly(urethanes) (PUs) allows to design materials with tunable mechanical properties for sustainable applications in advanced technological fields, such as the automotive sector.

Experimental Part

PUs, based on PCL and coumarin, were synthesized in two steps. In the first step coumarin diol (CD) and 1,6-hexamethylene diisocyanate (HDI) were prepared by condensation to form a pre-polymer based on HDI-CD and then PUs have been obtained by a posterior reaction with PCL-diol. In particular two PCL-diol, kindly donated by PERSTORP, with different molecular weights (M_w = 530 or 2000 g/mol) have been used. The physico-chemical properties of the synthesized materials have been characterized by ¹H-NMR and FT-IR spectroscopy. The photo-dimerization after irradiation at 365 nm of CD has been analyzed by UV-Vis analysis. The mechanical properties have been tested by stress-strain analysis in an Instron before and after irradiation at 365 nm.

Results and Discussions

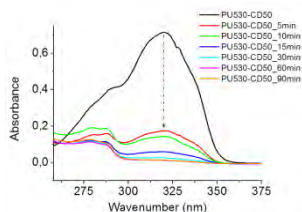


Fig. 1. Evolution of photo-dimerization at different times of irradiation

Initially, pre-polymers based on different amounts of CD (5, 15 and 25 mol %) and HDI were prepared by condensation and then reacted with PCL-diol, either with molecular weight M_w = 530 or

2000 g/mol, in dichloroethane. The obtained PU were photodimerized by means of a UV irradiation at 365nm. The photodimerization was followed by the reduction of the UV band at 320 nm (Fig.1). The maximum photodimerization yield took 90 min and was higher than 90% for PU530s than for PU2000s (> 65 %). CD reduced the Young modulus (E) of PU530s. CD increased the tensile strength (TS) and the elongation at break ($\epsilon\%$) of PU530s and PU2000s. In general, the photodimerization increased the mechanical performance (Table 1).

Table 1. Mechanical properties of PUs

Samples	E (MPa)		TS (MPa)		$\epsilon\%$	
	PU	365	PU	365	PU	365
PU530	36	36	1	2	8	8
PU530-CD5	37	8	22	12	107	710
PU530-CD15	2	7	43	8	530	370
PU530-CD25	3	2	43	3	460	405
PU2000	140	160	9	21	500	650
PU2000-CD5	180	160	10	21	880	590
PU2000-CD15	155	140	7	11	600	400
PU2000-CD25	165	70	8	20	510	480

Conclusions

PU based on PCL and CD, were successfully synthesized in two steps. Shorter PCL diol with higher amount of CD allowed higher photodimerization yields. The photo-dimerization of CD induces better mechanical properties. These PUs are promising coating systems for automotive applications.

Acknowledgment: We thanks Spanish Ministry of Economy and Competitiveness (MAT2013-48059-C2-1-R). L.P. and M.P.A. acknowledge MINECO for the "Ramon y Cajal" (RYC-2014-15595) and Juan de la Cierva contracts (FJCI-2014-20630).

References

- Seoane-Rivero ,R., Bilbao-Solaguren, P., Gondra-Zubieta, K., Peponi, L., Marcos-Fernández, A. *Express Polymer Letters*. 2015,10(2), 84.
- Peponi, L., Navarro-Baena, I, Báez, JE, Kenny, JM, Marcos-Fernández, A. *Polymer* 2012; 53(21), 4561.

